

**α,γ -Hybrid Pepbiotics: Exploration of α,γ -Hybrid
Peptides as a New Class of Antimicrobial
Peptidomimetics**

A thesis

Submitted in partial fulfilment of the requirements

Of the degree of

Doctor of Philosophy

By

Sushil Namdev Benke

ID: 20113135



Indian Institute of Science Education and Research, Pune.

*Dedicated to my family and
teachers*

CERTIFICATE

This is to certify that the work incorporated in the thesis entitled “ **α,γ -Hybrid Pepbiotics: Exploration of α,γ -Hybrid Peptides as a New Class of Antimicrobial Peptidomimetics**” submitted by **Sushil Namdev Benke** carried out by the candidate at the Indian Institute of Science Education and Research (IISER), Pune, under my supervision. The work presented here or any part of it has not been included in any other thesis submitted previously for the award of any degree or diploma from any other University or Institution.

Date: 28-08-2017

Dr. Hosahudya N. Gopi

(Research Supervisor)

Associate Professor, IISER-Pune

Pune-411008, India.

Declaration

I, hereby declare that the thesis entitled “ **α,γ -Hybrid Pepbiotics: Exploration of α,γ -Hybrid Peptides as a New Class of Antimicrobial Peptidomimetics**” submitted for the degree of Doctor of Philosophy in Department of chemistry at Indian Institute of Science Education and Research (IISER), Pune has not been submitted by me to any other University or Institution. This work was carried out at Indian Institute of Science Education and Research (IISER), Pune, India under the supervision of Dr. Hosahudya N. Gopi.

Date: 28-08-2017

Sushil Namdev Benke

ID: 20113135

Senior Research Fellow,

Dept. of Chemistry, IISER,

Pune-411008.

Acknowledgements

I would like to express special appreciation to my enthusiastic mentor Dr. H. N. Gopi for his constant support and guidance during the course of study. I admire his creativity in designing and executing experiments with great thinking. His guidance has helped me during the time of research and writing of this thesis. I thank Dr. Gopi, not only for his valuable inputs and consistent encouragement during my PhD, but also for his generous support in my personal life. I am very fortunate to have an opportunity to work under his supervision.

I sincerely thank to Prof. K. N. Ganesh (Director, IISER Pune) for providing the excellent infrastructure and facilities to pursue my doctoral research. I would like to express my sincere gratitude to Dr. S. Hotha and Dr. S. P. Chavan for being the research advisory committee (RAC) members and providing valuable suggestions during RAC meetings. I also would like to acknowledge Dr. H. V. Thulasiram (NCL, Pune) for providing facilities for conducting various experiments. I would also like to acknowledge Dr. S. Ragothama from IISc, Bangalore for carrying out the NMR calculations.

I am very fortunate to have wonderful colleagues working with me like Dr. Anupam, Dr. Sandip, Dr. Sachin, Dr. Ganesh, Rajkumar, Anindita, Rahi, Veeresh, Sachin, Puneet, Sanjit and Saikat. I thank them for their support and keeping cheerful atmosphere in the lab during my doctoral research. I am thankful to all the students of Dr. H. V. Thulasiram for their help in understanding the biological assays. I thank Anupam, Pramod and Balu for their help and support. I am thankful to all IISER Pune colleagues, with whom I discussed my ups and downs of research, and for giving the relaxation needed in tough times of research. I would like to extend my gratitude to all faculty members for their constant support and encouragement. It is my prime duty to acknowledge University Grants Commission (UGC) for my graduate research fellowship. I would like to thank those who helped me directly and indirectly during my research.

I shall always remain indebted to my parents and my entire family, for their unconditional love, blessings, sacrifices, patience and support during my study. The values and virtues they have instilled in me have made me to achieve whatever I have achieved so far. Finally, I would like to thank a very special person, my wife, Lalita for her unconditional support and trust.

Sushil Namdeo Benke

Contents

Abbreviations.....	i
Abstract.....	iv
Publications.....	v

Chapter 1

Antimicrobial Peptides

1.1	Antibiotics	1
1.1.1	Antimicrobial resistance	2
1.1.2	Strategy against the antibiotic resistance crisis	3
1.1.3	Antimicrobial peptides (AMP's)	3
1.1.3.1	Classification of antimicrobial peptides	4
1.1.3.1.1	Linear peptides	4
1.1.3.1.2	Helical peptides	4
1.1.3.1.3	β -sheet peptides	5
1.1.3.1.4	Macrocyclic peptides	5
1.1.3.1.5	Lipopeptides	5
1.1.3.2	Mechanism of action of AMP's	6
1.1.3.2.1	Membrane disruption	6
1.1.3.2.1.1	Barrel stave model	7
1.1.3.2.1.2	Carpet model	8
1.1.3.2.1.3	Toroidal pore model	9
1.1.3.2.2	Intracellular targets of antimicrobial peptides	10
1.1.4	AMP's as therapeutics	11
1.1.5	Drawbacks of AMP's	12
1.2	Antimicrobial peptidomimetics	12
1.2.1	Foldamers	13
1.2.1.1	β -peptides	13
1.2.1.2	Nylon-3 polymers	14
1.2.1.3	Cyclic peptides	15
1.2.1.4	Peptoids	16

1.2.1.5	α -AA peptides	16
1.2.1.6	γ -amino acid containing peptidomimetics	17
1.3	References	18

Chapter 2

Design, Synthesis, and Broad Spectrum Antimicrobial Properties of Short Hybrid *E*-Vinylogous Lipopeptides

2.1	Introduction	26
2.2	Aim and rational of the present work	29
2.3	Results and Discussion	30
2.3.1	Synthesis of monomers	30
2.3.2	Design, synthesis and purification of lipopeptides	31
2.3.3	Antimicrobial activity	32
2.3.4	Hemolytic activity	34
2.3.5	β -Galactosidase leakage assay	35
2.3.6	Membrane deformation study	37
2.3.7	FITC uptake assay	38
2.3.8	Dynamic light scattering studies	38
2.3.9	Field emission scanning electron microscope analysis	40
2.4	Conclusion	41
2.5	Experimental section	42
2.5.1	General experimental procedure	42
2.5.2	General procedure for the synthesis of Fmoc- α , β -unsaturated γ - amino acids	43
2.5.3	Solid phase peptide synthesis and purification	47
2.5.4	Procedure for testing antibacterial activity	47
2.5.5	Procedure for testing antifungal activity	48
2.5.6	Procedure for hemolysis assay	48
2.5.7	Procedure for atomic force microscopy imaging	49
2.5.8	Procedure for FITC uptake assay	49
2.5.9	Procedure for β -galactosidase leakage assay	50
2.5.10	Procedure for dynamic light scattering experiment	51
2.5.11	Scanning electron microscopy imaging	51

2.6	References	51
2.7	Appendix I. Characterisation data of synthesized compounds and peptides	57

Chapter 3

Chapter 3a

Potent Antimicrobial Activity of Lipidated Short α , γ -Hybrid Peptides

3a.1	Introduction	69
3a.2	Aim and rational of the present work	70
3a.3	Results and discussion	71
3a.3.1	Design and synthesis of peptides	71
3a.3.2	MIC determination	73
3a.3.3	Hemolytic activity of lipopeptides	74
3a.3.4	Membrane deformation study	76
3a.3.5	β -galactosidase leakage assay	77
3a.3.6	Time kill kinetics assay	78
3a.4	Conclusion	79
3a.5	Experimental section	80
3a.5.1	General experimental details	80
3a.5.2	Synthesis of <i>N</i> -Fmoc-protected γ -amino acids	80
3a.5.3	Synthesis of peptides	83
3a.5.4	Procedure for determining antibacterial activity	83
3a.5.5	Procedure for hemolysis assay	84
3a.5.6	FE-SEM Analysis	84
3a.5.7	Procedure for β -Galactosidase leakage assay	85
3a.5.8	Procedure for time kill kinetics	85
3a.6	References	86
3a.7	Appendix II: Characterisation data of synthesized peptides	89

Chapter 3b

Synthesis and Utilization of New $\gamma\gamma$ -diamino acids from *E*-Vinylogous Amino Acids and Their Utility in Design of α,γ -Hybrid Peptide Foldamers

3b.1	Introduction	99
3b.2	Aim and rational of the present work	100
3b.3	Results and discussion	101
3b.3.1	γ,γ -diamino acid synthesis	101
3b.3.2	Incorporation of γ,γ -diamino acid in peptidomimetics	103
3b.4	Conclusion	106
3b.5	General experimental details	107
3b.5.1	General procedure for the synthesis of β -nitromethane substituted γ -amino esters	107
3b.5.2	Solid phase synthesis of peptide N1	113
3b.5.3	Crystallographic information of peptide N1	114
3b.6	References	115
3b.7	Appendix IV: Characterisation data of synthesized peptides	118

Chapter 4

Design, Structure and Potent Antimicrobial Activity of $\alpha\alpha\gamma$ -Hybrid Peptide Helical Foldamers

4.1	Introduction	129
4.2	Aim and rational of the present work	131
4.3	Results	131
4.3.1	Peptide design and synthesis	131
4.3.2	Solution conformation of peptides	133
4.3.3	Antibacterial activity	140
4.3.4	Hemolytic activity	141
4.3.5	Field emission scanning electron microscopy studies	143
4.3.6	β -Galactosidase leakage assay	144

4.3.7	DNA Binding assay	145
4.3.8	Time kill kinetics assay	146
4.3.9	Serial passage assay	147
4.4	Discussion	148
4.5	Conclusion	150
4.6	Experimental section	151
4.6.1	Solid phase peptide synthesis and purification of $\alpha\alpha\gamma$ -hybrid peptides	151
4.6.2	NMR Structure Calculations	151
4.6.3	Procedure for determining MIC	152
4.6.4	Procedure for hemolysis assay	153
4.6.5	Procedure for β -galactosidase leakage assay	154
4.6.6	Procedure for peptide:DNA binding assay	154
4.6.7	Procedure for time kill kinetics assay	155
4.6.8	Procedure for membrane deformation study	155
4.6.9	Procedure for serial passage assay	156
4.7	References	157
4.8	Appendix IV: Characterisation data of synthesized peptides	161

Abbreviations

Ac₂O = Acetic anhydride

ACN = Acetonitrile

AcOH = Acetic acid

AFM = Atomic force microscopy

Aib = α -amino isobutyric acid

AMP = Antimicrobial peptide

ATCC = American type culture collection

aq. = Aqueous

Bn = Benzyl

Boc = tert-butoxycarbonyl

(Boc)₂O = Boc anhydride

tBu = tertiary Butyl

Calcd. = Calculated

Cbz = Bezyloxycarbonyl

Cbz-Cl = Benzyl chloroformate

CCDC no. = Cambridge Crystallographic Data Centre number

CFU = Colony forming unit

COSY = **C**ORrelation **S**pectroscop**Y**

CIF = Crystallographic Information File

Da = dalton

d γ = dehydro gamma

DBU = 1, 8-Diazabicyclo [5.4.0] undec-7-ene

DCC = N, N' -Dicyclohexylcarbodiimide

DCM = Dichloromethane

DiPEA = Diisopropyl ethyl amine

DMF = Dimethylformamide

DMSO = Dimethylsulfoxide

DNA = Deoxyribose nucleic acid

EDTA = Ethylene diamine tetra acetic acid

EtOH = Ethanol

Et = Ethyl

EtOAc = Ethyl acetate

FE-SEM = Field emission scanning electron microscopy

FITC = Fluorescein isothiocyanate
Fmoc = 9-Fluorenylmethoxycarbonyl
Fmoc-OSu = N-(9-Fluorenylmethoxycarbonyloxy) succinimide
g = gram
h = hours
HBTU = 2-(1H-benzotriazol-1-yl)-1, 1, 3, 3-tetramethyluronium hexafluorophosphate
H-bond = Hydrogen bond
HOBt = Hydroxybenzotriazole
HPLC = High performance liquid chromatography
hRBCs = Human red blood cells
HCl = Hydrochloric acid
IBX = 2-Iodoxybenzoic acid
M = Molar
MALDI-TOF/TOF = Matrix-Assisted Laser Desorption/Ionization-Time of Flight Time of Flight
Me = Methyl
MeOH = Methanol
mg = Milligram
MIC = Minimum inhibitory concentration
MHA = Mueller Hinton agar
MHB = Muller-Hinton broth
MHz = Mega hertz
min = Minutes
 μL = Micro litre
mL = Milli litre
mM = Milli molar
mmol = Milli moles
m.p = Melting Point
MRSA Methicillin resistant *Staphylococcus aureus*
MSSA Methicillin sensitive *Staphylococcus aureus*
MS = Mass Spectroscopy
ms = Milli second
MUG = 4-Methylumbelliferyl- β -galactosidase
N = Normal
NCIM = National Collection of Industrial Microorganisms
NHS = N-hydroxy succinimide

nm = Nano metre
NMP = N-methyl pyrrolidone
NMR = Nuclear Magnetic Resonance
NOE = Nuclear Overhauser Effect
NOESY = Nuclear Overhauser Effect Spectroscopy
O. D. = optical density
ORTEP = Oak Ridge Thermal-Ellipsoid Plot Program
PBS = Phosphate buffer saline
PG = Protecting Group
ppm = Parts per million
Py = Pyridine
R_t = Retention time
ROESY = **R**otating-frame nuclear **O**verhauser **E**ffect correlation **S**pectroscop**Y**
RP- HPLC = Reversed Phase-High Performance Liquid Chromatography
RT = Room Temperature
SDS = Sodium dodecyl sulphate
SR = selectivity ratio
TAE = Tris-acetate-EDTA
TFA = Trifluoroacetic acid
THF = Tetrahydrofuran
TOCSY = **T**otal **C**orrelation **S**pectroscop**Y**

Abstract

The emergence and spread of antibiotic resistant pathogens is one of the major health concerns of the 21st century, giving rise to an urgent need to develop new antibiotics with different mode of action. Peptides derived from non canonical amino acids such as β - and γ -amino acids have attracted greater interest due to their proteolytic resistance and predictable folding properties. These fascinating features encouraged us to explore the anti-microbial properties of hybrid peptides composed of α - and γ -amino acids. In this regard, we have designed two types of hybrid peptides, short lipopeptides and amphiphilic hybrid helices and investigated their antimicrobial properties. The short lipopeptides are composed of 1:1 α -, and γ -amino acids with varied length of lipid tail and the helical peptides are composed of repeating units of $\alpha\alpha\gamma$ tripeptide segment. These peptides were tested against various Gram positive, Gram negative bacteria as well as Fungi. In the first series, the designed lipopeptides displayed broad spectrum antimicrobial activity. The FITC uptake assay, β -galactosidase assay and AFM analysis reveal that peptides adopted different modes of action through membrane perturbation. In contrast to the lipopeptides composed of alpha and *E*-vinyllogous γ -amino acids, the second series of lipopeptides composed of 1:1 α - and saturated γ -amino acids showed better antimicrobial properties with less haemolytic activity. In the third series, the amphiphilic helical peptides were designed based on the single crystal conformation of α , α , γ -hybrid peptide 10/12-helices to mimic the structural and functional properties of natural helical antibiotic magainin and LL37. As predicted, the 2D NMR (TOCSY and NOESY) experiments reveal that the α,α,γ -hybrid peptides adopted 10/12-helical conformations of in SDS. Similar to the lipopeptides, these α,α,γ -helical peptides displayed potent broad spectrum antimicrobial activity across the panel of Gram positive, Gram negative bacteria including MRSA. The mode of action suggests that they not only inhibit the bacterial growth through membrane depolarisation but also showed their ability to bind DNA. These results suggest the dual mode of action of hybrid helical peptides. Overall, this study underlines the potential of α,γ -hybrid peptides in the development of next generation antimicrobial therapeutics.

Publications

1. A facile synthesis and crystallographic analysis of *N*-protected β -amino alcohols and short peptaibols. Sandip V. Jadhav, Anupam Bandyopadhyay, **Sushil N. Benke**, Sachitanand M. Mali and Hosahudya N. Gopi, *Org. Biomol. Chem.*, 2011,9 4182-4187.
2. Self-Assembly to Function: Design, Synthesis, and Broad Spectrum Antimicrobial Properties of Short Hybrid *E*-Vinylogous Lipopeptides S. Shiva Shankar, **Sushil N. Benke**, Narem Nagendra, Prabhakar Lal Srivastava, Hirekodathakallu V. Thulasiram, and Hosahudya N. Gopi. *J. Med. Chem.*, 2013, 56, 8468-8474.
3. Engineering polypeptide folding through trans double bonds: transformation of miniature β -meanders to hybrid helices. Mothukuri Ganesh Kumar, **Sushil N. Benke**, K. Muruga Poopathi Raja and Hosahudya N. Gopi. *Chem commun.*, 2015, 51, 13397-13399 .
4. Potent Antimicrobial activity of Lipidated Short α , γ -hybrid peptides. **Sushil N. Benke**, H. V. Thulasiram and H. N. Gopi. *ChemMedChem* 2017, 12, 1610-1615.
5. Novel γ -amino acids for the design of Hybrid peptide foldamers. **Sushil N. Benke** and H. N. Gopi. (Manuscript Submitted)
6. Foldamer antibiotics: Design, Structure and Potent Antimicrobial Activity of α,α,γ -hybrid helices. **Sushil N. Benke**, Mothukuri G. K., Shiva Shankar, G. George, S. S. Ragothama, H. V. Thulsiram, and H. N. Gopi. (Manuscript Submitted)

Chapter 1

Antimicrobial peptides

1.1 Antibiotics

Twentieth century has seen the rise of antibiotics as an indispensable weapon in the battle against the microorganisms. Antibiotics are medicines obtained from microorganisms that inhibit the growth of or destroy harmful microorganisms.¹ They have been useful tools to ward off deadly infections since 1940. The various classes of antibiotics are shown in Figure 1.1. Antibiotics have been instrumental not only in saving patients lives but also in achieving major advances in medicine and surgery.² They have successfully been used to treat various infections occurring in patients undergoing chemotherapy, patients having chronic diseases such as rheumatoid arthritis, kidney related diseases and diabetes.³

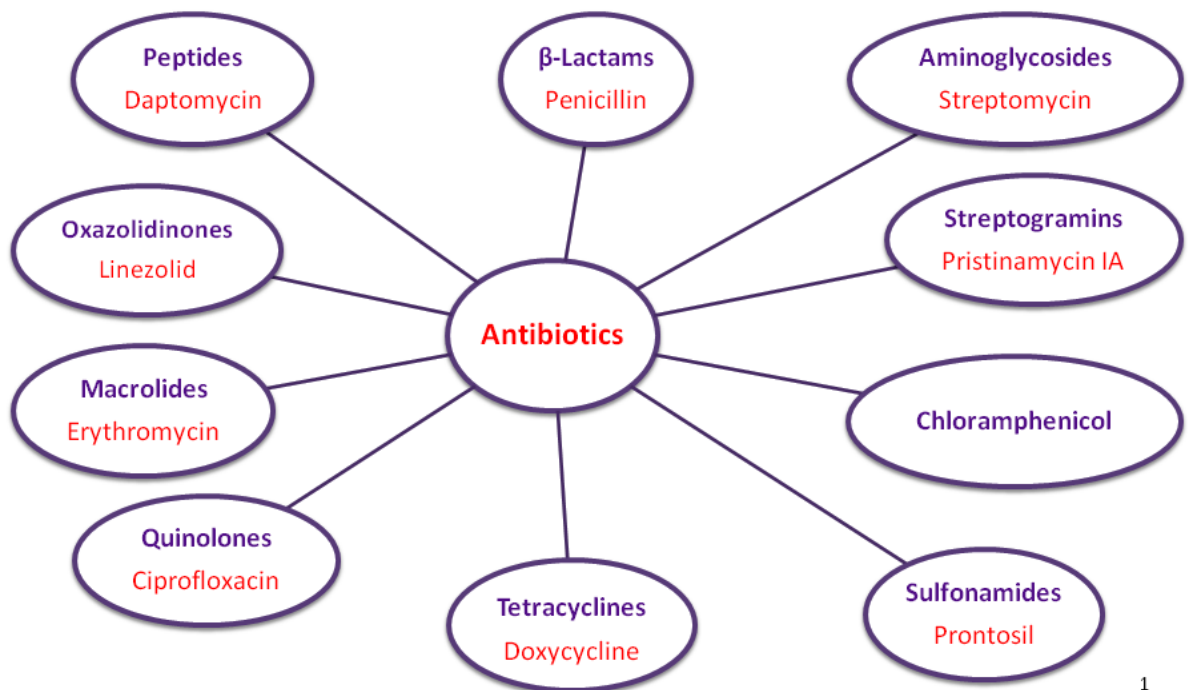


Figure 1.1. Classes of antibiotics with examples.

Also, antibiotics have been used extensively during organ transplants, joint replacements or cardiac surgery to ward off microbial infections. Overall use of antibiotics has resulted in extension of expected life spans worldwide.⁴

In developing countries, antibiotics have been crucial in improvement of the quality of the public health as antibiotics decrease the morbidity caused by food-borne as well as water-borne diseases and helped in avoiding sanitation related pandemics.^{3c} Lately, the antibiotics have lost their efficacy due to rapid emergence in antimicrobial resistance.

1.1.1 Antimicrobial resistance

The bacteria once exposed to an antibiotic, start evolving through mutation. It changes the physiological pathways the antibiotic attacks. The mutation renders the evolved strain of bacteria resistant towards the antibiotics.⁵ It was first observed in the case of Penicillin in the year 1943. Since then, antibiotic resistance has been detected for almost all the antibiotics introduced. In the beginning, it used to take 10-15 years for bacteria to become resistant to an antibiotic, but if we look at the development after 1980, it is observed that the response time is drastically reduced to 1-1.5 years.^{3b} In some cases, the resistance was observed in the same year the antibiotic was introduced. The timeline of antibiotic resistance developments for various antibiotics is showed in Figure 1.2.

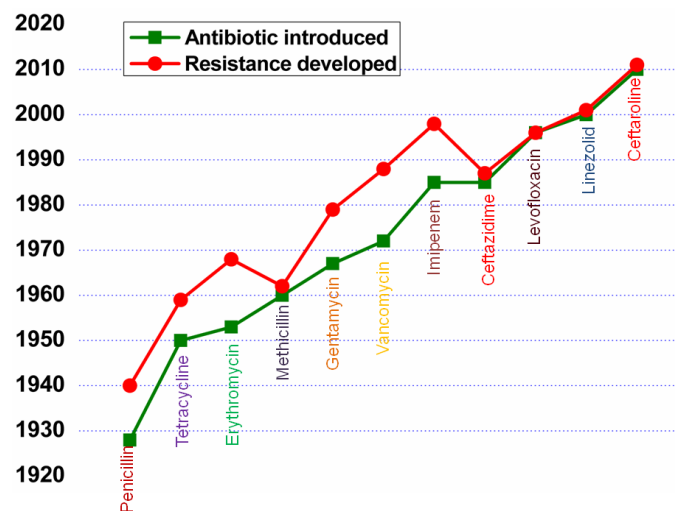


Figure 1.2. Timeline showing the emergence of antibiotic resistance.

1.1.2 Strategy against the antibiotic resistance crisis

Antibiotic resistance is increasing at alarming rate. Hence, there is urgent need for development of new class of antibiotics which would offer better and more sustainable alternative. Most of the antibiotics in use are either derived from natural substances produced by bacteria or fungi or modified analogues of these natural substances which show amplified activity.^{2a} Antimicrobial peptides are constituents of the innate immunity system and are ubiquitously found in almost all life forms.⁶

As the need for alternatives for antibiotics become pressing, antimicrobial peptides (AMP) both natural and synthetic, have emerged as a sustainable alternative in the battle against antibiotic resistance.

1.1.3 Antimicrobial peptides (AMP's)

Antimicrobial peptides (AMP's) are generally 10-50 amino acid long amphipathic peptides, carry a net positive charge more than 2 and have ~50% hydrophobic amino acids.⁶ AMP's represent a highly conserved part of innate immune system and they are present widespread in all plant and animal kingdoms. They are also called as Host defence peptides (HDP). They are ubiquitous in nature and a variety of AMP's are found in wide variety of living organisms such as bacteria, invertebrates, vertebrates and plants.⁷ The AMP's act through a different mechanism than that of antibiotics. They disrupt the microbial cellular membrane leading to the death of the microorganisms.⁸ The activity of the AMP's is due to their amphipathic design and the diverse AMP's can be classified on the basis of their secondary structure in various classes.

1.1.3.1 Classification of AMP's

The rich diversity of the antimicrobial peptides makes it difficult to categorize them. But the various AMP's adopt different secondary structures and can be classified into different classes such as linear, helical, β -sheet, cyclic or mixed peptides.⁹ The classes of AMP's based on secondary structure are described as below.

1.1.3.1.1 Linear Peptides

The linear AMP's do not fold into a regular secondary structure unless they come in contact with the hydrophobic bacterial membranes. The length of the peptide can vary from 6-40 residues and often contain high proportions of certain amino acids such as Arg, Trp or Pro. These are amphipathic peptides with balanced hydrophobicity and cationicity. They not only disrupt the membrane but also interact with intracellular proteins. Tryptophan rich Indolicidin obtained from cow,¹⁰ Proline-Arginine rich PR39 obtained from pig,¹¹ Apidaecin from honeybee,¹² Histatin 5 from humans¹³ fall into this category. They adopt α -helical secondary structure once they are exposed to the bacterial membrane.

1.1.3.1.2 Helical peptides

Cationic amphipathic helical peptides constitute a large class of AMP's which is extensively studied. The hydrophobic residues and cationic residues are evenly distributed along the axis of α -helix to attain amphipathicity. On the surface of the microbial membrane, the peptides form clusters around the Ca^{2+} binding sites and traverse through the microbial cellular membrane and eventually disrupts it. Silk moth's cecropin¹⁴ and African clawed frog's Magainin,¹⁵ Alamethicin,¹⁶ human AMP LL-37,¹⁷ synthetic peptide pexiganan,¹⁸ Buforin II obtained from vertebrates¹⁹ fall into this

category. Zasloff *et. al.* have studied the magainins extensively.²⁰ α -helical peptides serve as a template to design new synthetic antimicrobial peptides.

1.1.3.1.3 β -Sheet peptides

This class of AMP's consists of defence miniproteins and several β -hairpin peptides. They not only disrupt the bacterial cell membrane but also have been found to inhibit DNA, RNA and protein synthesis. The peptides disrupt the bacterial membranes by Toroidal pore formation. The β -sheet structures are stabilised by disulfide bridges (one, two or more) between the Cys residues.²¹ Human β -defensin-3 is a large 45 residues containing peptide containing three stranded antiparallel β -sheet. Human defensins,²² insect defensins²³ bovine lactoferricin,²⁴ Protegrin I²⁵ are β sheet AMP's.

1.1.3.1.4 Macrocyclic peptides

Circulin A and B are macrocyclic peptides (30 amino acid long) derived from plants of *Rubiaceae* family which show potent antimicrobial activity.²⁶ The cyclic backbone confers high rigidity to the structure of the peptides.

1.1.3.1.5 Lipopeptides

Lipopeptides are produced only in bacteria and fungi during cultivation.²⁷ They consist of a short linear or cyclic peptide sequence, to which a long chain fatty acid is covalently attached at the N-terminus. Lipopeptides display antibacterial as well as antifungal activity.²⁸ They can be cationic (e.g. Polymyxin)²⁹ as well as anionic (e.g. Daptomycin).³⁰ Lipopeptides tend to self aggregate on the bacterial membrane surface and disrupt the membrane through carpet mechanism. Unfortunately, native lipopeptides are non cell selective and therefore toxic to mammalian cells as well.

Although the antimicrobial peptides show rich diversity in structure, they have been found to act through the common mechanism of action i.e. disruption of cellular membrane.

1.1.3.2 Mechanism of action of AMP's

The AMP's carry out irreversible damage to the bacterial membrane by disturbing it. This can be achieved in various ways. Also, they are found to enter the microbial cell and disturb various intracellular functions leading to cell death. Hence, the antimicrobial peptides show dual mechanism of action. They act on membrane of the bacteria as well as on the intracellular targets. AMP's take advantage of their amphipathic design for interaction with the membrane. It is discussed in details below.

1.1.3.2.1 Membrane disruption

The antimicrobial peptides selectively target the bacterial cell membrane in contrast to the membranes of cells of plants and animals due to the difference in the membrane design.³¹ The interaction of antimicrobial peptide with the membrane of erythrocyte and bacterial cell membrane is shown in Figure 1.3. The outer layer of the bacterial cell membrane is heavily populated with negatively charged phospholipids. Hence, the cationic AMP's strongly interact with the bacterial membrane. Whereas, the outer membrane of plant and animal cells is neutral as the negatively charged head groups are projected inside the bilayer and not exposed on the surface. Also, the cholesterol present in animal cells stabilises the lipid bilayer and reduces the activity of antimicrobial peptide.³² The electrostatic interaction between the cationic residue of the antimicrobial peptide and the negative phospholipids in the bacterial outer membrane facilitate the action of AMP. Many hypotheses have been presented for the mechanism of killing of microbes by AMP, which include: depolarisation of normally energised membrane

leading to death of microbe,³³ the leaking of cellular contents due to disruption of membrane,³⁴ the damaging of intracellular targets by peptide after internalization,³⁵ induction of hydrolases leading to destruction of cell wall,³⁶ the change in lipid orientation in the membrane resulting in disturbance in normal membrane function.³²

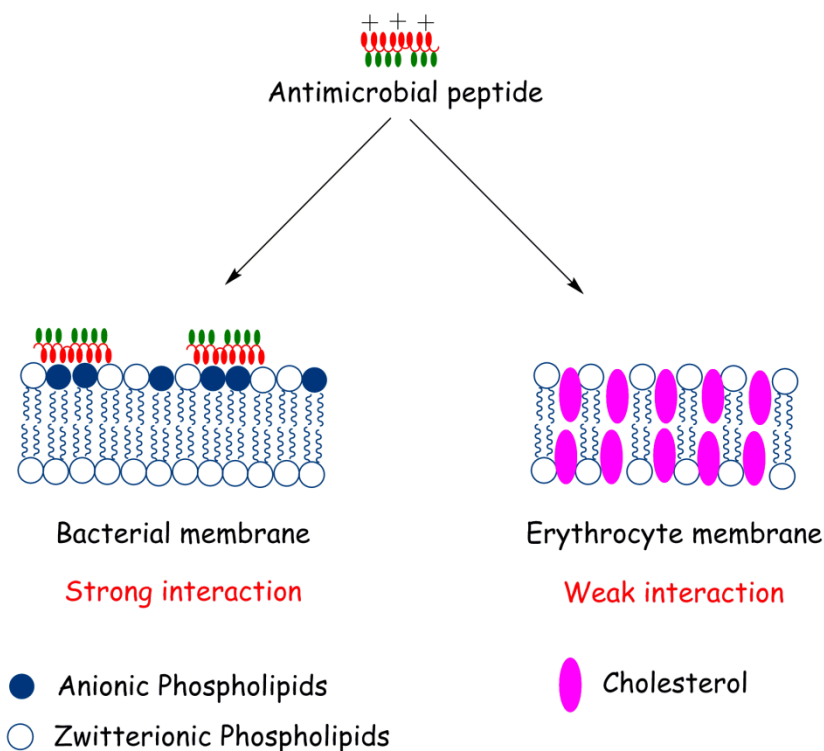


Figure 1.3. Specificity in action of AMP's against membrane of animal cells versus bacterial cells.

Different AMP's have different mode of action of membrane disruption. Various models of the mechanism of action of AMP are discussed as follows.

1.1.3.2.1.1 Barrel stave model

The α -helical antimicrobial peptides align themselves on the bacterial membrane perpendicularly. Peptide helices come together to form bundles which then get inserted into the membrane by forming a pore.

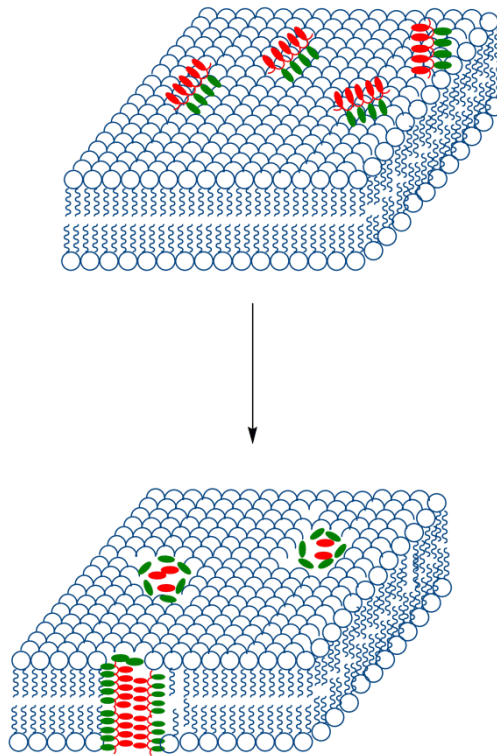


Figure 1.4. Barrel stave model of action of AMP.

The pore looks like a barrel made up of helical peptides which act as staves. The hydrophobic residues of the peptide align with the lipid core region of the membrane and the cationic residues are projected towards the interior of the pore.³⁷ Alamethicin acts through barrel stave model. 3-11 helices of Alamethicin come together to form the transmembrane pore.³⁸ Barrel formation leads to disturbance of membrane potential leading to collapse of membrane as well as initiates leakage of the intracellular contents resulting in cell death. The process is depicted in Figure 1.4.

1.1.3.2.1.2 Carpet model

In the carpet model, the peptides accumulate on the membrane surface and orient themselves parallel to the surface. The cationic residues of the peptides facilitate the interaction of the peptide with the negative phospholipid headgroups through electrostatic

attraction. The peptides interact at the numerous sites on the membrane and cover the membrane in a carpet like manner.

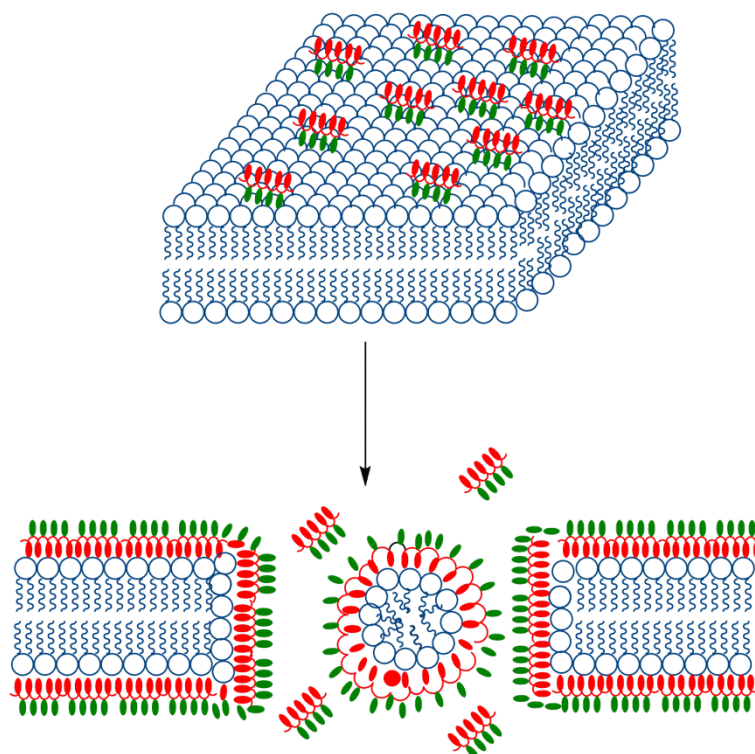


Figure 1.5. Carpet model of AMP action.

A threshold concentration of peptide is reached on the surface after which the surface oriented peptides are thought to act on the lipid bilayer of the membrane in a detergent like manner resulting in its disruption.³⁹ Finally, the membrane disintegrates and forms micelles leading to the collapse of the bilayer curvature. Lipopeptides act through the carpet mechanism. The process is shown in Figure 1.5.

1.1.3.2.1.3 Toroidal pore model

In this mode of action, the antimicrobial helical peptides aggregate on the outer surface and induce the lipid monolayers of the membrane to bend continuously through the pore. Due to this bending of lipid monolayer, the water core is lined by both the inserted peptides and lipid headgroups.

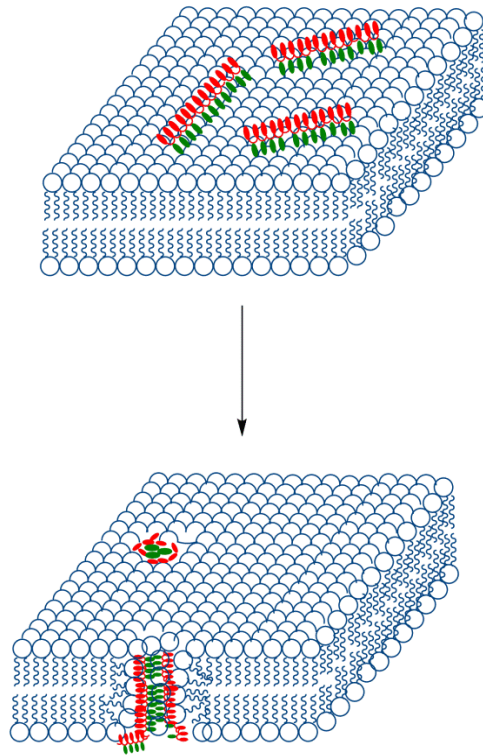


Figure 1.6. Toroidal pore model of AMP action.

The Toroidal pore model differs from the barrel stave model as the peptides are always associated with the lipid headgroups even when the peptides are perpendicularly inserted into the membrane. The cellular contents leak out the pore leading to the death of the microbe.⁴⁰ Magainins, protegrins and mellitin act on the membrane through Toroidal pore formation.⁴¹ The mechanism of Toroidal pore formation is shown in Figure 1.6. Apart from disrupting the membrane, some AMP's also bind to the intracellular targets leading to the death of microorganism.

1.1.3.2.2 Intracellular targets of antimicrobial peptides

Although the membrane disruption eventually leads to the lysis of the microbial cells, other mechanisms of action of AMP have also been speculated. AMP's have been found to act on various intracellular targets which are summarised in Figure 1.7. Non membrane external targets such as autolysins are activated by antimicrobial peptides.⁴²

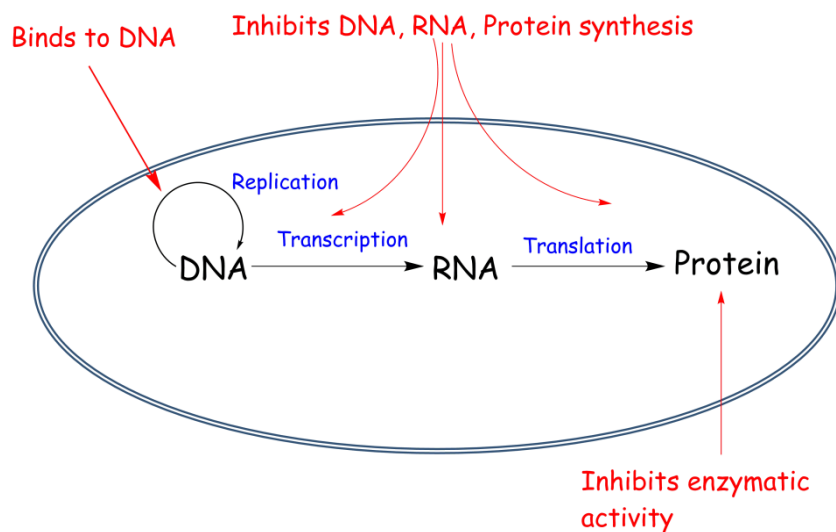


Figure 1.7. Intracellular targets of antimicrobial peptides.

Mersadicin inhibits the cell wall synthesis by combining with lipid II.⁴³ Histatins enter the cytoplasm and induce the non lytic loss of ATP from actively respiring cells resulting in disruption of the cell cycle.⁴⁴ Pyrrocoricin, Apidaecin have been found to bind specifically to DnaK, a heat shock protein.⁴⁵ PR-39 induces filamentation of *S. typhimurium* resulting in elongation of cells due to which the cells are unable to undergo cell division.⁴⁶ It also stops protein synthesis and induces degradation of some proteins required for DNA replication. Buforin II⁴⁷ and tachyplesin⁴⁸ bind to the DNA and RNA and alter the protein synthesis. Due to dual mode of action, AMP's are able to kill various bacteria in very short amount of time. For last two decades, large numbers of peptides have been explored for their ability as therapeutics against microbial infections.

1.1.4 AMP's as therapeutics

Antimicrobial peptides are in early stage of development as potential drug candidates and few AMP's have entered clinical trials, fewer have been approved as drug candidates.⁴⁹ Vancomycin and Teicoplanin are glycopeptides antibiotics which are used

as injectables.⁵⁰ The lipopeptides Polymyxin B and colistin have been extensively used for topical therapy but they are found to be cytotoxic. Hence, they can't be used as injectables.⁵¹ Although, colistin is used with Gentamycin and tobramycin in the form of aerosol to treat *P. aeruginosa* lung infections in patients suffering from cystic fibrosis. Nisin has entered early clinical trials and it can be administered orally to treat the gastrointestinal infections caused by *Helicobacter pylori*. Also, Telavancin, Dalbavancin and Oritavancin are new glycopeptides approved by FDA for treatment of skin and soft tissue infections.⁵²

Although, the number of antimicrobial peptides entering the antibiotic research pipeline is increasing, very few have been approved so far for clinical use. This is because of the inherent limitations of peptides such as poor bioavailability, protease instability.

1.1.5 Drawbacks of AMP's

Although the antimicrobial peptides have proved useful to treat microbial infections, they suffer from major drawbacks such as lack of selectivity, proteolytic instability and poor bioavailability. Various proteases attack the amide backbone of the peptides and cleave them into smaller pieces which no longer retain the activity. Hence, the AMP's have low serum stability. Backbone modification has been found out to be excellent strategy to increase the stability of peptides against proteases and several attempts have been documented in the literature in this regard.⁵²

1.2 Antimicrobial peptidomimetics

Naturally occurring antimicrobial peptides are susceptible to proteolytic degradation resulting in low bioavailability. In this regard, peptidomimetics offer better alternatives in

terms of activity and stability. Various attempts have been reported in the literature to mimic the antimicrobial peptides.⁵³ They are discussed as follows.

1.2.1 Foldamers

Significant attention has been paid over the past several decades on polypeptides composed of α -amino acids, with natural proteins and the use of stereochemically constrained amino acids and templates in the design of folded polypeptides. The success of this endeavor has also been applied to the design of well-defined secondary structures from the oligomers of non-biological amino acids such as β - and γ -amino acid templates.⁵⁴ The term “foldamers” was first introduced by Prof. Samuel H. Gellman, he propose that foldamer is “any polymer with strong tendency to adopt a specific compact conformation”.^{54c} A variety of foldamers that mimic the protein secondary structures have been designed using various organic templates and non-natural amino acids and their antimicrobial properties are studied. A few of them are discussed as follows.

1.2.1.1 β -peptides

β -Amino acid containing peptides are known to fold into turns, helices and sheet-like structures, similar to secondary structures of proteins.

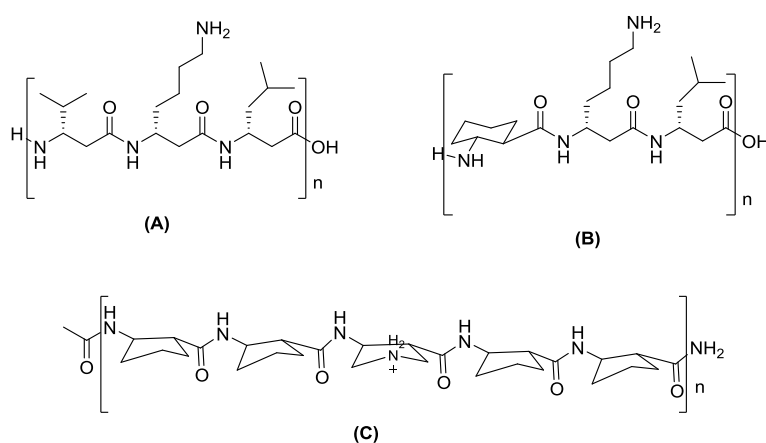


Figure 1.8. Amphipathic β -peptide helices. (A)⁵⁵ (B)^{56a} (C)^{56c}

Also, the unnatural β -peptide backbone makes them protease resistant as compared to the α -amino acid backbone.^{54j} β -peptides have been tested against various microorganisms and they have shown potent activity. DeGrado *et al.* demonstrated the design of amphipathic β -peptide helices which showed potent activity against *Escherichia coli*.⁵⁵ (Figure 1.8 A)

Besides their enormous contribution to the design of various foldamers composed of different types of β - and γ -amino acids, Gellman *et al.*⁵⁶ have extensively studied the antimicrobial activity of β -peptides and α/β - mixed peptides. In continuation, Schweizer *et al.*⁵⁷ studied cationic lipo β -peptides for their antibacterial activity and found that they work better than lipo α -peptides.

1.2.1.2 Nylon-3 polymers

In addition to the β - and α,β -hybrid peptide foldamers, Gellman *et al.*⁵⁸ also investigated the action of nylon-3 polymers (hybrid β -peptide polymers) active against the drug resistant *Candida albicans* biofilms. The antifungal nylon-3 polymers contain the cationic subunit β NM and the hydrophobic subunit CH in varying proportions. (Figure 1.9)

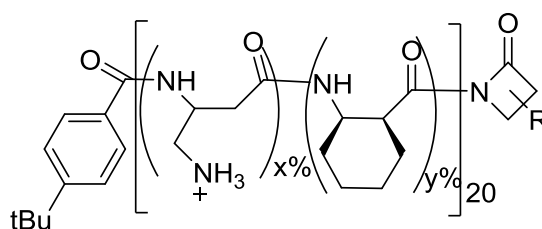


Figure 1.9 Structures of nylon-3 β NM:CH copolymers⁵⁸

1.2.1.3 Cyclic peptides

Alternative strategy to synthesize antimicrobial peptides involves cyclization. Cyclic peptides are stable against proteases. Daptomycin is a naturally occurring lipodepsipeptide recently approved by the Food and Drug Administration for use. It is used for the treatment of complicated skin and skin structure infections caused by several gram-positive bacteria. It acts through a calcium ion dependent pathway that helps to interact with phosphatidylglycerol (PG) of the bacterial membrane resulting in disruption of membrane.⁵⁹

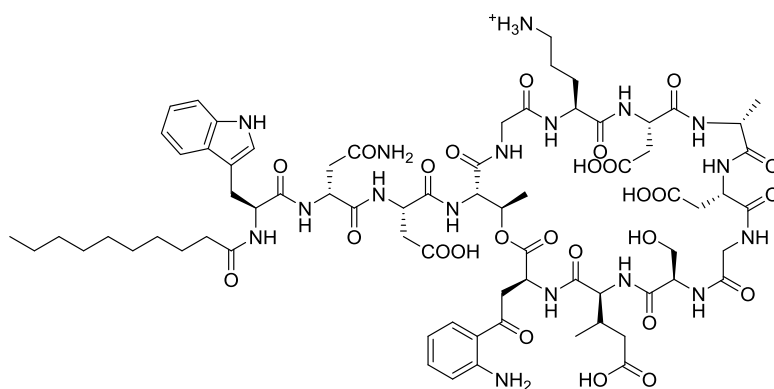


Figure 1.10 Structure of Daptomycin.

Various attempts have been reported to prepare cyclic peptides composed of alternating D and L α -amino acids. Gadhiri and co-workers have prepared a library of cyclic hexa and octapeptides and tested them against *S. aureus* and other gram positive strains.⁶⁰ Their study indicated that the cyclic cationic peptides show promising activity *in vitro* as well as *in vivo* and they can be considered as promising candidates for systemic administration and treatment of otherwise antibiotic resistant infections. Shai *et. al.*⁶¹ have reported that substitution of L-amino acid with D-amino acid in short antimicrobial lipopeptides which results in controlled enzymatic degradation.

1.2.1.4 Peptoids

Another strategy to stabilise the peptide structure involve methylation of backbone amide leading to formation of peptoids. Various peptoid building blocks are shown in Figure 1.11. Barron *et. al.* have reported broad spectrum antimicrobial activity of short alkylated peptoid mimics of antimicrobial peptides.⁶² They have also reported the helical “ampetoids” (antimicrobial peptoid oligomers) with micro molar antimicrobial activity.⁶³

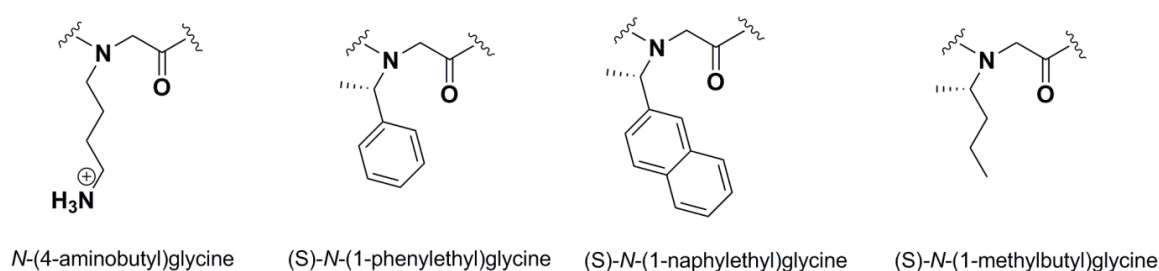


Figure 1.11 Various peptoid monomers used for antimicrobial peptoid construction.

Haldar *et al.* have investigated the small molecular antibacterial peptoids mimics which exhibit high potency against various Gram positive, Gram negative and drug resistant bacteria.⁶⁴

1.2.1.5 α -AA peptides

Cai *et al.* have extensively studied the α -AA peptides for their antimicrobial properties.⁶⁵ They tested linear, lipidated and cyclic α -AA peptides for antimicrobial activity. Short lipidated α -AA peptides showed broad spectrum activity against the Gram positive, Gram negative bacteria and fungi. Their activity was found to be comparable with the synthetic peptide pexiganan.

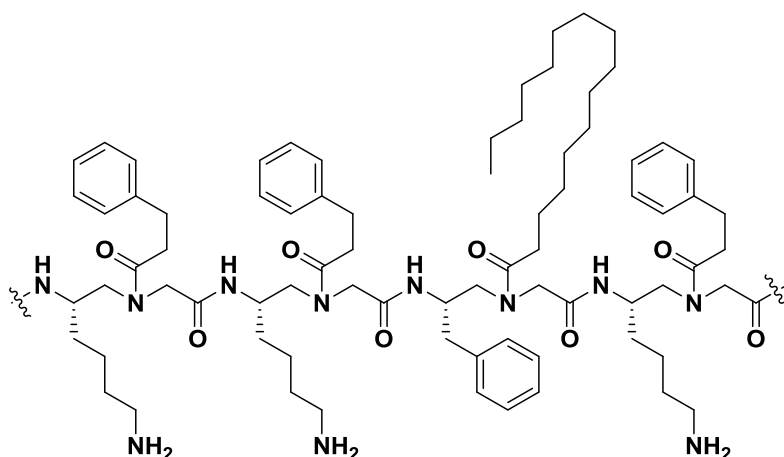


Figure 1.12 α -AA antimicrobial peptides.

1.2.1.6 γ -amino acid containing peptidomimetics

Our lab is involved in the synthesis of various gamma amino acids and their utility for building new functional peptidomimetics. We have demonstrated the successful incorporation of various γ -amino acids in secondary structural peptidomimetics such as α -helix, β -sheet, β -hairpin.⁶⁶ (Figure 1.13) Also, the preliminary protease studies suggested that the γ -amino acids containing peptides are more stable against proteases as compared to natural peptides. γ -amino acids have not been utilised in the design of antimicrobial peptidomimetics due to difficulty in obtaining stereochemically pure building block. Our group has established a convenient synthetic strategy to obtain γ -amino acids. In this regard, we designed two classes of antimicrobial peptidomimetics- lipopeptides and helical peptides and evaluated their antimicrobial activity. We also established the mechanism of action of the γ -amino acid containing antimicrobial peptidomimetics.

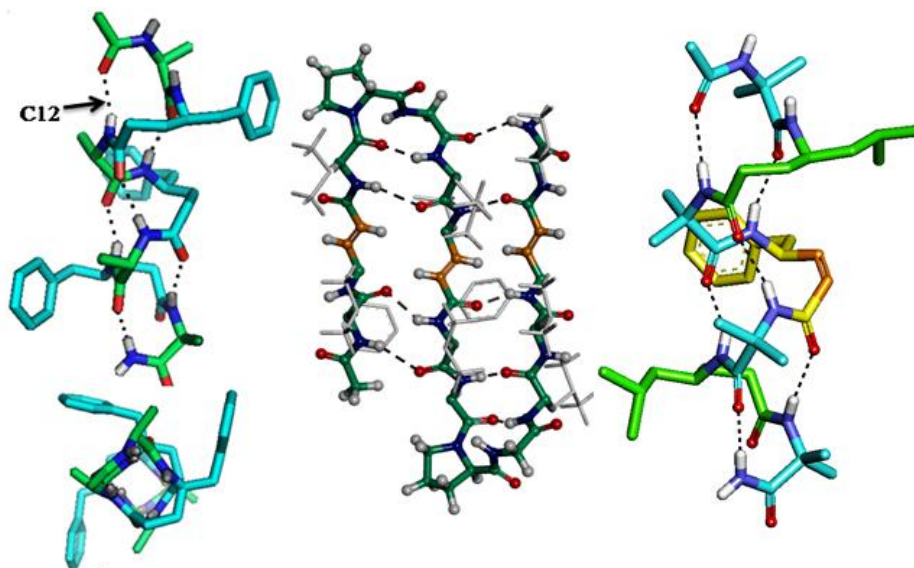


Figure 1.13: X-ray structures of helices and stranded β -sheets designed from the hybrid peptides composed of various types of γ -amino acids.

1.3 References

1. a) Zaffiri, L.; Gardner, J.; Toledo- Pereyra, L.H. *J. Investig. Surg.* **2012**, *25*, 67–77. b) Sengupta, S.; Chattopadhyay, M.; Grossart, H. *Front Microbiol*, **2013**, *4*, 47, 1-13.
2. a) Ventola, C. L. *Pharm. & Ther.*, **2015**, *40*, 277-283. b) Gould, I. M.; Bal, A. M. *Virulence*, **2013**, *4*, 185-191.
3. a) Wright, G. D. *Can. J. Microbiol.* **2014**, *60*, 147-154. b) Centres for disease control and prevention, office of infectious disease. Antibiotic resistant threats in the United states , 2013. April 2013. Available at: <http://www.cdc.gov/drugresistance/thret-report-2013>. c) Rossolini, G. M.; Arena, F.; Pecile, P.; Pollini, S. *Clin. Opin. Pharmacol.* **2014**, *18*, 56-60.
4. Piddock, L. J. *Lancet. Infect. Dis.* **2012**, *12*, 249-253.
5. Read, A. F.; Woods, R. J. *Evol. Med. Public Health* **2014**, *1*, 1-147.

6. a) Zasloff, M. *Nature*, **2002**, *415*, 389-395. b) Nakatsuji, T.; Gallo, R. L. *J. Investig. Dermat.* **2012**, *132*, 887-895. c) Hancock, R. E. W.; Brown, K. L.; Mookherjee, N. *Immunobiol.* **2006**, *211*, 315-322. d) Bulet, P.; Stocklin, R.; Menin, L. *Immunol. Rev.*, **2004**, *198*, 169-184.
7. a) Boman, H. G. *Annu. Rev. Immunol.* **1995**, *13*, 61-92. b) Nicolas, P.; Mor, A. *Annu. Rev. Microbiol.* **1995**, *49*, 277-304. c) Hancock, R. E. W.; Chapple, D. S. *Antimicrob. Agents. Chemother.* **1999**, *43*, 1317-1323. d) Hancock, R. E. W. Falla, T.; Brown, M. H. *Adv. Microb. Physiol.* **1995**, *37*, 135-175. e) Lehrer, R. I. *Nature Rev. Microbiol.* **2004**, *2*, 727-738. f) Brogden, K. A.; Ackermann, M.; McCray, P. B.; Tach, B. F. *Int. J. Atimicrob. Agents* **2003**, *22*, 465-478. g) Selsted, M.E.; Brown, D.M.; Delange, R.J.; Lehrer, R.I. *J. Biol. Chem.* **1983**, *258*, 4485-4489.
8. a) Shai, Y. *Biochim. Biophys. Acta.* **1999**, *1462*, 55-70. b) Saberwal, G.; Nagaraj, R. *Biochim. Biophys. Acta.* **1994**, *1197*, 109-131.
9. a) Zelezetsky, I.; Tossi, A. *Biochim. Biophys. Acta.* **2006**, *1758*, 1436-1449. b) Nguyen, L. T.; Haney, E. F.; Vogel, H. J. *Trends in Biotechnol.* **2011**, *29*, 464-472. c) Epand, R. M.; Vogel, H. J. *Biochim. Biophys. Acta.* **1999**, *1462*, 11-28. d) Hancock, R. E. W.; Chapple, D. S. *Antimicrob. Agents. Chemother.* **1999**, *43*, 1317-1323.
10. Selsted, M. E.; Novtny, M. J.; Morris, W. L.; Tang, Y. Q.; Smith, W.; Cullor, J. *S. J. Biol. Chem.* **1992**, *267*, 4292-4295.
11. Agerberth, B.; Lee, J. Y.; Bergman, T.; Carlquist, M.; Boman, H. G.; Mutt, V.; Jornvall, H. *Eur J. Biochem.* **1991**, *202*, 849-854.
12. Boman, H. G. *Annu. Rev. Immunol.* **1995**, *13*, 61-92.
13. Kavanagh, K.; Dowd, S. *J. Pharm. Pharmacol.* **2004**, *56*, 285-289.

14. Steiner, H.; Hultmark, D.; Engstrom, A.; Bennich, H.; Boman, H. G. *Nature* **1981**, 292, 246-268.
15. Zasloff, M. *Proc. Natl. Acad. Sci. USA* **1987**, 84, 5449-5453.
16. a) Sansom, M. S. P. *Prog. Biophys. Mol. Biol.* **1991**, 55, 139-235. b) Spaar, A.; Munster, C.; Salditt, T. *Biophys. J.* **2004**, 87, 9800-9812.
17. a) Oren, Z.; Lerman, J. C.; Gudmundsson, G. H.; Agerberth, B.; Shai, Y. *Biochem. J.* **1999**, 341, 501-513. b) Soehnlein, O. *J. Mol. Med.* **2009**, 87, 1157-1164. c) Mendez-Samperio, P. *Peptides*, **2010**, 31, 1791-1798.
18. Ge, Y.; MacDonald, D. L.; Holroyd, K. J.; Thornsberrry, C.; Wexler, H.; Zasloff, M. *Antimicrob. Agents. Chemother.* **1999**, 43, 782-788.
19. a) Kim, H. S.; Yoon, H. Minn, I.; Park, C. B.; Lee, W. T.; Zasloff, M.; Kim, S. C. *J. Immunol.* **2000**, 165, 3268-3274. b) Kobayashi, S.; Chikushi, A.; Tougu, S.; Imura, Y.; Nishida, M.; Yano, Y.; Matsuzaki, K. *Biochemistry*, **2004**, 43, 15610-15616.
20. a) Wang, G.; Li, X.; Zasloff, M. *Adv. in Mol. Cell. Microb.* **2010**, 18, 1-21. b) Zasloff, M. *Proc. Natl. Acad. Sci. USA* **1987**, 84, 5449-5453.
21. a) Srinivas, N.; Jetter, P.; Ueberbacher, B. J.; Werneburg, M.; Zerbe, K.; Steinmann, J.; Meijden, B. V.; Bernardini, F.; Lederer, A.; Dias, R. L. A.; Misson, P. E.; Henze, H.; Zumbunn, J.; Gombert, F. O.; Obrecht, D.; Hunziker, P.; Schauer, S.; Ziegler, U.; Käch, A.; Eberl, L.; Riedel, K.; DeMarco, S. J.; Robinson, J. A. *Science*, **2010**, 327, 1010-1013. b) Dimarcq, J.-L.; Bulet, P.; Hetru, C.; Hoffmann, J. *Pep. Sci.* **1998**, 47, 465-477. c) Zhu, S. *Molecular Immunology*, **2008**, 45, 828-838. c) Dassanayake, R.S.; Gunawardene, Y.; Tobe, S.S. *Peptides* **2007**, 28, 62-75.

22. a) Selsted, M. E.; Harwig, S. S.; Ganz, T.; Schilling, J. W.; Lehrer, R. I. *J. Clin. Invest.* **1985**, *76*, 1436-1439. b) Ganz, T.; Lehrer, R. I. *Curr. Opin. Hematol.* **1997**, *4*, 53-58. b) Ganz, T.; Selsted, M. E.; Szklarek, D.; Harwig, S. S. L.; Daher, K.; Bainton, D. F.; Lehrer, R. I. *J. Clin. Invest.* **1985**, *76*, 1427–1435.
23. Ravi, C.; Jeyashree, A.; Renuka Devi, K. *Res. In Biotech.* **2011**, *2*, 1–7.
24. Odell, E. W.; Sarra, R.; Foxworthy, M.; Chapple, D. S.; Evans, R. W. *FEBS Lett.* **1996**, *382*, 175-178.
25. Bolintineanu, D.S.; Kaznessis, Y.N. *Peptides*, **2011**, *32*, 188–201.
26. Tam, J. P.; Lu, Y. A.; Yang, J. L.; Chiu, K. W.; *Proc. Natl. Acad. Sci. USA* **1999**, *96*, 8913-8918.
27. a) Balkovec, J. *Exp. Opin. Investig. Drugs.* **1994**, *3*, 65-82. b) De Lucca, A. J.; Walsh, T. J. *Antimicrob. Agents. Chemother.* **1999**, *43*, 1-11.
28. a) Denning, D. W. *J. Antimicrob. Chemother.* **2002**, *49*, 889-891. b) Denning, D. W. *J. Antimicrob. Chemother.* **1997**, *40*, 611-614. c) Avrahami, D.; Shai, Y. *J. Biol. Chem.* **2004**, *279*, 12277-12285. d) Avrahami, D.; Shai, Y. *Biochemistry*, **2003**, *42*, 14946-14956. e) Horn, J. N.; Romo, T. D.; Grossfield, A. *Biochemistry* **2013**, *52*, 5604-5610.
29. a) Hancock, R. E. W.; Chapple, D. S. *Antimicrob. Agents. Chemother.* **1999**, *43*, 1317-1323. b) Storm, D. R.; Rosenthal, K. S.; Swanson, P. E. *Annu. Rev. Biochem.* **1977**, *46*, 723-763. c) Teuber, M.; Bader, J.; *Antimicrob. Agents. Chemother.* **1976**, *9*, 26-35.
30. a) Straus, S. K.; Hancock, R. E. W. *Biochim. Biophys. Acta.* **2006**, *1758*, 1215-1223. b) Steenbergen, J. N.; Alder, J.; Thorne, G. M.; Tally, F. P. *J. Antimicrob. Chemother.* **2005**, *55*, 283-288.
31. Zasloff, M. *Nature*, **2002**, *415*, 389-395.

32. Matsuzaki, K. *Biochim. Biophys. Acta.* **1999**, *1462*, 1-10.
33. Westerhoff, H. V.; Juretic, D.; Hendler, R. W.; Zasloff, M. *Proct. Natl. Acad. Sci. USA* **1989**, *86*, 6597-6601.
34. a) Yang, L.; Weiss, T. M.; Lehrer, R. I.; Huang, H. W. *Biophys. J.* **2000**, *79*, 2002-2009. b) Brogden, K. A.; De Lucca, A. J.; Bland, J.; Elliot, S. *Proct. Natl. Acad. Sci. USA* **1996**, *93*, 412-416.
35. Kragol, G.; Lovas, S.; Varadi, G.; Condie, B. A.; Hoffmann, R.; Otvos, L. *Biochemistry* **2001**, *40*, 3016-3026.
36. Bierbaum, G.; Sahl, H.-G. *Arch. Microbial.* **1985**, *141*, 249-254.
37. a) Oren, Z.; Shai, Y. *Biopolymers*, **1998**, *47*, 451-463. b) Christensen, B.; Fink, J.; Merrifield, R. B.; Mauzerall, D. *Proc. Natl. Acad. Sci. USA* **1988**, *85*, 5072-5076. c) Westerhoff, H. V.; Juretic, D.; Hendler, R. W.; Zasloff, M. *Proc. Natl. Acad. Sci. USA* **1989**, *86*, 6597-6601. d) Duclohier, H.; Molle, G.; Spach, G. *Biophys. J.* **1989**, *56*, 1017-1021. e) Matsuzaki, K.; Harada, M.; Funakoshi, S.; Fujii, N.; Miyajima, K. *Biochim. Biophys. Acta* **1991**, *1063*, 162-170.
38. a) Bechinger, B. *Biochim. Biophys. Acta.* **1999**, *1462*, 157-183. b) Yang, L.; Harroun, T. A.; Weiss, T. M.; Ding, L.; Huang, H. W. *Biophys. J.* **2001**, *81*, 1475-1485.
39. a) Pouny, Y.; Rapaport, D.; Mor, A.; Nicolas, P.; Shai, Y. *Biochemistry* **1992**, *31*, 12416-12423. b) Gazit, E.; Boman, A.; Boman, H. G.; Shai, Y. *Biochemistry*, **1995**, *34*, 11479-11488. c) Shai, Y. *Trends Biochim. Sci.* **1995**, *20*, 460-464. d) Naito, A. Nagao, T.; Norisada, K.; Mizuno, T.; Tuzi, S.; Saitô, H. *Biophys. J.* **2000**, *78*, 2405-2417. e) Wong, H.; Bowie, J. H.; Carver, J. A. *Eur. J. Biochim.* **1997**, *247*, 545-557. f) Yamaguchi, S.; Huster, D.; Waring, A.; Lehrer, R. I.; Kearney, W.; Tack, B. F.; Hong, M. *Biophys. J.* **2001**, *81*, 2203-2214.

40. a) Huang, H. W. *Phys. Rev. Lett.* **2004**, 92, 1983041-1983044. b) Henzler, W. K. A.; Lee, D. K.; Ramamoorthy, A. *Biochemistry*, **2003**, 42, 6546-6558.
41. a) Yang, L.; Harroun, T. A.; Heller, W. T.; Weiss, T.M.; Huang, H. W. *Biophys. J.* **1998**, 75, 641-645. b) Yamaguchi. S.; Hong, T.; Waring, A.; Lehrer, R. I; Hong, M. *Biochemistry*, **2002**, 41, 9852-9862. c) Lee, M. T.; Chen, F.Y.; Huang, H. W. *Biochemistry*, **2004**, 43, 3590-3599.
42. Bierbaum, G.; Sahl, H. G. *J. Bacteriol.* **1987**, 169, 5452-5458.
43. Brotz, H.; Bierbaum, G.; Leopold, K.; Reynolds, P. E.; Sahl, H. G. *Antimicrob. Agents. Chemother.* **1998**, 42, 154-160.
44. Andreu, D.; Rivas, L. *Biopolymers* **1998**, 47, 415-433.
45. Otvás, L.; Rogers, M. E.; Consolvo, P. J.; Condie, B. A.; Lovas, S.; Bulet, P.; Blaszczyk-Thurin, M. *Biochemistry* **2000**, 39, 14150-14159.
46. Boman, H. G.; Agerberth, B.; Boman, A. *Infect. Immun.* **1993**, 61, 2978-2984.
47. Park, C. B.; Kim, H. S.; Kim, S. C. *Biochem. Biophys. Res. Commun.* **1998**, 244, 253-257.
48. Yonezawa, A.; Kuwahara, J.; Fujii, N.; Sugiura, Y. *Biochemistry*, **1992**, 31, 2998-3004.
49. Hancock, R. E. W. *Lancet*, **1997**, 349, 418-422.
50. Hancock, R. E. W.; Farmer, S. W. *Antimicrob. Agents. Chemother.* **1993**, 37, 453-456.
51. a) Jensen, T.; Pedersen, S. S.; Garne, S.; Heilmann, C.; Høiby, N.; Koch, C. J. *J. Antimicrob. Chemother.* **1987**, 19, 831-838. b) Wright, W. W.; Welch, H. *Antibiot. Annu.* **1960**, 61-74.
52. Ventola, C. L. *Pharm. & Ther.*, **2015**, 40, 344-352.
53. Wade, D.; Englund, J. *Prot. Pep. Lett.*, **2002**, 9, 53-57.

54. a) Seebach, D.; Beck A. K.; Bierbaum, D. J. *Chem. Biodiv.*, **2004**, *1*, 1111-1239.
b) Seebach D.; Gardiner, J. *Acc. Chem. Res.*, **2008**, *41*, 1366-1375. c) Gellman, S. H. *Acc. Chem. Res.* **1998**, *31*, 173-180. d) Horne, W. S.; Gellmann, S. H. *Acc. Chem. Res.*, **2008**, *41*, 1399-1408. e) Vasudev, P. G.; Chatterjee, S.; Shamala N.; Balaram, P. *Chem. Rev.*, **2011**, *111*, 657-687. f) Martinek T. A.; Fulop, F. *Chem. Soc. Rev.* **2012**, *41*, 687-702. g) Hecht, S.; Huc, I. (Eds.), *Foldamers: Structure, Properties and Applications*, Wiley-VCH, Weinheim, 2007. h) Bouillère, F.; Thétiot-Laurent, S.; Kouklovsky, C.; Alezra, V. *Amino Acids* **2011**, *41*, 687-707
i) Goodman, C. M.; Choi, S.; Shandler, S.; DeGrado, W. F. *Nat. Chem. Biol.*, **2007**, *3*, 252-262. j) Hook, D. F.; Bindschadler, P.; Mahajan, Y. R.; Sebesta, R.; Kast, P.; Seebach, D. *Chem. Biodiv.* **2005**, *2*, 591 - 632.
55. a) Hamuro, Y.; Schneider, J. P.; DeGrado, W. F. *J. Am. Chem. Soc.* **1999**, *121*, 12200 - 12201. b) Liu, D.; DeGrado, W. F. *J. Am. Chem. Soc.* **2001**, *123*, 7553-7559.
56. a) Schmitt, M. A.; Weisblum, B.; Gellman, S. H. *J. Am. Chem. Soc.* **2007**, *129*, 417-428. b) Porter, E. A.; Wang, X.; Lee, H. S.; Weisblum, B.; Gellman, S. H. *Nature* **2000**, *404*, 565 - 565. c) Raguse, T. L.; Porter, E. A.; Weisblum, B.; Gellman, S. H. *J. Am. Chem. Soc.* **2002**, *124*, 12774 - 12785. d) Porter E. A.; Weisblum, B.; Gellman S.H. *J. Am. Chem. Soc.* **2002**, *124*, 7324-7330.
57. Serrano, G.; Zhanel, G.; Schweizer, F. *Antimicrob. Agents. Chemother.* **2009**, *53*, 2215-2217.
58. a) Liu, R.; Chen, X.; Falk, S. P.; Masters, K. S.; Weisblum, B.; Gellman, S. H. *J. Am. Chem. Soc.* **2015**, *137*, 2183. b) Chakraborty, S.; Liu, R.; Hayouka, Z.; Chen, X.; Ehrhardt, J.; Lu, Q.; Burke, E.; Yang, Y.; Weisblum, B.; Wong, G. C.; Masters, K. S.; Gellman, S. H. *J. Am. Chem. Soc.* **2014**, *136*, 14530.

59. Jeu, L.; Fung, H. B. *Clin. Ther.* **2004**, *26*, 1728–1757.
60. Dartois, V.; Ghadiri, M. R. *Antimicrob. Agents. Chemother.* **2005**, *49*, 3302–3310.
61. Makovitzki, A.; Avrahami, D.; Shai, Y. *Proc. Natl. Acad. Sci. USA* **2006**, *103*, 15997-16002.
62. Chongsiriwatana, N. P.; Miller, T. M.; Wetzler, M.; Vakulenko, S.; Karlsson, A. J.; Palecek, S. P.; Mobashery, S.; Barron A. E. *Antimicrob. Agents. Chemother.* **2011**, *55*, 417-420.
63. Chongsiriwatana, N. P.; Patch, J. A.; Czyzewski, A. M.; Dohm, M. T.; Ivankin, A.; Gidalevitz, D.; Zuckermann, R. N.; Barron, A. E. *Proc. Natl. Acad. Sci. USA* **2008**, *105*, 2794-2799.
64. a) Ghosh, C.; Konai, M. M.; Sarkar, P.; Samaddar, S. Haldar J. *ChemMedChem*, **2016**, *11*, 2376-2371. b) Ghosh, C.; Manjunath, G. B.; Akkapeddi, P.; Yarlagadda, V.; Hoque, J.; Uppu, D. S. S. M.; Konai, M. M.; Haldar, J. *J. Med. Chem.* **2014**, *57*, 1428–1436.
65. a) Hu, Y.; Amin, M. N.; Padhee, S.; Wang, R. E.; Qiao, Q.; Bai, G.; Li, Y.; Mathew, A.; Cao, C.; Cai J. *ACS Med. Chem. Lett.* **2012**, *3*, 683-686. b) Niu, Y.; Padhee, S.; Wu, H.; Bai, G.; Qiao, Q.; Hu, Y.; Harrington, L.; Burda, W. N.; Shaw, L. N.; Cao, C.; Cai J. *J. Med. Chem.* **2012**, *55*, 4003-4009.
66. a) Jadhav, S. V.; Bandyopadhyay, A.; Gopi, H. N. *Org. Biomol. Chem.* **2013**, *11*, 509-514. b) Bandyopadhyay, A.; Jadhav, S. V.; Gopi H. N. *Chem. Commun.* **2012**, *48*, 7170-7172. c) Misra, R.; Saseendran, A.; George, G.; Veeresh, K.; Raja, K. M. P.; Raghothama, S.; Hofmann, H. -J.; Gopi, H. N. *Chem. Eur. J.* **2017**, *23*, 3764 – 3772. d) Ganesh Kumar, M.; Thombare, V. J.; Katariya, M. M.; Veeresh, K.; Raja, K. M. P.; Gopi, H. N. *Angew. Chem. Int. Ed.* **2016**, *55*, 7847-7851.

Chapter 2

Design, Synthesis and Broad Spectrum Antimicrobial Properties of Short Hybrid *E*-Vinyllogous Lipopeptides

2.1 Introduction

As a consequence of evolution, a large number of bacterial and fungal strains have developed resistance towards the conventional antibiotics, creating an urgent need for the design of new antibiotics with different mode of action. Indeed an overwhelming body of literature over the past several years demonstrated that naturally occurring antimicrobial peptides (AMPs) are evolutionary conserved components of the innate immune response capable of targeting wide range of “multidrug resistant” strains.¹ However, potential therapeutic applications of AMPs have been suffering with several inherent problems including selectivity, toxicity and bioavailability. In this regard, various approaches have been adopted to mimic the cationic and amphiphilic nature of natural AMPs including synthetic peptides,² β -peptides,³ peptoids,^{4, 5} polypyridines,⁶ polynorboranes,⁷ polysaccharides,⁸ peptidopolysaccharides,⁹ and so on. Lipopeptides are a recently emerged class of AMPs and the broad spectrum of natural lipopeptides has paved way for the development of new class of synthetic analogues.¹⁰ Most of the native lipopeptides isolated from bacteria and fungi are non-specific and highly toxic. However, after the approval of drug daptomycin as a potential chemotherapeutic agent for the treatment of skin infections, these lipopeptides have attracted considerable attention of medicinal chemists.¹¹ Previous studies of many natural and synthetic hybrid lipopeptides revealed that the antimicrobial activity of lipopeptides mainly depends on the sequence of peptides, length of fatty acid chain and overall hydrophobicity of the peptides.¹² These lipopeptides permeate rapidly and disintegrate the membrane morphology of pathogens.¹³ In addition to this, many *N*-terminal fatty acid acylated amphiphilic peptides are self-assembled into cylindrical nanofibers with diameters ranging from nanometers to micrometers, lead to the formation of hydrogels, nanotubes, nanobelts and nanoribbons.¹⁴ Various strategies have been employed in the designing of peptides that can undergo

self-assembly in response to environmental and chemical stimuli, including ionic strength, temperature, pH, and also by enzymes.

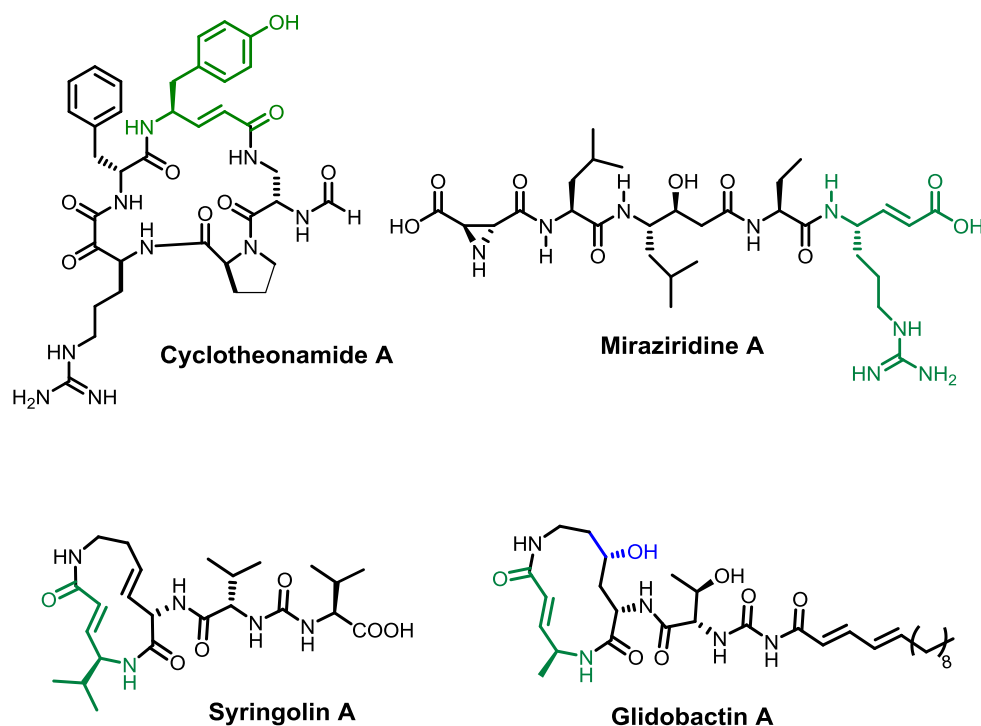


Figure 2.1: Peptide natural products containing *E*-vinylogous amino acids.

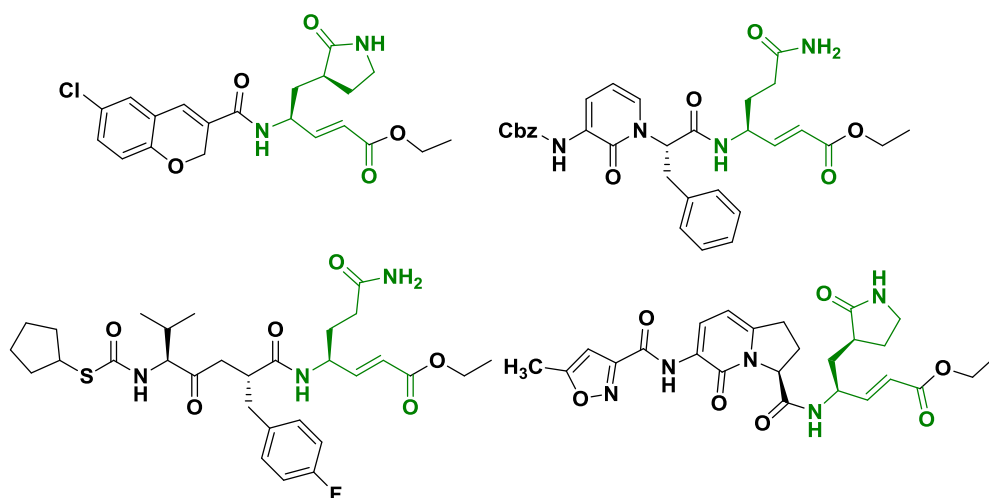


Figure 2.2. Synthetic peptides contained *E*-vinylogous amino acid residues used for various protease inhibitors.

The applications of self-assembled nanostructures of amphiphilic peptide based materials have been found in various fields like bone regeneration and enamel formation.¹⁶

α , β -Unsaturated γ -amino acids (*E*-vinylogous amino acids) are important components of many biologically active peptides¹⁷ and also have been used as potential candidates for design of inhibitors of serine and cysteine protease.¹⁸ Some of the naturally occurring antibiotics containing *E*-vinylogous amino acids as well as biologically active synthetic peptides containing *E*-vinylogous amino acids are shown in the Figure 2.1 and 2.2. Natural products Cyclotheonamide (A, B, C, D, E) have been shown act as inhibitors for serine proteases.¹⁹ Gallinamide A has shown a potent anti-malarial activity.²⁰ Miraziridine A is a natural cyclic peptide that inhibits variety of proteases like trypsin-like protease, papain-like cysteine protease and pepsin-like aspartyl protease.²¹

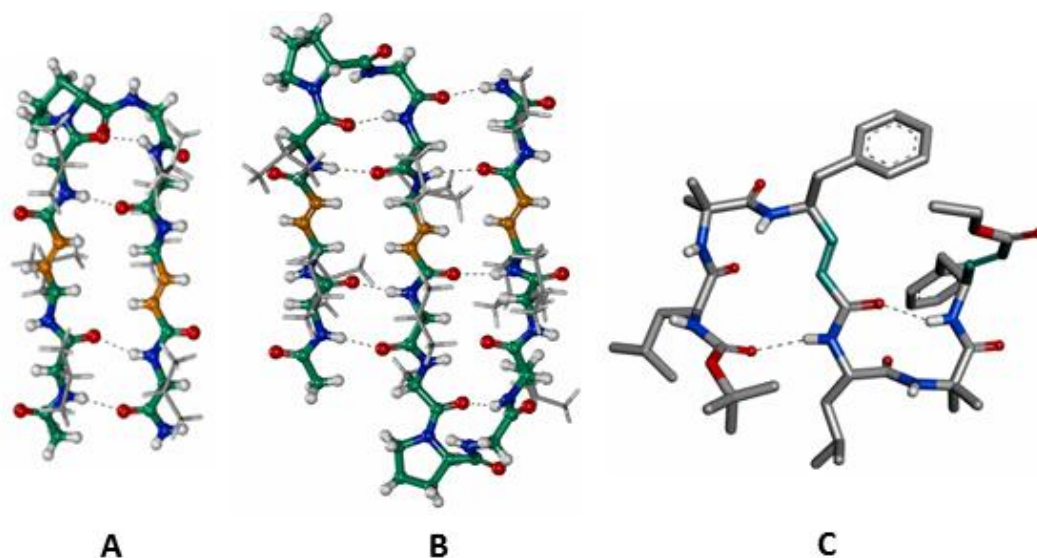


Figure 2.3: X-ray structures of (A) β -Hairpin, (B) Three-stranded β -sheet and (C) miniature β -meander from hybrid peptides composed of *E*-vinylogous residues.

Both syringolins and glidobactins have shown 20s proteasome inhibition activity.²² These excellent biological activity and natural occurrence of vinylogous amino acid

residues motivated many synthetic chemists to design peptide inhibitors against serine and cysteine proteases.²³

In their preliminary work, Schneider and colleagues demonstrated the extended conformations of *E*-vinylogous dipeptides.²⁴ Using extensive *ab initio* theoretical calculations Hofmann and colleagues predicted a variety of helical conformations from *E*-vinylogous amino acid oligomers.²⁵ In addition, Chakraborty *et al.* demonstrated the utility of *E*-vinylogous amino acids as β -turn inducers.²⁶ We have been interested in the synthesis and conformational analysis of hybrid peptides containing *E*-vinylogous amino acids. The structural analysis of the *E*-vinylogous amino acids in hybrid peptides reveal that due to the geometrical constraints of the double bonds they prefer to adopt extended β -sheet type of structures.^{27, 28} By exploiting the geometrical constraints of *E*-vinylogous amino acid residues we have designed β -hairpins,²⁹ three-stranded β -sheets³⁰ and miniature β -meander³¹ type supersecondary structure mimetics and studied their conformations in single crystals. Some of these X-ray structures are shown in the Figure 2.3. Besides using *E*-vinylogous amino acids as β -sheet inducing templates, we also explored them as Michael acceptors to derive β -substituted γ -amino acids and their utility in the foldamers design.³²⁻³⁴

2.2 Aim and rational of the present work

As *E*-vinylogous amino acids promote β -sheet type structures, we sought to explore the antimicrobial properties of short hybrid lipopeptides containing geometrically constrained *E*-vinylogous amino acids. In this Chapter, we are reporting the design, antimicrobial activities, self-assembling properties and the mode of action of short 1:1 alternating alpha and *E*-vinylogous hybrid lipopeptides. Systematic investigation of the mode of action reveals that the nature of the self-assemblies of these hybrid lipopeptides

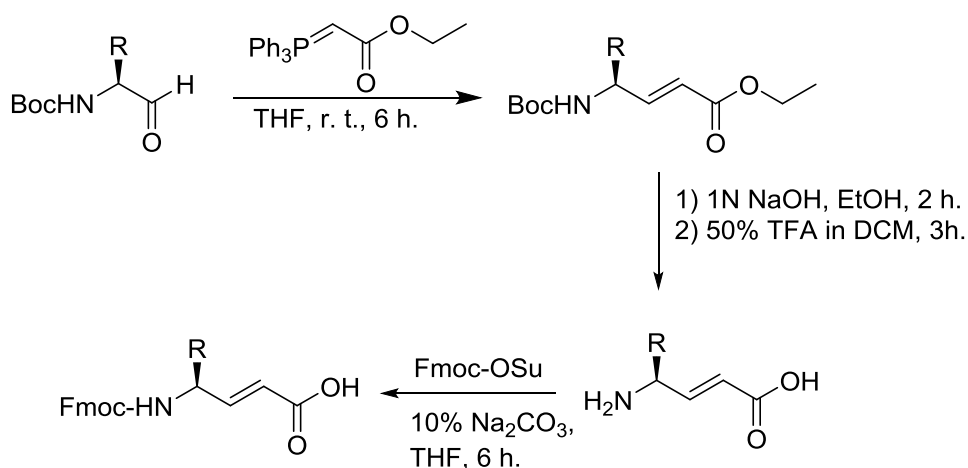
plays a crucial role in their antimicrobial activities and the mechanism of action. The self-assembly properties associated with the mode of action can be controlled by tuning the hydrophobic threshold of lipopeptides.

2.3 Results and Discussion

2.3.1 Synthesis of monomers

Synthesis of ethyl ester of Boc-protected α , β -unsaturated γ - amino acids:

We have synthesized (*E*)- α , β -unsaturated γ -amino esters through Wittig reaction starting from α -amino aldehydes as reported earlier.²⁸ The schematic representation of the synthesis of *E*-vinylogous amino esters is shown in Scheme 2.1.



R =	-CH ₃	-CH(CH ₃) ₂	-CH ₂ -CH(CH ₃) ₂	-CH ₂ -C ₆ H ₅	-CH ₂ -C ₆ H ₄ - OBu ^t
dg amino acid	dgAla	dgVal	dgLeu	dgPhe	dgTyr(OBu ^t)

Scheme 2.1: Schematic representation of the synthesis of Fmoc- α , β -unsaturated γ - amino acids

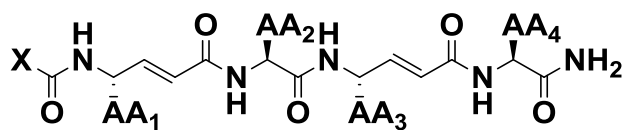
The Boc-amino aldehyde was synthesized from the LAH (Lithium aluminium hydride) reduction of the corresponding Weinreb amide and subjected immediately to the Wittig reaction. The Wittig products were isolated in excellent yields after column purification. To obtain solid phase compatible Fmoc- protected *E*-vinylogous amino acids, ethyl ester

of the Boc-protected amino acids were subjected to saponification using 1N NaOH in ethanol and Boc- group was deprotected using 50% TFA in DCM. The free amino acid was finally protected with Fmoc- group, purified through column chromatography and used for solid phase synthesis.

2.3.2 Design, synthesis and purification of lipopeptides

In order to understand their antimicrobial activity, we designed two series of short hybrid *E*-vinyllogous lipopeptides containing C₁₂ and C₈ fatty acids. The schematic representation of the short hybrid lipopeptides is shown in Table 2.1.

The design is based on the analysis of the natural lipopeptides which generally constitute equal proportions of hydrophobic and hydrophilic residues. The α -amino acids were chosen to be hydrophilic residues (Lysine, Arginine) while *E*-vinyllogous amino acids as hydrophobic residues in short tetrapeptide sequences. All *E*-vinyllogous amino acids were synthesized using Wittig reaction as reported earlier.^{27, 28} All peptides were synthesized by solid phase method on Knorr amide resin and purified through reverse phase HPLC on C₁₈ column. Based on the reverse phase HPLC retention time the order of hydrophobicity of the lipopeptides was found to be **S7> S1>S11> S3> S10>S8> S5> S2> S6> S4> S9**.

Table 2.1: List of α,γ -hybrid vinylogous lipopeptides

Peptide	X	AA1	AA2	AA3	AA4	t_R (min)
S1	C ₁₁ H ₂₃	dgAla	Lys	dgAla	Lys	41.14
S2	C ₇ H ₁₅	dgAla	Lys	dgAla	Lys	31.96
S3	C ₁₁ H ₂₃	dgTyr	Lys	dgTyr	Lys	38.61
S4	C ₇ H ₁₅	dgTyr	Lys	dgTyr	Lys	30.65
S5	C ₁₁ H ₂₃	dgAla	Arg	dgAla	Arg	33.30
S6	C ₇ H ₁₅	dgAla	Arg	dgAla	Arg	31.63
S7	C ₁₁ H ₂₃	dgPhe	Lys	dgPhe	Lys	48.19
S8	C ₇ H ₁₅	dgPhe	Lys	dgPhe	Lys	35.60
S9	C ₇ H ₁₅	dgLeu	Lys	dgVal	Lys	37.50
S10	CH ₃	dgPhe	Lys	dgPhe	Lys	25.25
S11	C ₇ H ₁₅	Leu	Lys	Val	Lys	39.22

2.3.3 Antimicrobial activity

All *E*-vinylogous hybrid peptides with N-terminal C₁₂ fatty acid (**S1**, **S3**, **S5**, and **S7**) and C₈ fatty acid (**S2**, **S4**, **S6**, **S8**, **S9**, **S10**) along with α -peptide control **S11** were subjected to

antimicrobial studies. Instructively, except **S7**, all peptides with C₁₂ fatty acids, displayed potent antimicrobial activity with various gram-negative and gram-positive bacterial strains as well as various fungal strains.

Table 2.2: MICs of vinylogous hybrid lipopeptides (µg/mL)

Microorganisms	S1	S2	S3	S4	S5	S6	S7	S8	S9	S10	S11
<i>Escherichia coli</i>	6.25	>100	6.25	25	12.5	>100	25	1.56	12.5	>100	>100
<i>Escherichia coli</i> <i>K12</i>	6.25	>100	6.25	25	12.5	>100	25	1.56	-	>100	>100
<i>Klebsiella pneumoniae</i>	3.12	>100	3.12	50	6.25	>100	25	3.12	25	>100	>100
<i>Pseudomonas aeruginosa</i>	6.25	>100	3.12	50	3.12	>100	25	3.12	50	>100	>100
<i>Staphylococcus aureus</i>	6.25	>100	3.12	50	6.25	>100	25	3.12	50	>100	>100
<i>Salmonella typhimurium</i>	6.25	>100	3.12	50	3.12	>100	25	3.12	50	>100	>100
<i>Candida albicans</i>	3.12	>100	1.56	12.5	3.12	>100	3.12	3.12	25	>100	>100
<i>Candida glabrata</i>	6.25	50	3.12	25	6.25	>100	6.25	3.12	50	>100	>100
<i>Cryptococcus neoformans</i>	6.25	>100	6.25	25	12.5	>100	6.25	3.12	6.25	>100	>100
<i>Saccharomyces cerevisiae</i>	3.12	>100	3.12	12.5	3.12	>100	6.25	3.12	50	>100	>100
Hemolytic HD₁₀	48	58	2.5	54	22	52	<1.56	16	Nil-	-Nil-	-Nil-

Among all lipopeptides in the series of C₈ fatty acid containing hybrid peptides, **S8** displayed potent activity against all bacterial and fungal strains while moderate activities were observed for **S4** and **S9**. The MIC values of all the peptides are given in the Table 2.2. Similar MIC values of the individual peptides against Gram-positive, Gram-negative

and fungal strains suggest the unique mode of action of these lipopeptides. Peptides which showed strong inhibitory action against bacteria also displayed the strong inhibitory action against fungi (**S1**, **S3**, **S5** and **S8**). In comparison with **S7**, **S3** containing phenolic –OH groups displayed excellent antimicrobial activity. Interestingly, **S8** showed more potent activity than **S7**, while **S4** showed lower potency than that of the C₁₂ analogue **S3**. In order to understand the role of basic residues, we replaced Lys with Arg in the peptides **S5** and **S6**. Results reveal that the peptides containing Arg also displayed similar antimicrobial activities. Further the control peptides, protected with acetyl group (**S10**) and the α -peptide with C₈ fatty acid (**S11**) showed no activity even at higher concentration. These results suggest that *E*-vinylogous hybrid peptides can be used as potential antimicrobial candidates compared to that of α -peptide counterparts. In addition, the antimicrobial activity further depends on the side-chains of amino acids as well as length of the fatty acids. The disparity in the antimicrobial activity of these hybrid lipopeptides can be directly correlated with their hydrophobicity. All active peptides showing similar MIC values promoted us to probe the plausible mechanism of action of these lipopeptides.

2.3.4 Hemolytic activity

The encouraging results of the antimicrobial activities of these peptides inspired us to subject them for hemolytic activity. Results of the hemolytic activities are shown in Figure 2.4. Out of all the peptides tested, **S7** and **S3** (both highly hydrophobic) showed the highest hemolytic activity followed by **S8**. In contrast the highly potent antimicrobial peptide **S1** displayed comparatively lesser hemolytic activity. Other peptides which show poor activity against the bacteria and fungi have shown lesser hemolytic activity.

Analysis of these results reveals that peptides containing aromatic side chains have shown greater hemolytic activity

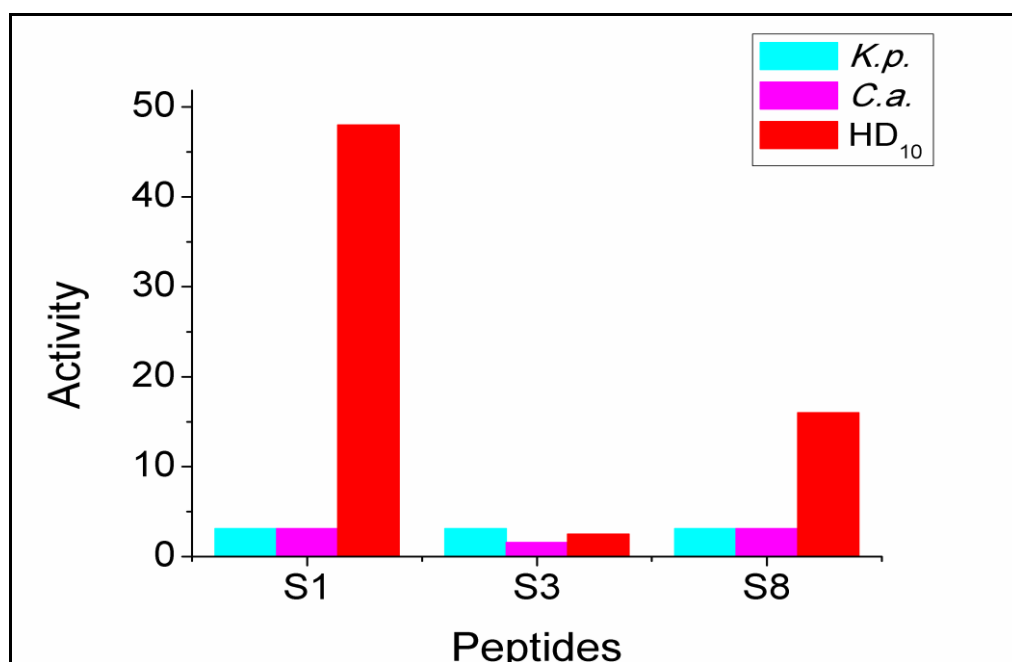


Figure 2.4. Comparison of MIC and hemolytic activity of hybrid lipopeptides **S1**, **S3** and **S8**.

than those containing aliphatic side chain amino acids. Even though **S1** is more hydrophobic than **S8**, it displayed lower hemolytic activity. Except **S3** and **S7** all other peptides which showed antimicrobial activities are non-hemolytic at their MICs. The specificity of the peptides **S1**, **S3** and **S8** is shown in Figure 2.4.

2.3.5 β -Galactosidase leakage assay

Further, to understand the mechanism of the action of these peptides on the inner cell membrane, we studied the enzyme β -galactosidase leakage assay³⁵ using peptides **S1**, **S3** and **S8** on *E.coli* (pUC19 plasmid transformed Top10 (Invitrogen) competent cells). The leakage of β -galactosidase (MW \approx 116kDa) from *E.coli* was used as an indicator of the disruption of the cytoplasmic membrane. β -Galactosidase release was measured using the initial velocity of the reaction by standard fluorogenic substrate. Results reveal very

intriguing information regarding the action of lipopeptides (Figure 2.5). No reaction of β -galactosidase with the

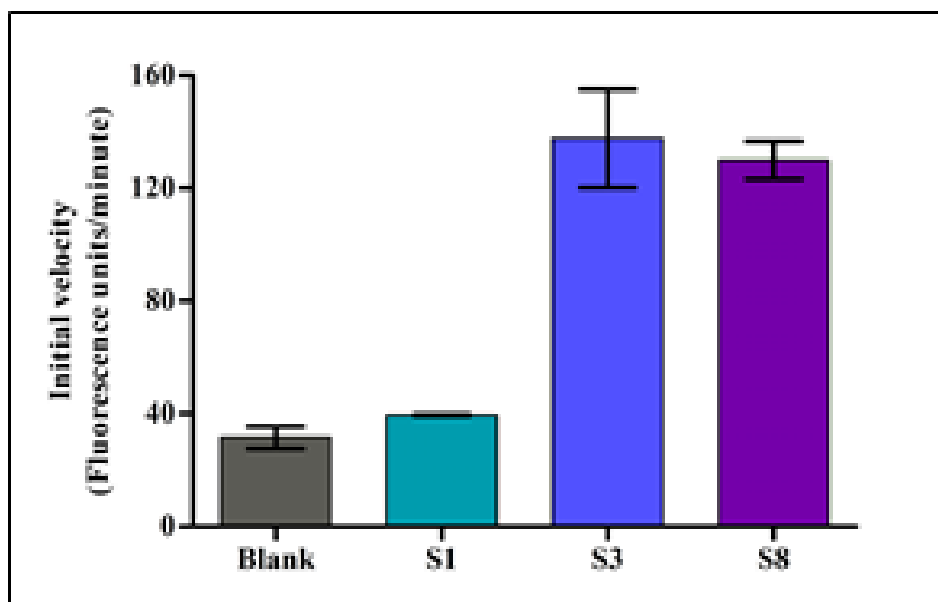


Figure 2.5. Peptide induced leakage of β -galactosidase from *Escherichia coli* Top10 (Invitrogen) cells. The graph represents relative amount of β -galactosidase present in the medium after treating with the peptides. Error bars are based on triplicate experiments for each peptide.

substrate observed in the case **S1** suggests that the peptide probably disrupts the outer cell membrane by binding through the negatively charged lipopolysaccharides. In contrast, **S3** and **S8** displayed equal amount of fluorescence intensity indicating the release of β -galactosidase upon the treatment of lipopeptides. This experiment suggests that these lipopeptides act on the cytoplasmic membrane and facilitate the release of β -galactosidase. Though the peptides **S1**, **S3** and **S8** display nearly similar MIC values, these results suggest their different mode of action.

2.3.6 Membrane deformation study

We further examine the membrane disruption of these peptides using atomic force microscopy (AFM). The images of *Escherichia coli* (*E. coli*) and fungus *Candida albicans*

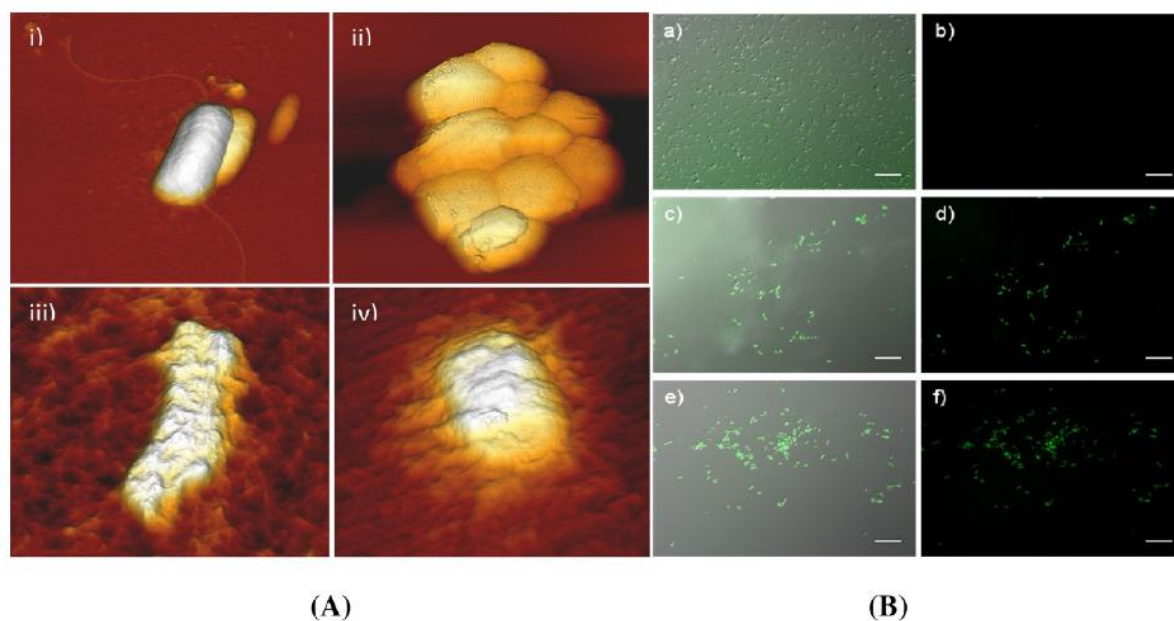


Figure 2.6 A) Atomic Force Microscopy images of *Escherichia coli* K12 (i) and *Candida albicans* (ii) before the treatment of lipopeptides, iii and iv after the treatment lipopeptide S1, respectively. B) Fluorescence images (FITC) of *E.coli* without peptides (a) and (b). Fluorescence images (FITC) of the *E. coli* after the treatment of S3 (c and d) and S8 (e and f) lipopeptides (Scale bar 10 μm).

(*C. albicans*) before and after the treatment of S1 lipopeptide obtained from AFM are shown in Figure 2.6A. The change in the morphology of both the organisms clearly indicates that the possible action of these peptides is through the disruption of cell membrane.

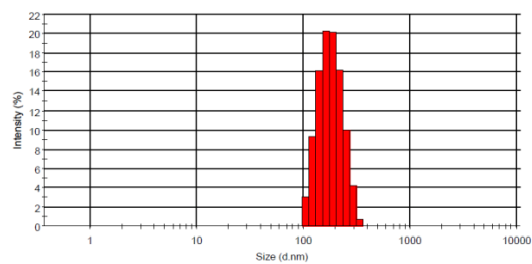
2.3.7 FITC uptake assay

Though the cell wall components are different for bacteria and fungi, the mode of action of these peptides indeed appears to be the perturbation of the cell membrane. We further validate the ability of cell membrane disruption by the lipopeptides using FITC (MW 389.4 Da) uptake assay using *E.coli*.³⁶ Since the entry of FITC requires significant membrane damage, the collapse of the transmembrane was studied using **S3** and **S8**. The fluorescent image of *E.coli* before and after the treatment of the lipopeptides is shown in Figure 2.6B. No fluorescence was observed in *E.coli* cells in the absence of hybrid peptides. The observed fluorescence behaviour of the cells suggests that lipopeptides render *E. coli* cells permeable to FITC.

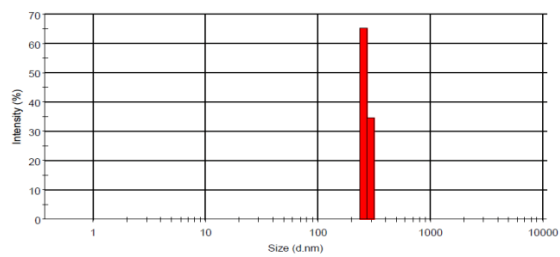
2.3.8 Dynamic light scattering studies

The disparity in the antimicrobial activities upon addition or truncation of N-terminal fatty acid between **S7** and **S8**, also the different mode of action between **S1**, **S3** and **S8** promoted us to speculate the role of self-organization of these lipopeptides. To address this possibility and gain further knowledge regarding their mode of action we analyzed the self-assembly patterns of lipopeptides in both solution and on the surface.

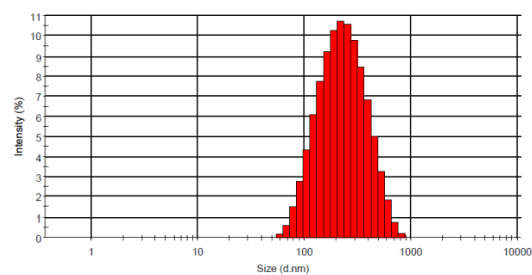
Dynamic light scattering experiments confirm that all lipopeptides undergo a spontaneous self-association to give nano-assemblies in solution. Mono dispersed self-assemblies of peptides shown in Figure 2.7. Intriguingly, the size of the mono dispersed self- assemblies are ranging from 124 to 950 nm. Lipopeptides **S1**, **S3**, **S7** and **S8** displayed



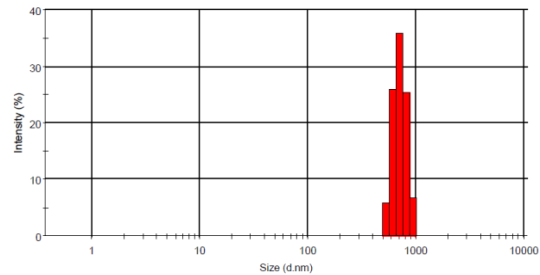
S1



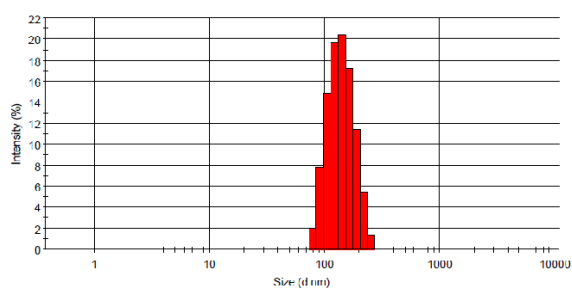
S2



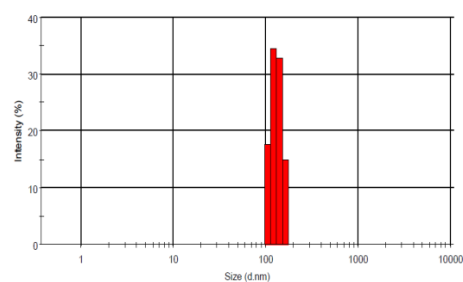
S3



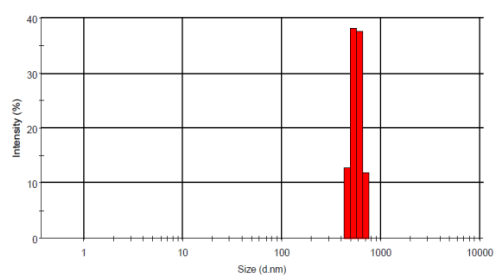
S4



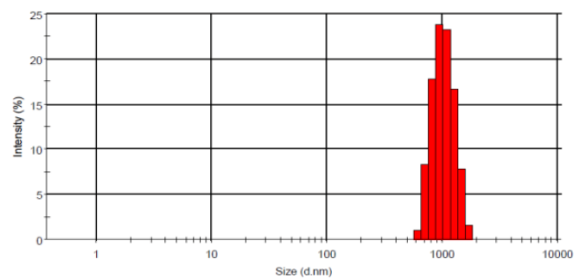
S5



S6



S7



S8

Figure 2.7: DLS histogram of S1, S2, S3, S4, S5, S6, S7 and S8 lipopeptides.

average size of the nano-assemblies 164 ± 12 , 220 ± 8 , 615 ± 20 and 950 ± 22 nm, respectively. Interestingly, the zeta-potential values of these self-assembled lipopeptides were found to be $+57\pm 5$, $+56\pm 5$, $+43\pm 4$ and $+48\pm 7$ respectively. The peptides with aromatic residues showed larger sized self-assemblies, while peptides with aliphatic amino acids displayed smaller sized nano-assemblies. Irrespective to the size of assembly, these peptides showed excellent surface potential charges.

2.3.9 Field emission scanning electron microscope analysis:

In order to understand the pattern of self-association, we subjected them to FE-SEM (Field Emission Scanning Electron Microscope) analysis. The FE-SEM images of **S1**, **S3**, **S5**, and **S8** are shown in Figure 2.8. Peptides **S1** and **S5** containing dehydro alanine (dgA) adopted nanofibers type of morphology similar to the amyloid fibrils.³⁷ Peptide **S3** and **S8** with aromatic amino acid side chains underwent diffusion limited aggregation, however, with a different morphology. Peptide **S3** was found to be composed of fractals with a needle shaped nano-structures. Ironically, **S8** displayed spectacular fractal trees similar to the polyelectrolyte complexes and peptide containing aromatic amino acids.³⁸⁻⁴⁰ Peptide **S7** display fractals different than that of **S8**. Though the higher concentrations are required for the SEM analysis, however, the different morphologies observed in the self-assembly of these hybrid lipopeptides partially explains the disparity in their biological activity. Even though electric potential of self-assemblies are very similar, substantial change in the self-assembly pattern is observed between the peptides **S1** and **S3**. The robust growth of fractals and needle shaped nano-structures from **S3** and **S8** may be influencing their antimicrobial and high hemolytic activities. As **S7** showed poor antimicrobial activity, we anticipate that this peptide might have adopted different mechanism from that of **S3** and **S8**. The low hydrophobicity and

low surface charges of **S2**, **S4** and **S6** is reflected in their poor antimicrobial and lower hemolytic activity values.

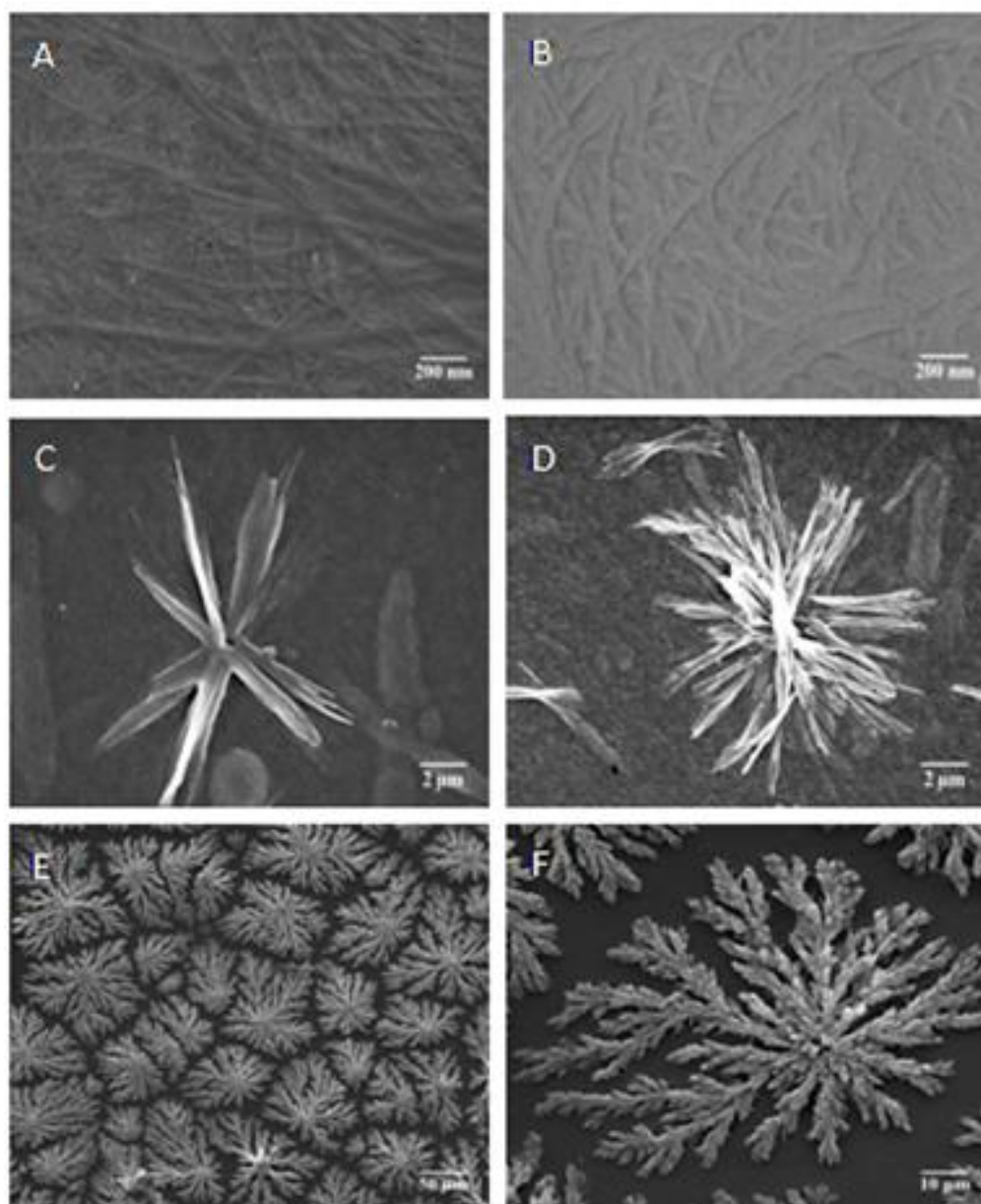


Figure 2.8: FE-SEM images of **S1** (A), **S5** (B), **S3** (C, D) and **S8** (E, F) hybrid lipopeptides.

2.4 Conclusion

We demonstrated the broad spectrum antimicrobial properties of short hybrid lipopeptides composed α - and *E*-vinylous amino acids. Due to their geometrical restriction of the

backbone double bonds, these short hybrid peptides showed highly potent antimicrobial activity compared to that of their α -peptide counterparts. In addition, hybrid peptides with C₁₂ and C₈ N-terminal fatty acids displayed better activity than the α - as well as β -lipopeptides containing C₁₆ fatty acid at the N-terminal.^{12c, 12d} The hybrid peptides with moderate hydrophobicity and high electrical potential of self-assemblies showed high antimicrobial and low hemolytic activities. These peptides may possibly bind to the negatively charged outer membrane of the microorganisms and affecting the transmembrane electric potential. The antimicrobial activity, the mode of action and the self-assembly patterns of these short *E*-vinylogous hybrid lipopeptides, particularly **S1** and **S8** provide unique opportunity to further design potent antimicrobial candidates as well as to explore their utility as smart biomaterials.

2.5 Experimental section

2.5.1 General experimental procedure

All amino acids, DCC, PPh₃ were purchased from Aldrich. The solvents THF, DCM, Toluene were purchased from Merck. Ethyl bromoacetate, di-tert-butyl dicarbonate, Fmoc-OSu were purchased from Spectrochem and used without further purification. Column chromatography was performed on Merck silica gel (100-200 mesh). Peptides were filtered and purified through reverse phase HPLC on C₁₈ column using MeOH/H₂O gradient: ¹H NMR spectra were recorded on Jeol 400 MHz and ¹³C NMR on 100 MHz spectrometer using residual solvent as internal standard (DMSO-*d*₆ δ_H , 2.5 ppm, δ_C 39.51 ppm) The chemical shifts (δ) were reported in ppm and coupling constant (*J*) in Hz. Mass spectra were obtained from the MALDI-TOF/TOF.

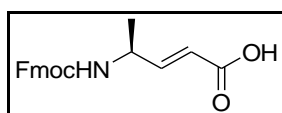
2.5.2 General procedure for the synthesis of Fmoc- α , β -unsaturated γ - amino acids

The Boc-amino aldehyde (10 mmol) and ylide (15 mmol, 5.22 g) were dissolved in 30 mL of dry THF at room temperature and stirred for about 5 h. Completion of reaction was monitored by TLC. The reaction mixture was concentrated under reduced pressure to give crude product, which was purified with silica gel column chromatography using EtOAc/ petroleum ether (1:5) to afford the pure ethyl ester of the Boc-protected α,β -unsaturated γ -amino acid. To a solution of the ethyl ester of the Boc- α,β -unsaturated γ -amino acid (2 mmol) in 5 mL of ethanol was added 5 mL of 1 N NaOH dropwise. After completion of the reaction (~30 min), ethanol was evaporated and the residue was acidified using 10 mL of 5% HCl (5% volume in water) under cold conditions. The product was extracted with ethyl acetate (3 \times 40 mL). The combined organic layer was washed with brine (30 mL) and dried over anhydrous Na₂SO₄. The solvent was concentrated under reduced pressure to give the Boc- α,β -unsaturated γ -amino acid as a gummy product in quantitative yield. The Boc- α,β -unsaturated γ -amino acid (1 mmol) was dissolved in 5 mL of DCM and cooled to 0 °C in an ice bath followed by addition of 5 mL of neat TFA to the reaction mixture. After 30 min, TFA was removed from the reaction mixture under vacuum. The residue was dissolved in 15 mL of water (15 mL), and the pH was adjusted to ~9-10 by the slow addition of solid Na₂CO₃. A solution of Fmoc-OSu (1 mmol) in 10 mL of THF was added slowly to the reaction mixture and stirred overnight at room temperature. After completion of the reaction, the reaction mixture was acidified with 20 mL of 20% HCl (20% volume in water) under cold conditions. The product was extracted with ethyl acetate (3 \times 50 mL). The combined organic layer was washed with brine (30 mL) and dried over anhydrous Na₂SO₄. The solvent was concentrated under reduced pressure to give a gummy product, which was

recrystallized using EtOAc/petroleum ether. The pure solid Fmoc- α,β -unsaturated γ -amino acid was used for solid-phase peptide synthesis.

Characterisation of N-Fmoc-protected α,β -unsaturated γ - amino acids

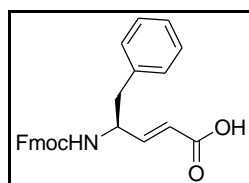
(S,E)-4-(((9H-Fluoren-9-yl)methoxy)carbonyl)amino)pent-2-enoic acid): White solid; yield (0.30 g, 89%) ^1H NMR (400 MHz, DMSO- d_6) δ 12.27 (s, 1H) , 7.89(d, $J = 8$ Hz,2H),7.71 (d, $J = 8$ Hz,2H), 7.60 (d, , $J = 8$ Hz,1H, NH),7.41 (t, $J = 8$ Hz,2H), 7.33 (t, $J = 8$ Hz,2H), 6.76 (dd, $J = 16$ Hz,8 Hz,1H vinylic β proton),5.77 (d, , $J = 16$ Hz,1H, vinylic α proton), 4.33-4.28 (br, 2H), 4.26-4.21 (br, 2H), 1.22-1.15 (m, 3H, CH₃). ^{13}C NMR (100 MHz, DMSO- d_6) δ 167.6, 155.9, 150.1, 144.4, 141.2, 128.1 127.5, 125.6, 120.7, 65.9, 47.6, 47.2, 20.3; m/z value for C₂₀H₁₈O₄ [M+Na]⁺. 360.1212 (calcd) , 360.1242(observed).



Fmoc-(*S, E*)-dgAla-OH

(S,E)-4-(((9H-Fluoren-9-yl)methoxy)carbonyl)amino)-5-phenylpent-2-enoic acid): White solid; yield (0.38 g, 92%) ^1H NMR (400 MHz, DMSO- d_6) δ 12.29 (s, 1H , OH) ,7.83 (d, $J = 8$ Hz,2H), 7.63(d, $J = 8$ Hz,1H, NH),7.59 (t, $J = 8$ Hz,2H), 7.37-7.34 (m, 2H), 7.29-7.21 (m, 7H), 6.79-6.74(dd, $J = 8$ Hz,16Hz,1H vinylic β proton), 5.73(d, $J = 16$ Hz,1H, vinylic α proton), 4.34 (br, 1H), 4.19-4.17 (br, 2H), 4.12-4.11 (m, 1H, CH), 2.84 (dd, $J = 8$ Hz, 4Hz, 1H), 2.72-2.66 (m, 1H). ^{13}C NMR (100 MHz, DMSO- d_6) δ 167.5, 156.0, 148.6, 144.3, 141.2, 138.5, 129.7, 128.6, 128.1, 127.5, 126.8, 125.7, 121.5, 120.6,

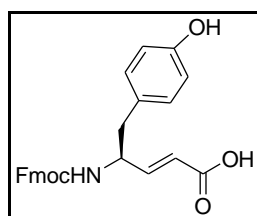
65.9, 53.7, 47.1, 31.2 ; m/z value for $C_{26}H_{22}O_4$ $[M+Na]^+$. 436.1497 (calcd), 436.1521(observed).



Fmoc-(*S, E*)-dgPhe-OH

(*S, E*)-4-(((9H-Fluoren-9-yl)methoxy)carbonyl)amino)-5-(4-hydroxyphenyl)pent-2-enoic acid): White solid; yield(0.42 g, 90%) 1H NMR (400 MHz, $DMSO-d_6$) δ 12.25 (s, 1H), 9.16(s, 1H), 7.84 (d, $J = 8$ Hz, 2H), 7.62-7.57 (m, 3H), 7.38-7.34 (m, 2H), 7.30-7.24 (m, 2H), 6.98 (d, $J = 8$ Hz, 2H), 6.74 (dd, $J = 16$ Hz, 8 Hz, 1H vinylic β proton), 6.61 (d, $J = 8$ Hz, 2H), 5.71 (d, $J = 16$ Hz, 1H, vinylic α proton), 4.25-4.233 (br, 1H), 4.20-4.11 (br, 3H), 2.71 (dd, $J = 12$ Hz, 8 Hz, 1H), 2.58 (dd, $J = 12$ Hz, 8 Hz, 1H)

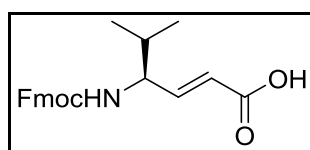
^{13}C NMR (100 MHz, $DMSO-d_6$) δ 167.5, 156.2, 155.9, 148.8, 144.3, 144.2, 141.2, 130.6, 128.5, 128.1, 127.5, 125.7, 125.6, 121.4, 120.6, 155.4, 65.9, 54.0, 47.1 m/z value for $C_{26}H_{22}O_5$ $[M+Na]^+$. -486.2279(calcd.), 486.2268(observed).



Fmoc-(*S, E*)-dgTyr-OH

(S,E)-4-(((9H-fluoren-9-yl)methoxy)carbonyl)amino)-5-methylhex-2-enoic acid:

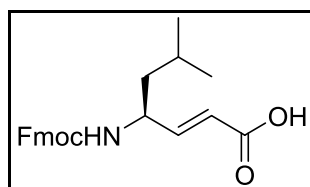
White solid; yield (0.33 g, 90%); ^1H NMR (400 MHz, $\text{DMSO-}d_6$) δ 12.31 (s, 1H), 7.84 (d, $J=8$ Hz, 2H), 7.67 (d, $J=8$ Hz, 2H), 7.28 (t, $J=8$ Hz, 2H), 6.69 (dd, $J=8$ Hz, 16 Hz, 2H), 5.79 (d, $J=8$ Hz, 1H), 4.32-4.18 (m, 3H), 3.95-3.93 (m, 1H), 1.76-1.74 (m, 1H), 0.80 (d, $J=8$ Hz, 6H); ^{13}C NMR (100 MHz, $\text{DMSO-}d_6$) δ 167.4, 156.3, 147.7, 144.3, 141.2, 128.1, 127.5, 125.7, 122.4, 120.6, 65.9, 57.8, 47.2, 32.1, 19.5, 19.0; m/z value for $\text{C}_{22}\text{H}_{23}\text{NO}_4$ $[\text{M}+\text{Na}]^+$. 388.1525 (calcd.), 388.1483 (observed).



Fmoc-(*S, E*)-dgVal-OH

(S,E)-4-(((9H-fluoren-9-yl)methoxy)carbonyl)amino)-6-methylhept-2-enoic acid:

White solid; yield (0.35 g, 92%); ^1H NMR (400 MHz, $\text{DMSO-}d_6$) δ 12.27 (s, 1H), 7.86-7.26 (m, 10H), 6.65 (dd, $J=8$ Hz, 16 Hz, 1H), 5.72 (d, $J=8$ Hz, 1H), 4.34-4.14 (m, 4H), 1.56-1.50 (m, 1H), 1.39-1.19 (m, 2H), 0.82 (t, $J=8$ Hz, 6H); ^{13}C NMR (100 MHz, $\text{DMSO-}d_6$) δ 167.5, 156.1, 149.6, 144.3, 141.2, 128.1, 127.5, 125.6, 121.0, 120.6, 65.7, 50.2, 47.3, 42.9, 24.8, 23.3, 22.1; m/z value for $\text{C}_{23}\text{H}_{25}\text{NO}_4$ $[\text{M}+\text{Na}]^+$. 402.1681 (calcd.), 402.1712 (observed).



Fmoc-(*S, E*)-dgLeu-OH

2.5.3 Solid phase peptide synthesis and purification

. Peptides were synthesized on a 0.25 mmol scale on Knorr amide resin using standard Fmoc-chemistry. The combination of HBTU/HOBt (1:1) was used as coupling reagents. The coupling reactions were monitored by the Kaiser test. After completion of the synthesis, peptides were cleaved from the resin using a cocktail mixture of TFA:water:thioanisole (98:1:1). After cleavage, the resin was filtered and washed with TFA. The cleavage mixture was then evaporated under reduced pressure to give a gummy product and purified through reverse phase HPLC on a C₁₈ column using a MeOH/H₂O gradient. The purity of the peptides was further confirmed by an analytical C₁₈ column with the same gradient system

2.5.4 Procedure for testing antibacterial activity

The bacteria used in these experiments were collected from National Collection of Industrial Microorganisms (NCIM) *Escherichia coli* (NCIM 2065), *Escherichia coli* K12 (NCIM2563), *Klebsiella pneumoniae* (NCIM 2957), *Pseudomonas aeruginosa* (NCIM 5029), *Salmonella typhimurium* (NCIM 2501), and *Staphylococcus aureus* (NCIM 5021).

The antibacterial activities of lipopeptides were carried out in 96-well microtiter plate using broth dilution method. The bacterial cultures were grown over night at 37 °C and serially diluted to a concentration of 10⁶ colony forming units/mL with sterile MHB (Muller-Hinton broth) medium. Two-fold serial dilutions with MHB medium were performed triplicate for each lipopeptide in a sterile 96-well plate to a final volume of 50 µL in each well. The final volume was made to 100 µL by adding an aliquot of 50 µL bacterial suspension to each well, and the plate was incubated at 37 °C for 18-20 h. Controls were done without peptide and the MIC of peptide was defined as the lowest concentration of the peptide required for the complete inhibition or killing the bacterial

inoculum. the growth inhibition was monitored by measuring the absorbance at 492 nm. The MIC values reported were reproducible between three independent triplicates.

2.5.5 Procedure for testing antifungal activity

The antifungal activity of lipopeptides was performed using 96 well plate methods (TPP brand) as follows: The 50 μL of water containing peptide was serially two fold diluted in PDB (Potato dextrose broth, Hi-Media) medium. The final volume was adjusted to 100 μL by adding 50 μL of yeast suspension containing a concentration of 2×10^3 colony forming units/ml. A culture without peptide was also grown parallel as a control. Inoculated plates were incubated at 25 °C for 48-72 h and the growth inhibition was determined by measuring the absorbance at 620 nm. The yeasts used were *Candida albicans* (NCIM 3471), *Candida glabrata* (NCIM 3237), *Cryptococcus neoformans* (NCIM 3542), and *Saccharomyces cerevisiae* (NCIM 3454). Experiments were carried out in triplicate. The MIC was determined as the lowest concentration of peptide required for the complete growth inhibition of each organism after 48-72 h incubation.

2.5.6 Procedure for hemolysis assay

Fresh hRBCs (Human Red Blood Cells) were collected with EDTA. The hRBCs were washed with Tris buffered saline (10 mM Tris, 150 mM NaCl, and pH 7.2) four times and diluted to a final concentration of 4% v/v. The assay was performed in sterile 96-well plate in a final volume of 100 μL as follows: aliquot of 50 μL of hRBC suspension were added to 50 μL (100 $\mu\text{g}/\text{mL}$) of two-fold serial diluted lipopeptide in Tris buffer. The plate was incubated at 37 °C for 1 h and then centrifuged for 15 min at 3000 rpm. The supernatant (50 μL) from each well was transferred to a fresh 96-well plate containing 50 μL of water and release of haemoglobin was monitored by measuring the absorbance at 540 nm. The experiments were performed in duplicate and the hRBCs suspensions with

Tris buffer and 1% Triton-X was consisted as negative and positive controls. Percentage of hemolysis was defined as $(A-A_N)/(A_P-A_N) \times 100$, where A is the absorbance of test well, A_N is the absorbance of the negative control and A_P is the absorbance of the positive control (100% hemolysis).

2.5.7 Procedure for atomic force microscopy imaging

A culture of *E. coli* K12 (NCIM 2563) were grown in MHB medium and *Candida albicans* (NCIM 3471) were grown in potato dextrose broth. The cells were centrifuged and resuspended in deionized distilled water. The bacteria were incubated with 50 μ M of S1 and S8 lipopeptide at 37 °C for 1 h. After incubation, 50 μ L droplets of each sample were applied onto Poly-L-Lysine (PLL) pretreated glass slides and allowed to dry for 30 min at 25 °C. For control, cells without peptide were similarly prepared and imaged within 2 h of being resuspended in distilled water.

For AFM analysis of peptides the samples were applied on the freshly cleaved mica surface and dried for 10 min at 25 °C. The AFM images were acquired using a JPK Nano Wizard (Berlin, Germany) mounted on a Zeiss Axiovert 200 inverted microscope. Measurements were carried out in Intermittent contact (IC) mode using Tap 300 E-G (Cr/Pt Conductive coating) cantilevers from silicon AFM probes (Spring constant, $k = 40$ N/m, Resonance Frequency around 300 KHz, Radius <10 nm). Height and size information were acquired using JPK data processing software.

2.5.8 Procedure for FITC uptake assay

To analyze the membrane permeabilization of lipopeptides, impermeable fluorescent probe Fluorescein isothiocyanate (FITC) was used. Culture of *E.coli* K12 (NCIM 2563) were grown to absorbance OD 0.6 in MHB medium. The bacteria were washed and

suspended (2×10^7 cfu /mL) in 10 mM sodium phosphate buffer (pH 7.4). The bacterial suspension was incubated with 50 μ M of **S1**, **S3** and **S8** lipopeptides at 37 °C for 60 min. The microorganisms were immobilized on Poly-L-Lysine (PLL) coated glass slide for 50 min at 30 °C, followed by addition of 100 μ L FITC (10 μ g/mL) suspended in the same buffer. The slides were washed with 10 mM sodium phosphate buffer (pH 7.4) and viewed under Zeiss Axiovert apotome microscope equipped with an AxioCam camera. The images were processed with Axiovision 4.7 software. The samples with peptide solvents were taken as a control.

2.5.9 Procedure for β -galactosidase leakage assay

The PUC19 plasmid containing LacZ reporter gene was transformed in to the chemically competent *Escherichia coli* (TOP10, Invitrogen) cells. *E.coli* cells were grown in Luria Bertani broth with 100 μ g/mL of ampicillin at 37 °C to an absorbance 0.6 at 660 nm. The cells were centrifuged and washed with fresh medium for three times to remove extracellular β -galactosidase. The 10 μ L of water containing peptide of stock solution (200 μ g/mL) were added in a sterile 96-well plate. The final volume was adjusted to 100 μ L by adding an aliquot of 90 μ L bacterial suspensions to each well, and the plate was incubated at 37 °C for 1 h. After 1 h, the plate was centrifuged at 4000 rpm for 10 min to remove cell debris and 80 μ L of supernatant was removed and separated in a fresh well. An aliquot 20 μ L (0.4 mg/mL) of fluorescent indicator 4-methylumbelliferyl- β -galactosidase (MUG, Sigma) was added to the well and β -galactosidase release was monitored for 1 h. Initial velocities of enzyme reaction were taken from the linear plot of fluorescence versus time. The samples with water were taken as a blank.

2.5.10 Procedure for dynamic light scattering experiment

For DLS measurements, lipopeptides of concentration 1mg/mL were dissolved in water and by using poly propylene glass cuvette measurements were performed in Zeta sizer (Malvern Instrument). The average count rate at each time point was recorded.

2.5.11 Scanning electron microscopy imaging:

The peptides were dissolved in water of concentration (50 µg/mL) was spotted on silicon wafers and air dried for 45 min. The samples were sputter coated with gold and observed in Zeiss FE-SEM. The sample was spotted on silicon wafers and recorded on FE-SEM. The images were converted to binary file and fractal dimension were analyzed by using fractal box count of Image J software.

2.6 References

1. a) Zasloff, M. *Nature* **2002**, *415*, 389-395. b) Brogden, K. A. *Nat. Rev. Microbiol.* **2005**, *3*, 238-250. c) Hancock, R. E.; Sahl, H. G. *Nat. Biotechnol.* **2006**, *24*, 1551-1557. d) Boman, H. G. *Cell* **1991**, *65*, 205-207. e) Bulet, P.; Stocklin, R.; Menin, L. *Immunol. Rev.* **2004**, *198*, 169-184.
2. a) Srinivas, N.; Jetter, P.; Ueberbacher, B. J.; Werneburg, M.; Zerbe, K.; Steinmann, J.; Meijden, B. V.; Bernardini, F.; Lederer, A.; Dias, R. L. A.; Misson, P. E.; Henze, H.; Zumbrunn J.; Gombert, F. O.; Obrecht, D.; Hunziker, P.; Schauer, S.; Ziegler, U.; Käch, A.; Eberl, L.; Riedel, K.; DeMarco, S. J.; Robinson, J. A. *Science* **2010**, *327*, 1010-1013. b) Findlay, B.; Zhanel, G. G.; Schweizer, F. *Antimicrob. Agents Chemother.* **2010**, *54*, 4049-4058. c) Liu, L.; Xu, K.; Wang, H.; Tan, P. K. J.; Fan, W.; Venkatraman, S. S.; Li, L.; Yang, Y. Y. *Nature Nanotechnology* **2009**, *4*, 457-463.

3. a) Porter, E. A.; Wang, X.; Lee, H. S.; Weisblum, B.; Gellman, S. H. *Nature* **2000**, *404*, 565. b) Hansen, T.; Alst, T.; Havelkova, M.; Strøm, M. B. *J. Med. Chem.* **2010**, *53*, 595-606. c) Hamuro, Y.; Schneider, J. P.; DeGrado, W. F. *J. Am. Chem. Soc.* **1999**, *121*, 12200-12201. d) Porter, E. A.; Weisblum, B.; Gellman, S. H. *J. Am. Chem. Soc.* **2002**, *124*, 7324-7330. e) Arvidsson, P. I.; Frackenpohl, J.; Ryder, N. S.; Liechty, B.; Petersen, F.; Zimmermann, H.; Camenisch, G. P.; Woessner, R.; Seebach, D. *ChemBioChem* **2001**, *2*, 771-773. f) Schmitt M. A.; Weisblum B.; Gellman S. H. *J. Am. Chem. Soc.* **2007**, *129*, 417-428.
4. a) Chongsiriwatana, N. P.; Patch, J. A.; Czyzewski, A. M.; Dohm, M. T.; Ivankin, A.; Gidalevitz, D.; Zuckermann, R. N.; Barron, A. E. *Proc. Nat. Acad. Sci. U.S.A.* **2008**, *105*, 2794-2799. b) Shuey S. W.; Delaney W. J.; Shah M. C.; Scialdone M. A. *Bioorg. Med. Chem. Lett.* **2006**, *16*, 1245-1248. c) Olsen C. A.; Ziegler H. L.; Nielsen H. M.; Frimodt-Møller N.; Jaroszewski J. W.; Franzyk, H. *ChemBioChem* **2010**, *11*, 1356-1360.
5. Chongsiriwatana, N. P.; Miller, T. M.; Wetzler, M.; Vakulenko, S.; Karlsson, A. J.; Palecek, S. P.; Mobashery, S.; Barron, A. E. *Antimicrob. Agents Chemother.* **2011**, *55*, 417-420.
6. Stratton, T. R.; Applegate, B. M.; Youngblood, J. P.; **2011**, *12*, 50-56.
7. Lienkamp, K.; Madkour, A. E.; Musante, A.; Nelson, C. F.; Nusslein, K.; Tew, G. N. *J. Am. Chem. Soc.* **2008**, *130*, 9836-9843 .
8. Li, P.; Poon, Y. F.; Li, W.; Zhu, H. Y.; Yeap, S. H.; Cao, Y.; Qi, X.; Zhou, C.; Lamrani, M.; Beuerman, R. W.; Kang, E. T.; Mu, Y.; Li, C. M.; Chang, M. W.; Jan Leong, S. S.; Chan-Park, M. B. *Nature Mater.* **2011**, *10*, 149-156.
9. Li, P.; Zhou, C.; Rayatpisheh, S.; Ye, K.; Poon, Y. F.; Hammond, P. T.; Duan, H.; Chan-Park, M. B. *Adv. Mater.* **2012**, *24*, 4130-4137.

10. a) Ongena, M.; Jacques, P. *Trends in Microbiol.* **2008**, *16*, 115-125. b) Koehn, F. E.; Kirsch, D. R.; Feng, X.; Janso, J.; Young, M. *J. Nat. Prod.* **2008**, *71*, 2045-2048. c) McPhail, K. L.; Correa, J.; Linington, R. G.; Gonzalez, J.; Ortega-Barria, E.; Capson, T. L.; Gerwick W. H. *J. Nat. Prod.* **2007**, *70*, 984-988. d) Gu, J. Q.; Nguyen, K. T.; Gandhi, C.; Rajgarhia, V.; Baltz, R. H.; Brian, P.; Chu, M. *J. Nat. Prod.* **2009**, *70*, 233-240. e) Grunewald, J.; Sieber, S. A.; Mahlert, C.; Linne, U.; Marahiel, M. A. *J. Am. Chem. Soc.* **2004**, *126*, 17025-17031. f) Curran, W. V.; Leese, R. A.; Jarolmen, H.; Borders, D. B.; Dugourd, D.; Chen, Y.; Cameron, D. R. *J. Nat. Prod.* **2007**, *70*, 447-450.
11. Steenbergen, J. N.; Alder, J.; Thorne, G. M.; Tally, F. P. *J. Antimicrob Chemother.* **2005**, *55*, 283-288.
12. a) Avrahami, D.; Shai, Y. *J. Biol. Chem.* **2004**, *279*, 12277-12285. b) Makovitzki, A.; Avrahami, D.; Shai, Y. *Proc. Nat. Acad. Sci. U.S.A.* **2006**, *103*, 15997-16002. c) Serrano, G. N.; Zhanel, G. G.; Schweizer, F. *Antimicrob. Agents Chemother.* **2009**, *53*, 2215-2217. d) Makovitzki, A.; Baram, J.; Shai, Y. *Biochemistry* **2008**, *47*, 10630-10636. e) Mangoni, M. L.; Shai, Y. *Cell. Mol. Life Sci.* **2011**, *68*, 2267-2280. f) Toniolo, C.; Crisma, M.; Formaggio, F.; Peggion, C.; Epand, R. F.; Epand, R. M. *Cell. Mol. Life Sci.* **2001**, *58*, 1179-1188. g) Radzishovsky, I. S.; Rotem, S.; Bourdetsky, D.; Navon-Venezia, S.; Carmeli, Y.; Mor, A. *Nat. Biotechnol.* **2007**, *25*, 657-659.
13. a) Nguyen, L. T.; Haney, E. F.; Vogel H. J. *Trends in Biotechnol.* **2011**, *29*, 464-472. b) Shai, Y. *Biopolymers* **2002**, *66*, 236-248.
14. Matson, J. B.; Stupp, S. I. *Chem Commun.* **2012**, *48*, 26-33.
15. Cui, H.; Muraoka, T.; Cheetham, A. G.; Stupp S. I. *Nano Lett.* **2009**, *9*, 945-951.
16. a) Hartgenik, J. D.; Beniash, E.; Stupp S.I. *Science* **2001**, *294*, 1684-1688. b) Hartgenik, J. D.; Beniash, E.; Stupp, S. I. *Proc. Natl. Acad. Sci. U. S. A.* **2002**,

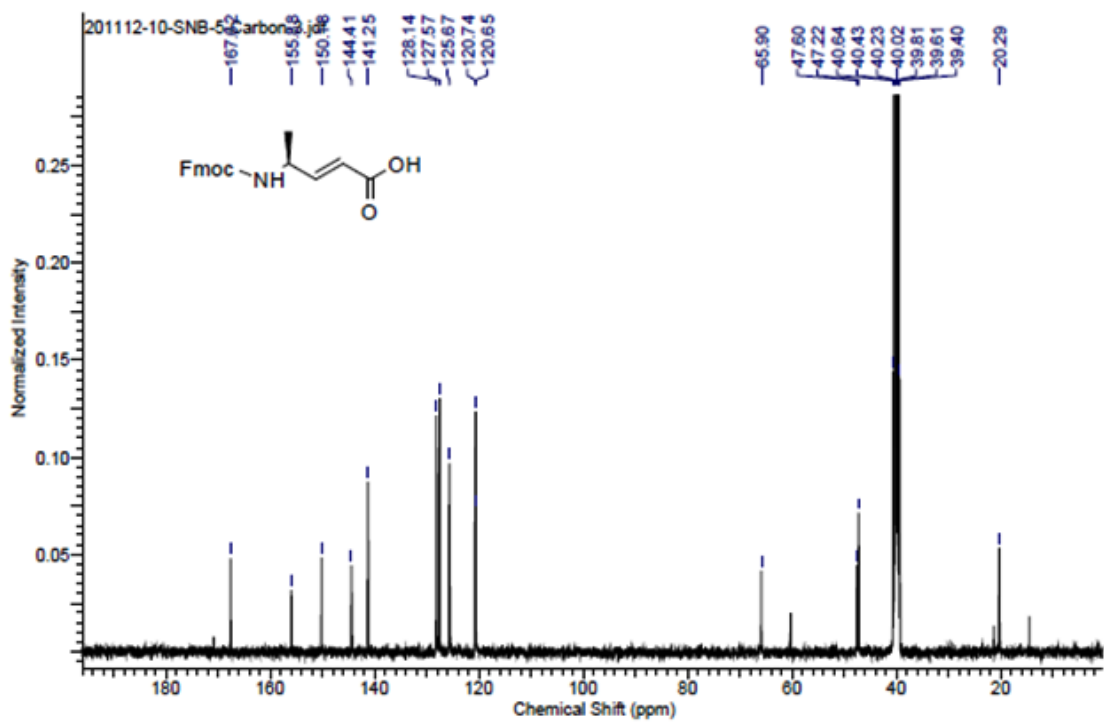
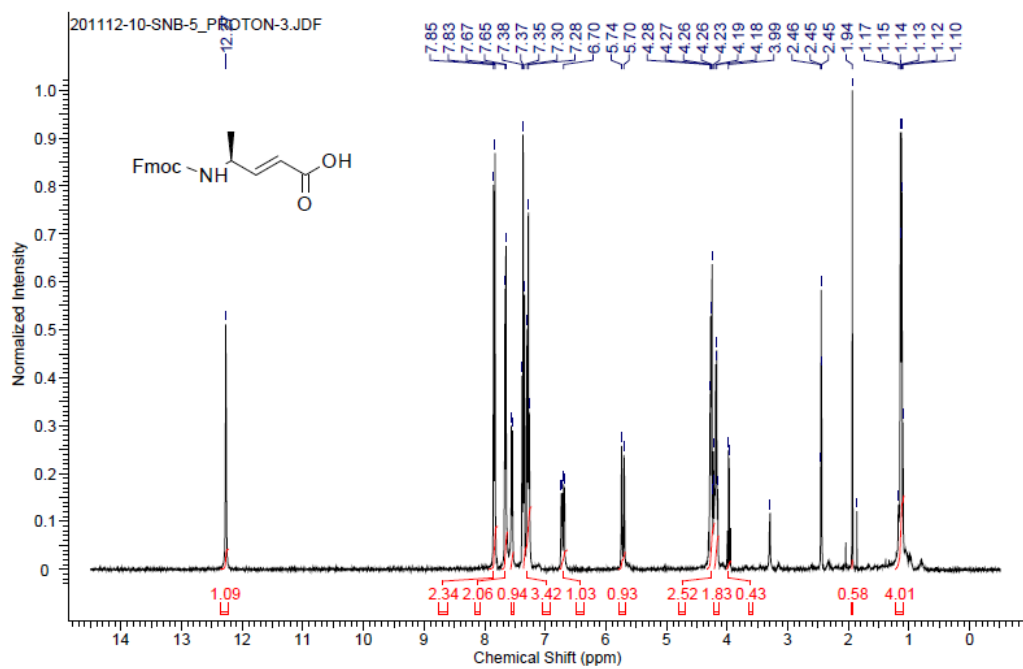
- 99, 5133-5138. c) Zubarev, R. E.; Pralle, M. U.; Sone, D. E.; Stupp S. I. *Adv. Mater.* **2002**, *14*, 198-203. d) Palmer, L. C.; Newcomb, C.J.; Kaltz, R. S.; Spoerke, E. D.; Stupp, S. I. *Chem. Rev.* **2008**, *108*, 4754-4783. e) Spoerke, E. D.; Anthony, G. S.; Stupp, S. I. *Adv. Mater.* **2009**, *21*, 425-430.
17. a) Linington, R. G.; Clark, B. R.; Trimble, E. E.; Almanza, A.; Urena, L. D.; Kyle, D. E.; Gerwick, W. H. *J. Nat. Prod.* **2009**, *72*, 14-17. b) Hagihara, M.; Schreiber, S. L.; *J. Am. Chem. Soc.* **1992**, *114*, 6570-6571. d) Coleman, J. E.; de Silva, E. D.; Kong, F.; Andersen, R. J.; Allen, T. M. *Tetrahedron* **1995**, *51*, 10653-10662.
18. a) Schaschke, N.; Sommerhoff, C. P. *ChemMedChem* **2010**, *5*, 367-370. b) Breuning, A.; Degel, B.; Schulz, F.; Buchold, C.; Stempka, M.; Machon, U.; Heppner, S.; Gelhaus, C.; Leippe, M.; Leyh, M.; Kisker, C.; Rath, J.; Stich, A.; Gut, J.; Rosenthal, P. J.; Schmuck, C.; Schirmeister, T. *J. Med. Chem.* **2010**, *53*, 1951-1963. c) Kong, J. S.; Venkatraman, S.; Furness, K.; Nimkar, S.; Shepherd, T. A.; Wang, Q. M.; Aube, J.; Hanzlik, R. P. *J. Med. Chem.* **1998**, *41*, 2579-2587.
19. Hagihara, M.; Schreiber, S. L. *J. Am. Chem. Soc.* **1992**, *114*, 6570.
20. Linington, R. G.; Clark, B. R.; Trimble, E. E.; Almanza, A.; Uren, L.-D.; Kyle, D. E.; Gerwick, W. H. *J. Nat. Prod.* **2009**, *72*, 14.
21. Nakao, Y.; Fujita, M.; Warabi, K.; Matsunaga, S.; Fusetani, N. *J. Am. Chem. Soc.* **2000**, *122*, 10462.
22. a) Totaro, K. A.; Barthelme, D.; Simpson, P. T.; Jiang, X.; Lin, G.; Nathan, C. F.; Sauer, R. T.; Sello, J. K. *ACS Infect. Dis.* **2017**, *3*, 176-181. b) Krahn, D.; Ottmann, C.; Kaiser, M. *Nat. Prod. Rep.*, **2011**, *28*, 1854-1867.
23. a) Hanzlik, R. P.; Thompson, S. A. *J. Med. Chem.* **1984**, *27*, 711. b) Bastiaans, H. M. M.; Van der Baan, J. L.; Ottenheijm, H. C. J. *J. Org. Chem.* **1997**, *62*, 3880. c) Liu, S.; Hanzlik, R. P. *J. Med. Chem.* **1992**, *35*, 1067. d) Kong, J-S.; Venkatraman, S.;

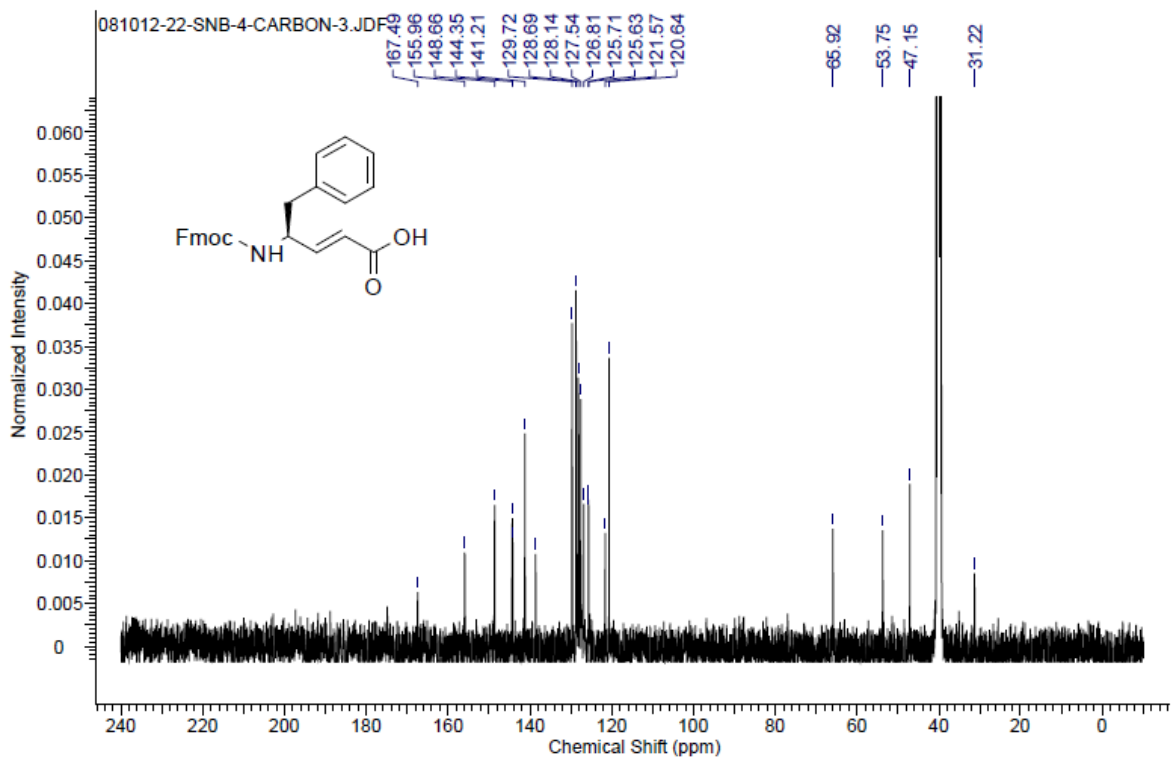
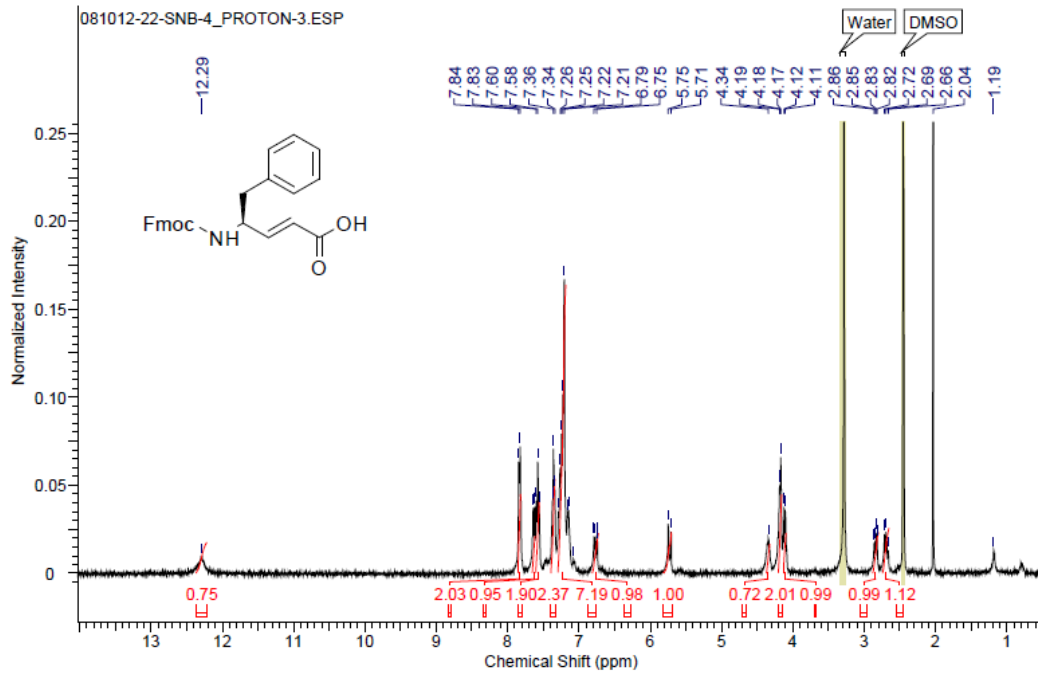
- Furness, K.; Nimkar, S.; Shepherd, T. A.; Wang, Q. M.; Aube, J.; Hanzlik, R. P. *J. Med. Chem.* **1998**, *41*, 2579. e) Schaschke, N.; Sommerhoff, C. P. *ChemMedChem***2010**, *5*, 367.
24. Hagihara, M.; Anthony, N. J.; Stout, T. J.; Clardy, J.; Schreiber, S. L. *J. Am. Chem. Soc.* **1992**, *114*, 6568.
25. Baldauf, C.; Gunther, R.; Hofmann, H.-J. *J. Org. Chem.* **2005**, *70*, 5351.
26. Chakraborty, T. K.; Ghosh, A.; Kumar, S. K.; Kunwar, A. C. *J. Org. Chem.* **2003**, *68*, 6459.
27. Mali, S. M.; Bandyopadhyay, A.; Jadhav, S. V.; Ganesh Kumar, M.; Gopi, H. N. *Org. Biomol. Chem.* **2011**, *9*, 6566.
28. Bandyopadhyay, A.; Gopi, H. N. *Org. Lett.* **2012**, *14*, 2770.
29. Bandyopadhyay, A.; Mali, S. M.; Lunawat, P.; Raja, K. M. P.; Gopi, H. N. *Org. Lett.* **2011**, *13*, 4482-4485.
30. Bandyopadhyay, A.; Misra, R.; Gopi, H. N. *Chem Commun.* **2016**, *52*, 4938-4941.
31. Ganesh Kumar M.; Benke, S. N.; Raja, K. M. P.; Gopi, H. N. *Chem Commun.* **2015**, *51*, 13397-13399.
32. Ganesh Kumar, M.; Mali, S. M.; Raja, K. M.; Gopi, H. N. *Org Lett.* **2015**, *17*, 230-233.
33. Ganesh Kumar, M.; Gopi, H. N. *Org Lett.* **2015**, *17*, 4738-4741.
34. Ganesh Kumar, M.; Mali, S. M.; Gopi, H. N. *Org. Biomol. Chem.* **2013**, *11*, 803-813.
35. Ulijasz, A. T.; Grenader, A.; Weisblum, B. *J. Bacteriol.* **1996**, *178*, 6305-6309.
36. Gopinath, K.; Praveen, P.; Martin, K.; Victoria, R.; Matthias, M.; Barbara, A.; Martin, M.; Artur, S. *Antimicrob. Agents Chemother.* **2011**, *55*, 2880-2890.
37. Lakshmanan, A.; Cheong, D. W.; Accardo, A.; Fabrizio, E. D.; Riekkel, C.; Hauser, C. A. E. *Proc. Natl. Acad. Sci. USA* **2013**, *110*, 519-524.

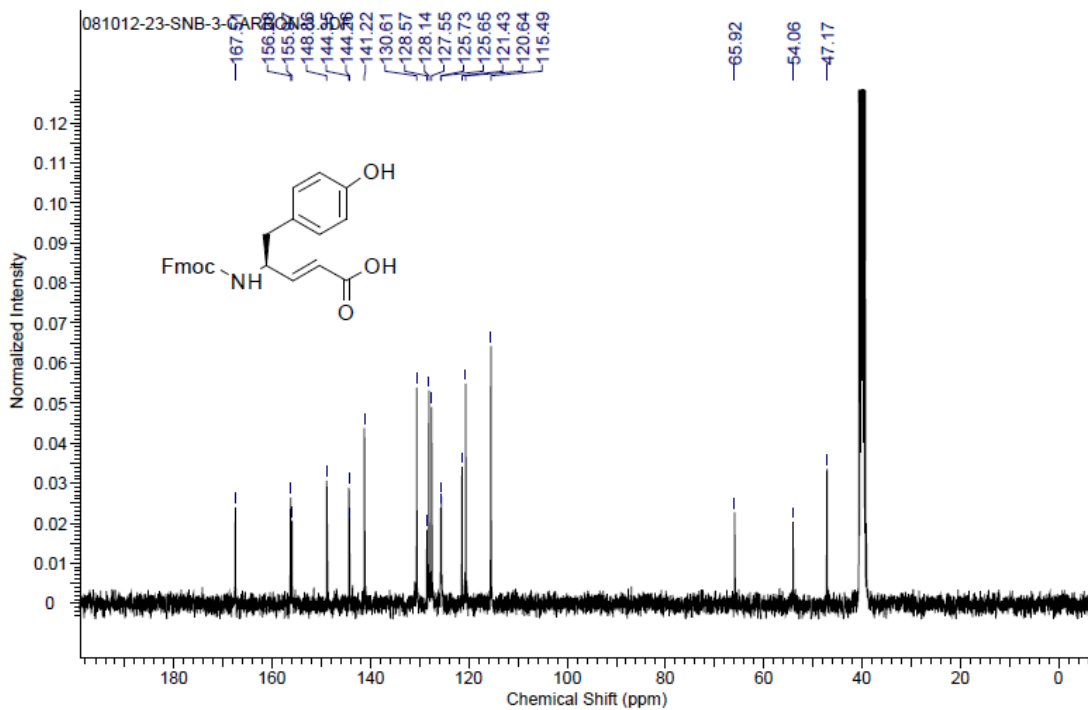
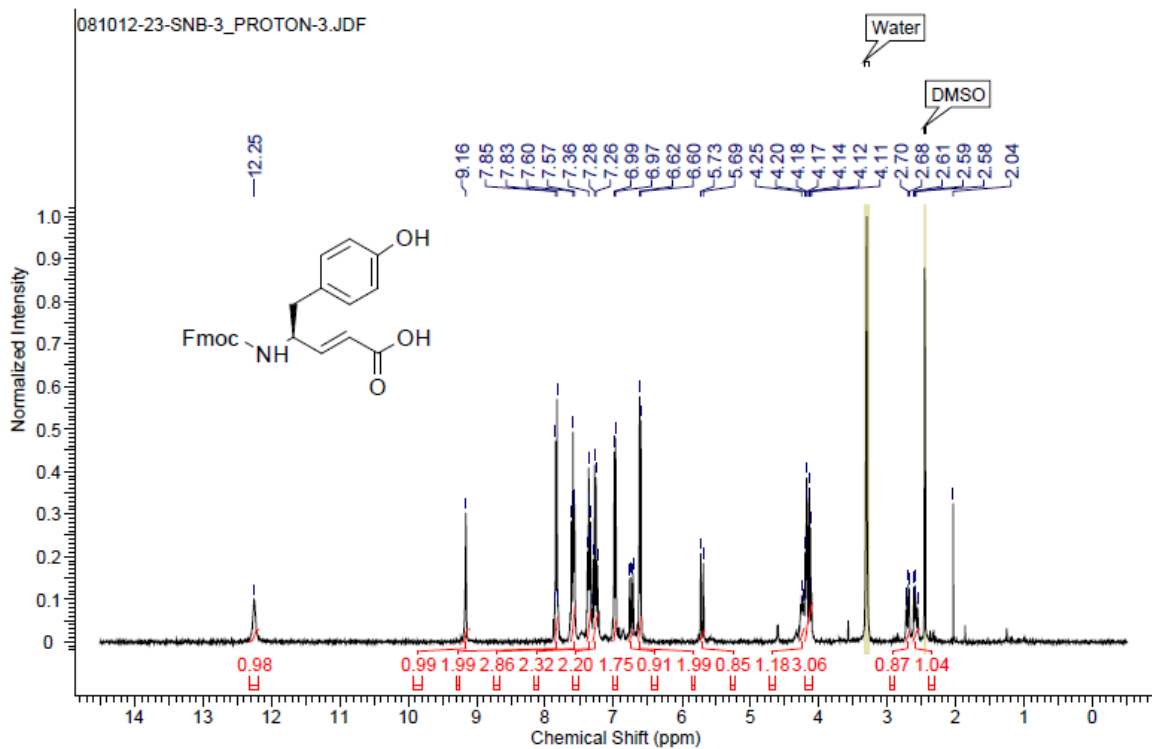
38. Zhao, Q.; An, Q.; Qian, J.; Wang, X.; Zhou, Y. *J. Phy. Chem. B* **2011**, *115*, 14901-14911.
39. Zhao, Q.; Qian, J.; Gui, Z.; An, Q.; Zhu M *Soft Matter* **2010**, *6*, 1129-1137.
40. Wang W.; Chau, Y. *Soft Matter* **2009**, *5*, 4893-4898.

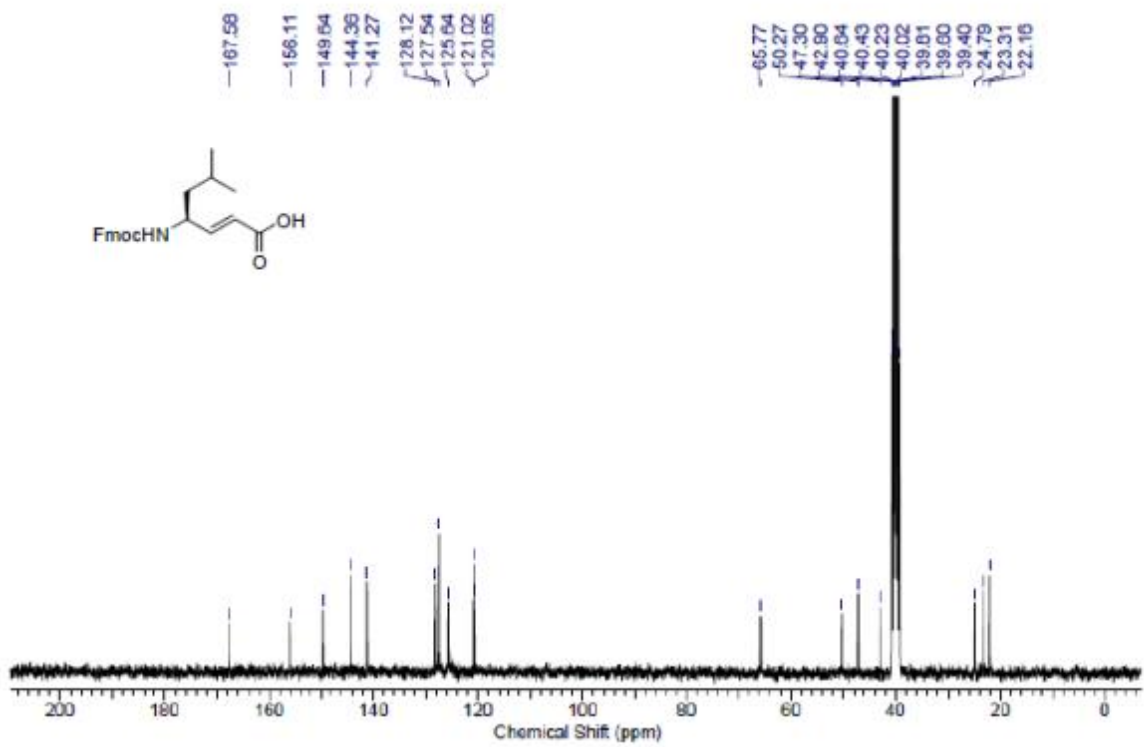
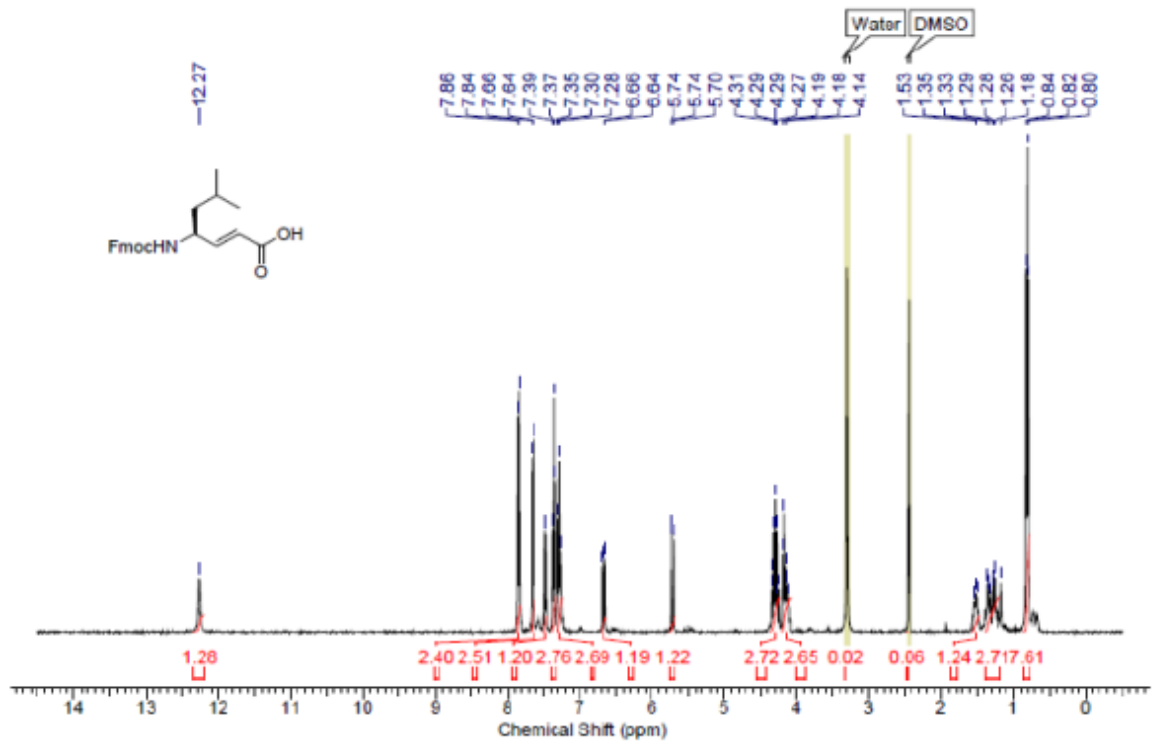
2.7 Appendix I. Characterisation data of synthesized compounds and peptides

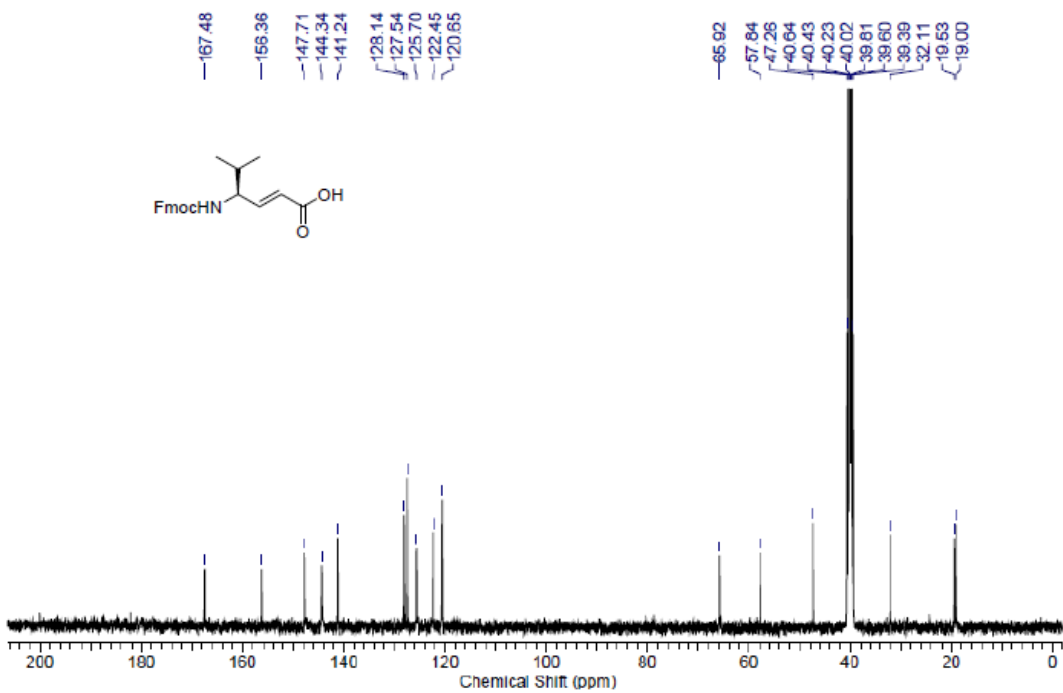
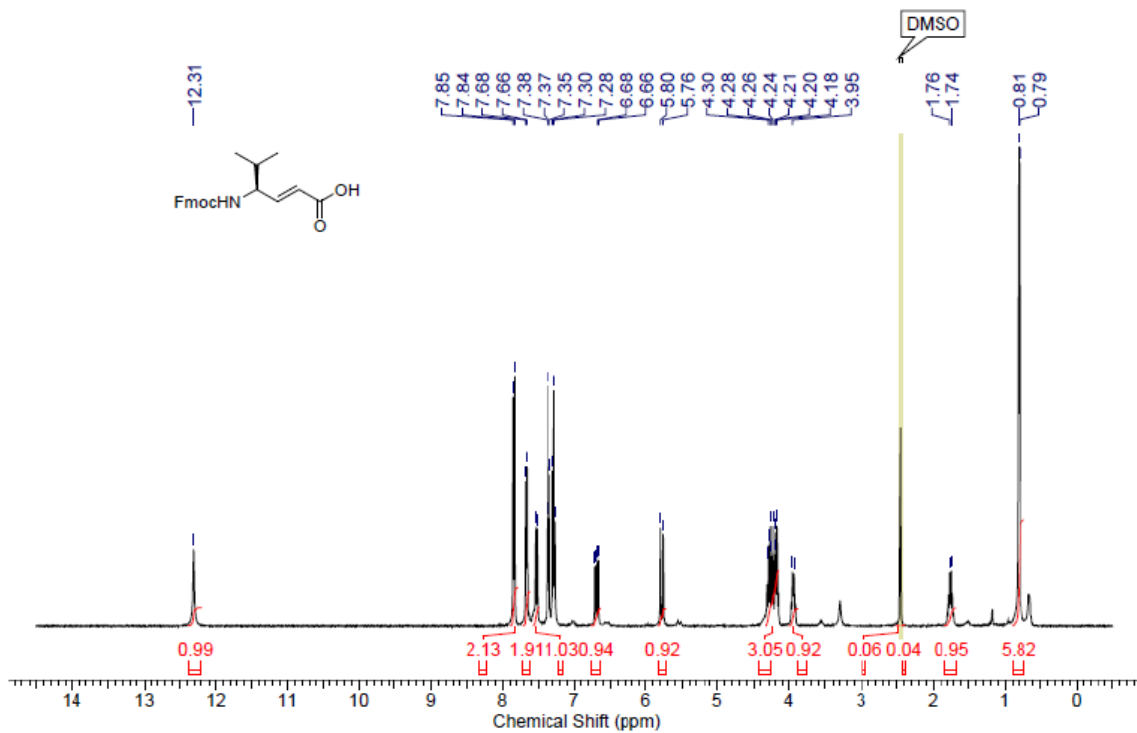
Designation	Description	Page No.
Fmoc-(<i>S,E</i>)-dgAla-OH	¹ H and ¹³ C spectra	58
Fmoc-(<i>S,E</i>)-dgPhe-OH	¹ H and ¹³ C spectra	59
Fmoc-(<i>S,E</i>)-dgTyr-OH	¹ H and ¹³ C spectra	60
Fmoc-(<i>S,E</i>)-dgLeu-OH	¹ H and ¹³ C spectra	61
Fmoc-(<i>S,E</i>)-dgVal-OH	¹ H and ¹³ C spectra	62
S1	HPLC trace and Mass spectrum	63
S2	HPLC trace and Mass spectrum	63
S3	HPLC trace and Mass spectrum	64
S4	HPLC trace and Mass spectrum	64
S5	HPLC trace and Mass spectrum	65
S6	HPLC trace and Mass spectrum	65
S7	HPLC trace and Mass spectrum	66
S8	HPLC trace and Mass spectrum	66
S9	HPLC trace and Mass spectrum	67
S10	HPLC trace and Mass spectrum	67
S11	HPLC trace and Mass spectrum	68



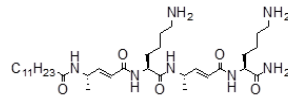








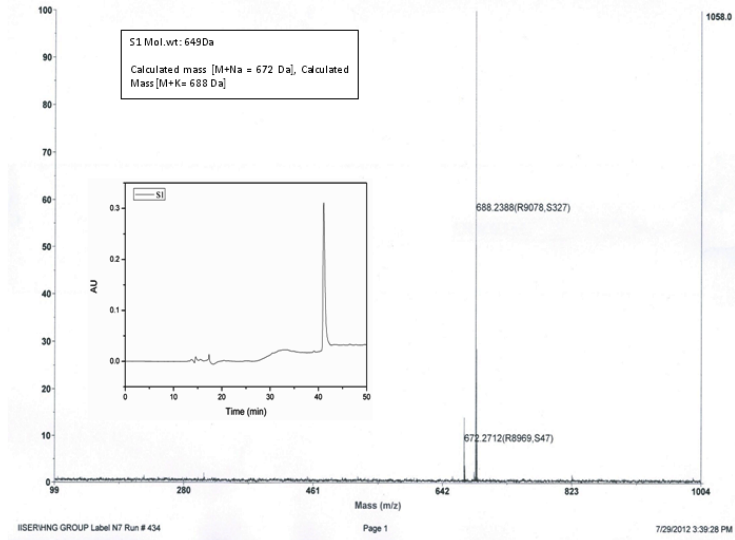
S1



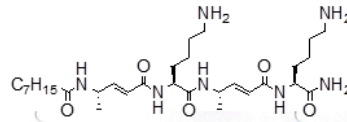
Spectrum Report

S5-1)

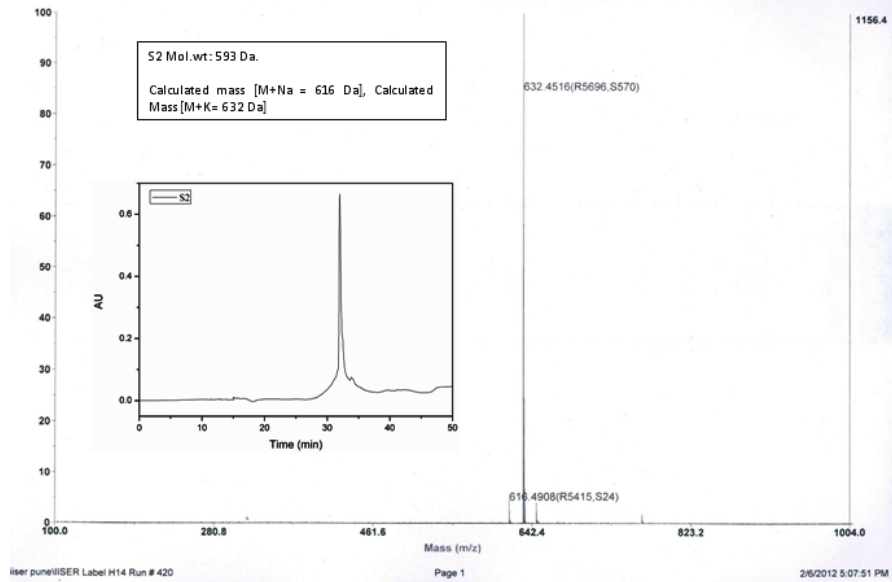
Final - Shots 450 - HNG GROUP: Label N7

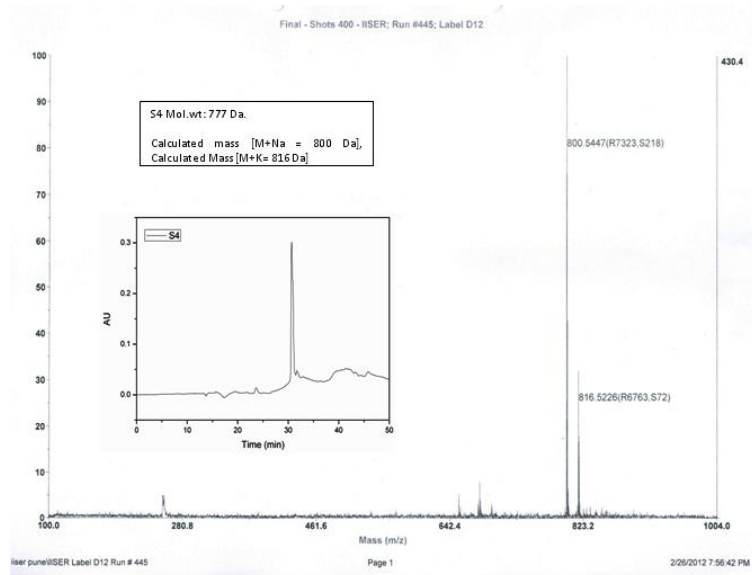
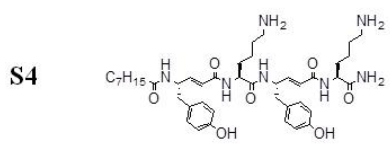
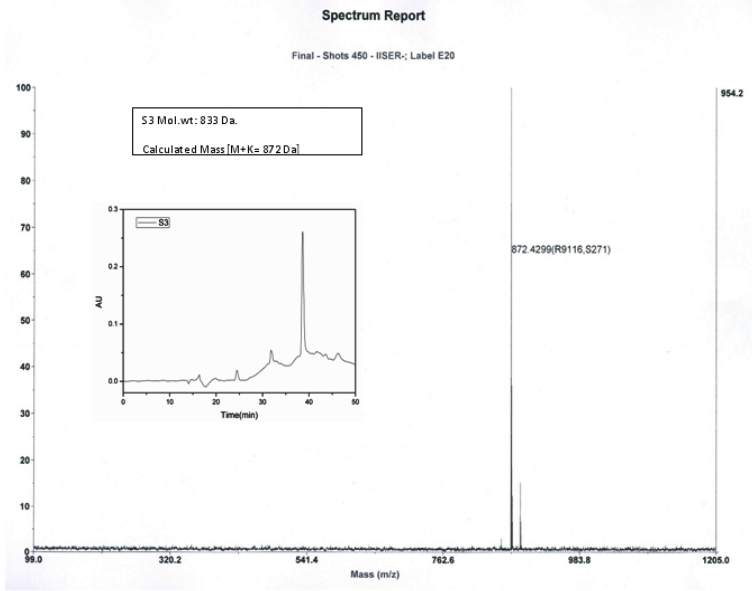
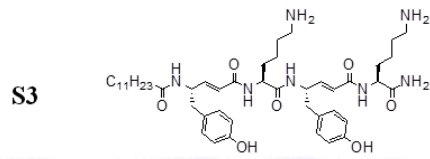


S2

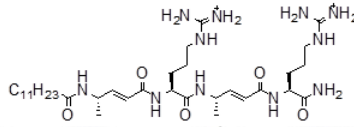


Final - Shots 400 - IISER: Run #420; Label H14

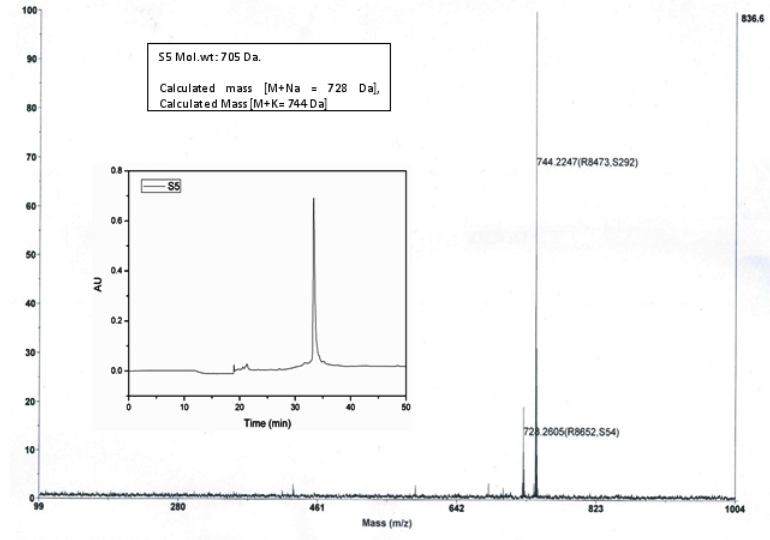




S5



Final - Shots 450 - HNG GROUP, Label N9

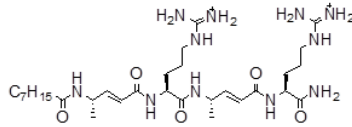


ERHNG GROUP Label N9 Run # 434

Page 1

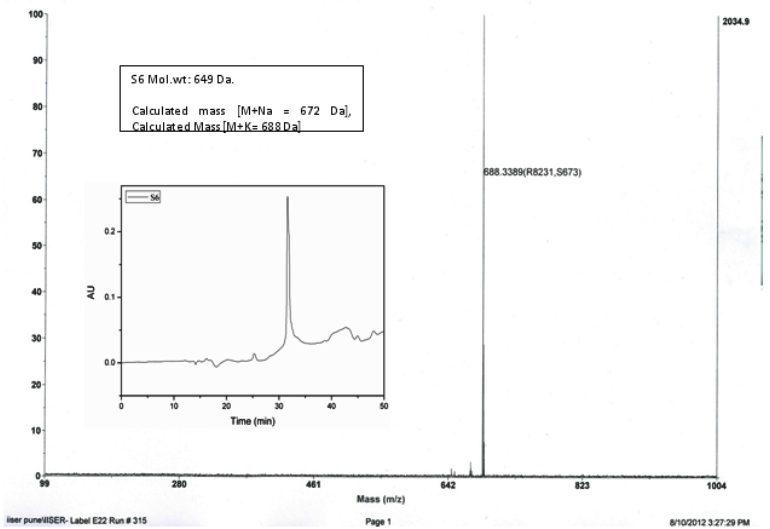
7/29/2012 3:46:21 PM

S6



Spectrum Report

Final - Shots 450 - IISER, Label E22

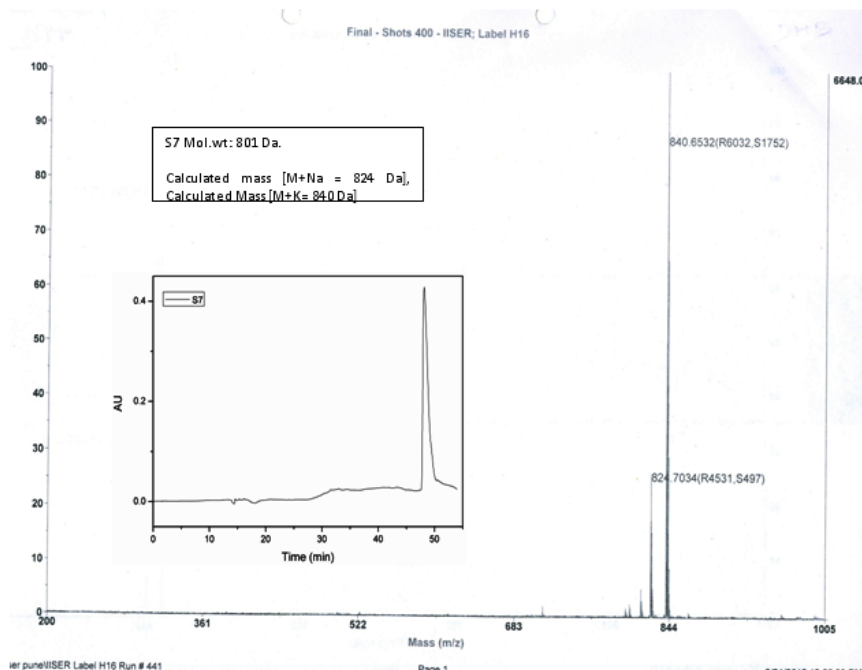
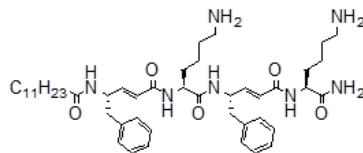


IISER punj/IISER- Label E22 Run # 315

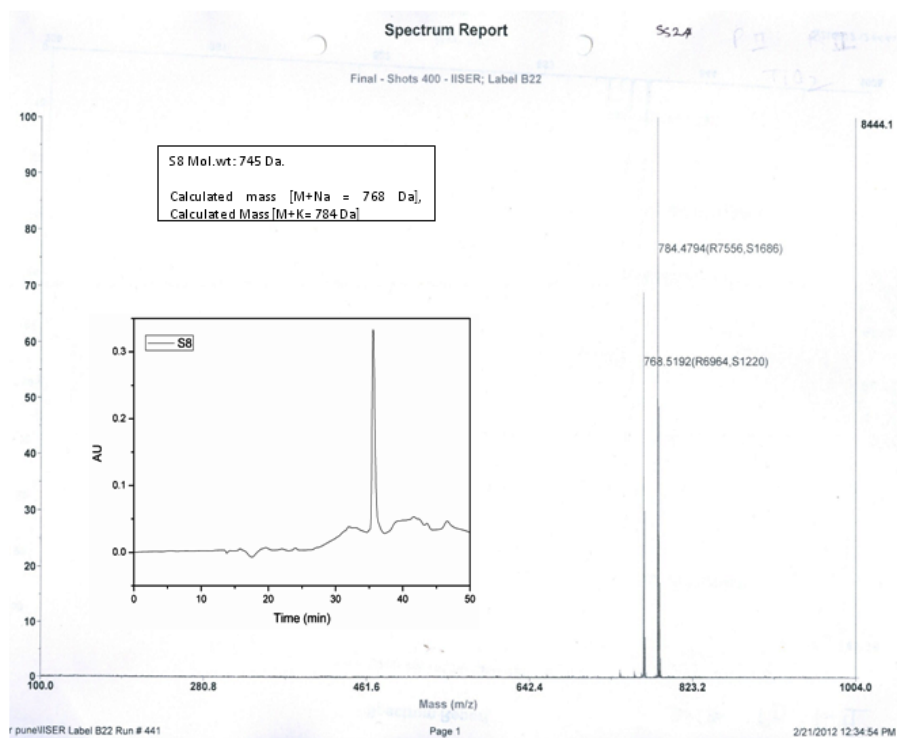
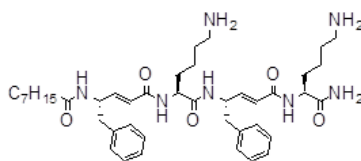
Page 1

8/10/2012 3:27:29 PM

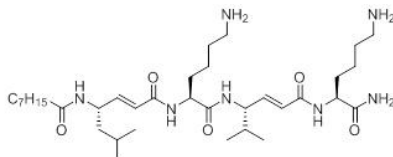
S7



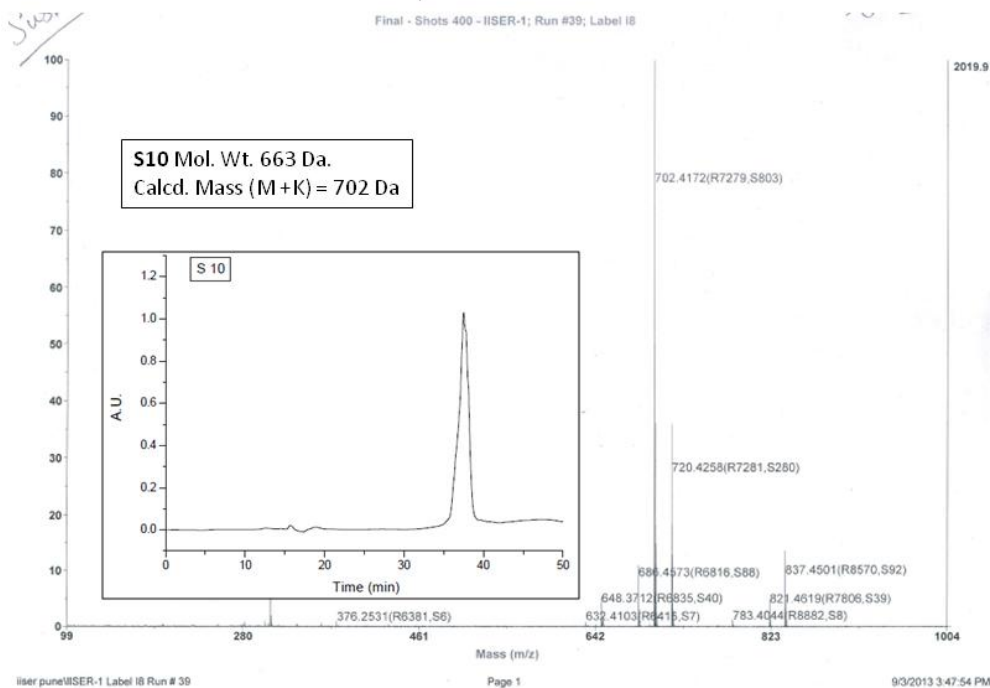
S8



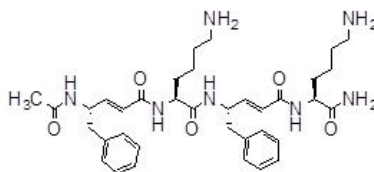
S9



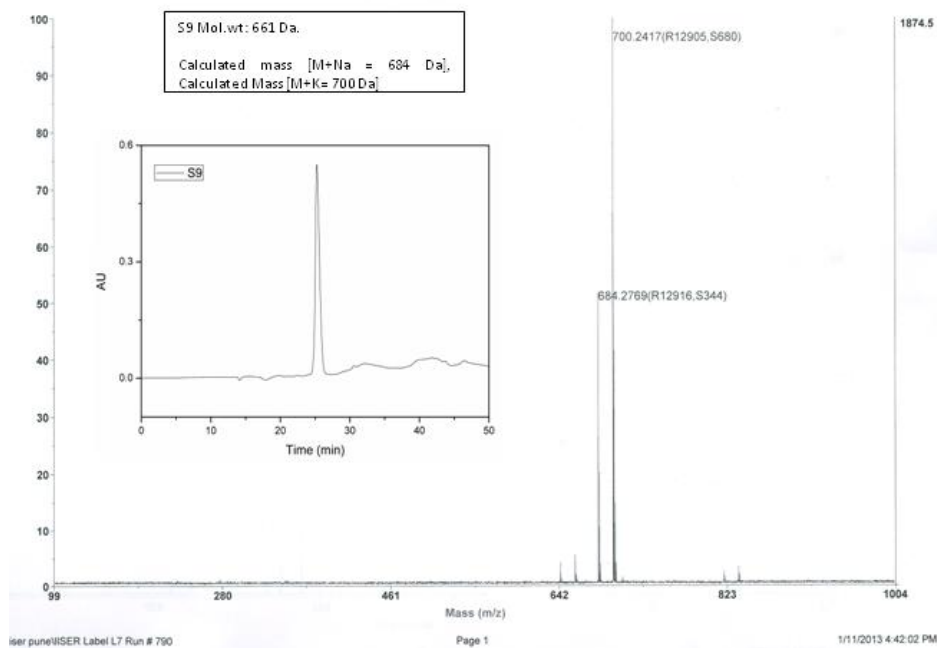
Final - Shots 400 - IISER-1; Run #39; Label I8



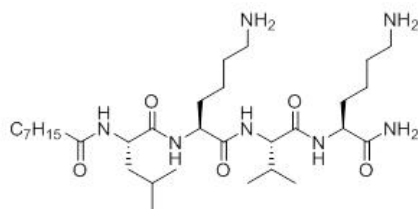
S10



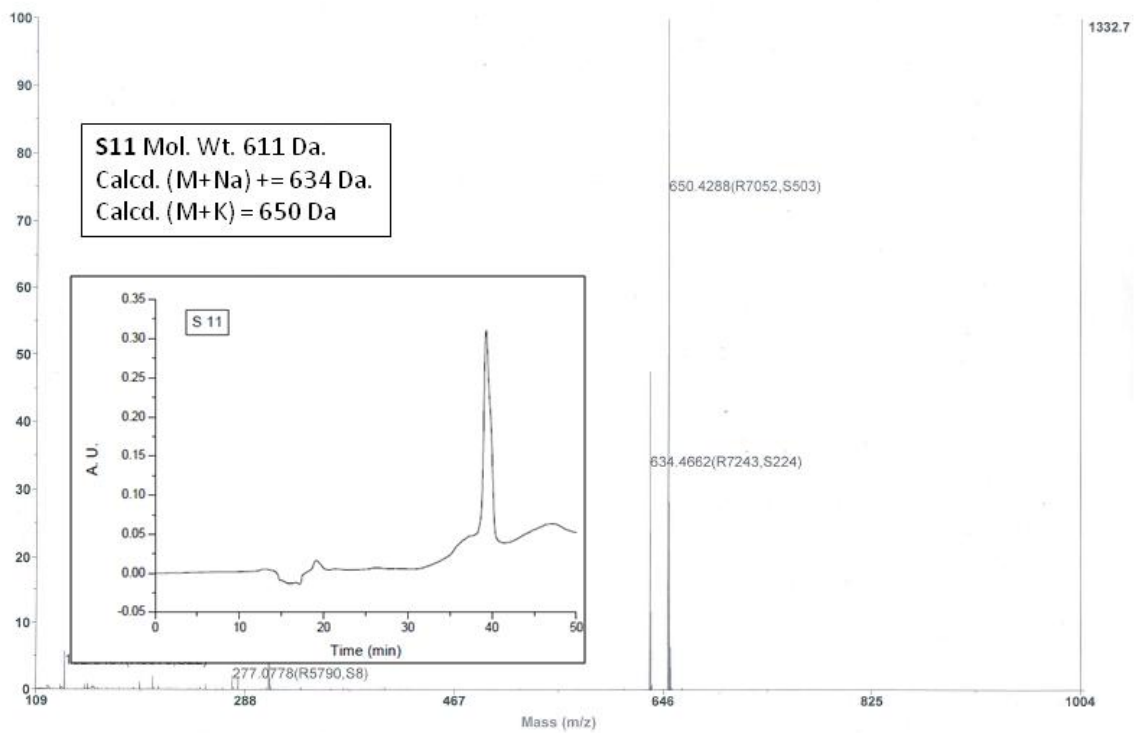
Final - Shots 400 - IISER; Run #790; Label L7



S11



Final - Shots 400 - IISER-2; Label M24



Chapter 3

Chapter 3a

Potent Antimicrobial Activity of Lipidated Short α , γ - Hybrid Peptides

3a.1 Introduction

In chapter 2, we have demonstrated the design and broad spectrum antimicrobial activities of α,γ -hybrid peptides containing 1:1 alternating α - and *E*-vinylogous γ -amino acids. The *E*-vinylogous amino acids have been used as starting materials for the synthesis of γ -amino acids.¹ In addition, we have recently demonstrated utility of the esters of *E*-vinylogous γ -amino acids as Michael acceptors to derive β -substituted γ -amino acids. Using nitromethane Michael donor, we have synthesized a variety of β -nitromethyl substituted γ -amino acids² and demonstrated their utility in design of hybrid peptide

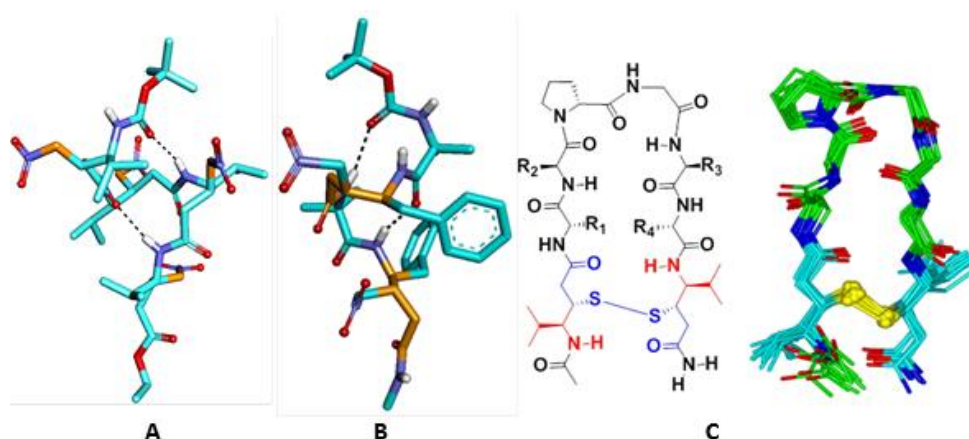


Figure 3a.1: A) 14-Helix from the tetrapeptide of β -nitromethyl substituted γ -Val homooligomer. B) 12-Helix conformation of a tetrapeptide composed of 1:1 alternating α -amino acid, Aib and β -nitromethyl substituted γ -Phe. C) Utilization of β -sulfhydryl γ -Val in the design of stable β -hairpin mimetics.

foldamers (Figure 3a.1A).³ In addition to the nitromethyl substituted γ -amino acids, our group also demonstrated the synthesis of β -sulfhydryl γ -amino acids and their utility in the design of β -hairpin mimetics.⁴ Nevertheless, antimicrobial activities of γ - and α,γ -hybrid peptides have not been systematically investigated.

As discussed in the previous chapter, the cationic host-defence antimicrobial peptides (AMPs) and native lipopeptides have attracted considerable attention due to their broad spectrum antimicrobial activity.⁵ Nevertheless, their inherent limitations such as higher haemolytic activity, poor selectivity and bioavailability and high toxicity of natural AMPs and native lipopeptides have hindered their potential therapeutic values. To improve their activity and selectivity, Shai and colleagues⁶ and others⁷ have designed a variety of short lipopeptides and examined their potential antimicrobial properties. In addition to the lipopeptides consisting of completely L-amino acids as well as alternating L- and D-amino acids,⁸ Schweizer and colleagues demonstrated the antimicrobial activity of short lipo- β -peptides.⁹ Besides the utility of β -peptides to mimic protein secondary structures,¹⁰ they have also been explored to design potent antimicrobial candidates.¹¹ In addition to the β -peptides, potential of γ -peptides built from γ -amino acids have been examined to derive protein secondary structure mimetics.¹² In contrast to β -peptides, the antimicrobial activity of γ -peptides have not been systematically investigated. The advantage of β - and γ -peptides compared to the α -peptides is that they are proteolytically and metabolically stable.¹³ We hypothesize that the conformationally flexible γ - and hybrid γ -peptides can be explored to design potent antimicrobial candidates.

3a.2 Aim and rational of the present work

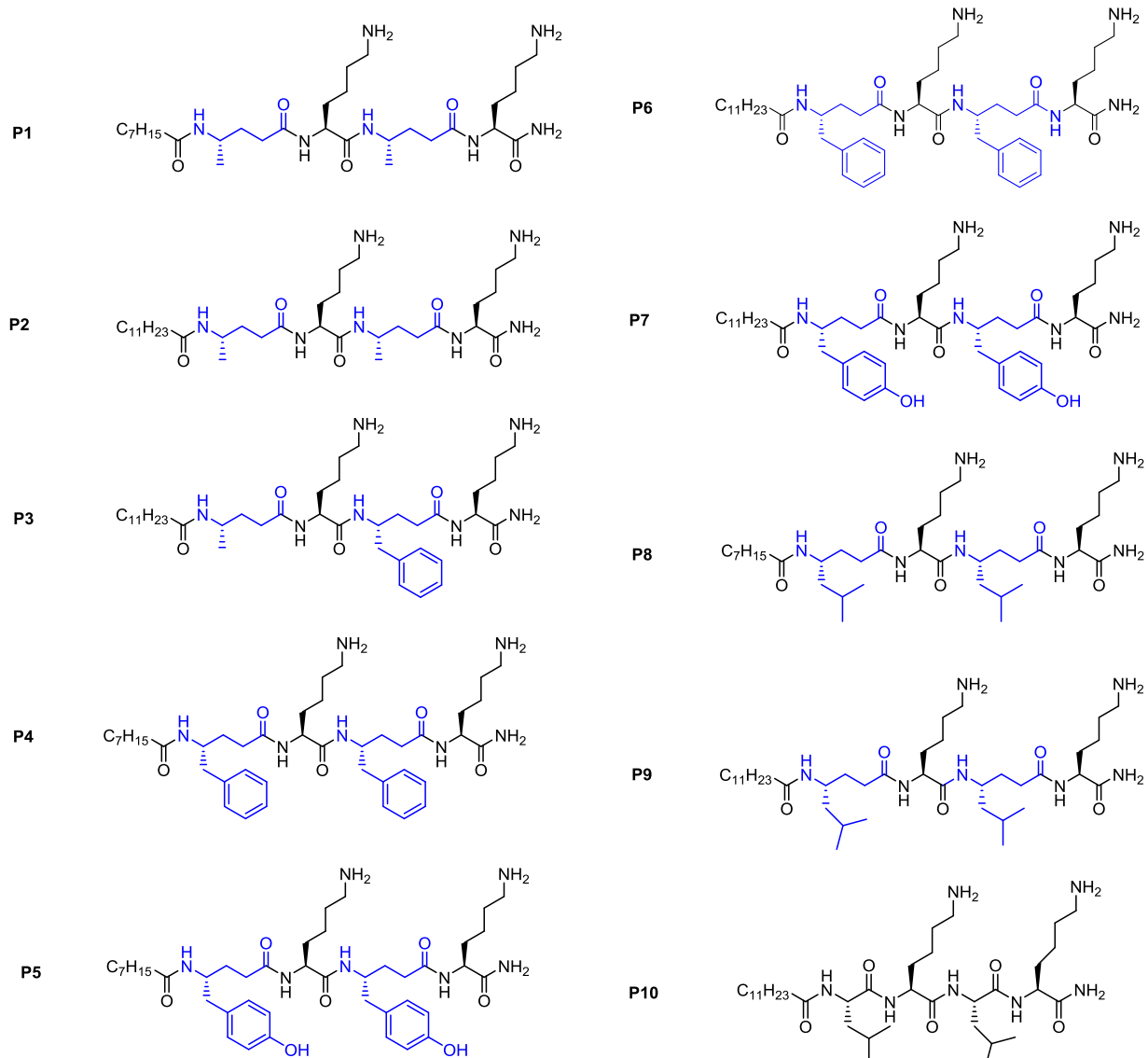
In the previous chapter, we have studied the antimicrobial activities of the short lipopeptides composed of α - and *E*-vinyllogous residues. In this chapter, we sought to investigate the antimicrobial activities of short α,γ -hybrid peptides composed saturated γ -amino acids. Here in, we are reporting the design, synthesis and antimicrobial activity of various short α,γ -hybrid lipopeptides composed of saturated γ -amino acids. In addition to their

antibacterial activity, we also investigated their mechanism of action and hemolytic activity. In comparison with α -peptide counterparts, these short α,γ -hybrid lipopeptides showed potent antimicrobial activity against various bacterial strains and lower hemolytic activity. Additionally, the time kill kinetics assay was performed to assess the amount of time required for complete killing of bacteria.

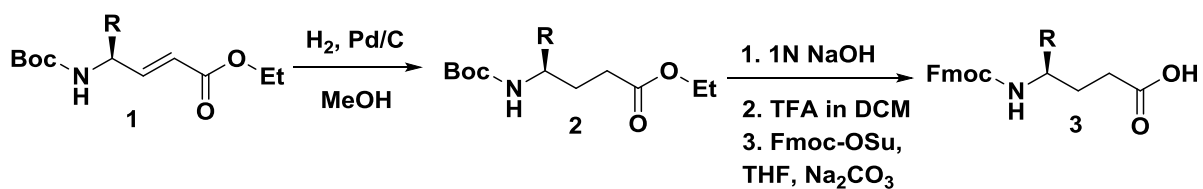
3a.3 Results and Discussion

3a.3.1 Design and synthesis of peptides

To examine the antimicrobial activity of short α,γ -hybrid lipopeptides, we have designed nine α,γ -hybrid peptides (**P1-P9**) and an α -peptide **P10**. The sequences of these lipopeptides are shown in the Scheme 3a.1. We have utilized both octanoic acid and dodecanoic acid to understand the importance of lipids in antimicrobial activity. Required γ -amino acids (γ -Ala, γ -Leu, γ -Tyr and γ -Phe) were synthesized starting from α , β -unsaturated γ -amino esters through catalytic hydrogenation.¹⁴ The *N*-Boc protected γ -amino esters were subsequently hydrolyzed to corresponding free carboxylic acids. Finally, the Boc- group was deprotected using TFA and the free amine was protected again with solid phase compatible Fmoc- group. Schematic representation of the synthesis of γ -amino acids is shown in Scheme 3a.2. Using solid phase synthesis, we have synthesized all peptides on Knorr amide resin. All α,γ -hybrid peptides and the control α -peptide were purified using reverse phase-HPLC on a C₁₈ column. The α,γ -lipopeptides and the control α -peptide were subjected to antimicrobial and haemolytic activity.



Scheme 3a.1. Sequences of α,γ -hybrid lipopeptides (**P1-P9**) and control α -lipopeptide (**P10**).



R= -CH₃ (**a**, γ Ala); -CH₂-Ph (**b**, γ Phe); -CH₂-C₆H₄-OH (**c**, γ Tyr); -CH₂-CH(CH₃)₂ (**d**, γ Leu)

Scheme 3a.2: Schematic representation of the synthesis of solid phase compatible Fmoc- γ -amino acids.

3a.3.2 MIC determination

We examined the antibacterial activity of short lipopeptides, **P1-P10** against Gram negative bacteria *Escherichia coli* (NCIM 2065), *Escherichia coli* K12 (NCIM2563), *Klebsiella pneumoniae* (NCIM 2957), *Pseudomonas aeruginosa* (NCIM 5029), *Salmonella typhimurium* (NCIM 2501) and Gram positive *Staphylococcus aureus* (NCIM 5021). The antibacterial activity of all peptides were carried out using microbroth dilution method in a 96-well microtiter plate. The minimum inhibitory concentration (MIC) was measured in triplicate and average values are given in the Table 3a.1. Among all α,γ -hybrid lipopeptides, peptides coupled with dodecanoic acid showed better antimicrobial activity than the peptides coupled with octanoic acid. Among the dodecanoic acid coupled α,γ -hybrid peptides (**P2**, **P3**, **P6**, **P7** and **P9**), peptide **P9** with γ -Leu residues was found to be the best antimicrobial candidate. They inhibit various Gram negative and Gram Positive bacteria with low MIC (6 $\mu\text{g/mL}$) value. The excellent activity of **P9** among all the hybrid peptides motivated us to design α -peptide analogue **P10**. More interestingly, the α -peptide counterpart displayed much higher MIC value under identical conditions. Replacing dodecanoic acid by octanoic acid (**P8**) leads to drastic decrease in the antimicrobial activity of the peptide. Among the C₈-fatty acid containing peptides, **P8** was found to be the best. The α -peptide counterpart of **P9**, peptide **P10** showed poor antimicrobial activity under identical conditions. It is worth mentioning that both amino acids side-chains and fatty acids play crucial role in the antimicrobial activity.

Table 3a.1. Minimum inhibitory concentration* of α,γ -hybrid lipopeptides in $\mu\text{g/mL}$

Bacteria	P1	P2	P3	P4	P5	P6	P7	P8	P9	P10
<i>E. coli</i>	>250	163	32	250	>250	13	26	170	6	>250
<i>E. coli K12</i>	>250	163	32	250	>250	26	26	85	12	>250
<i>K. pneumoniae</i>	>250	81	16	125	97	6	3.3	85	3	>250
<i>P. aeruginosa</i>	>250	163	16	62	97	13	13	42	6	>250
<i>S. aureus</i>	>250	81	16	125	195	13	13	85	6	>250
<i>S. typhimurium</i>	>250	81	8	62	195	13	6	42	6	>250
Hemolysis	>250	135	93	>250	>250	136	26	>250	183	>250
HD₁₀										

*The experiments were performed in triplicates and the least concentration of peptide required for complete killing of bacteria is reported as minimum inhibitory concentration (MIC).

3a.3.3 Hemolytic activity of lipopeptides

The encouraging antimicrobial activity of short α,γ -hybrid lipopeptides motivated us to investigate their haemolytic activity. We subjected all lipopeptides including control α -peptide **P10** for the haemolytic assay. Results of haemolytic activity of all lipopeptides are shown in Figure 3a.2. The HD₁₀ values are given in the Table 1. Among the active peptides, peptide **P7** with γ -Tyr residues and **P3** with γ -Ala and γ -Phe were found to most haemolytic in the series. Highly active peptide **P9** showed comparatively less haemolytic activity.

The active peptide **P6** with γ -Phe was found to be relatively less haemolytic than **P7**. More importantly, at their MICs these peptides are not haemolytic. Further, the peptides which displayed weak antimicrobial activity (**P1**, **P4**, **P5** and **P8**) were also found to be less haemolytic.

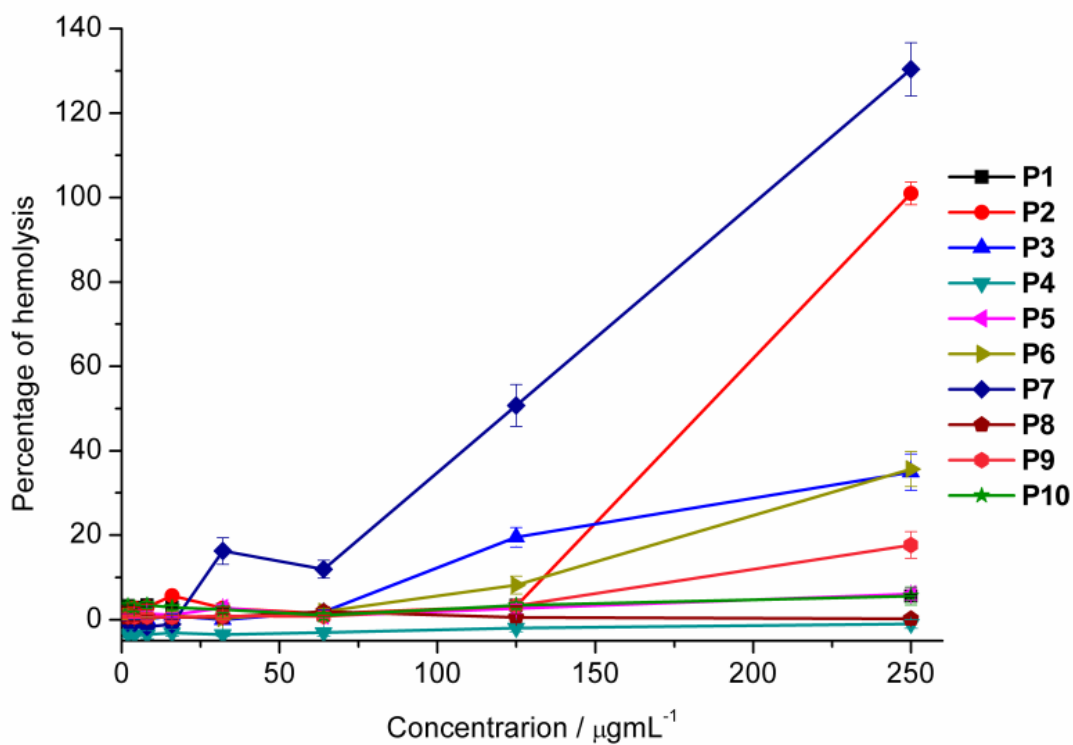


Figure 3a.2. Hemolytic activity of short lipopeptides

3a.3.4 Membrane deformation study

As α,γ -hybrid lipopeptides **P6** and **P9** inhibit the growth of Gram positive and Gram negative bacteria with comparable MIC values across the panel motivated us to examine their mode of action. In order to understand whether these peptides act through membrane disruption similar to other native antimicrobial peptides,⁵ we undertook Field-emission scanning electron microscopy analysis (FE-SEM). Figure 3a.3 depicts the FE-SEM images of the bacteria before and after the treatment of peptides **P6** and **P9**.

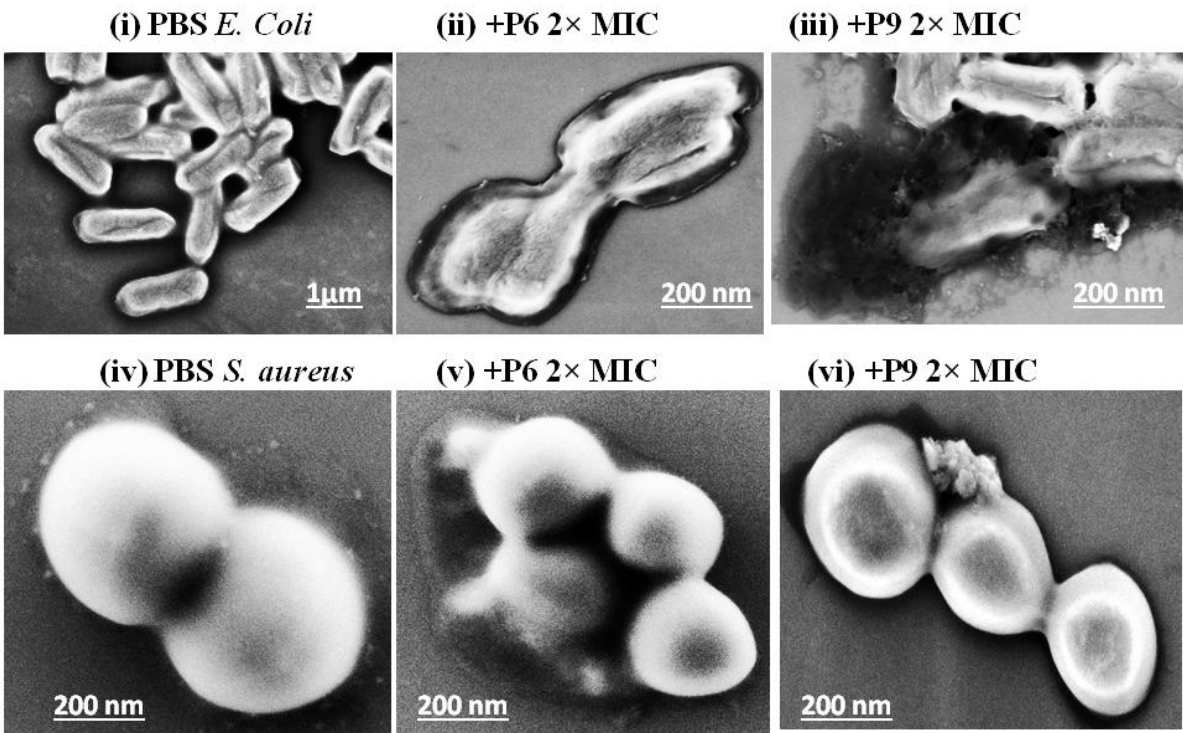


Figure 3a.3 FE-SEM images of bacteria *E. coli* K12 (i) and *S. aureus* (iv) without lipopeptides. Images of *E. coli* after the treatment with lipopeptides **P6** (ii) and **P9** (iii). Images of *S. aureus* after the treatment with lipopeptides **P6** (v) and **P9** (vi).

The FE-SEM images clearly suggested the change in morphology of the microorganisms after the treatment of α,γ -hybrid lipopeptides. These results indeed indicate that the α,γ -hybrid lipopeptides disrupt the bacterial membrane.

3a.3.5 β -galactosidase leakage assay

In order to authenticate whether these peptides really disrupt the bacterial membrane, β -galactosidase leakage experiment was performed using *E. coli* containing LacZ reporter gene.¹⁵ The β -galactosidase is expected to leak out from the *E-coli* upon disruption of the bacterial cell wall. The peptides **P6** and **P9** were incubated with *E. coli* (TOP 10) and the release of β -galactosidase was measured using standard fluorogenic substrate, 4-methylumbelliferyl- β -galactosidase. The results are shown in the Figure 3a.4.

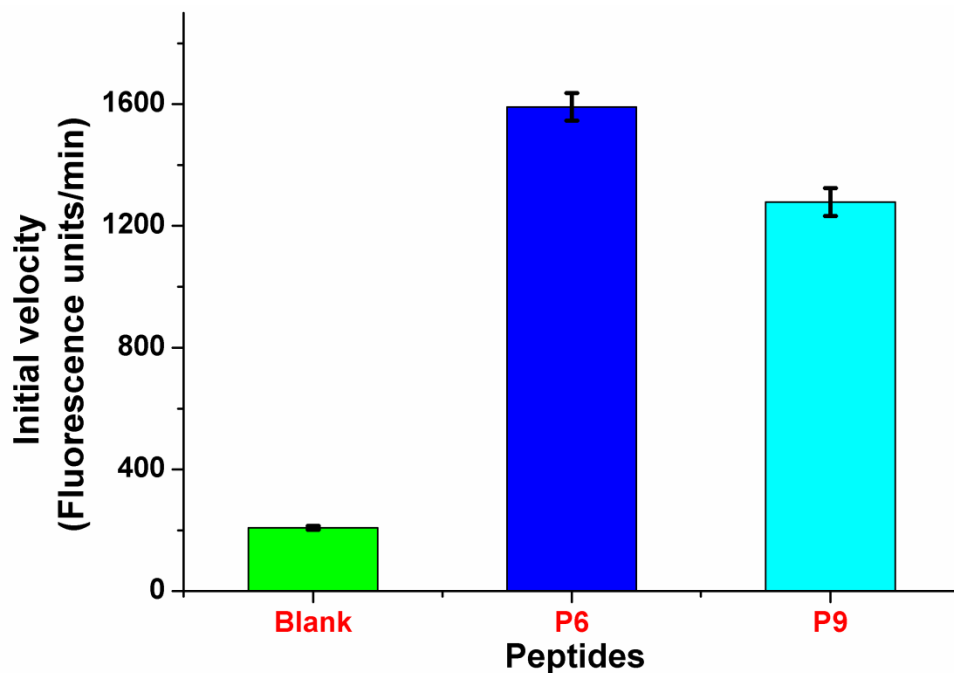


Figure 3a.4 Peptide mediated β -galactosidase leakage. The height of the graphs indicates the relative amount of β -galactosidase present in the medium after the treatment of peptides.

Increased fluorescence intensity indicating the release of β -galactosidase upon the treatment of lipopeptides. In contrast, no β -galactosidase release was observed in the control experiment without lipopeptides. The enzyme leakage assay suggested that these lipopeptides bind and disrupt the bacterial cell membrane.

3a.3.6 Time kill kinetics assay

The potent antibacterial activity of lipopeptide **P9** inspired us to further evaluate its activity through time kill kinetics assay. This experiment gives the information about the rate at which the lipopeptide is acting on the bacteria

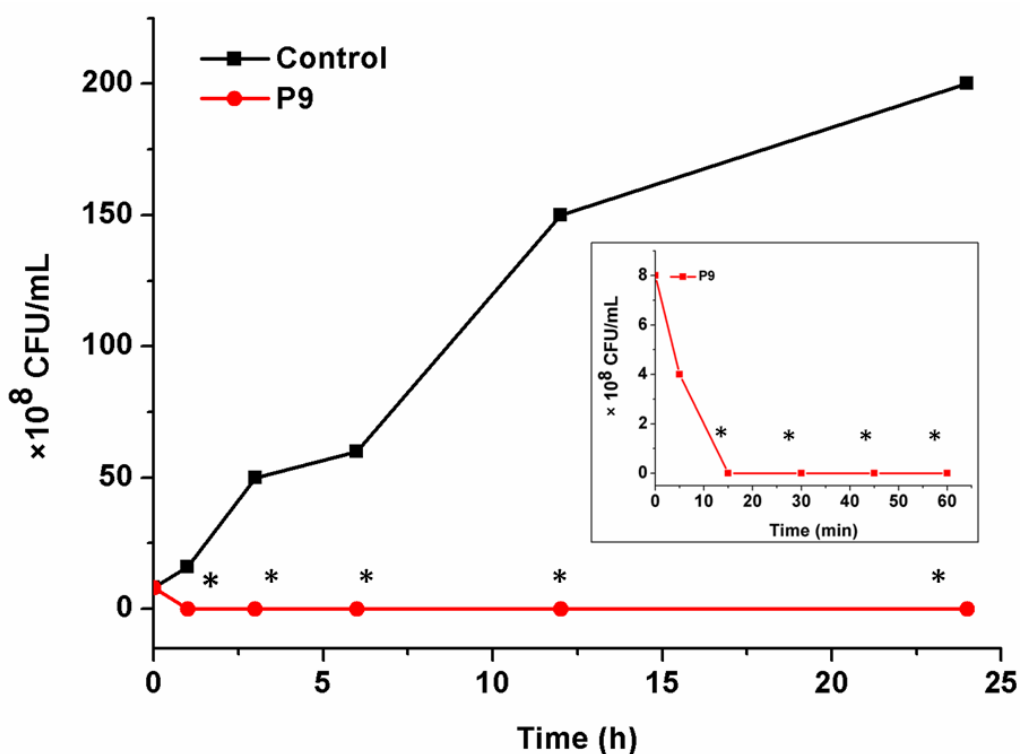


Figure 3a.5. Time–kill kinetics of peptide **P9** ($2 \times$ MIC) against *K. pneumoniae* (asterisks correspond to <50 CFU/mL). (The experiments were performed in triplicates and the average CFU values are reported.)

. We selected *K. pneumoniae* for time kill kinetics experiment as the peptide displayed better MIC values against this microorganism. The peptide was incubated with the bacterial solution at $2 \times \text{MIC}$ (6 $\mu\text{g/mL}$) and 20 μL of the peptide treated bacterial solution was drawn with increasing time intervals and diluted to ten times using 0.9% saline and plated again on Mueller Hinton agar plates. After incubating for about 24 h, the bacterial colonies were counted. These results were represented in CFU/mL scale. Results of time kill kinetics assay are shown in Figure 3a.4. These results clearly suggested that the lipopeptide **P9** completely eradicate the bacteria within 20 min.

3a.4 Conclusion:

In conclusion, we have shown the potent antibacterial activity and the mechanism of action of short α,γ -hybrid lipopeptides. The hybrid peptides coupled with dodecanoic acids showed better activity compared to the octanoic acid coupled hybrid peptides. Among the active lipopeptides, peptides composed of aromatic residues showed higher haemolytic activity compared to peptides with aliphatic residues. The mechanism of action suggested that these cationic lipopeptides bind and disrupt the bacterial cell wall. Informatively, lipopeptide **P10** with α -amino acid showed weaker antimicrobial activity compared to the α,γ -hybrid lipopeptides. Moreover, the time kill kinetics assay suggested that the lipopeptide **P9** completely inhibit the growth of bacteria within 20 min. Overall, the potent antibacterial activity, mechanism of action, and fast killing of bacteria, less haemolytic activity displayed by the short α,γ -hybrid peptides, particularly peptide **P9**, provided an unique opportunity to further design peptide antibiotics.

3a.5 Experimental section

3a.5.1 General experimental details

. All reagents, amino acids, solvents were obtained from commercial sources and used without further purification. Peptides were purified through reverse phase HPLC on a C₁₈ column using MeOH/H₂O gradient. ¹H NMR spectra were recorded on 400 MHz and ¹³C NMR on 100 MHz spectrometer using residual solvent as internal standard (DMSO-*d*₆ δ_H , 2.5 ppm, δ_C 39.51 ppm) The chemical shifts (δ) were reported in ppm and coupling constant (*J*) in Hz. Mass spectra of the peptides were obtained from the MALDI-TOF/TOF.

3a.5.2 Synthesis of *N*-Fmoc-protected γ -amino acids

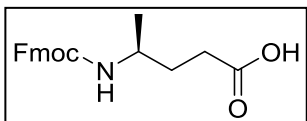
Boc- α , β -unsaturated γ -amino acid (2 mmol) was dissolved in 5 mL of ethanol under inert atmosphere. Then 20% Pd/C was added slowly to the reaction mixture and the reaction mixture was stirred under Hydrogen atmosphere for 2 hours. After completion of the reaction, Pd/C was filtered and ethanol was evaporated from the reaction mixture to give Boc- γ -amino acid as gummy product in a quantitative yield.

The Boc- γ gamma amino acid (1 mmol) was dissolved in 5 mL of DCM and cooled to 0 °C in ice bath followed by 5 mL of neat TFA was added to the reaction mixture. After 30 min, TFA was removed from reaction mixture under *vacuum*. Residue was dissolved in 15 mL of water (15 mL) and the pH was adjusted to ~10 by the slow addition of solid Na₂CO₃. The solution of Fmoc-OSu (1 mmol) in 10 mL of THF was added slowly to the reaction mixture at 0 °C. Reaction mixture was stirred overnight at RT. After completion of the reaction, the reaction mixture was acidified with 20 mL of 20% HCl (20% volume in water) in cold condition. Product

was extracted with ethyl acetate (3× 50 mL). Combined organic layer was washed with brine (30 mL) and dried over anhydrous Na₂SO₄. The solvent was concentrated under reduced pressure to give gummy product, which was recrystallized using EtOAc/Pet-ether. The pure Fmoc- γ -amino acid was utilised for SPPS.

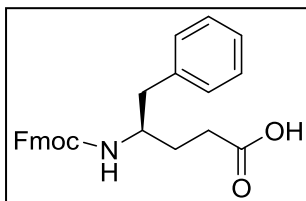
(S)-4-(((9H-fluoren-9-yl)methoxy)carbonyl)amino)pentanoic acid (3a)

White solid; yield (83%) m. p. 148-150 °C ; $[\alpha]_D^{25} +6.0^\circ$ (c 1.0, MeOH); ¹H NMR (400 MHz, DMSO-*d*₆) δ 11.98 (s, 1H, COOH), 7.83(d, 2H, aromatic), 7.64 (d, 2H, aromatic), 7.35 (t, 2H, aromatic), 7.27 (t, 2H, aromatic), 7.11 (d, 1H), 4.28-4.15 (m, 3H), 3.97-3.43(m, 1H), 2.14 (t, 2H), 1.58-1.50 (m, 2H), 0.98 (d, 3H): ¹³C NMR (100 MHz, DMSO-*d*₆) δ 193.8, 174.8, 156.1, 144.4, 141.2, 128.1, 127.5, 120.6, 65.6, 47.3, 46.4, 40.6, 31.7, 31.0, 21.3; *m/z* value for C₂₀H₂₁NO₄ [M+Na]⁺ 362.1368 (calcd), 362.1376(observed).



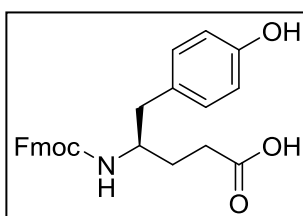
(R)-4-(((9H-fluoren-9-yl)methoxy)carbonyl)amino)-5-phenylpentanoic acid(3b)

White solid; yield (85%) mp.143-145 °C ; $[\alpha]_D^{25} -10.4^\circ$ (c 1.0, MeOH); ¹H NMR (400 MHz, DMSO-*d*₆) δ 12.00 (br, 1H), 7.82 (d, 2H), 7.58 (d, 2H), 7.35 (t, 2H), 7.26 (t, 2H), 7.17 (t, 3H), 7.12 (d, 2H), 6.9 (d,1H), 4.16 (d, 2H), 4.08 (d, 2H), 3.63-3.57(m, 1H), 2.63(d, 2H), 2.24-2.08 (m, 2H), 1.69-1.63(m, 1H), 1.55-1.46 (m, 1H) ¹³C NMR (100 MHz, DMSO-*d*₆) δ 174.8,156.2, 144.4, 141.2, 139.4, 129.7, 128.6, 127.5, 126.5, 125.7, 120.6, 65.6, 52.2, 47.3, 41.0, 40.6, 30.9, 29.9; *m/z* value for C₂₅H₂₅NO₄ (M+Na⁺). 438.1681 (calcd), 438.1147(observed).



(R)-4-((((9H-fluoren-9-yl)methoxy)carbonyl)amino)-5-(4-hydroxyphenyl)pentanoic acid(3c)

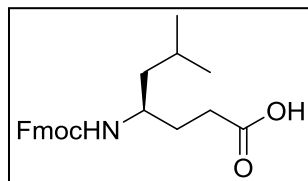
White solid; yield (80%) mp.162-164 °C ; $[\alpha]_D^{25}$ -9.0° (c 1.0, MeOH); ^1H NMR (400 MHz, DMSO- d_6) δ 7.77 (d, 2H), 7.73 (d, 1H), 7.54 (d, 2H), 7.31 (t, 3H), 7.25-7.21 (m, 3H), 7.09 (d, 1H), 6.85 (d, 1H), 6.53 (d, 1H), 6.17 (s, 1H), 4.16-4.05 (m, 3H), 2.49-2.45 (m, 2H), 2.26-2.21(m, 1H), 2.15-2.02 (m, 2H), 1.63-1.50 (m,1H), 1.49-1.37 (m, 1H) ^{13}C NMR (100 MHz, DMSO- d_6) δ 174.9,156.2, 144.4, 143.1, 141.2, 139.9, 137.9, 130.5, 129.5, 128.1, 127.8, 127.6, 125.7, 121.9, 120.6, 115.4, 110.3, 65.6, 52.5, 47.3, 40.6, 31.1, 29.9 ; m/z value for $\text{C}_{26}\text{H}_{25}\text{NO}_5$ $[\text{M}+\text{Na}]^+$ 454.1630 (calcd), 454.2030.



(R)-4-((((9H-fluoren-9-yl)methoxy)carbonyl)amino)-6-methylheptanoic acid(3d).

White solid; yield (87%), mp.130-132 °C ; $[\alpha]_D^{25}$ -3.4° (c 1.0, MeOH); ^1H NMR (400 MHz, DMSO- d_6) δ 7.88 (d, 2H), 7.69 (d, 2H), 7.41 (t, 2H), 7.31(t, 2H), 7.04 (d, 1H), 4.31 (d, 2H), 4.22 (t, 1H), 3.56-3.44(m, 1H), 2.17 (t, 2H), 1.76-1.38 (m, 1H), 1.65-1.57 (m, 2H), 1.44-1.38 (m, 1H), 1.29-1.19 (m, 1H), 0.85 (d, 7H) ^{13}C NMR (100 MHz, DMSO- d_6) δ 175.3, 155.9,

144.7, 140.6, 129.3, 128.2, 127.1, 125.8, 124.9, 121.8, 111.6, 65.4, 48.3, 47.2, 44.8, 30.7, 24.8, 23.3, 21.9; m/z value for $C_{23}H_{27}NO_4$ $[M+Na]^+$ 404.1838(calcd), 404.1837 (observed).



3a.5.3 Synthesis of peptides

All peptides were synthesized on Knorr amide resin at 0.25 mmol scale using standard Fmoc-chemistry. All coupling reactions were performed using HBTU along with HOBt and monitored by Kaiser Test. Finally, peptides were cleaved from the resin using the combination of TFA: water: thioanisole (98:1:1) and filtered. The cleavage solution was evaporated under reduced pressure to obtain crude product. The crude peptides were purified through reverse phase HPLC on C_{18} column using MeOH/ H_2O gradient.

3a.5.4 Procedure for determining antibacterial activity

The bacterial strains *Escherichia coli* (NCIM 2065), *Escherichia coli* K12 (NCIM2563), *Klebsiella pneumoniae* (NCIM 2957), *Pseudomonas aeruginosa* (NCIM 5029), *Salmonella typhimurium* (NCIM 2501), *Staphylococcus aureus* (NCIM 5021) used for the antibacterial activity were obtained from National Collection of Industrial Microorganisms (NCIM).

The antibacterial activity of peptides were carried out in a 96-well microtiter plate using microbroth dilution method. The cultures of bacteria were incubated over night at 37 °C, and the solution was diluted with sterile MHB (Muller-Hinton broth) medium to a concentration of 10^6 colony forming units/mL. Increasing concentration of peptides **P1-P10** with the volume of 50

μL was added to the 50 μL bacterial suspension to each well, and incubated for about 18 h at 37 °C. Control experiment was performed without peptides. The inhibition of the growth of bacteria was monitored through measuring the absorbance at 492 nm. The lowest peptide concentration required for the complete killing was defined as the MIC value.

3a.5.5 Procedure for hemolysis assay

Hemolytic activity was performed on human red blood cells (hRBCs). The fresh hRBCs collected with EDTA were washed four times with Tris-buffered saline (10 mM Tris, 150mM NaCl, and pH 7.2). The hRBCs were again diluted to 4% v/v with Tris buffer. To the solution of hRBCs (50 μL), increasing concentration of the peptides in Tris buffer were added by keeping the total volume 100 μL . The combined hRBCs and peptides solution was incubated at 37 °C for about 1 h. After 1 h, the solution was centrifuged for about 15 min at 3000 rpm. The supernatant (50 μL) of the each well was transferred to another 96-well plated and diluted with 50 μL of water and measure the absorbance of released hemoglobin at 540 nm. Simple Tris buffer without peptides was used as a negative control and 1% Triton-X was used as a positive control. All experiments were performed in triplicate.

3a.5.6 FE-SEM analysis

Peptides **P6** and **P9** (100 μL) at $2 \times \text{MIC}$ values were pipetted into a 96-well cell culture plate. To this peptide solution, 100 μL of either *E. coli* or *S. aureus* bacterial solution in Mueller Hinton broth was added. The bacterial concentration was adjusted to 0.1-0.2 optical density at 600 nm. The peptide treated bacterial solution was incubated for about 2 h at 37 °C. The bacterial cells were centrifuged and the pellet was washed with PBS. Using 2.5% glutaraldehyde the cells were fixed and washed with PBS. The bacterial cells were centrifuged and washed with

30%, 50%, 70%, 95%, and 100% graded ethanol solution and finally with water. Finally, the dried bacterial cells were mounted on a silicon wafer and imaged under a field emission scanning electron microscope after the gold coating.

3a.5.7 Procedure for β -Galactosidase leakage assay

Membrane deformation studies were performed using *Escherichia coli* (TOP10, Invitrogen) cells containing LacZ reporter gene as reported earlier. Briefly, 90 μ L of Luria Bertani broth containing the *E.coli* cells producing β -galactosidase were incubated separately with 10 μ L (200 μ g/mL) of peptides **P6** and **P9**. After incubating for about 1h, the bacterial solution was centrifuged for 10 min at 4000 rpm. The clear supernatant solution (80 μ L) was treated with 20 μ L (400 μ g/mL) of 4-methylumbelliferyl- β -galactosidase indicator. The release of the β -galactosidase was monitored for about 1 h by recording the fluorescence emission at 445 nm after exciting the solution at 365 nm. The linear plot of fluorescence versus time gave the initial velocity of the enzyme reaction. The control experiment was performed without peptides.

3a.5.8 Procedure for time kill kinetics

To understand the rate at which the peptides can completely inhibit bacterial growth we have performed the time kill kinetics assay. The potent peptide **P9** (6 μ g/mL, $2 \times$ MIC)was added to the solution of *K. pneumoniae* grown in Mueller Hinton broth (approximately 1.8×10^5 CFU/mL) and incubated at 37 °C. From this solution, 20 μ L were drawn at 0, 1, 3, 6, 12, and 24 h intervals and diluted 10 times with 0.9% saline. The solution extracted at different time intervals were plated again on Mueller Hinton agar plates and incubated at 37 °C. Similar experiments were performed at shorter time intervals 0, 10, 20, 30, 45, and 60 min. After 24 h incubation, the bacterial colonies were counted.

3a.6 References

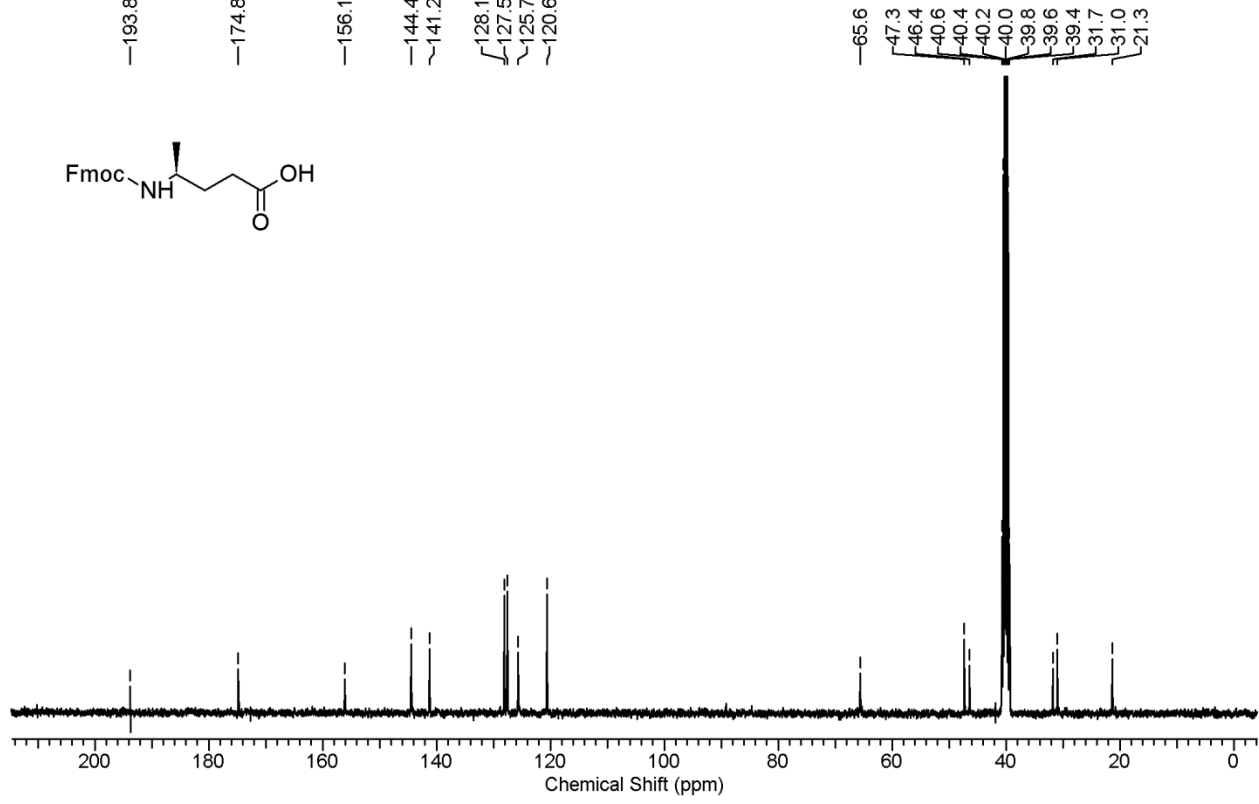
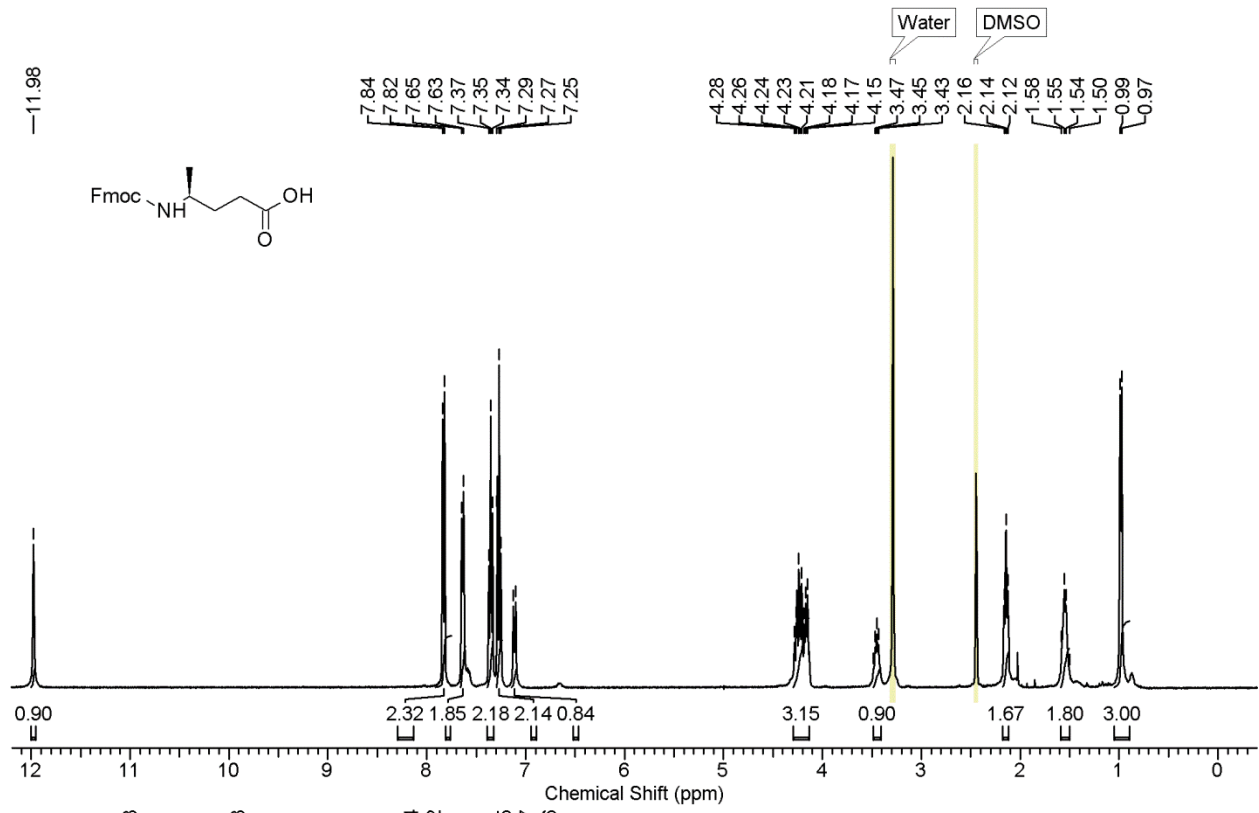
1. a) Hintermann, T.; Gademann, K.; Jaun B.; Seebach, D. *Helv. Chim. Acta*, **1998**, *81*, 983–1002. b) Brenner, M.; Seebach, D. *Helv. Chim. Acta.*, **2001**, *84*, 1181–1189 c) Hanessian, S.; Luo, X.; Schaum, R.; Michnick, S. *J. Am. Chem. Soc.*, **1998**, *120*, 8569–8570.
2. Mothukuri, G.; Mali, S. M.; Gopi, H. N. *Org. Biomol. Chem.*, **2013**, *11*, 803–813.
3. Mothukuri, G.; Gopi, H. N. *Org. Lett.* **2015**, *17*, 4738–4741.
4. Mothukuri, G.; Mali, S. M.; Raja, K. M. P.; Gopi, H. N. *Org. Lett.* **2015**, *17*, 230–233.
5. a) Hancock, R. E. W. *Lancet* **1997**, *349*, 418–422; b) Zasloff, M. *Nature* **2002**, *415*, 389–395; c) Maróti, G.; Kereszt, A.; Kondorosi, É.; Mergaert, P. *Res in Microbiol.* **2011**, *162*, 363–374; d) Hancock, R. E. W.; Sahl, H. -G. *Nat. Biotechnol.* **2006**, *24*, 1551–1557. d) Fjell, C. D.; Hiss, J. A.; Hancock, R. E. W.; Schneider G. *Nat. Rev.* **2012**, *11*, 37–51; e) Nguyen, L. T.; Haney, E. F.; Vogel, H. J. *Trends in Biotechnol.* **2011**, *29*, 464–472.
6. a) Oren, Z.; Shai, Y. *Biochemistry* **1997**, *36*, 1826–1835; b) Makovitzki, A.; Avrahami, D. ; Shai, Y. *Proc. Natl. Acad. Sci. USA* **2006**, *103*, 15997–16002; c) Avrahami, D.; Shai, Y. *J. Biol. Chem.* **2004**, *279*, 12277–12285; d) Makovitzki, A.; Baram, J.; Shai, Y. *Biochemistry* **2008**, *47*, 10630–10636; e) Arnusch, C. J.; Albada, H. B.; Vaardegem, M. V.; Liskamp, R. M. J.; Sahl, H-G.; Shadkchan, Y., Osherov, N.; Shai, Y. *J. Med. Chem.* **2012**, *55*, 1296–1302.
7. a) Hu, Y.; Amin, M. N.; Padhee, S.; Wang, R. E.; Qiao, Q.; Bai, G.; Li, Y.; Mathew, A.; Cao, C.; Cai, J. *ACS Med. Chem. Lett.* **2012**, *3*, 683–686. b) Toniolo, C.; Crisma, M.; Formaggio, F.; Peggion, C.; Epand, R. F.; Epand, R. M. *Cell. Mol. Life Sci.* **2001**, *58*, 1179–1188. c) Lavery, G.; McLaughlin, M.; Shaw, C.; Gorman, S. P.; Gilmore, B. F.

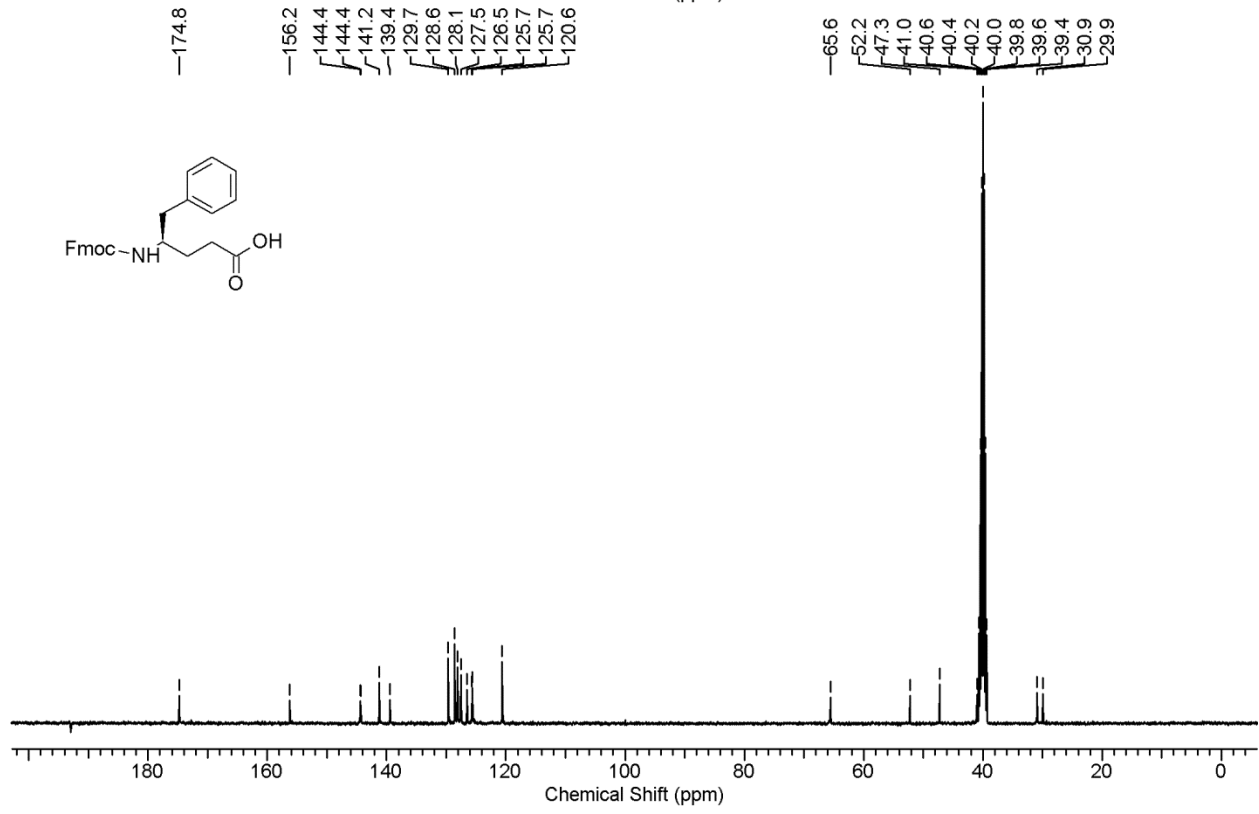
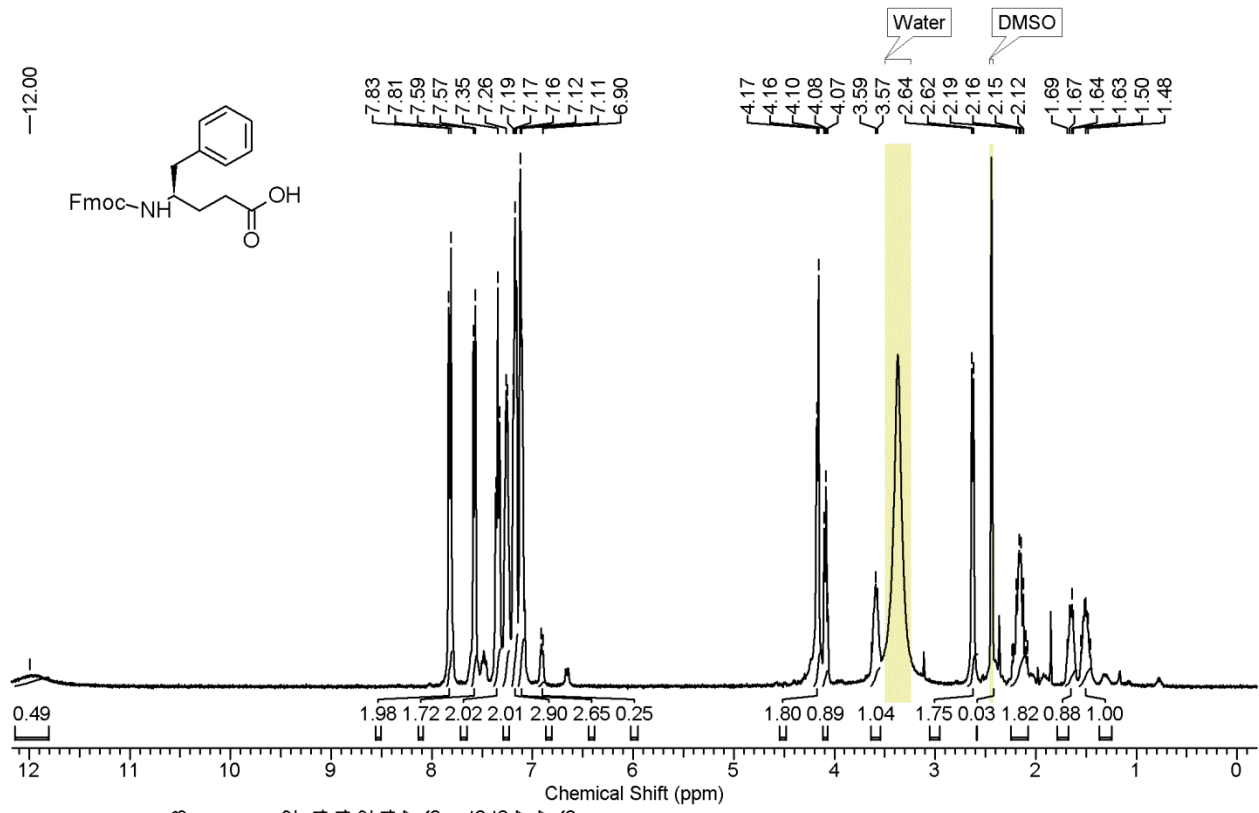
- Chem. Biol. Drug. Des.* **2010**, *75*, 563–569; d) Ghosh, C.; Konai, M. M.; Sarkar, P.; Samaddar, S.; Haldar, J. *ChemMedChem* **2016**, *11*, 2367-2371; e) Koh, J. -J.; Lin, H.; Caroline, V.; Chew, Y. S.; Pang, L. M.; Aung, T. T.; Li, J.; Lakshminarayanan, R Tan, .; D. T. H.; Verma, C.; Tan, A. L.; Beurman, R. W.; Liu, S. *J. Med. Chem.* **2015**, *58*, 6533–6548 f) Sarig, H.; Rotem, S.; Ziserman, L.; Danino, D.; Mor, A. *Antimicrob. agents. Chemother.* **2008**, *52*, 4308–4314.
8. Avrahami, D.; Shai, Y. *Biochemistry* **2003**, *42*, 14946-14956.
9. Serrano, G.; Zhanel, G.; Schweizer, F. *Antimicrob. Agents. Chemother.* **2009**, *53*, 2215–2217.
10. a) Seebach, D.; Beck, A. K.; Bierbaum, D. J. *Chem. Biodiversity* **2004**, *1*, 1111-1239; b) Horne, W. S.; Gellman, S. H. *Acc. Chem. Res.* **2008**, *41*, 1399-1408.
11. a) Arvidsson, P. I.; Frackenpohl, J.; Ryder, N. S.; Liechty, B.; Petersen, F.; Zimmermann, H.; Camenisch, G. P.; Woessner, R.; Seebach, D. *ChemBioChem* **2001**, *2*, 771-773; b) Raguse, T. L.; Porter, E. A.; Weisblum, B.; Gellman, S. H. *J. Am. Chem. Soc.* **2002**, *124*, 12774-12785; c) Porter, E. A.; Weisblum, B.; Gellman, S. H. *J. Am. Chem. Soc.* **2002**, *124*, 7324-7330. d) Schmitt, M. A.; Weisblum, B.; Gellman, S. H. *J. Am. Chem. Soc.* **2007**, *129*, 417-428. e) Liu D.; DeGrado, W. F. *J. Am. Chem. Soc.* **2001**, *123*, 7553-7559. f) Hansen, T.; Alst, T.; Havelkova, M.; Strøm, M. B. *J. Med. Chem.* **2010**, *53*, 595–606.
- 12 a) Vasudev, P. G.; Chatterjee, S.; Shamala, N.; Balaram, P. *Chem. Rev.* **2011**, *111*, 657-687. b) Bouillère, F.; Thétiot-Laurent, S.; Kouklovsky, C.; Alezra, V. *Amino Acids* **2011**, *41*, 687-707. c) Seebach, D.; Gardiner, J. *Acc. Chem. Res.* **2008**, *41*, 1366-1375. d) Jadhav, S. V.; Bandyopadhyay, A.; Gopi, H. N. *Org. Biomol. Chem.* **2013**, *11*, 509 –514.

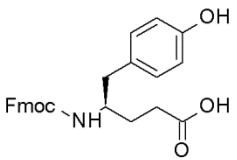
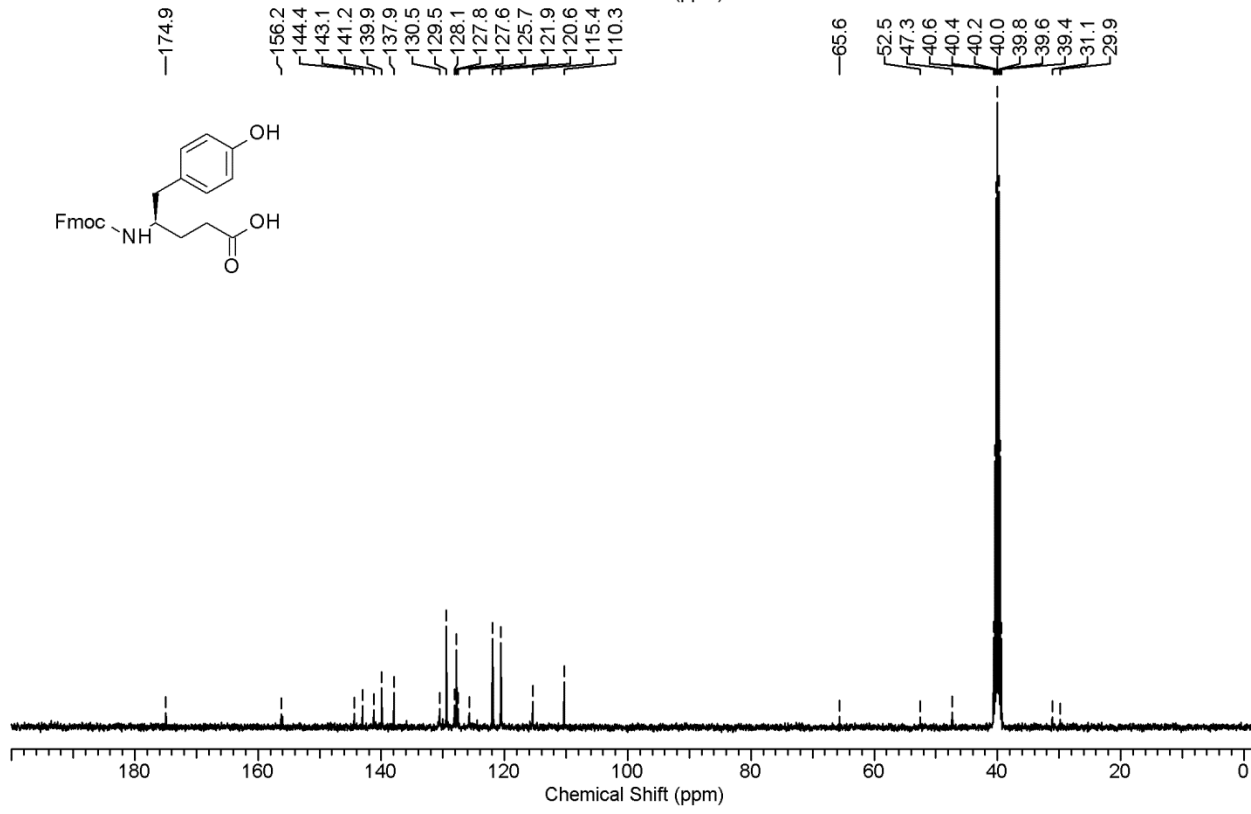
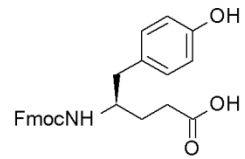
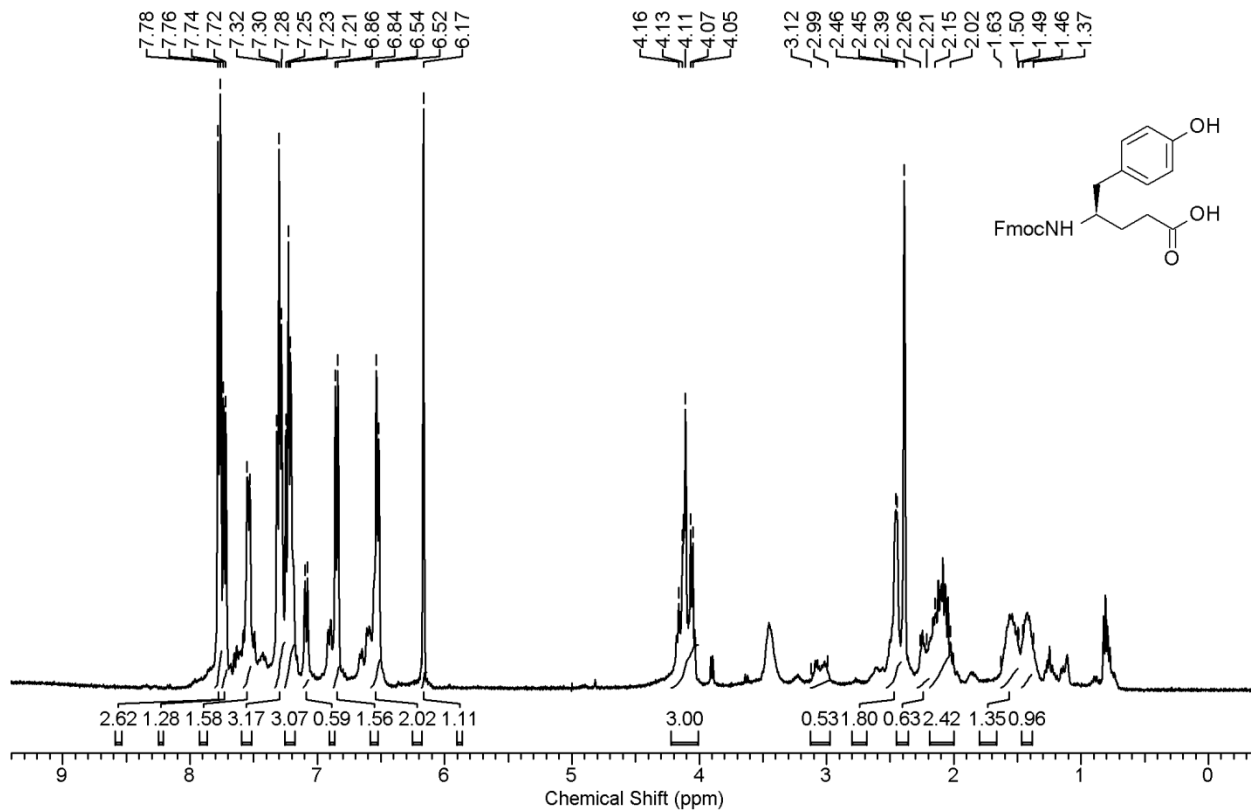
- e) Bandyopadhyay, A.; Jadhav, S. V.; Gopi, H. N. *Chem. Commun.* **2012**, *48*, 7170-7172.
- f) Guo, L.; Chi, Y.; Almeida, A. M.; Guzei, I. A.; Parker, B. K.; Gellman, S. H. *J. Am. Chem. Soc.* **2009**, *131*, 16018–16020.
- 13 Frackenpohl, J.; Arvidsson, P. I.; Schreiber, J. V.; Seebach, D. *ChemBioChem* **2001**, *2*, 445- 455.
- 14 Jadhav, S. V.; Misra, R.; Singh, S. K.; Gopi, H. N. *Chemistry* **2013**, *25*, 16256-16262.
- 15 Ulijasz, A. T.; Grenader, A.; Weisblum, B. *J. Bacteriol.* **1996**, *178*, 6305–6309.

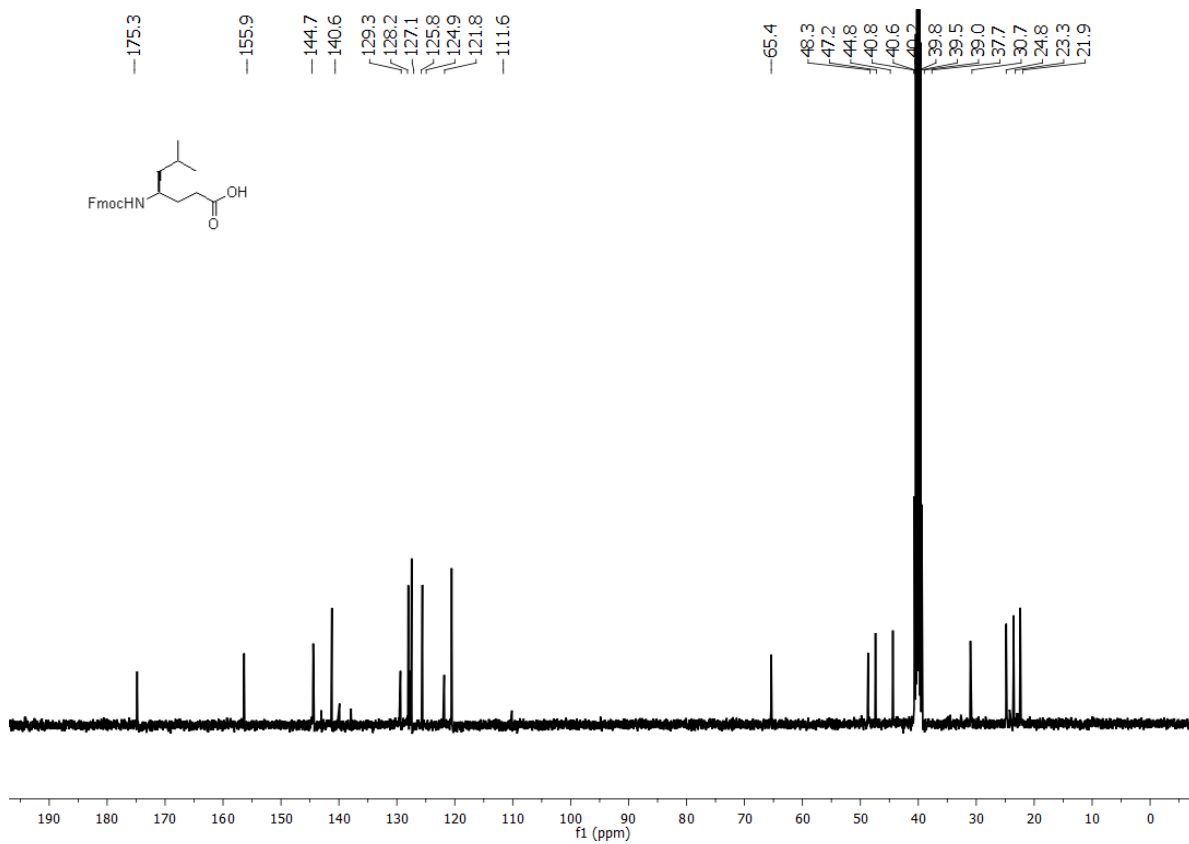
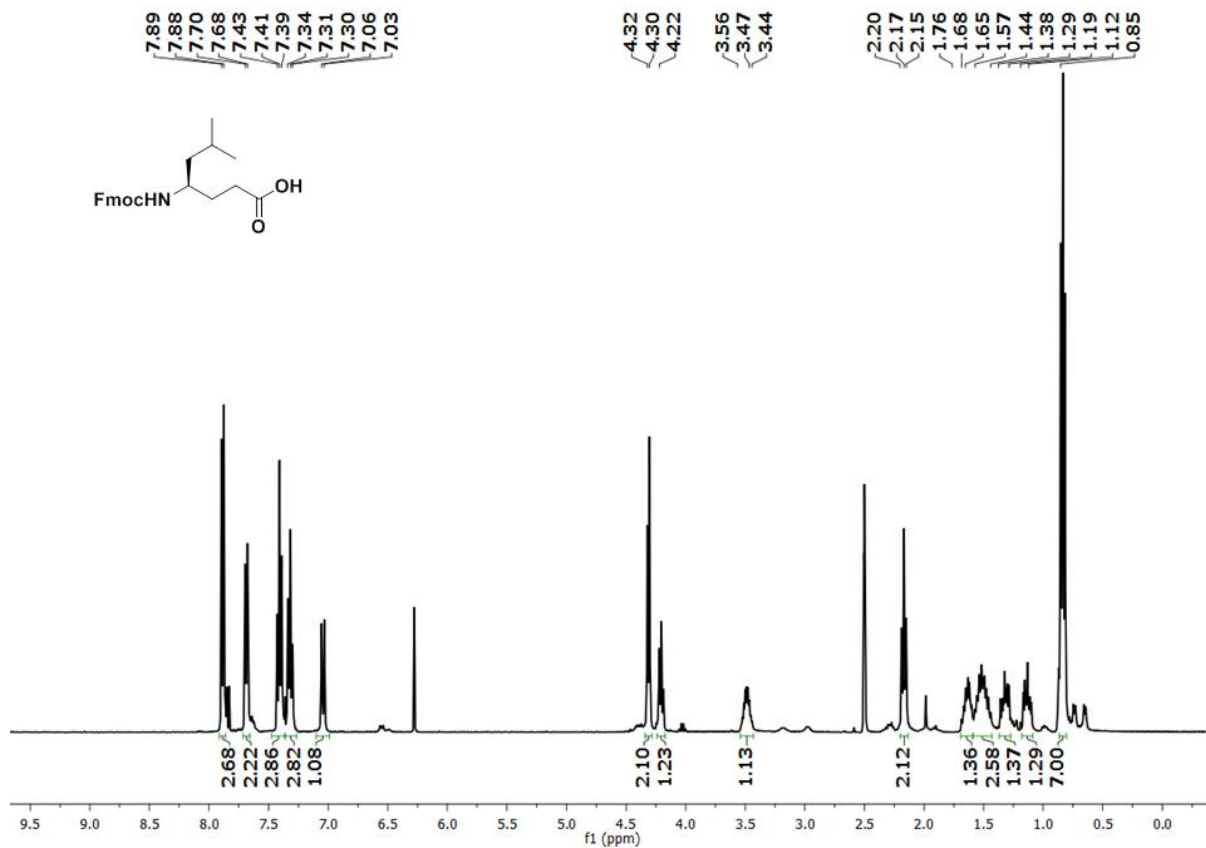
3a.7 Appendix II: Characterisation data of synthesized peptides

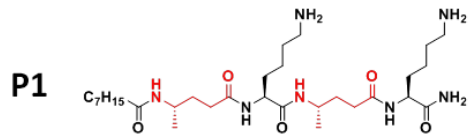
Designation	Description	Page No.
3a	^1H and ^{13}C NMR spectra	90
3b	^1H and ^{13}C NMR spectra	91
3c	^1H and ^{13}C NMR spectra	92
3d	^1H and ^{13}C NMR spectra	93
P1	HPLC trace and Mass spectrum	94
P2	HPLC trace and Mass spectrum	94
P3	HPLC trace and Mass spectrum	95
P4	HPLC trace and Mass spectrum	95
P5	HPLC trace and Mass spectrum	96
P6	HPLC trace and Mass spectrum	96
P7	HPLC trace and Mass spectrum	97
P8	HPLC trace and Mass spectrum	97
P9	HPLC trace and Mass spectrum	98
P10	HPLC trace and Mass spectrum	98







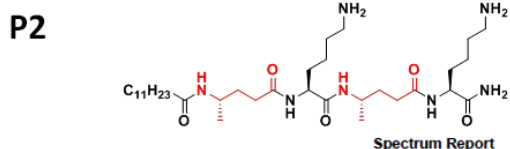
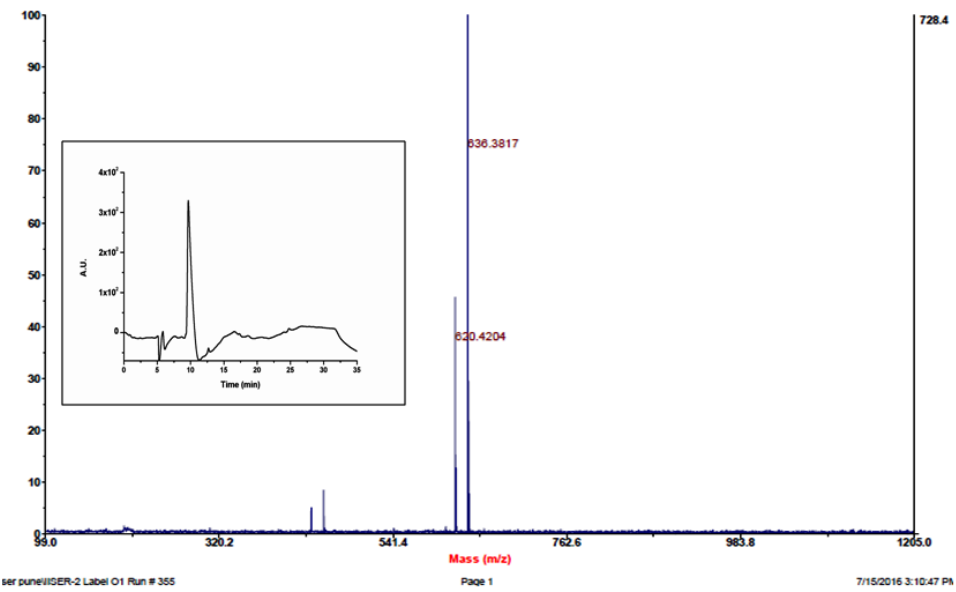




MW-597 Da
 Calc. mass [M+Na]⁺=620 Da
 Calc. mass [M+K]⁺ = 636 Da

Spectrum Report

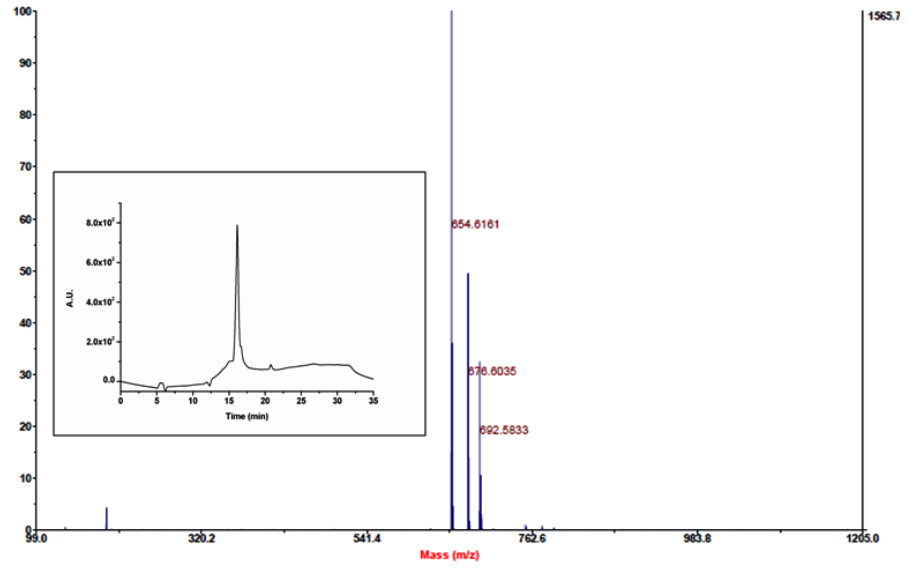
Final - Shots 400 - IISER-2; Run #355; Label O1

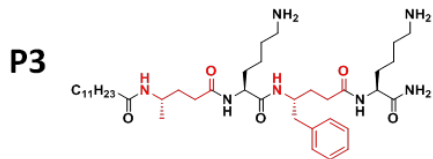


MW-653 Da
 Calc. mass [M+H]⁺ =654 Da
 Calc. mass [M+Na]⁺=676 Da
 Calc. mass [M+K]⁺ = 692 Da

Spectrum Report

Final - Shots 400 - IISER-2; Run #339; Label H16

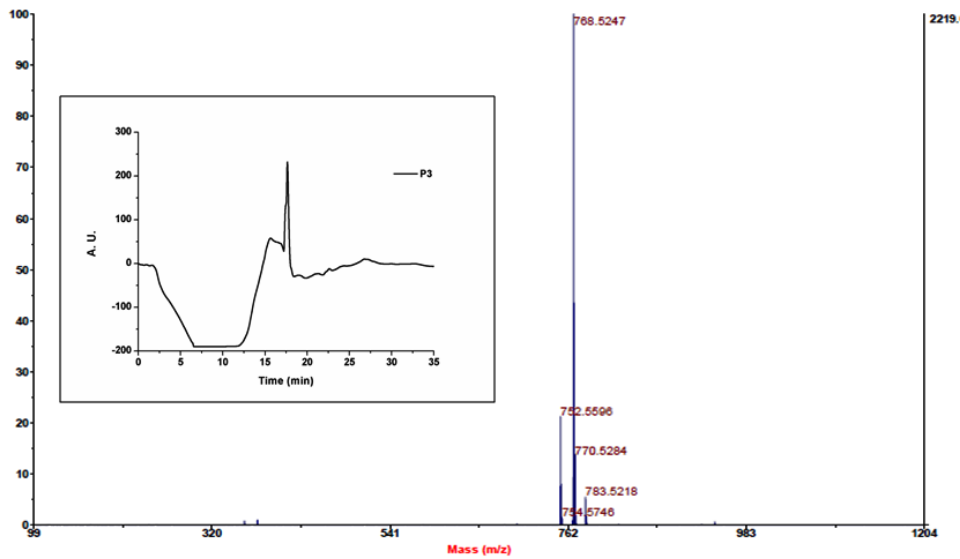




MW=729 Da
 Calc. mass [M+Na]⁺=752 Da
 Calc. mass [M+K]⁺ = 768 Da

Spectrum Report

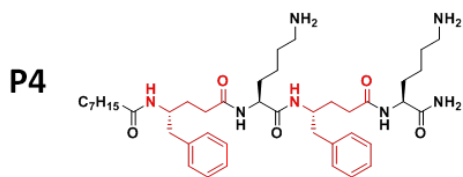
Final - Shots 1000 - IISER-3; Run #340; Label N19



SER New\IISER-3 Label N19 Run # 340

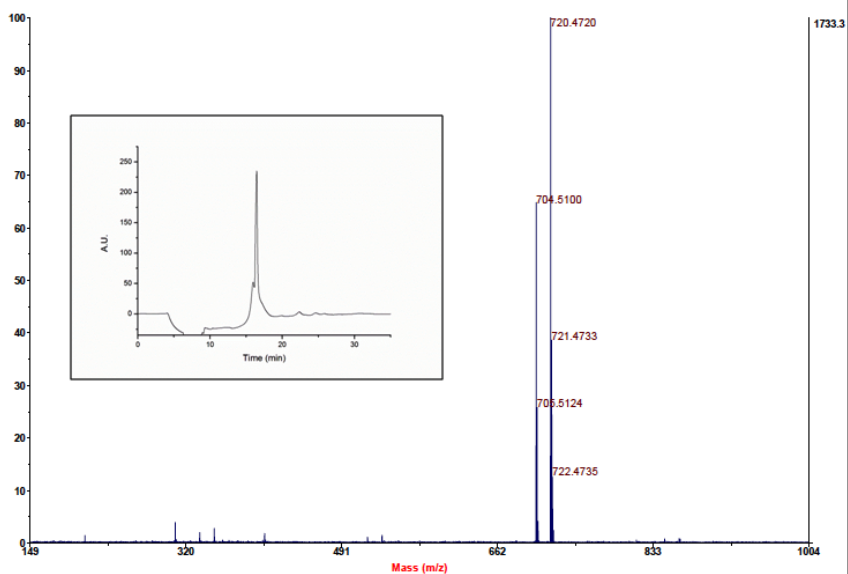
Page 1

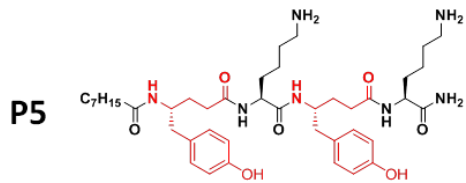
7/15/2016 3:15:04 P



MW=749 Da
 Calc. mass [M+Na]⁺=772 Da
 Calc. mass [M+K]⁺ = 788 Da

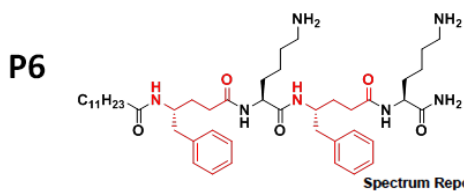
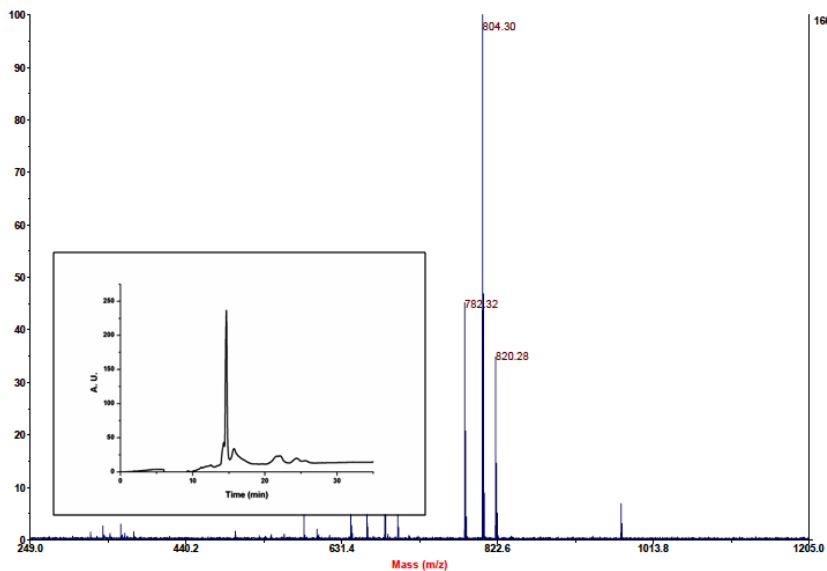
Final - Shots 400 - IISER-3; Run #19; Label F1





MW=781Da
 Calc. mass [M+Na]⁺=804 Da
 Calc. mass [M+K]⁺= 820 Da

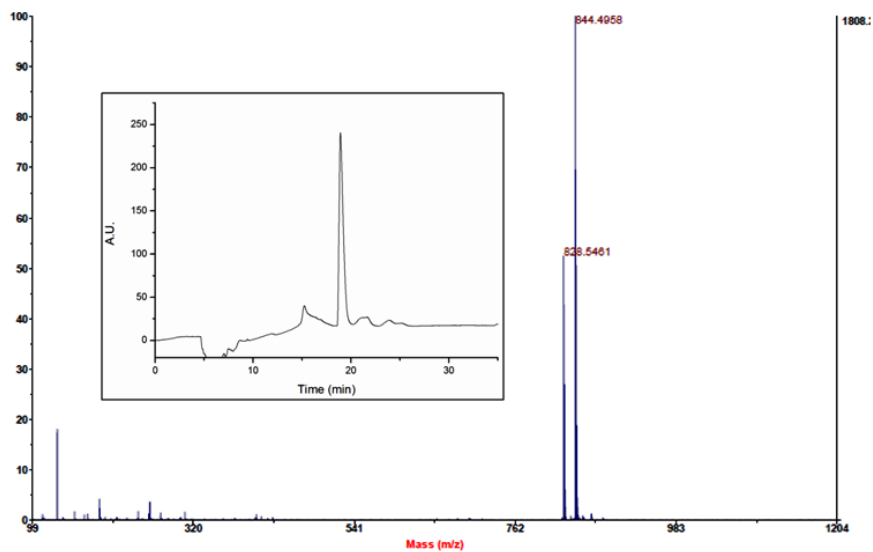
Final - Shots 500 - IISER-96-1; Run #217; Label G2



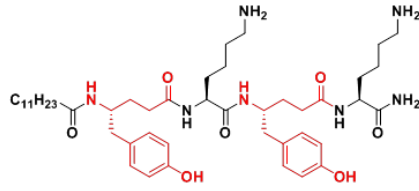
MW=805 Da
 Calc. mass [M+Na]⁺=828 Da
 Calc. mass [M+K]⁺= 844 Da

Spectrum Report

Final - Shots 1000 - IISER-3; Run #23; Label E10



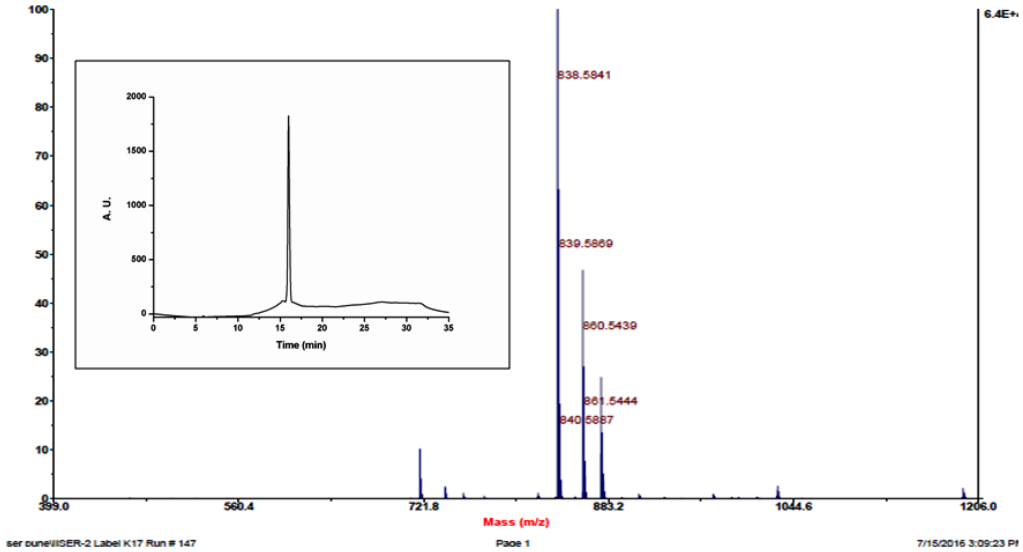
P7



MW=837 Da
Calc. mass [M+Na]⁺= 860 Da
Calc. mass [M+K]⁺= 876 Da

Spectrum Report

Final - Shots 400 - IISER-2; Run #147; Label K17

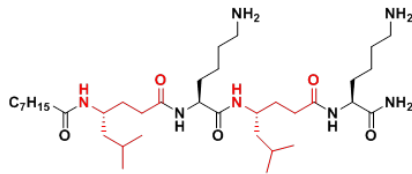


ser ouneIISER-2 Label K17 Run # 147

Page 1

7/15/2016 3:05:23 PM

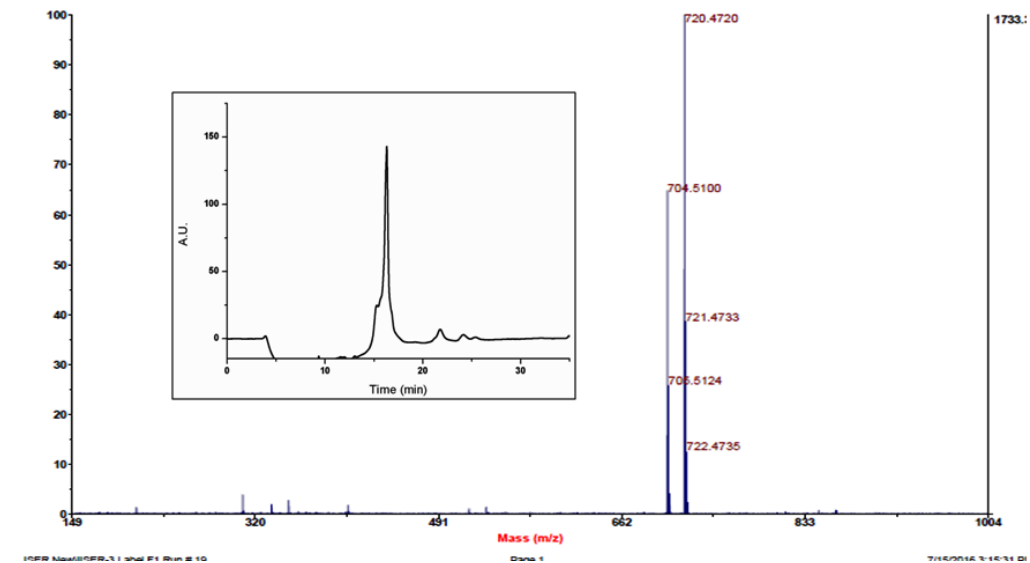
P8



MW=681 Da
Calc. mass [M+Na]⁺=704 Da
Calc. mass [M+K]⁺= 720 Da

Spectrum Report

Final - Shots 400 - IISER-3; Run #19; Label F1

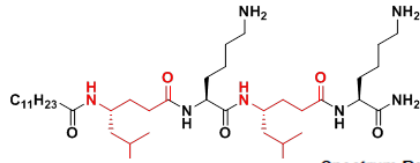


IISER-Nanobiosci, Label F1 Run # 19

Page 1

7/15/2016 3:14:31 PM

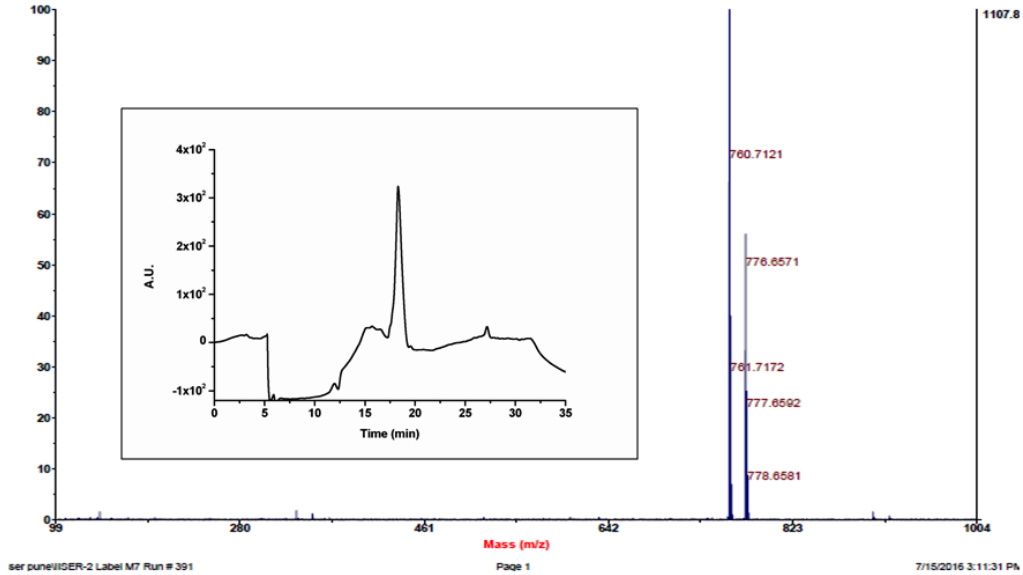
P9



MW-737 Da
Calc. mass [M+Na]⁺ = 760 Da
Calc. mass [M+K]⁺ = 776 Da

Spectrum Report

Final - Shots 400 - IISER-2; Run #391; Label M7

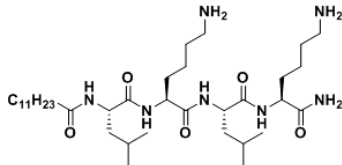


ser pure IISER-2 Label M7 Run # 391

Page 1

7/15/2016 3:11:31 PM

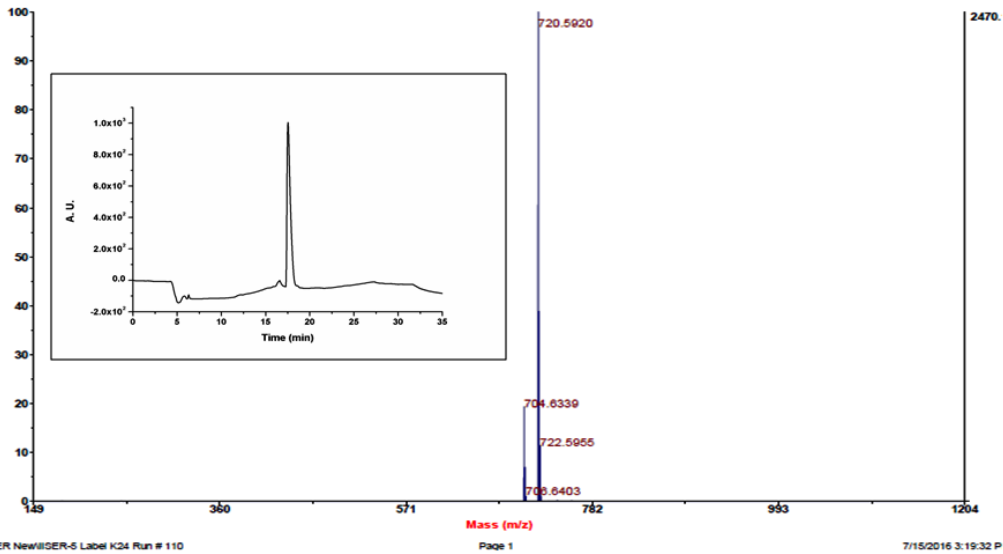
P10



MW-682 Da
Calc. mass [M+Na]⁺ = 704 Da
Calc. mass [M+K]⁺ = 720 Da

Spectrum Report

Final - Shots 750 - IISER-5; Run #110; Label K24



DER New IISER-5 Label K24 Run # 110

Page 1

7/15/2016 3:19:32 PM

Chapter 3b

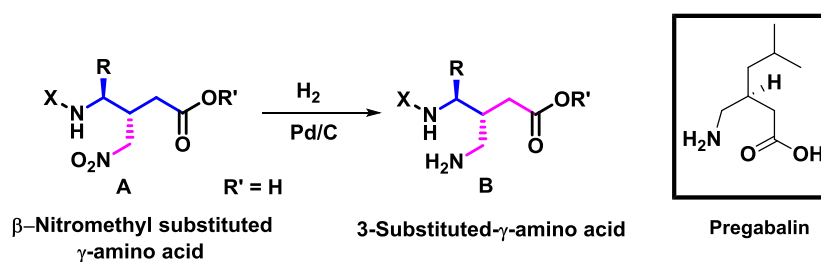
**Synthesis and Utilization of New $\gamma\gamma$ -diamino Acids from *E*-
Vinylogous Amino Acids and Their Utility in the Design of
 α,γ -Hybrid Peptide Foldamers**

3b.1 Introduction

In the previous section, we have demonstrated the potent antimicrobial activity of lipidated α,γ -hybrid peptides. The γ -amino acids are directly derived from the catalytic hydrogenation of *E*-vinylogous amino acids. In addition to the synthesis of γ -amino acids, recently we demonstrated the utility of *E*-vinylogous amino esters as Michael acceptors. In this chapter 3b, we are reporting the synthesis of novel $\gamma\gamma$ -diamino acids starting from *E*-vinylogous amino acids and their utility in the design of hybrid peptide foldamers.

Over the last two decades, a variety of non-natural β - and γ -amino acids have been explored to design protein secondary structure mimetics.^{1,2} In addition to the homooligomers of β - and γ -amino acids, the mixed $(\alpha\beta)_n$,³ $(\alpha\gamma)_n$,⁴ and $(\beta\gamma)_n$,⁵ sequences have shown to adopt helical structures with a variety of intramolecular H-bonding patterns. The lessons learned from the diverse folding properties of β -, γ - and mixed hybrid peptide helical foldamers have been utilized further to design inhibitors for protein-protein interactions,⁶ antimicrobials⁷ and soft biomaterials.⁸ We have been interested in understanding the conformational properties of γ - and α,γ -hybrid peptide foldamers composed of various types of γ -amino acids. Recently we have shown the folding properties of (*E*)- and (*Z*)- α,β -unsaturated γ -amino acids.⁹ The (*E*)-vinylogous amino acids preferred to adopt extended conformation,^{9a} while (*Z*)-vinylogous amino acids can be readily accommodated into the helical structures.^{9b} Besides serving as starting materials for the synthesis of saturated γ -amino acids through the reduction of double bonds, these unsaturated amino acids also provided an opportunity to drive 3,4-disubstituted γ -amino acids through Michael addition.¹⁰ We have reported the helical conformations of hybrid peptides composed of 3-nitromethyl substituted γ -amino acids derived from the nitromethane Michael addition on *E*-vinylogous γ amino acids.^{10,11} The hybrid peptides composed of alternative α - and 3-nitromethyl substituted γ -amino acids

adopted 12-helix conformations and self-assembled nanotubes in single crystals.¹¹ We hypothesize that the reduction of 3-nitromethyl functional group in the 3,4-disubstituted γ -amino acids may leads to new γ -amino acids with different side-chains (Scheme 3b.1). Interesting fact is that the 3-substituted γ -amino acid consists of both amine and amino acid side-chain functionality cab be placed as a side-chain. In addition, this transformation also leads



Scheme 3b.1: Transformation of β -nitromethyl substituted γ -amino acid to 3-Substituted γ -amino acid.

to easy access to the drug pregabalin (Scheme 3b.1) analogues. Pregabalin has been marketed to treat epilepsy, neuropathic pain, fibromyalgia, etc.¹²

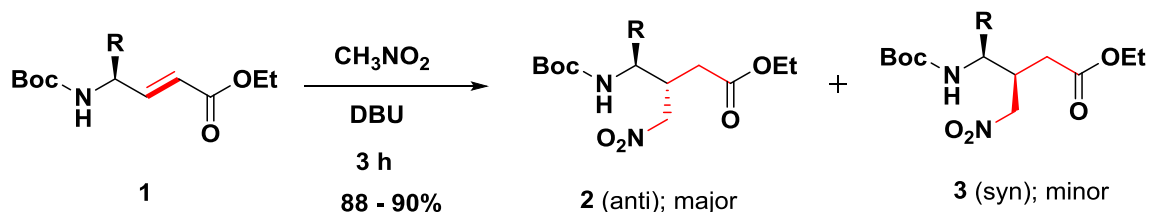
3b.2 Aim and rational of the work

α , β -Unsaturated γ -amino acids have been serving as intermediates for the synthesis of various substituted γ -amino acids as well as saturated γ -amino acids. In addition, hybrid lipopeptides composed of unsaturated γ -amino acids have shown the potent and broad spectrum antimicrobial activity. In the previous section, we have shown the potent antibacterial activities of short hybrid lipopeptides derived from α - and saturated γ -amino acids. In this chapter, we sought to investigate the synthesis and conformational properties of new β -aminomethyl γ -amino acids derived from the Michael addition of nitromethane to the α,β -unsaturated γ -amino acids. Herein, we are reporting the synthesis of new 3-substituted γ -

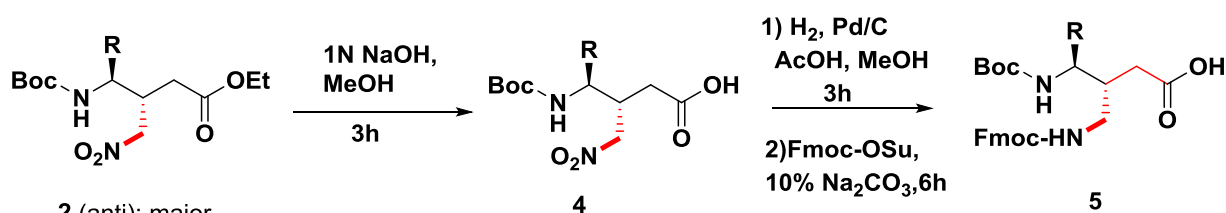
amino acids, their utility in the design of hybrid peptide foldamers and the single crystal conformation of α,γ -hybrid heptapeptide composed of 3-substituted γ -amino acid.

3b.3 Results and Discussion

3b.3.1 $\gamma\gamma$ -diamino acid synthesis



Scheme 3b.2: Synthesis of β -nitromethyl substituted γ -amino acids



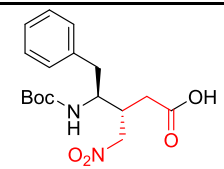
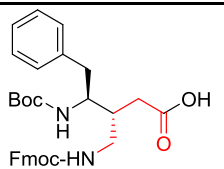
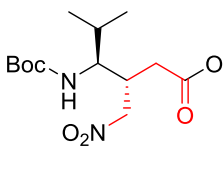
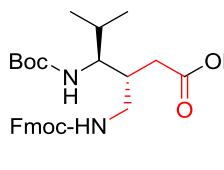
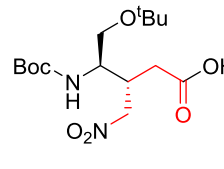
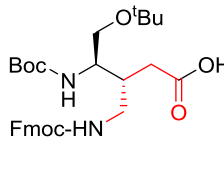
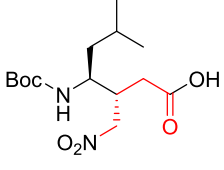
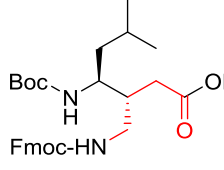
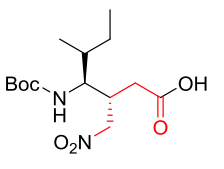
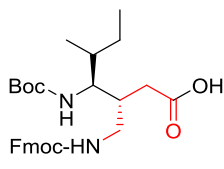
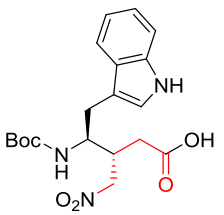
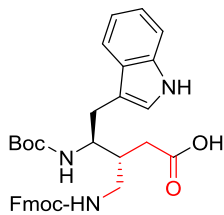
R = **a**: $-\text{CH}_2\text{C}_6\text{H}_5$; **b**: $-\text{CH}(\text{CH}_3)_2$; **c**: $-\text{CH}_2-\text{O}^t\text{Bu}$; **d**: $-\text{CH}_2-\text{CH}(\text{CH}_3)_2$; **e**: $-\text{CH}(\text{CH}_3)-\text{CH}_2-\text{CH}_3$; **f**: $-\text{CH}_2-$ (3-indole); **g**: $\text{CH}_2-\text{C}_6\text{H}_4-(4-\text{O}^t\text{Bu})$

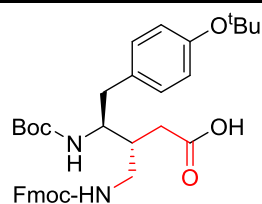
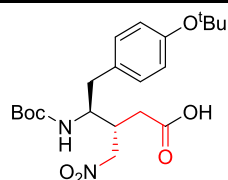
Scheme 3b.3: Synthesis of orthogonally protected compatible β -amino methyl substituted γ -amino acids

The schematic representation of the syntheses of ethyl ester β -nitromethyl substituted γ -amino acids from ethyl esters of *N*-Boc protected α,β -unsaturated amino acids (1) is shown in Scheme 3b.2. The ethyl ester of *N*-Boc- α,β -unsaturated γ -amino acids (**1a-g**) were synthesized through Wittig reaction starting from *N*-Boc-amino aldehydes as reported earlier.^{9a} All unsaturated amino acid esters were subjected to nitromethane Michael addition in the presence DBU as reported earlier.^{10,13} Both major (**2**) and minor (**3**) diastereoisomers obtained after the Michael addition reaction were separated using through column chromatography.¹⁰ All major diastereoisomers were isolated in good to excellent yields and characterized. The pure diastereoisomers (**2a-g**) were subjected to the saponification using 1N NaOH in methanol to obtain corresponding free carboxylic acid derivatives (**4a-g**). To

understand the feasibility of transforming β -nitromethyl substituted γ -amino acids into 3-substituted and/or 3, 4-disubstituted γ -amino acids ($\gamma\gamma$ -diamino acids), we subjected **4a** to the catalytic hydrogenation using 20% Pd/C in methanol.

Table 3b.1: Orthogonally protected 3-substituted (and/or 3,4-disubstituted) γ -amino acids

Entry	4	5	Yield (%)
a			85
b			85
c			90
d			87
e			80
f			78

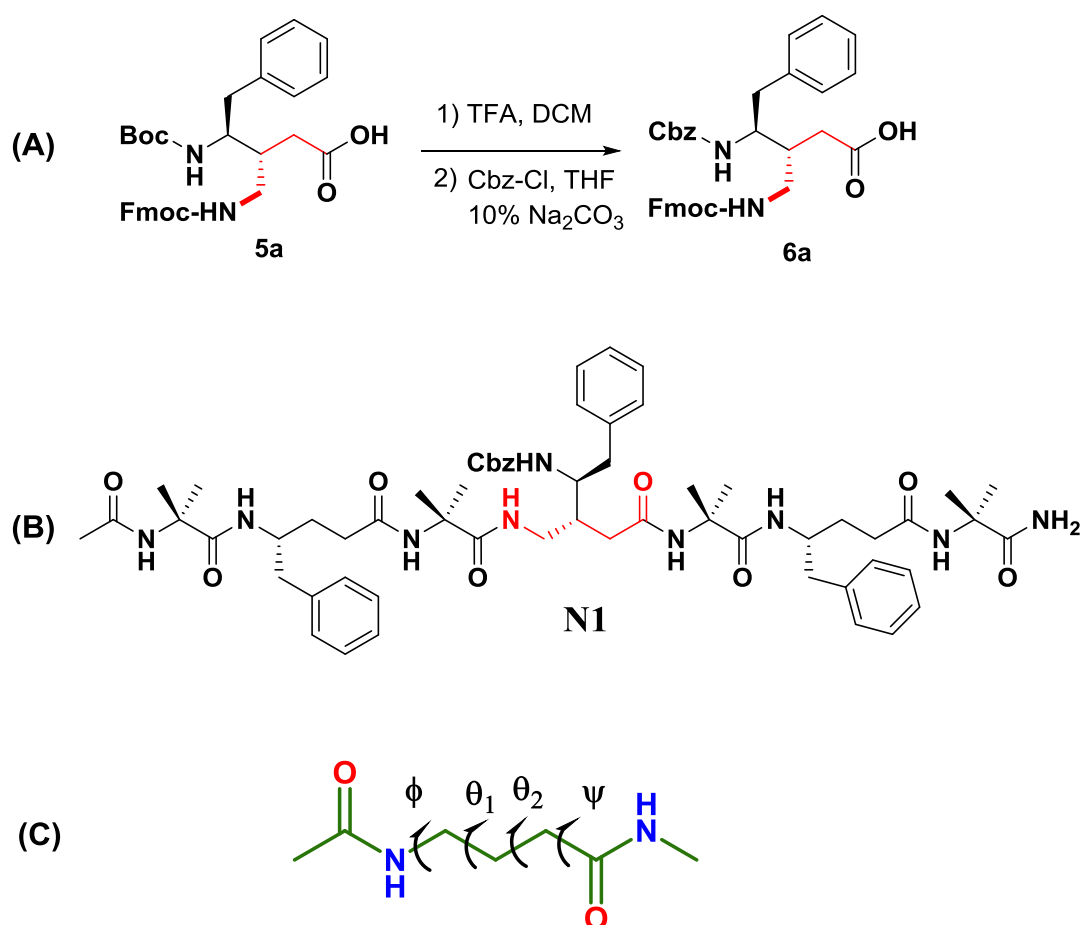


The free amine obtained after the completion of reaction was protected with Fmoc- group to obtain compound **5a** in excellent yield. The $\gamma\gamma$ -diamino acid **5a** can serve as both 3,4-disubstituted γ -amino acid as well as 3-substituted γ -amino acid. Motivated by the simple the transformation of β -nitromethyl γ -amino acid **4a** into dual γ -amino acid **5a** in a single step, we subjected other β -nitromethyl γ -amino acids (**4b-g**) to the catalytic hydrogenation. The free amine of all β -amino methyl substituted γ -amino acids was protected with Fmoc- group (**5b-g**) and isolated in good to excellent yields. The list of orthogonally protected β -amino methyl- γ -amino acids is shown in Table 3b.1.

3b.3.2 Incorporation of $\gamma\gamma$ -diamino acid in peptidomimetics

In order to understand the conformational properties of new 3-substituted γ -amino acids in peptide sequence, heptapeptide **N1** was designed (Scheme 3b.3). The amino acid **5a** was transformed into **6a** to accommodate Cbz-group for side-chain protection instead of Boc- group (Scheme 3b.3A). The protected amino acid was directly used for the peptide synthesis. The α,γ -hybrid peptide **N1** was synthesized using solid phase method on Rink amide resin. The γ^4 -amino acids were synthesized from the reduction of α,β -unsaturated γ -amino acids as reported earlier.^{4d} All coupling reactions were performed using HBTU as a coupling agent in the presence of additive HOBt and base DIEA. The peptide **N1** was purified by reverse phase HPLC on a C₁₈ column and pure peptide was subjected to the crystallization in various solvent combinations. Peptide gave X-ray quality crystals in a solution of aqueous methanol and its X-ray structure is shown in Figure 3b.1. There are two

molecules in the asymmetric unit. The heptapeptide **N1** adopted a right handed helical conformation stabilized by six intramolecular 12-membered H-bonds (12-helix) between the residues i and $i+3$. The H-bond parameters are tabulated in the Table 3b.2.



Scheme 3b.4 A) Synthesis of Cbz-protected γ -diamino acid (**6a**). B) Sequence of the peptide **N1** incorporating amino acid **6a**. C) Local torsion variables of γ -amino acids are also shown.

Both backbone homologated γ^4 -Phe2 and γ^4 -Phe6 adopted g^+ , g^+ conformation along C^α - C^β and C^β - C^γ bonds in the helix. Similar to γ^4 -Phe residues, the new γ^3 -amino acids at position 4 also adopted g^+ , g^+ conformation along C^α - C^β and C^β - C^γ bonds and nicely accommodated into the helix. The torsion variables ϕ , θ_1 , θ_2 and ψ are used to describe the local

conformations of the γ -residues (Scheme 3b.4C). The torsion angles of peptide **N1** (one of molecules) are tabulated in Table 3b.2.

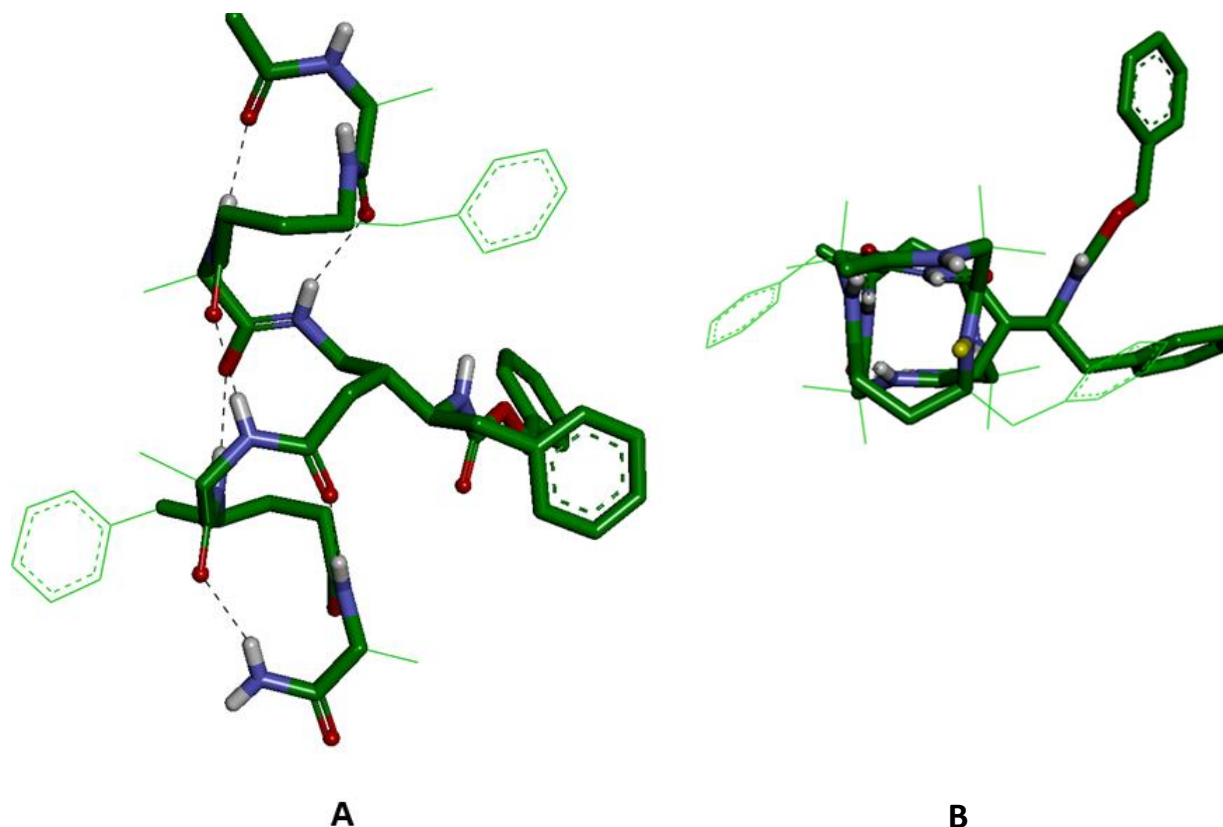


Figure 3b.1. Crystal structure of peptide **N1**. (A) side view (B) top view.

Similar to the reported α,γ -hybrid peptide 12-helices,^{4a-f} the all three γ -residues displayed θ_1 and $\theta_2 \sim +60^\circ$ and ϕ and $\psi \sim -120^\circ$. The Aib residues adopted an average ϕ and ψ values $\sim -60^\circ$ and $\sim -40^\circ$ respectively. Inspection of the crystal structure reveals that the Cbz protected amine and Phe groups of the γ^3 -amino acid are projected outwards. In the contrast to the backbone amide bonds, the side-chain amide bond of γ^3 -residue is not involved in inter or intramolecular H-bonds. As compared to other γ -amino acids, the side-chain of the new γ -amino acid is elongated and possible to cover larger surface if the foldamers are constructed from these new γ -amino acids.

Table 3b.2. Torsion angles for Peptide **N1** (°)*

Residue	ϕ	θ_1	θ_2	ψ	Backbone coformation
Aib1	-56	-	-	-39	-
γ^4 Phe 2	-123	49	63°	-122	g^+, g^+
Aib3	-58	-	-	-37°	-
γ^3 Phe4	-135	60	52	-110	g^+, g^+
Aib5	-63	-	-	-44	
γ^4 Phe 6	-129	58	59	-117	g^+, g^+
Aib7	-57°	-	-	-44	-

*The other molecule in the asymmetric unit also displayed similar torsion angles.

3b.4 Conclusion

We have demonstrated the synthesis of new γ -amino acids starting from *E*-vinyllogous amino acids through the Michael addition. The mild reduction of 3-nitromethyl group led to the generation of a new γ -amino acid. Using this simple and facile method it is possible to generate pregabalin analogues. The orthogonally protected 3-substituted γ -amino acids were isolated in excellent yields and utilized in the construction of hybrid peptide foldamer. The single crystal conformational analysis of hybrid heptapeptide suggested that these amino acids can be accommodated into the helix similar to the other γ -amino acids. Overall the synthesis and isolation of different side-chain substituted γ -amino acids and their conformations in the single crystals reported here can be explored to design functional peptide foldamers.

3b.5 General Experimental Details

Column chromatography was performed on silica gel (100-200 mesh). ^1H NMR and ^{13}C NMR spectra were recorded on 400 MHz and on 100 MHz respectively, using residual solvent signal as internal standards ($\text{DMSO-}d_6$). Chemical shifts (δ) reported in parts per million (*ppm*) and coupling constants (*J*) reported in Hz. Mass spectra were recorded using MALDI TOF/TOF.

3b.5.1 General procedure for the synthesis of β -nitromethane substituted γ -amino esters through the Michael addition of nitromethane to N-protected α,β -unsaturated γ -amino esters.

The N-Boc α,β -unsaturated γ -amino ester **1** (2.0 mmol) was dissolved in neat nitromethane (10.0 mmol). To this solution, DBU (2.0 mmol) was added under a N_2 atmosphere. The reaction mixture was stirred at room temperature for about 3 h and the progress of the reaction was monitored by TLC. After completion of the reaction, EtOAc (100 mL) was added to the reaction mixture, and washed with H_2O (3×50 mL), 1N HCl (2×50 mL) and brine (2×50 mL) solution. Then the organic layer was dried over anhydrous Na_2SO_4 and concentrated under reduced pressure. The diastereoisomers **2** and **3** were separated through silica gel column chromatography.

General procedure for the synthesis of **4**

N-Boc protected ethyl ester of β -nitromethyl substituted γ -amino acid (**2**, 5 mmol) was dissolved in MeOH (5 mL) and 1N NaOH was slowly added to the reaction mixture until the solution turns turbid and stir the reaction mixture for about 3 h. The progress of the reaction was monitored by TLC. After completion of the reaction, MeOH was evaporated using rotary evaporator and the aqueous layer was acidified using 10% HCl solution. The product was extracted in EtOAc (3×40 mL). The combined organic layer was

washed with brine (2×50 mL), dried over Na_2SO_4 and concentrated under reduced pressure to give free carboxylic acid **4**. The product was used further without purification.

General procedure for the synthesis of 5

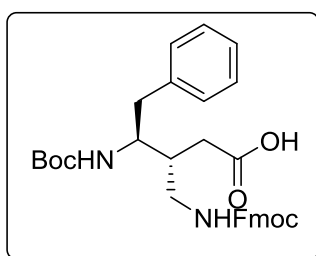
The free carboxylic acid (**4**, 1 mmol) was dissolved in distilled MeOH (10 mL) under N_2 atmosphere and subjected to hydrogenation using Pd/C (10 % w/w) under H_2 atmosphere. The progress of the reaction was monitored by TLC. After the completion of reaction (~ 3 h), Pd/C was filtered using a sintered funnel, MeOH was evaporated to get N-Boc-protected β -aminomethyl γ -amino acid. The free amino acid was dissolved in 10 mL of THF and 15 mL 10% Na_2CO_3 was added while stirring. The Fmoc-OSu (0.9 mmol) dissolved in 5 mL THF was added drop wise to the ice cold reaction mixture. The reaction mixture was stirred and completion of reaction was monitored by TLC. After 6 h, the THF was evaporated and aqueous layer was acidified with 10% HCl. The product was extracted using EtOAc (3×50 mL). The combined organic layer was washed with brine (3×50 mL), dried over Na_2SO_4 and concentrated under reduced pressure. The crude product was purified using silica gel column chromatography to get pure compound **5**.

Synthesis of 6a from 5a:

Compound **5a** (1 mmol) was dissolved in 5 mL DCM and cooled to 0°C . To this cold solution 5 mL TFA was added and the reaction mixture was stirred for about 1 h. After 1 h, the solvent was evaporated under reduced pressure and the product was washed with DCM. The free amino acid was dissolved in 10 mL of THF, and 15 mL 10% Na_2CO_3 was added to it while stirring. To this solution, Cbz-Cl (0.9 mmol) dissolved in 5 mL THF was added drop wise. The reaction mixture was stirred for 6 h and progress of the reaction was monitored by TLC. After 6h, the THF was evaporated under reduced pressure and aqueous layer was acidified with 10% HCl. The product was extracted using EtOAc (3×50 mL). The

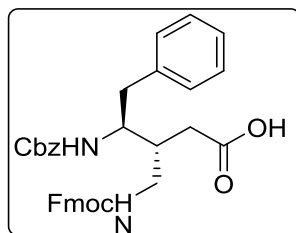
combined organic layer was washed with brine (3 × 50 mL), dried over Na₂SO₄ and concentrated under reduced pressure. The product was purified using silica gel column chromatography to give Cbz- γ Phe(β CH₂NHFmoc)-OH (**6a**).

(3R,4S)-3-((((9H-fluoren-9-yl)methoxy)carbonyl)amino)methyl)-4-((tert-butoxycarbonyl)amino)-5-phenylpentanoic acid (5a): White solid; (85%); m. p. 136 °C ; $[\alpha]_D^{25} +11.8$ (c 1.0, MeOH); ¹H NMR (400 MHz, DMSO-*d*₆); δ 11.99 (s, 1H, COOH), 7.83 (d, *J* =8 Hz, 2H, -Fmoc Aromatic), 7.65(d, *J* =8 Hz, 2H, -Fmoc Aromatic), 7.35 (t, *J* =8 Hz, 2H, -Fmoc Aromatic), 7.26(t, *J* =8 Hz, 2H, -Fmoc Aromatic), 7.18-7.15 (m, 5H, phenyl), 6.66 (d, *J* =12 Hz, 1H, NH), 6.27 (d, *J* = 12 Hz, 1H, NH), 4.24 (d, *J* = 8 Hz, 2H, -CH₂-Fmoc), 4.19-4.17 (m, 1H, -CH-Fmoc), 3.82-3.77 (m, 1H,CH), 3.20-3.14 (m, 1H,CH), 2.93-2.86(m, 1H,CH), 2.72-2.65(m, 1H,CH), 2.56-2.48(m, 1H,CH), 2.30-2.23 (m, 1H,CH), 2.16-2.07(m, 2H,CH₂), 1.20 (s, 9H, Boc); ¹³C NMR (100 MHz, DMSO-*d*₆) δ 174.3, 156.9, 155.9, 144.4, 141.2, 139.9, 129.5, 128.3, 128.1, 127.5, 126.2, 125.7, 120.6, 77.9, 65.9, 52.7, 49.1, 47.2, 37.3, 28.6, 28.1; ESI HRMS *m/z* value for C₃₂H₃₆N₂O₆ [M + Na]⁺ 567.2471 (calcd), 567.2470 (observed).

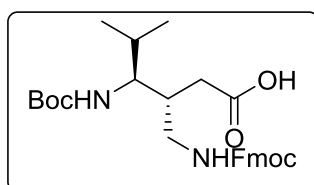


(3R,4S)-3-((((9H-fluoren-9-yl)methoxy)carbonyl)amino)methyl)-4-((benzyloxy)carbonyl)amino)-5-phenylpentanoic acid (6a): White solid; (78%); m. p. 122 °C; $[\alpha]_D^{25} -1.4$ (c 1.0, MeOH); ¹H NMR (400 MHz, DMSO-*d*₆) δ 12.04 (s, 1H), 9.60(s, 1H), 7.84-7.09(m, 18H), 4.91-4.80(m, 2H), 4.26-4.24(m, 3H), 3.88-3.84(m, 1H), 3.75-3.51(m, 1H), 3.23-3.16(m, 1H), 2.98-2.90(m, 1H), 2.76-2.73(m, 1H), 2.57-2.49(m, 1H), 2.35-2.27(m, 1H),

2.18-2.13(m, 2H); ^{13}C NMR (100 MHz, DMSO- d_6) δ 174.3, 144.4, 141.2, 139.8, 137.9, 129.7, 129.6, 128.8, 128.4, 128.1, 128.0, 127.6, 126.4, 125.7, 120.6, 68.1, 66.0, 65.3, 53.6, 47.3, 37.2, 33.6, 29.5; ESI HRMS m/z value for $\text{C}_{35}\text{H}_{34}\text{N}_2\text{O}_6$ $[\text{M} + \text{Na}]^+$ 601.2315(calcd), 601.2515 (observed).

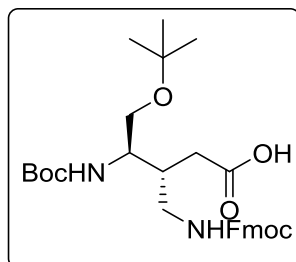


(3R,4S)-3-((((9H-fluoren-9-yl)methoxy)carbonyl)amino)methyl)-4-((tert-butoxycarbonyl)amino)-5-methylhexanoic acid (5b): White solid; (85%); m. p. 89 °C; $[\alpha]_{\text{D}}^{25}$ -6.4 (c 1.0, MeOH); ^1H NMR (400 MHz, CDCl_3) δ 7.74 (d, J = 8 Hz, 2H,-Fmoc Aromatic), 7.58 (d, J = 8 Hz, 2H, -Fmoc Aromatic), 7.38(t, J = 8 Hz, 2H, -Fmoc Aromatic), 7.29 (t, J = 8 Hz, 2H, -Fmoc Aromatic), 5.84 (m,1H),4.64 (d, J =12 Hz, 1H), 4.36 (d, J =8 Hz, 2H), 4.21 (t, J =8 Hz, 1H), 3.54-3.50 (m, 1H), 3.42-3.35 (m, 1H), 3.12-3.09 (m, 1H), 2.72 (d, J =8 Hz, 1H), 2.37-2.27 (m, 2H), 1.46-1.38 (m, 11H), 1.27-1.24 (m,1H), 1.03-0.82(m, 6H); ^{13}C NMR (100 MHz, CDCl_3) δ 175.1, 172.8, 157.5, 143.8, 141.4, 127.8, 127.1, 125.2, 123.0, 120.1, 67.3, 56.5, 47.2, 40.6, 38.6, 34.8, 28.7, 28.4, 28.3, 20.3, 16.9 ESI HRMS m/z value for $\text{C}_{28}\text{H}_{36}\text{N}_2\text{O}_6$ $[\text{M} + \text{Na}]^+$ 519.2471 (calcd), 519.2477 (observed).

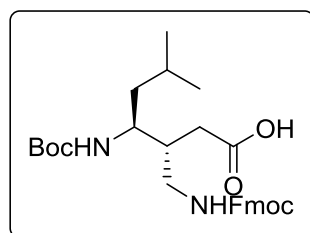


(3R,4R)-3-((((9H-fluoren-9-yl)methoxy)carbonyl)amino)methyl)-5-(tert-butoxy)-4-((tert-butoxycarbonyl) amino)pentanoic acid (5c): White solid; (90%); m. p. 76 °C; $[\alpha]_{\text{D}}^{25}$ +9.6 (c 1.0, MeOH); ^1H NMR (400 MHz, DMSO- d_6) δ 11.95(s, 1H), 7.84-7.24(m,8H), 6.42-

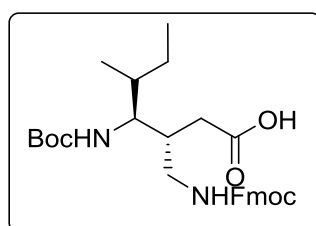
6.38(m, 1H), 4.23-4.15(m, 3H), 3.64-3.59(m, 1H), 3.20(m, 1H), 3.04-2.82(m,1H), 2.15-2.06(m, 2H), 1.31(s, 9H), 1.04(s,9H); ^{13}C NMR (100 MHz, DMSO- d_6) δ 174.3, 157.8, 156.2, 144.4, 141.2, 129.4, 128.1, 127.8, 125.7, 120.6, 78.1, 72.9, 65.9, 62.3, 51.8, 47.2, 37.4, 33.7, 28.7, 27.8; ESI HRMS m/z value for $\text{C}_{30}\text{H}_{40}\text{N}_2\text{O}_7$ $[\text{M} + \text{Na}]^+$ 563.2733 (calcd.), 563.2811(observed).



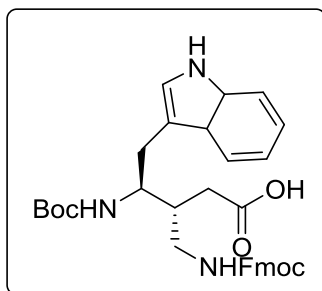
(3R,4S)-3-((((9H-fluoren-9-yl)methoxy)carbonyl)amino)methyl)-4-((tert-butoxycarbonyl)amino)-6-methylheptanoic acid (5d): White solid; (87%); m. p. 80 °C , $[\alpha]_D^{25}$ -16 (c 1.0, MeOH); ^1H NMR (400 MHz, DMSO- d_6) δ 11.92 (s, 1H, COOH),7.89-7.88 (d, J = 8 Hz, 2H, -Fmoc Aromatic),7.68-7.67(d, J =8 Hz, 2H, -Fmoc Aromatic), 7.43-7.39 (t, J =8Hz, 2H, -Fmoc Aromatic),7.33-7.30(t, J =8Hz, 2H, -Fmoc Aromatic), 6.81-6.79 (d, J = 9.16 Hz, 1H, NH),6.59-6.57(d, J = 8 Hz, 1H, NH),4.27-4.26 (d, J = 4 Hz, 2H, -CH₂-Fmoc), 4.22-4.21 (m, 1H, CH-Fmoc),3.73-3.65 (m, 1H,CH), 3.17-3.16 (m, 1H,CH), 3.10-3.02 (m, 1H,CH), 2.82-2.77 (m, 1H,CH), 2.17-2.12 ((m, 1H,CH),2.03-2.19(m, 1H,CH),1.57-1.52(m, 1H,CH),1.37-1.34 (m, 11H, Boc, CH₂), 0.86-0.80(m, 6H, CH₃); ^{13}C NMR (100 MHz, DMSO- d_6) δ 176.7, 156.3, 143.1, 139.9, 137.9, 129.4, 127.8, 121.9, 120.5, 77.9, 51.1, 49.1, 43.9, 41.9, 39.4, 29.4, 28.7, 24.9, 24.0, 23.0, 21.9 ; ESI HRMS m/z value for $\text{C}_{29}\text{H}_{38}\text{N}_2\text{O}_6$ $[\text{M} + \text{Na}]^+$ 533.2628 (calcd), 533.2627 (observed).



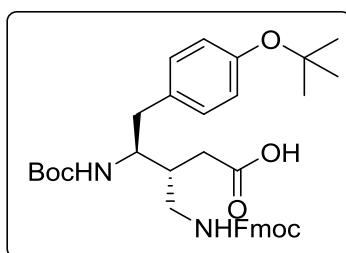
(3*R*,4*S*,5*R*)-3-((((9*H*-fluoren-9-yl)methoxy)carbonyl)amino)methyl)-4-((*tert*-butoxycarbonyl)amino)-5-methylheptanoic acid (5e): White solid (80%), m. p. 95 °C ; $[\alpha]_D^{25}$ -7.0 (c 1.0, MeOH); $^1\text{H NMR}$ (400 MHz, $\text{DMSO-}d_6$) δ 11.89 (s, 1H, COOH), 7.84 (d, J = 7.32 Hz, 2H, -Fmoc Aromatic), 7.61 (d, J = 8 Hz, 2H, -Fmoc Aromatic), 7.35 (t, J = 8 Hz, 2H, -Fmoc Aromatic), 7.29-7.24(m, 2H, -Fmoc Aromatic), 6.45 (d, J = 12 Hz, 1H, NH), 4.27-4.13(m, 3H, -OCH₂, -CH of Fmoc),3.00-2.96 (m, 1H, CH),2.64-2.62 (m, 1H, CH),2.16-2.10(m, 2H, CH₂), 2.02-1.93 (m, 1H, CH),1.42-1.29 (m, 11H, Boc, CH₂),0.83-0.73 (m, 6H, CH₃); $^{13}\text{C NMR}$ (100 MHz, $\text{DMSO-}d_6$) δ 174.2, 156.8, 144.4, 142.2, 128.1, 17.5, 125.6, 120.6, 77.9, 65.7,55.6, 47.2, 39.4, 36.3, 28.7, 26.0, 16.1, 11.1; ESI HRMS m/z value for $\text{C}_{29}\text{H}_{38}\text{N}_2\text{O}_6$ $[\text{M} + \text{Na}]^+$ 533.2628 (calcd), 533.2627 (observed).



(3*R*,4*S*)-3-((((9*H*-fluoren-9-yl)methoxy)carbonyl)amino)methyl)-4-((*tert*-butoxycarbonyl)amino)-5-(12,18-dihydro-1*H*-indol-3-yl)pentanoic acid (5f): Yellow colored solid; (78%); m. p. 121 °C; $[\alpha]_D^{25}$ -7.6 (c 1.0, MeOH); $^1\text{H NMR}$ (400 MHz, $\text{DMSO-}d_6$) δ 11.98 (s, 1H), 10.69(s, 1H), 7.85-6.63(m,19H), 4.25-4.18(m, 3H), 3.89(m,1H), 2.94-2.93(m, 1H), 2.78-2.73(m 1H), 2.27-2.19(, 3H), 1.24(s, 9H); $^{13}\text{C NMR}$ (100 MHz, $\text{DMSO-}d_6$) δ 176.1, 156.1, 143.0, 139.9, 137.9, 136.6, 129.4, 127.8, 123.5, 121.8, 121.2, 120..5, 118.8, 118.6, 117.5, 111.5, 110.2, 78.0, 53.9, 44.0, 38.6, 34.5, 28.7, 28.5. ESI HRMS m/z value for $\text{C}_{34}\text{H}_{39}\text{N}_3\text{O}_6$ $[\text{M} + \text{Na}]^+$ 608.2737 (calcd), 606.2581(observed).



(3R,4S)-3-((((9H-fluoren-9-yl)methoxy)carbonyl)amino)methyl)-5-(4-(tert-butoxy)phenyl)-4-((tert-butoxycarbonyl)amino)pentanoic acid (5g): White solid; (87%); m. p. 74 °C; $[\alpha]_D^{25}$ -2.0 (c 1.0, MeOH); $^1\text{H NMR}$ (400 MHz, $\text{DMSO-}d_6$) δ 7.84(d, $J=8\text{Hz}$, 2H), 7.64(t, $J=8\text{Hz}$, 2H), 7.36(t, $J=8\text{Hz}$, 2H), 7.31-7.25(m, 3H), 7.05(d, $J=8\text{Hz}$, 2H), 6.83-6.74(m, 2H), 4.26-4.15(m, 3H), 3.81-3.74(m, 1H), 3.17-3.12(m, 1H), 2.91-2.87(m, 1H), 2.33(t, $J=8\text{Hz}$, 1H), 2.14-2.06(m, 1H), 1.24-1.17(m, 18H); $^{13}\text{C NMR}$ (100 MHz, $\text{DMSO-}d_6$) 176.7, 156.7, 143.1, 139.9, 137.9, 129.4, 127.8, 121.9, 120.5, 110.3, 78.0, 58.1, 56.3, 44.3, 36.7, 34.5, 31.9, 30.1, 28.7, 20.6, 17.8, 17.6; ESI HRMS m/z value for $\text{C}_{36}\text{H}_{44}\text{N}_2\text{O}_7$ $[\text{M} + \text{Na}]^+$ 639.3036 (calcd), 639.3054(observed).



3b.5.2 Solid phase synthesis of peptide N1:

Peptide **N1** was synthesized at 0.1 mmol scale on Rink amide resin using standard Fmoc-chemistry. The combination of HBTU/HOBt was used as coupling reagents. The coupling reactions were monitored by Kaiser Test. After completion of the synthesis, peptide was cleaved from the resin using TFA/ H_2O (9.5:0.5). After cleavage, the resin was filtered and washed with TFA. The cleavage mixture was then evaporated under reduced pressure to give

gummy product and purified through reverse phase HPLC on C₁₈ column using MeOH/H₂O gradient.

White solid; ¹H NMR (400 MHz, CD₃OH) δ 8.28-8.25 (m, 2H), 8.21 (s, 1H), 8.15 (s, 1H), 8.01 (s, 1H), 7.90 (s, 1H), 7.85-7.83 (d, 8Hz, 1H), 7.66-7.63 (d, 12Hz, 1H), 7.56 (s, 1H), 7.35-7.04 (m, 15H), 6.60 (s, 1H), 5.21-5.18 (d, 12Hz, 1H), 4.15-4.01 (m, 4H), 3.49-3.46 (m, 3H), 3.04-3.00 (m, 2H), 2.91-2.78 (m, 3H), 2.68 (s, 3H), 2.67-2.26 (m, 12H), 2.13-2.06 (m, 3H), 1.87-1.73 9m, 4H), 1.67-1.60 (m, 2H), 1.49 (s, 3H), 1.41-1.40 (m, 5H), 1.34 (s, 2H), 1.27 (m, 6H), 1.16 (s, 2H), 0.93 (s, 3H); ¹³C NMR (100 MHz, DMSO-*d*₆) δ 176.2, 175.7, 173.8, 173.1, 171.7, 157.3, 139.3, 138.6, 137.3, 129.4, 129.0, 128.1, 127.9, 126.6, 126.1, 125.7, 65.8, 56.4, 53.7, 48.5, 47.1, 42.1, 41.4, 34.8, 32.2, 31.6, 29.9, 28.2, 26.4, 25.7, 23.1, 22.3, 21.9, 10.2; MALDI-TOF mass *m/z* value for C₆₀H₈₁N₉O₁₀ [M + Na]⁺ 1110.6106 (calcd.), 1110.3234 (observed).

3b.5.3 Crystallographic information of peptide N1:

Crystals of peptide N1 were grown by slow evaporation from a solution of MeOH. A single crystal (0.11 × 0.09 × 0.06 mm) was mounted on loop with a small amount of the paraffin oil. The X-ray data were collected at 100K temperature on a Bruker APEX(II) DUO CCD diffractometer using Mo K_α radiation (λ = 0.71073 Å), ω-scans (2θ = 68.26), for a total of 10595 independent reflections. Space group P 1, a = 13.057 (2), b = 14.859 (3), c = 20.089 (3), β = 72.034 (8), V = 3467.0 (10) Å³, Monoclinic, Z = 2 for chemical formula C₆₀H₈₁N₉O₁₀, with two molecules in asymmetric unit; ρ_{calcd} = 1.043 gcm⁻³, μ = 0.579 mm⁻¹, F(000) = 1168, R_{int} = 0.0555 The structure was obtained by direct methods using SHELXS-97. The final R value was 0.0962 (wR2 = 0.2401) 21325 observed reflections (F_o ≥ 4σ(|F_o|)) and 1441 variables, S = 1.047. The largest difference peak and hole were 0.738 and -0.642 eÅ³, respectively.

3b.6 References

- 1 a) Seebach, D.; Beck A. K.; Bierbaum, D. J. *Chem. Biodiv.*, **2004**, *1*, 1111-1239. b) Seebach D.; Gardiner, J. *Acc. Chem. Res.*, **2008**, *41*, 1366-1375. c) Horne, W. S.; Gellmann, S. H. *Acc. Chem. Res.*, **2008**, *41*, 1399-1408. d) Vasudev, P. G.; Chatterjee, S.; Shamala N.; Balaram, P. *Chem. Rev.*, **2011**, *111*, 657-687. e) Pils, L. K. A.; Reiser, O. *Amino Acids*, **2011**, *41*, 709-718. f) Martinek T. A.; Fulop, F. *Chem. Soc. Rev.* **2012**, *41*, 687-702. g) Hecht, S.; Huc, I. (Eds.), *Foldamers: Structure, Properties and Applications*, Wiley-VCH, Weinheim, 2007. h) Bouillère, F.; Thétiot-Laurent, S.; Kouklovsky, C.; Alezra, V. *Amino Acids* **2011**, *41*, 687-707. i) Baldauf, C.; Hofmann, H.-J. *Helv. Chim. Acta* **2012**, *95*, 2348-2383. j) Goodman, C. M.; Choi, S.; Shandler, S.; DeGrado, W. F. *Nat. Chem. Biol.*, **2007**, *3*, 252-262.
2. a) Hanessian, S.; Luo, X.; Schaum R.; Michnick, S. *J. Am. Chem. Soc.*, **1998**, *120*, 8569-8570. b) Petersson, E. J.; Schepartz, A. *J. Am. Chem. Soc.*, **2008**, *130*, 821-823. c) Guichard G.; Huc, I. *Chem. Commun.* **2011**, *47*, 5933-5941. d) Reinert, Z. E.; Horne, W. S. *Org. Biomol. Chem.* **2014**, *12*, 8796-8802. e) Bonnel, C.; Legrand, B.; Bantignies, J. -L.; Petitjean, H.; Martinez, J.; Masurier N.; Maillard, L. T. *Org. Biomol. Chem.* **2016**, *14*, 8664-8669.
3. a) De Pol, S.; Zorn, C.; Klein, C. D.; Zerbe O.; Reiser, O. *Angew. Chem. Int. Ed.* **2004**, *43*, 511-514. b) Sharma, G. V. M.; Nagendar, P.; Jayaprakash, P.; Krishna, P.R.; Ramakrishna, K. V. S.; Kunwar, A. C. *Angew. Chem. Int. Ed.* **2005**, *44*, 5878-5882. c) Horne, W. S.; Price, J. L.; Keck J. L.; Gellman, S. H. *J. Am. Chem. Soc.* **2007**, *129*, 4178-4180. d) Choi, S. H.; Guzei I. A.; Gellman, S. H.; *J. Am. Chem. Soc.* **2007**, *129*, 13780-13781. e) Choi, S. H.; Guzei, I. A.; Spencer, L. C.; Gellman, S. H. *J. Am. Chem. Soc.* **2008**, *130*, 6544-6550. f) Baldauf, C.; Günther, R.; Hofmann, H. -J. *Biopolymers* **2006**, *84*, 408-413. g) Lee, M.; Shim, J.; Kang, P.; Guzei I. A.; Choi, S. H. *Angew. Chem., Int. Ed.* **2013**, *52*, 12564-12567. h) Legrand, B.; André, C.; Moulat, L.; Wenger, E.; Didierjean, C.; Aubert, E.; Averlant-Petit,

M. C.; Martinez, J.; Calmes, M.; Amblard, M. *Angew. Chem., Int. Ed.* **2014**, *53*, 13131-13135.

4. a) Baldauf, C.; Günther, R.; Hofmann, H. -J. *J. Org. Chem.* **2006**, *71*, 1200-1208. b) Guo, L.; Zhang, W.; Guzei, I. A.; Spencer, L. C.; Gellman, S. H. *Org. Lett.* **2012**, *14*, 2582-2585.

c) Sonti, R.; Dinesh, B.; Basuroy, K.; Raghothama, S.; Shamala, N.; Balaram, P. *Org. Lett.* **2014**, *16*, 1656-1659. d) Jadhav, S. V.; Bandyopadhyay, A.; Gopi, H. N. *Org. Biomol. Chem.*

2013, *11*, 509-514. e) Sharma, G. V. M.; Chandramouli, N.; Choudhary, M.; Nagendar, P.; Ramakrishna, K. V. S.; Kunwar, A. C.; Hofmann, H.-J. *J. Am. Chem. Soc.* **2009**, *131*, 17335-17344. f) Fisher, B. F.; Gellman, S. H. *J. Am. Chem. Soc.*, **2016**, *138*, 10766-10769. g) Misra,

R.; Saseendran, A.; George, G.; Veeresh, K.; Raja, K. M. P.; Raghothama, S.; Hofmann, H. -J.; Gopi, H. N. *Chem. Eur. J.* **2017**, *23*, 3764-3772. h) Stanovych, A.; Guillot, R.; Kouklovsky, C.; Miclet, E.; Alezra, V. *Amino Acids*, **2014**, *46*, 2753-2757.

5. a) Grison, C. M.; Robin, S.; Aitken, D. J. *Chem. Commun.* **2016**, *52*, 7802-7805. b) Guo, L.; Almeida, A. M.; Zhang, W.; Reidenbach, A. G.; Choi, S. H.; Guzei, I. A.; Gellman, S. H. *J. Am. Chem. Soc.* **2010**, *132*, 7868-7869. c) Araghi, R. R.; Jäckel, C.; Cölfen, H.; Salwiczek, M.; Völkel, A.; Wagner, S. C.; Wieczorek, S.; Baldauf, C.; Kocsch, B. *ChemBioChem* **2010**, *11*, 335-339.

6. a) Checco, J. W.; Gellman, S. H. *ChemBioChem* **2017**, *18*, 291-299. b) Checco, J. W.; Kreitler, D. F.; Thomas, N. C.; Belair, D. G.; Rettko, N. J.; Murphy, W. L.; Forest, K. T.; Gellman, S. H. *Proc. Natl. Acad. Sci. USA*, **2015**, *112*, 4552-4557. c) Bartus, É.; Hegedüs, Z.; Wéber, E.; Csipak, B.; Szakonyi, G.; Martinek, T. A. *ChemistryOpen* **2017**, *6*, 236-241. d) Grison, C. M.; Miles, J. A.; Robin, S.; Wilson, A. J.; Aitken, D. J. *Angew. Chem. Int. Ed.* **2016**, *55*, 11096-11100.

7. a) Choi, H.; Chakraborty, S.; Liu, R.; Gellman, S. H.; Weisshaar, J. *ACS Chem. Biol.* **2016**, *11*, 113-120. b) Arvidsson, P. I.; Frackenpohl, J.; Ryder, N. S.; Liechty, B.;

Petersen, F.; Zimmermann, H.; Camenisch, G. P.; Woessner, R.; Seebach, D. *ChemBioChem* **2001**, *2*, 771-773. c) Liu, R.; Chen, X.; Falk, S.; Masters, K.; Weisblum, B.; Gellman, S. H. *J. Am. Chem. Soc.* **2015**, *137*, 2183-2186. d) Cabrele, C.; Martinek, T. A.; Reiser O.; Berlicki, Ł. *J. Med. Chem.* **2014**, *57*, 9718-9739.

8. (a) Kulkarni, K.; Motamed, S.; Habila, N.; Perlmutter, P.; Forsythe, J. S.; Aquilar, M. I.; Del Borgo, M. P. *Chem. Commun.*, **2016**, *52*, 5844-5847. b) Misra, R.; Reja, R. M.; Narendra, L. V.; George, G.; Raghothama, S.; Gopi, H. N. *Chem. Commun.*, **2016**, *52*, 9597-9600. c) Mándity, I. M.; Monsignori, A.; Fülöp, L.; Forró, E.; Fülöp, F. *Chem. Eur. J.* **2014**, *20*, 4591-4597. d) Kim, J.; Kwon, S.; Kim, S. H.; Lee, C. -K.; Lee, J. -H.; Cho, S. J.; Lee H. -S.; Ihee, H. *J. Am. Chem. Soc.* **2012**, *134*, 20573-20576.

9. a) Mali, S. M.; Bandyopadhyay, A.; Jadhav, S. V.; Mothukuri, G.; Gopi, H. N. *Org. Biomol. Chem.* **2011**, *9*, 6566-6574. b) Mothukuri, G. K.; Thombare, V. J.; Katariya, M. M.; Veeresh, K.; Raja, K. M. P.; Gopi, H. N. *Angew. Chem. Int. Ed.*, **2016**, *55*, 7847-7851.

10. Mothukuri, G. K.; Mali, S. M.; Gopi, H. N. *Org. Biomol. Chem.*, **2013**, *11*, 803-813.

11. Mothukuri, G. K.; Gopi, H. N. *Org. Lett.* **2015**, *17*, 4738-4741.

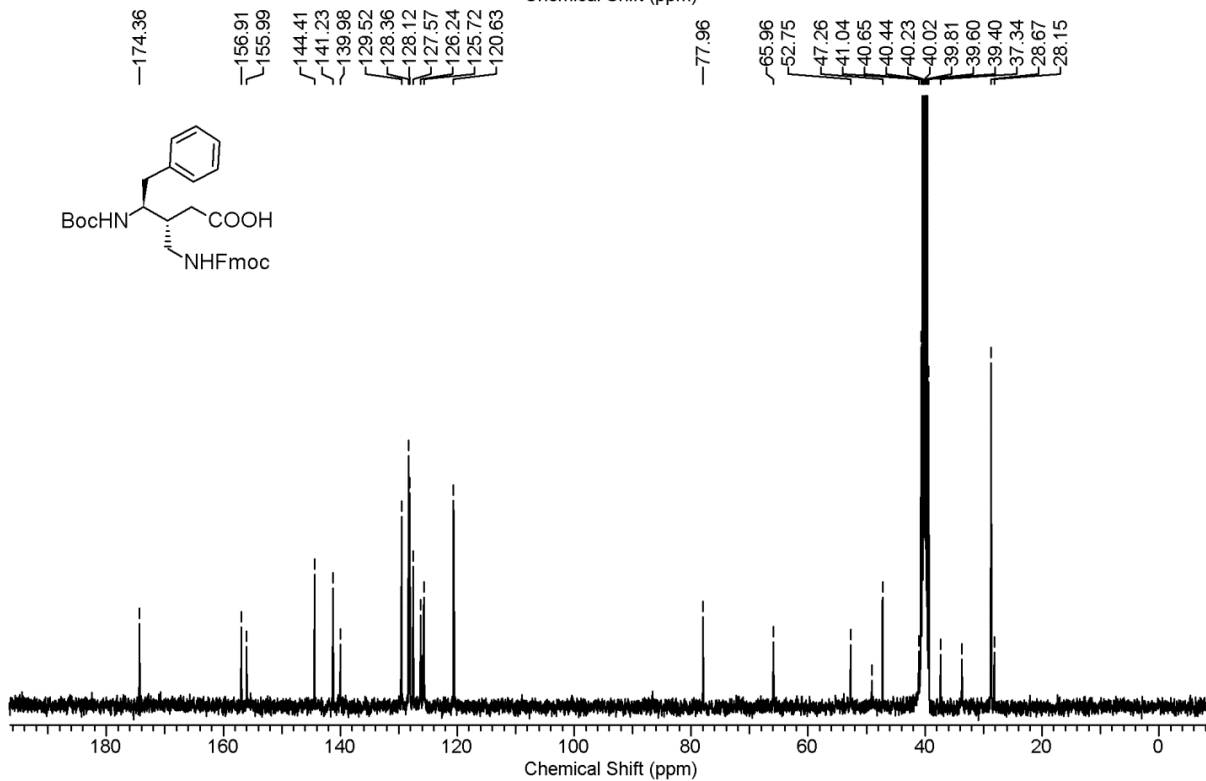
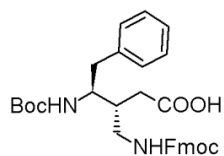
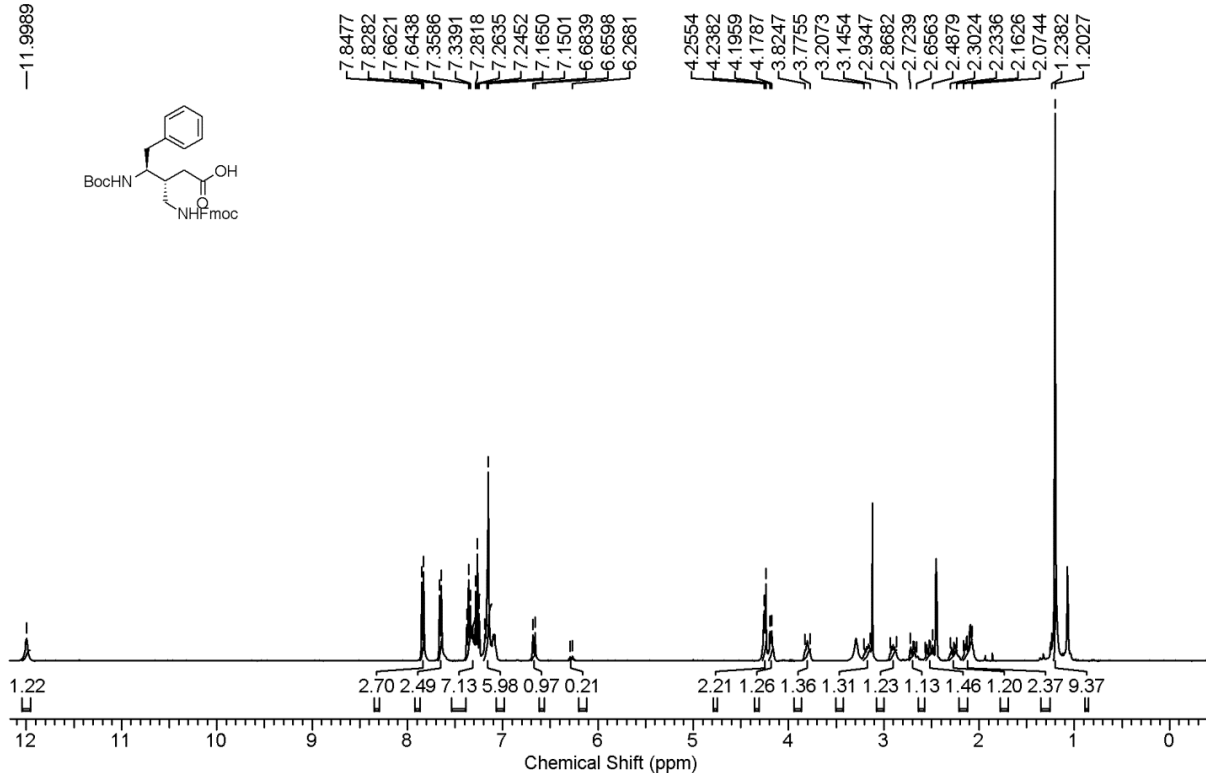
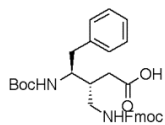
12. a) Sill, G. J. *Curr. Opin. Pharmacol.*, **2006**, *6*, 108-113. b) Silverman, R. B. *Angew. Chem. Int. Ed.* **2008**, *47*, 3500-3504.

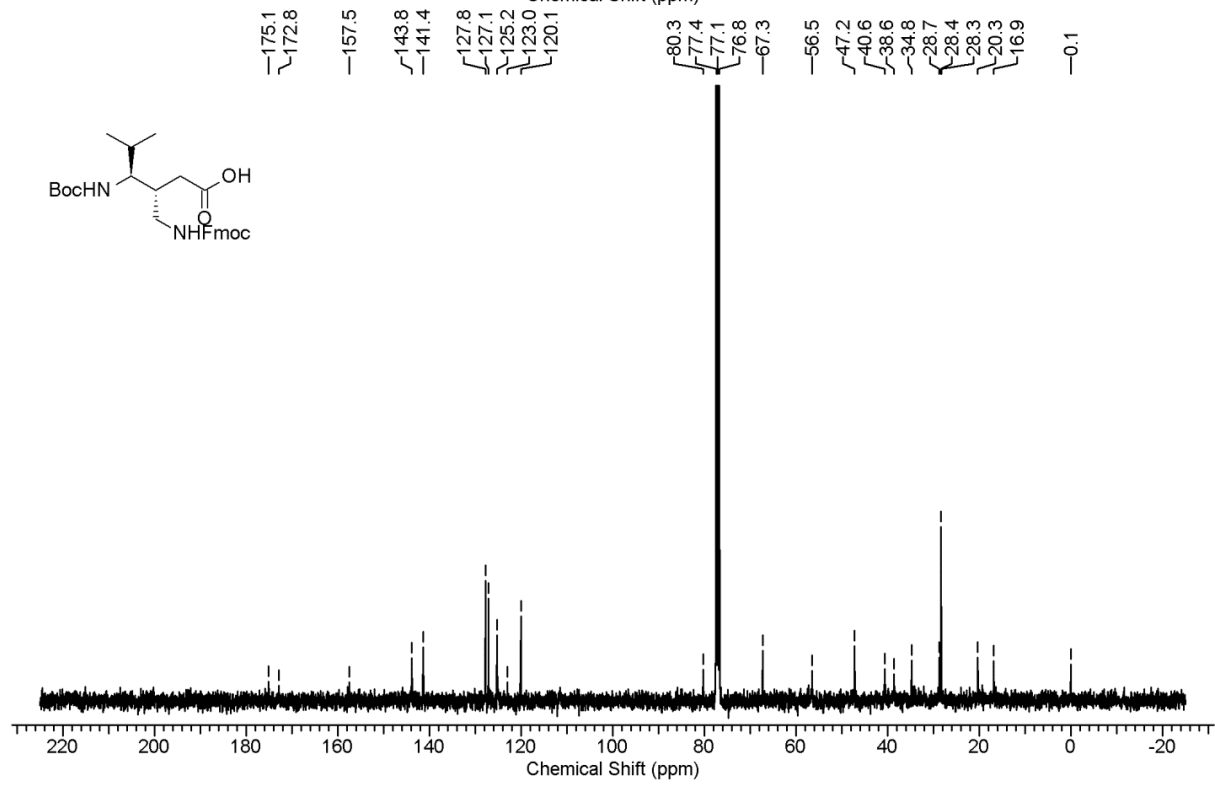
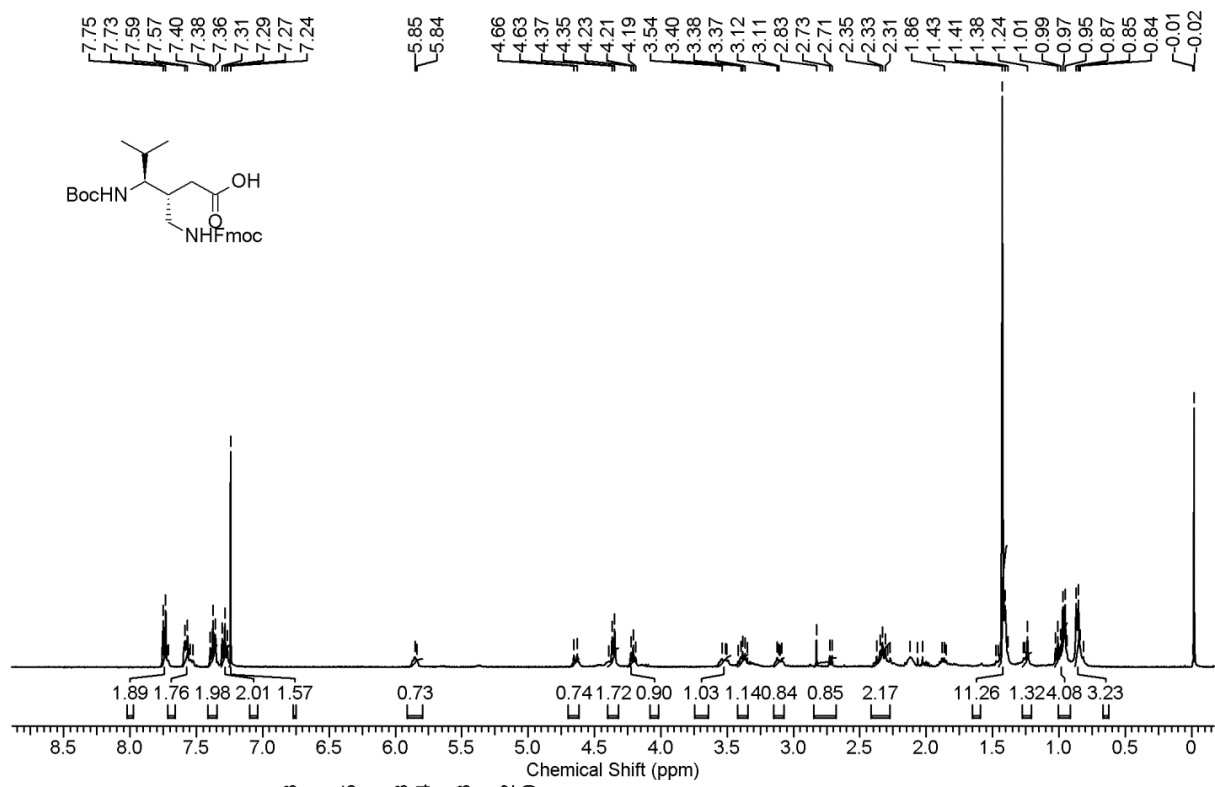
13. Plummer, J. S.; Emery, L. A.; Stier M. A.; Suto, M. J. *Tetrahedron Lett.*, **1993**, *34*, 7529-7532.

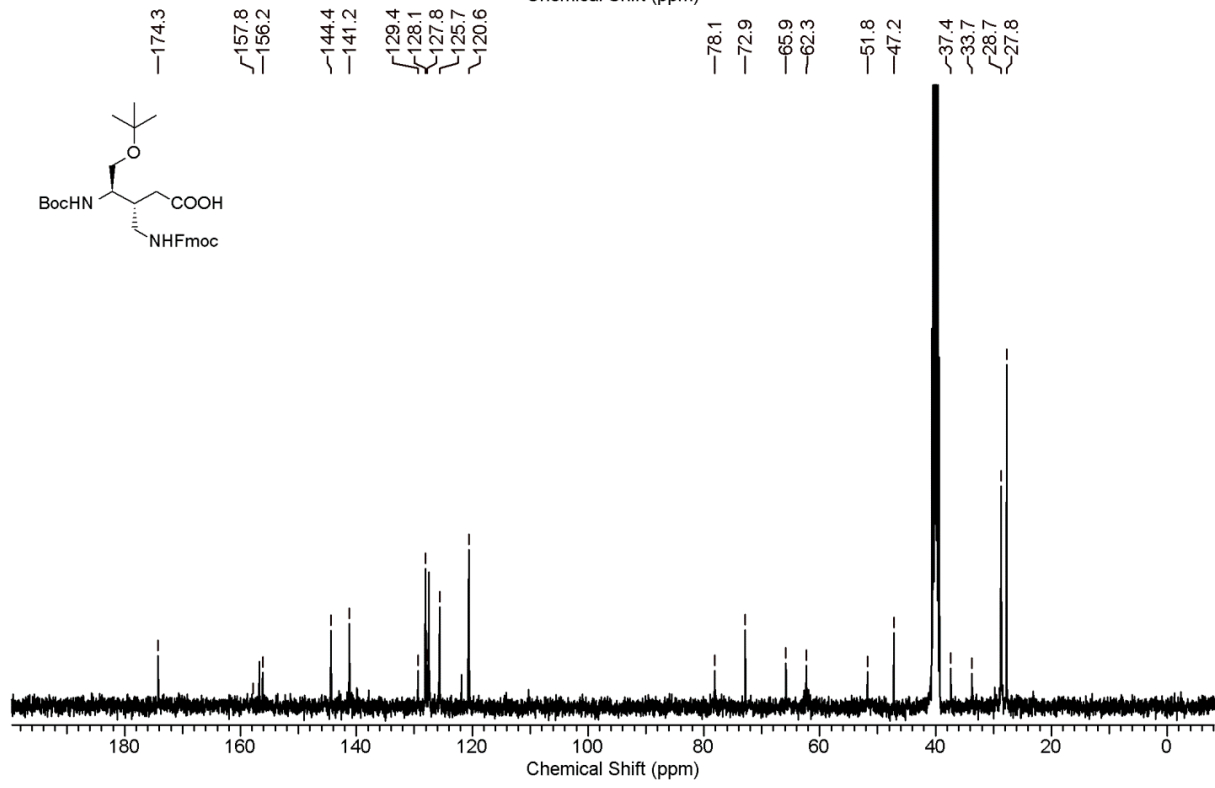
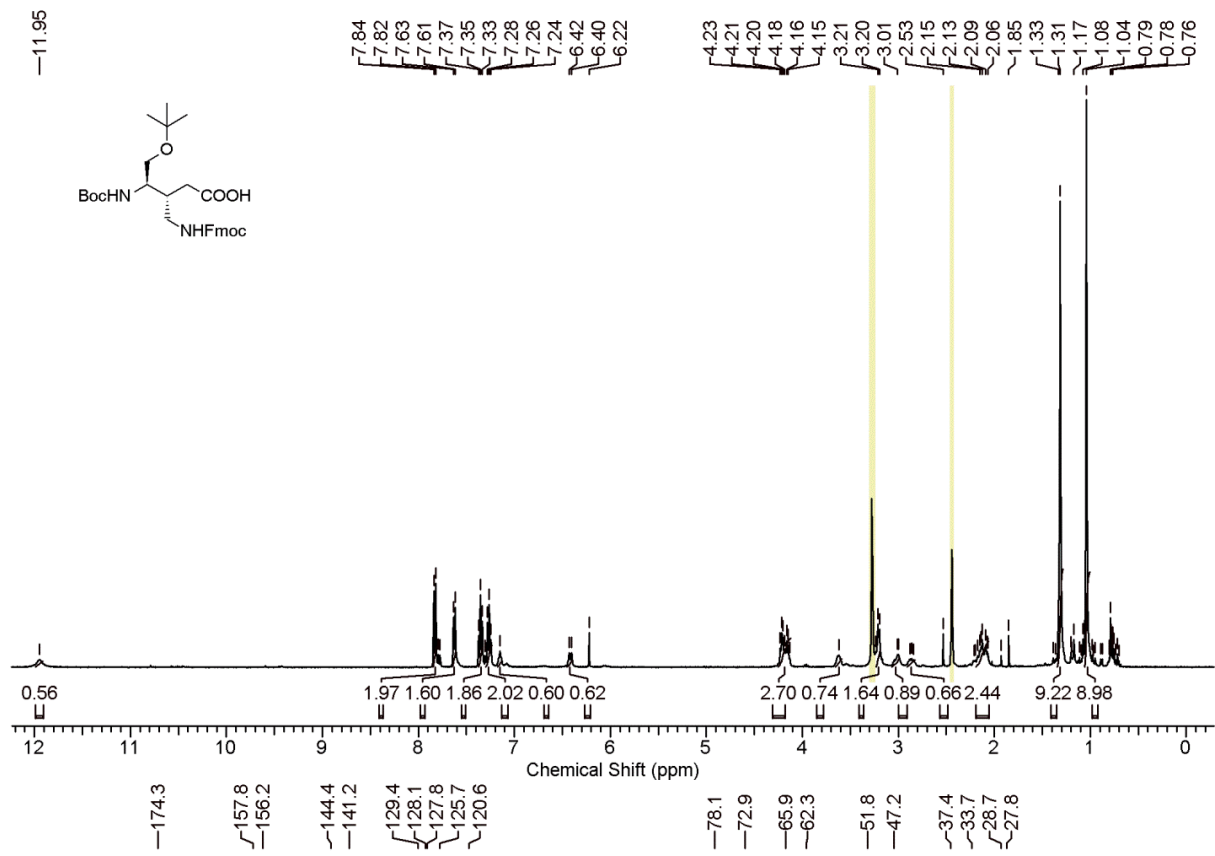
3b.7 Appendix IV: Characterisation data of synthesized peptides

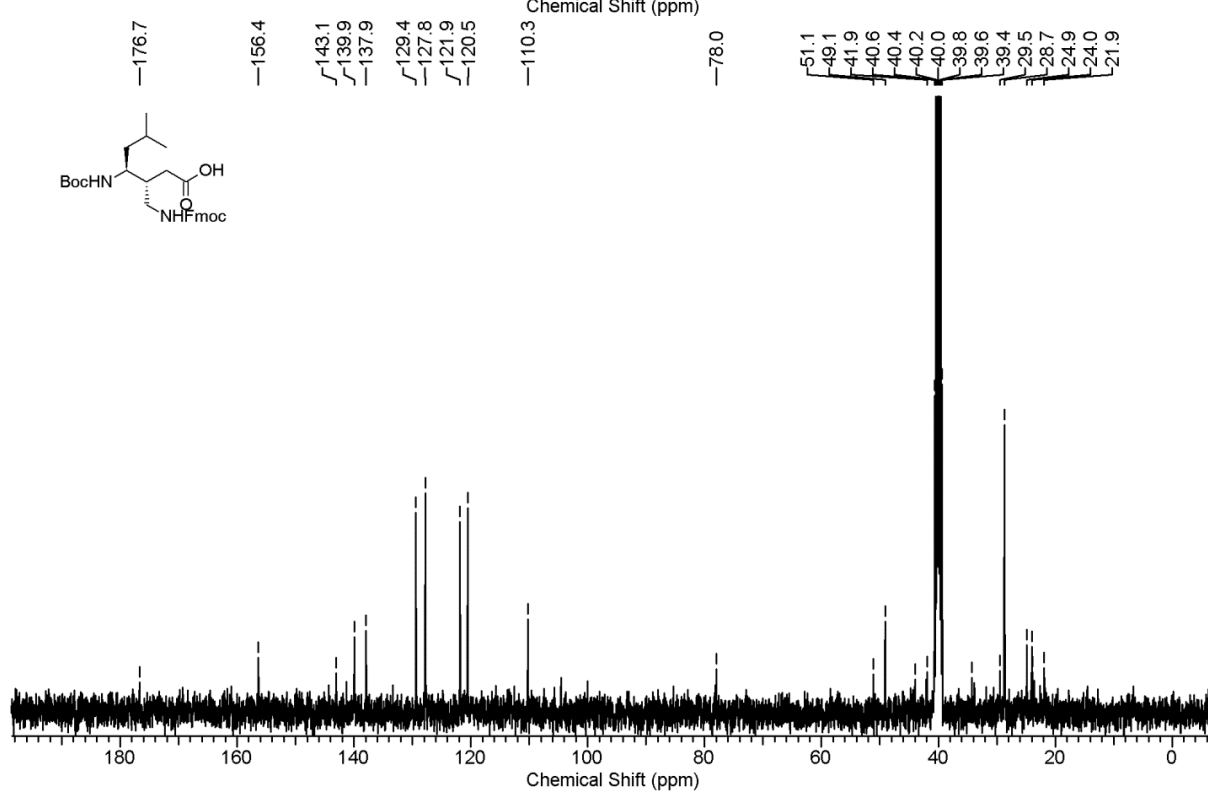
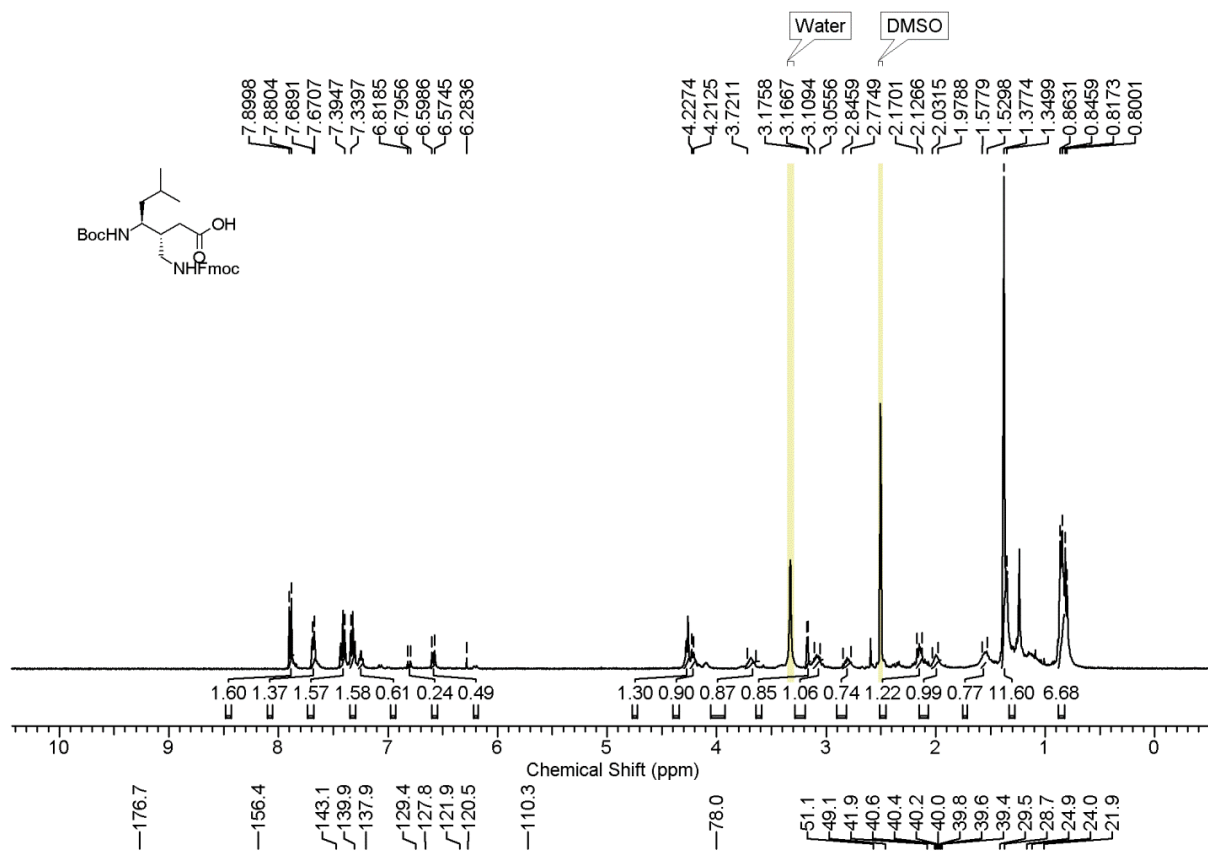
Designation	Description	Page No.
5a	^1H and ^{13}C NMR spectra	119
5b	^1H and ^{13}C NMR spectra	120
5c	^1H and ^{13}C NMR spectra	121
5d	^1H and ^{13}C NMR spectra	122
5e	^1H and ^{13}C NMR spectra	123
5f	^1H and ^{13}C NMR spectra	124
5g	^1H and ^{13}C NMR spectra	125
6a	^1H and ^{13}C NMR spectra	126
N1	^1H and ^{13}C NMR spectra	127
	MALDI-TOF spectrum	128

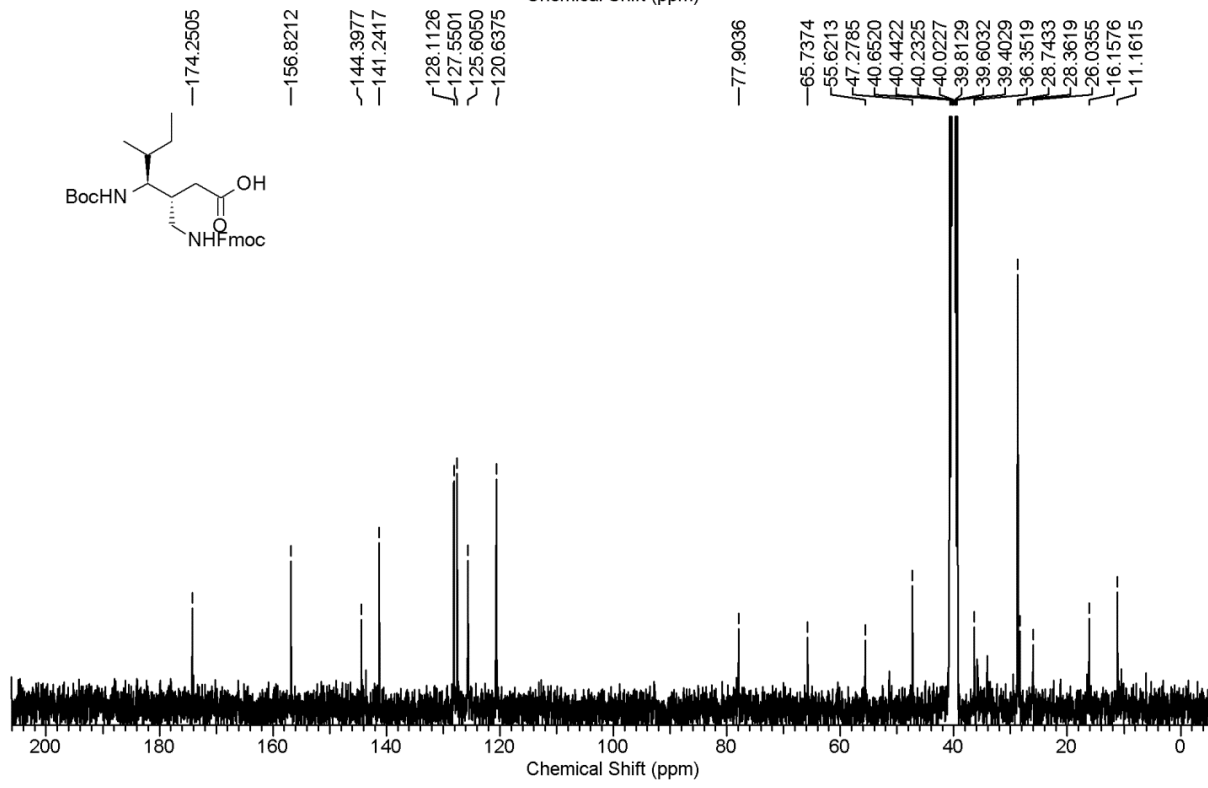
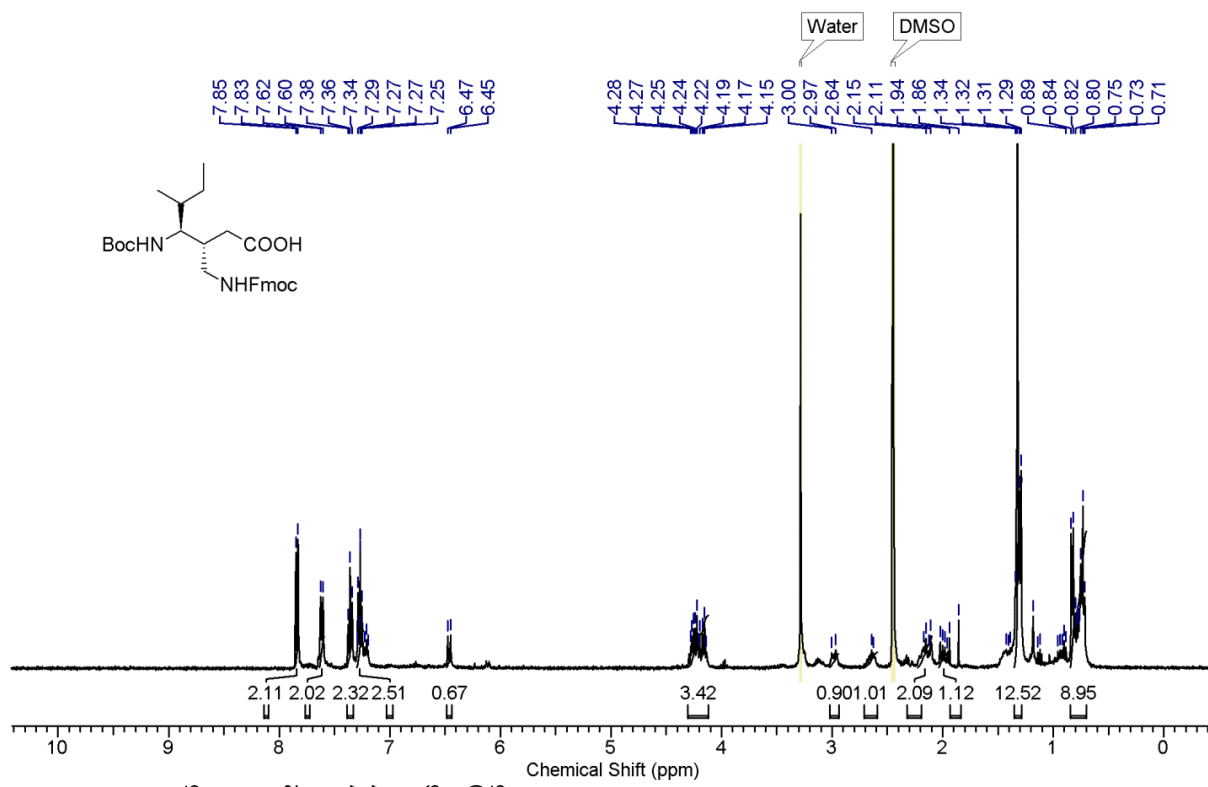
—11.9989

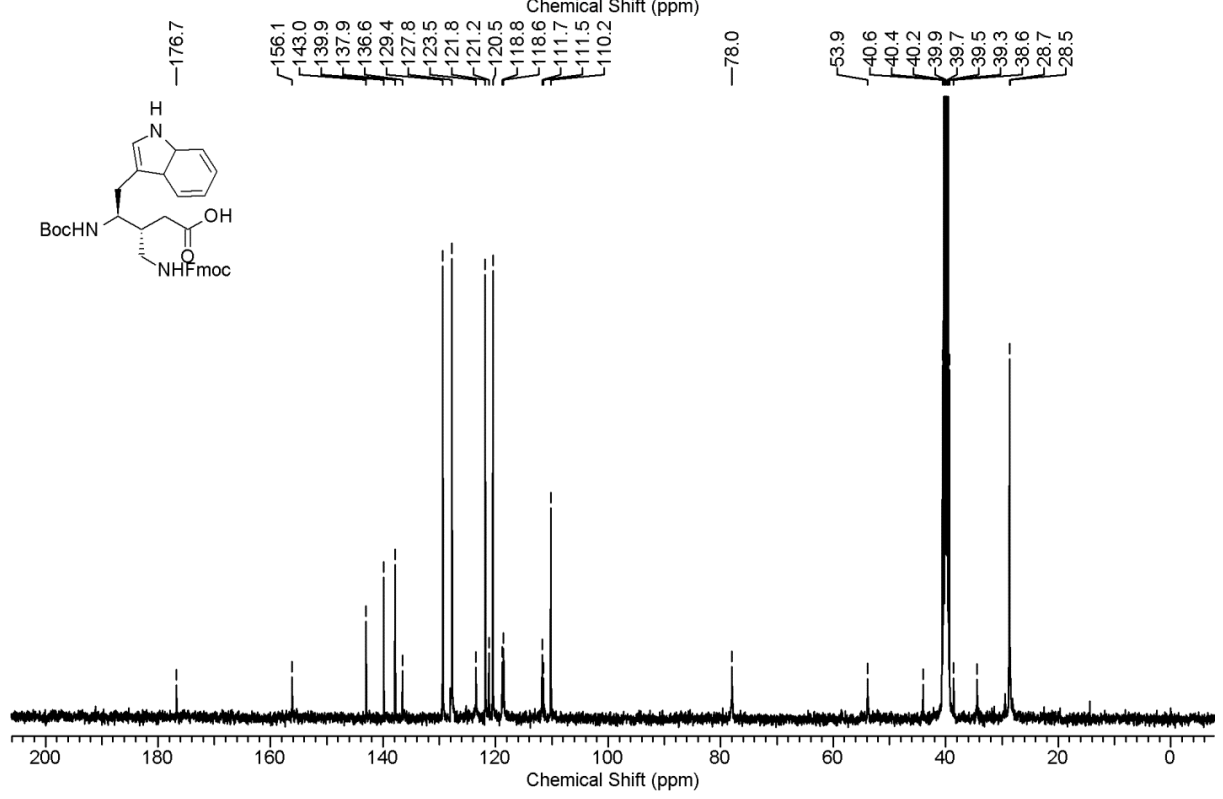
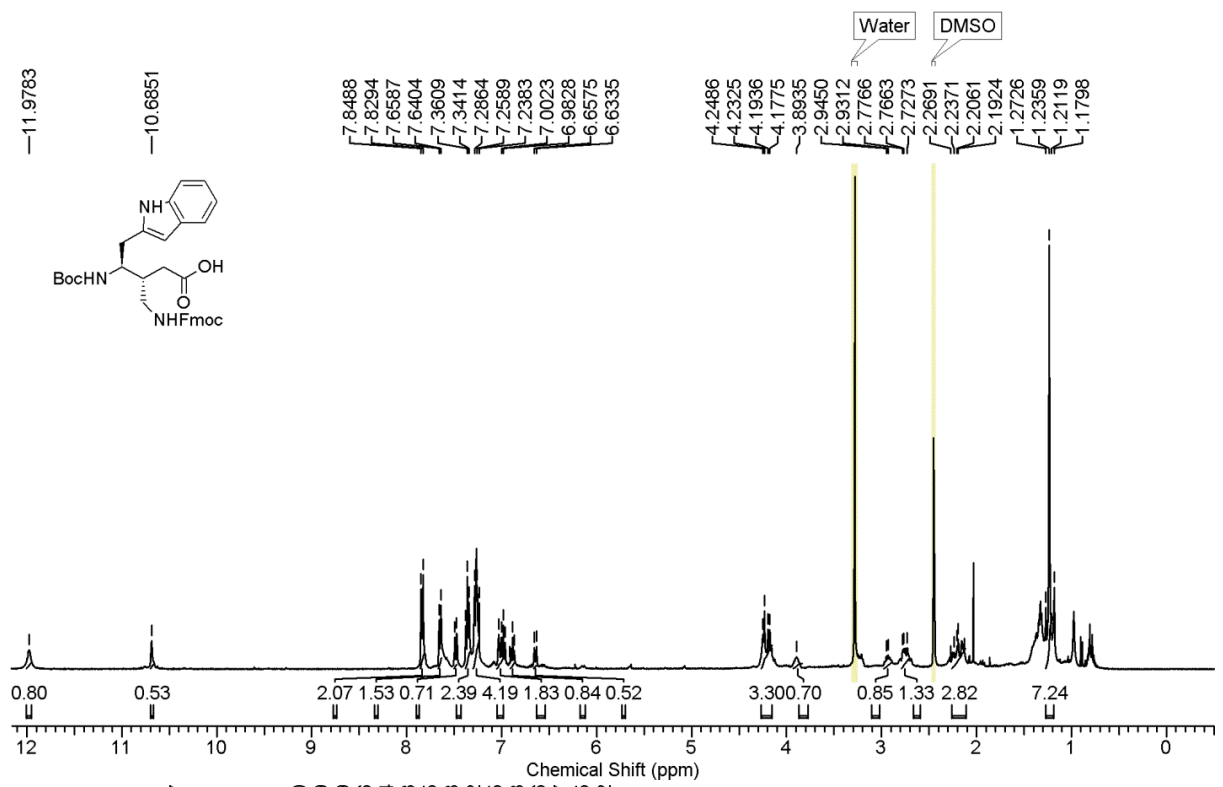


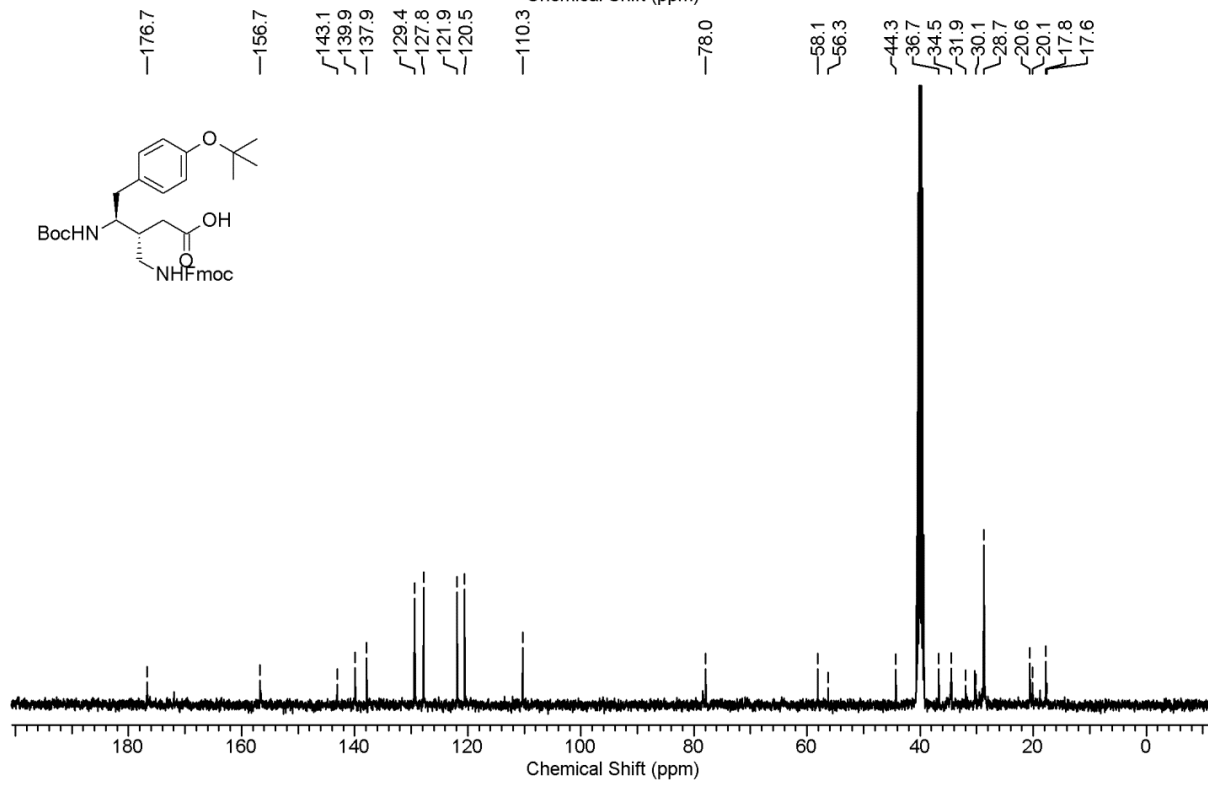
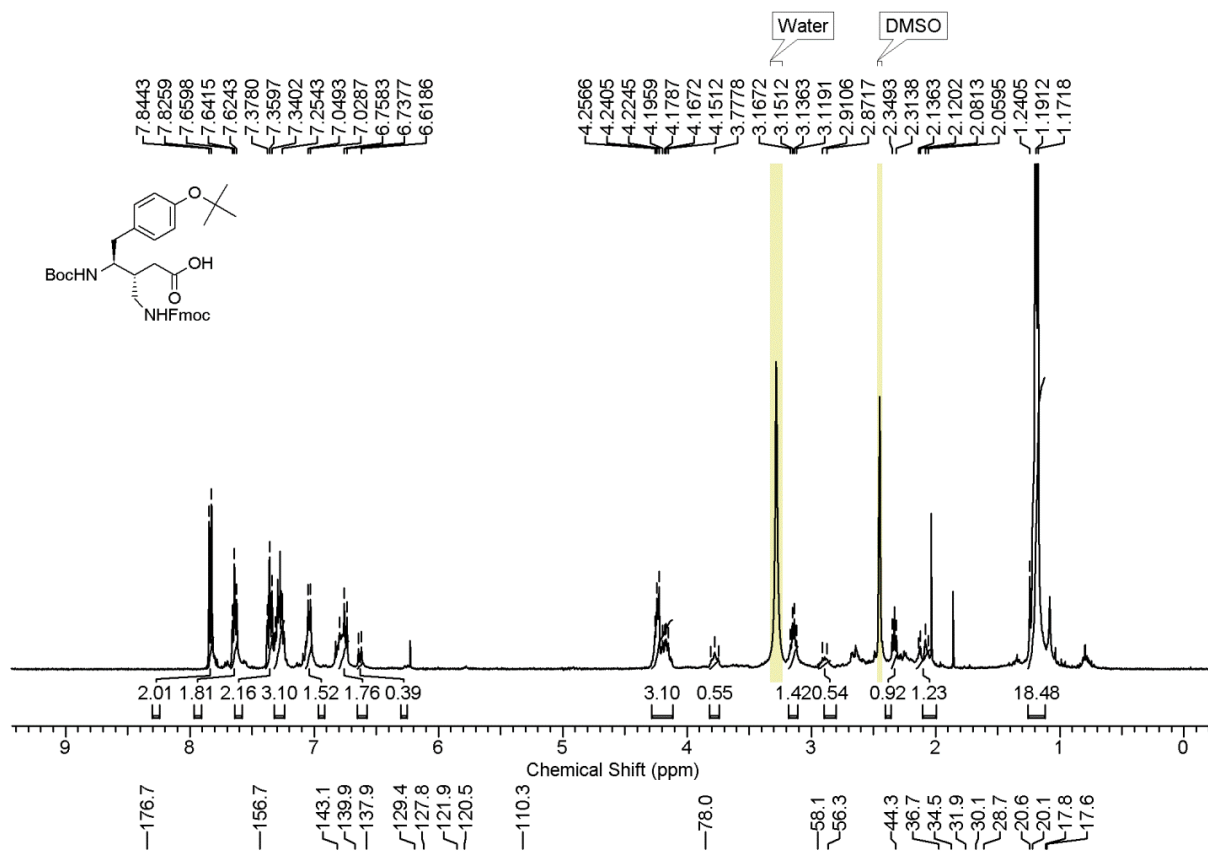


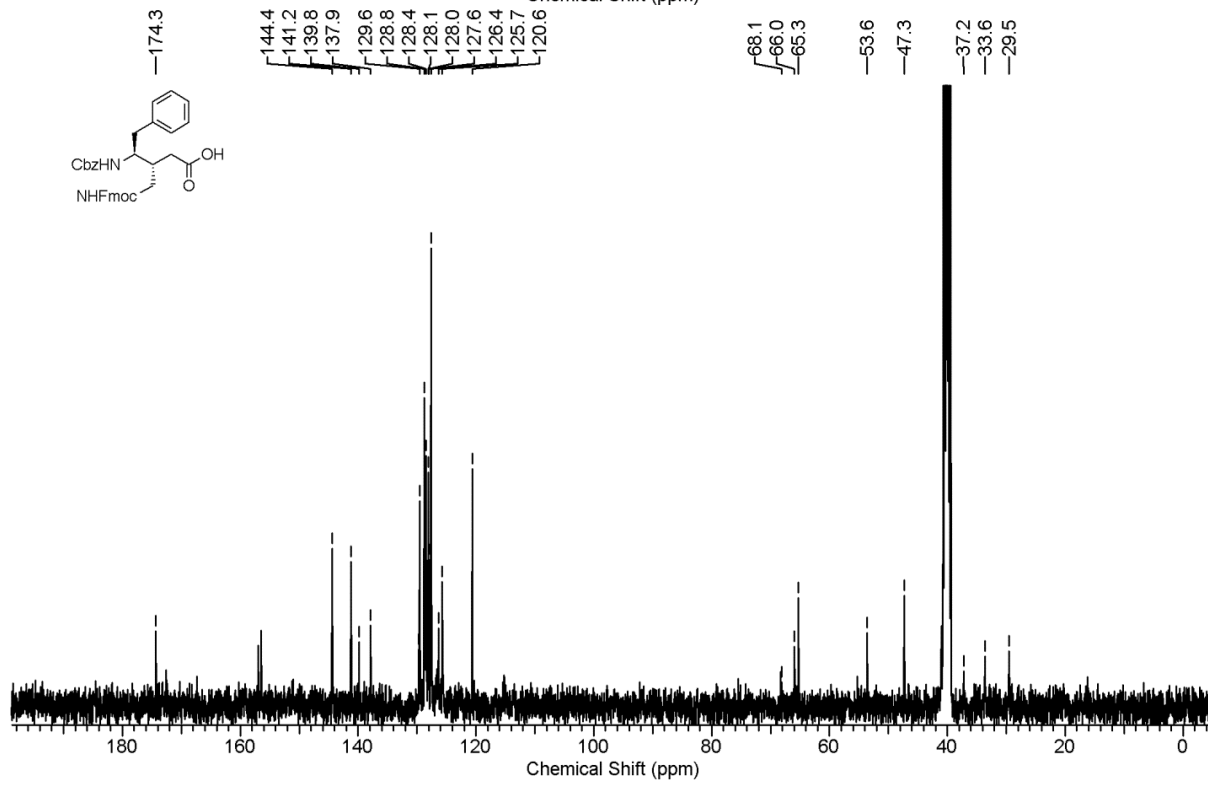
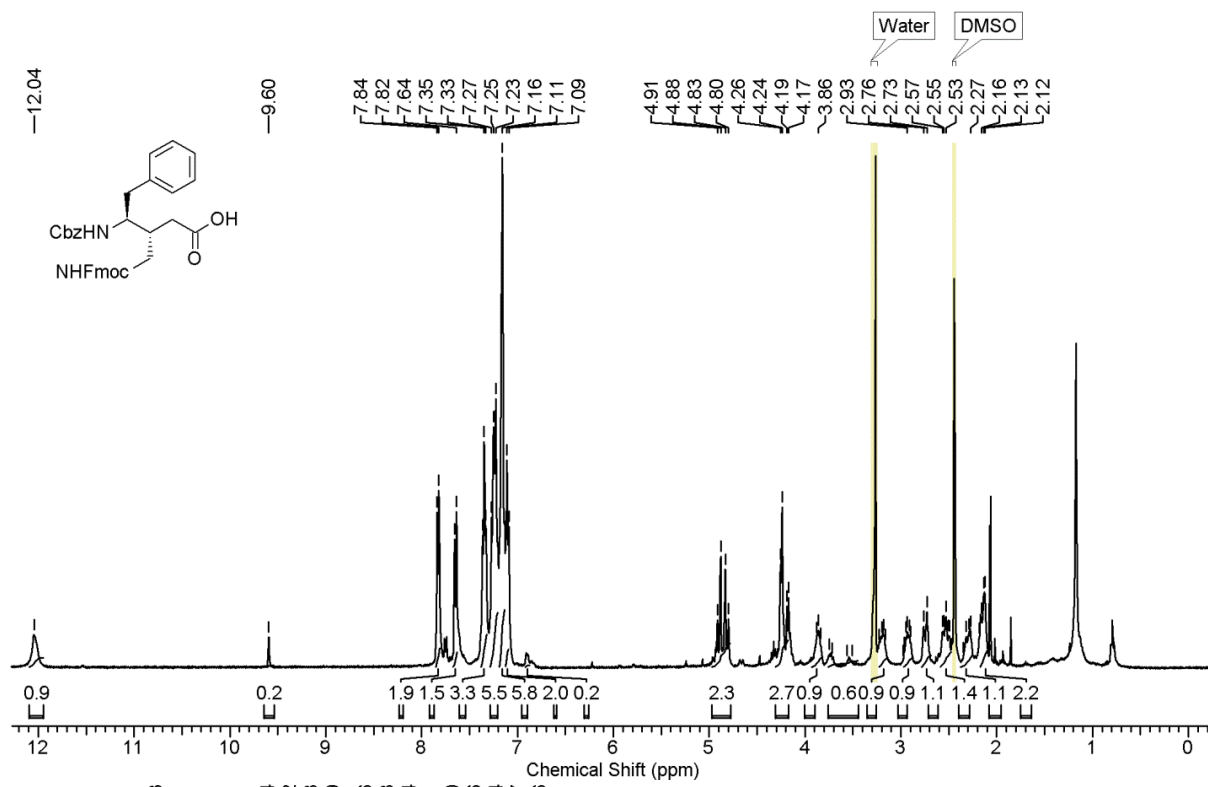


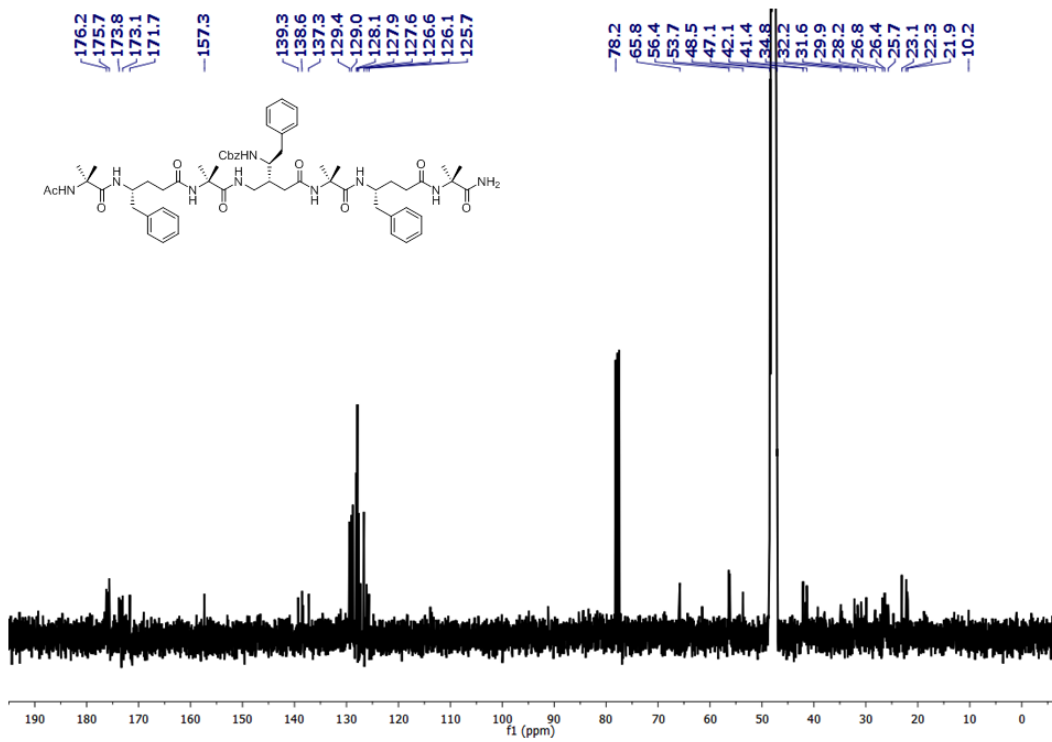
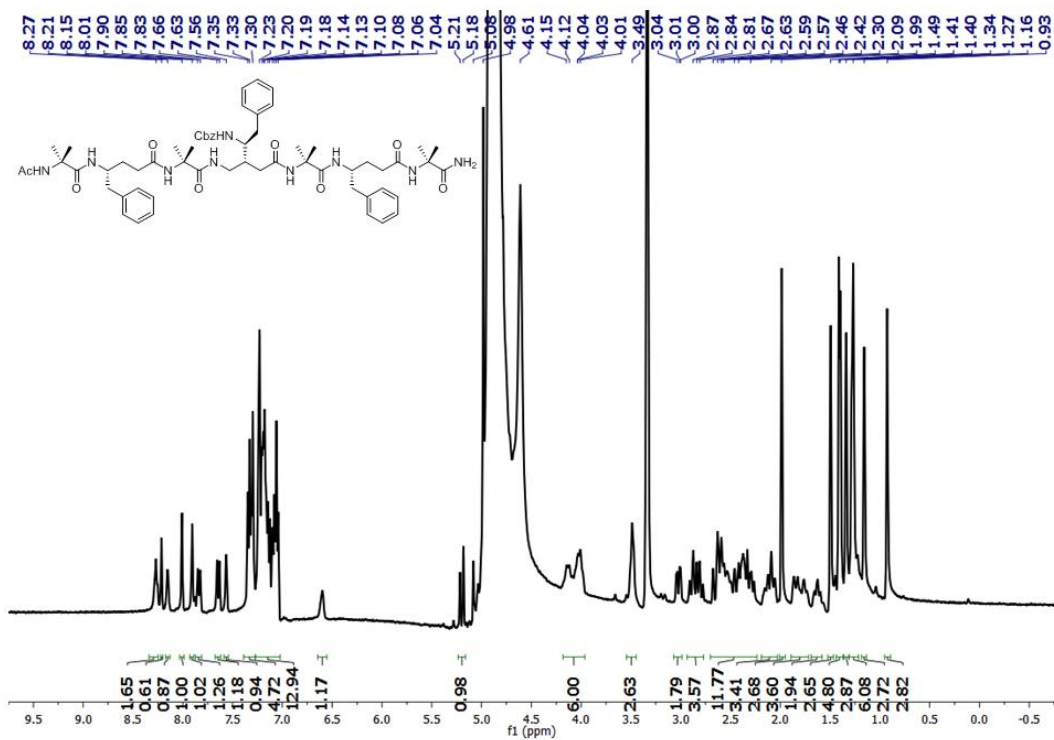






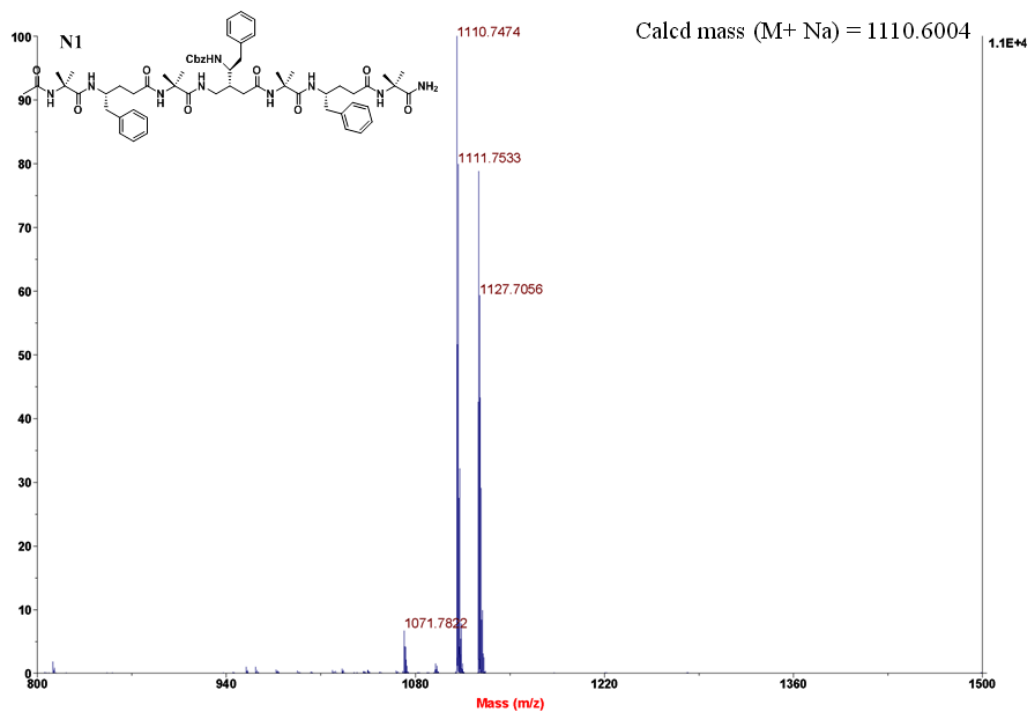






Spectrum Report

Final - Shots 400 - IISER-96-3; Run #171; Label C12



Chapter 4

Design, Structure and Potent Antimicrobial Activity of α,α,γ -Hybrid Peptide Helical Foldamers

4.1 Introduction

The raise in microbial resistance towards the conventional antibiotics has created an urgent need to develop antibiotics with different mode of action to combat microbial infections.¹ In addition, the modern medical advancements such as organ transplantation and invasive surgeries that depend heavily on the antibiotics are also at high risk. In this context, host-defense peptides have attracted considerable attention due to their broad spectrum antimicrobial activities.² The mechanism of action of these peptides showed that they target and disrupt the bacterial cell membrane.³ The issues such as poor selectivity, high dosage requirement, proteolytic instability and high hemolytic activities have hampered the practical applications of most of these natural peptides.⁴ However they have provided key structural features to develop new generation of potential antibiotics. Among the various types of the host-defense peptides, α -helical peptides are predominant.⁵ Along with helical propensity, the facial amphiphilicity and hydrophobicity are the crucial factors that are responsible for the antimicrobial activities of these helical peptides. Extensive efforts have been made in the literature to improve to the activity and proteolytic stability of natural antimicrobial peptides using D-amino acid oligomers,⁶ β -peptides,⁷ peptoids,⁸ mixed α/β -hybrid peptides,⁹ polymers of β -amino acids,¹⁰ substituted polyproline¹¹ and oligomers of aromatic subunits.¹² Some of these antimicrobial foldamers have been described in the Chapter 1. All these designs maintain the global amphiphilic and hydrophobic nature of the natural helical antibiotics. Recent advances in the structural analysis of γ -and hybrid γ -peptides reveal that γ -amino acids have shown grater helical propensity.¹³ The homooligomers of γ -amino acids have shown to adopt 14-helical conformations (14-atom H-bonds) without any stereochemical constraints.¹⁴ The hybrid peptides with 1:1 alternating α - and γ -amino acids have shown to adopt stable 12-helical (12-atom H-bonds) conformations.¹⁵ Recently, Balaram and

colleagues and we reported the 10/12-helical conformation of a hybrid peptide constituted with 2:1 α - and γ -amino acids in single crystals.^{16,17} The sequences of the peptides (**A** and **B**) and their structures are shown in Figure 4.1. The interesting feature of the 10/12-helix

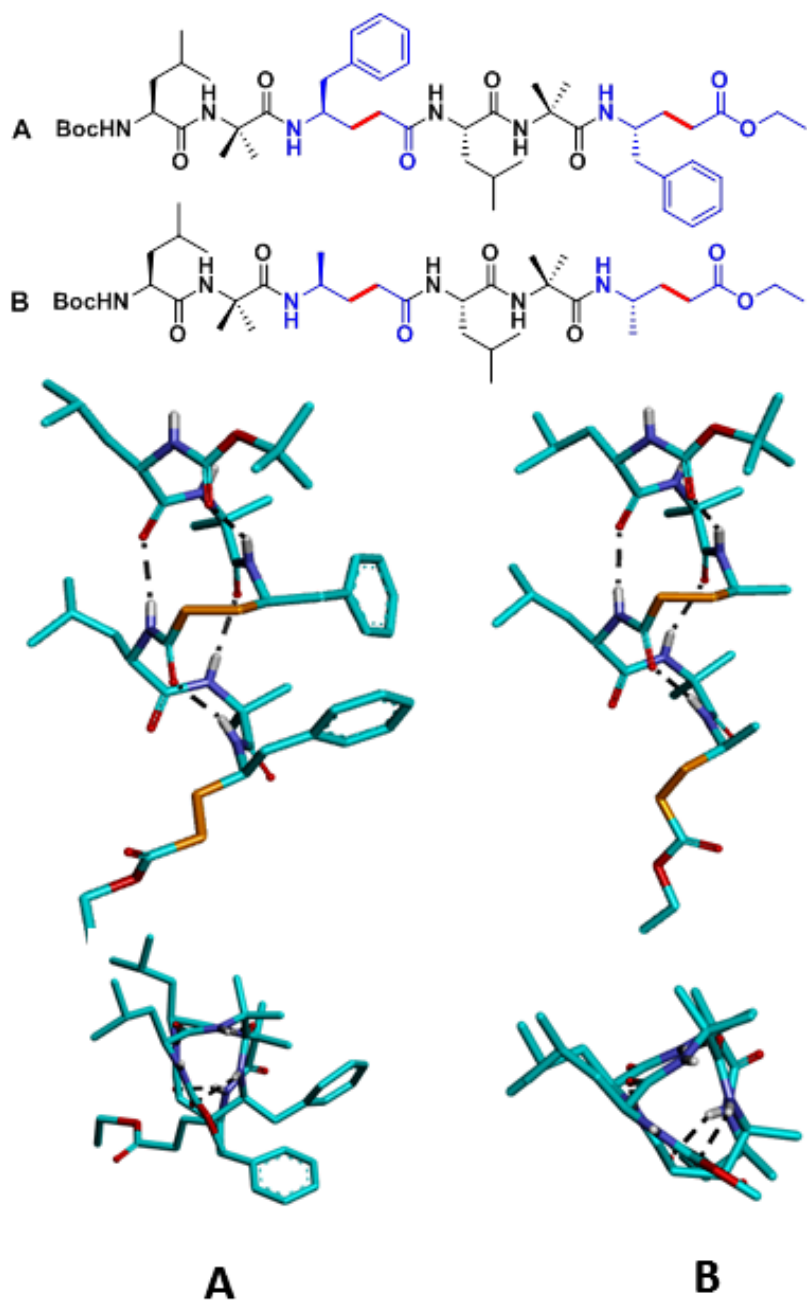


Figure 4.1: Sequence of $\alpha\gamma$ -hybrid peptides (**A** and **B**) and their X-ray structures.¹⁷ B) Top view of the 10/12-helical structures are shown in the bottom plane.

is that the side-chains of the amino acids are oriented at the three faces of the helical cylinder (Figure 4.1 top view). The spatial arrangement of amino acid side-chains along the helical cylinder provided an excellent opportunity to design amphiphilic helices with lesser number of γ -amino acids.

4.2 Aim and rational of the present work

Based on the structural evidences of the $\alpha\gamma$ -hybrid peptides from the previous studies, we sought to investigate their antimicrobial properties and their solution conformations. In addition, there is no report on whether these peptides can adopt 10/12-helix conformation in solution. In this chapter, we are reporting the design, synthesis, conformational analysis in solution and antimicrobial properties of various amphiphilic $\alpha\gamma$ -hybrid peptides. We explored 2D NMR analysis to understand their conformations in solution. To understand the antibacterial activity of these designed amphiphilic foldamers, various Gram positive and Gram negative bacteria and Methicillin-resistant *Staphylococcus aureus* (MRSA) and Methicillin-sensitive *Staphylococcus aureus* (MSSA) were tested. Along with the antibacterial activities, their hemolytic activity and DNA binding ability were also investigated.

4.3 Results

4.3.1 Peptide design and synthesis

The sequence of the designed $\alpha\gamma$ -hybrid peptides are shown in Scheme 4.1. Peptides **H1-H6** are Leu-Lys- γ Leu tripeptide repeats. Peptide **H7** is an analogue of peptide **H3** where the γ -Leu was replaced with γ -Ala. Peptide **H8** is a control α -peptide. The γ -amino acids were synthesized starting from α -amino acids through Wittig reaction as reported earlier.¹⁵ All the peptides were synthesized on Knorr Amide resin using standard Fmoc-Chemistry. Except **H6**, the *N*-terminus of all other peptides was not capped with acetyl group for better solubility

in aqueous solutions. All peptides were purified using reverse phase HPLC and pure peptides were subjected to the antibacterial activities and solution conformation analysis.



Scheme 4.1: Sequences of $\alpha\gamma$ -hybrid peptides (**H1-H7**) and α -peptide counterpart **H8**.

4.3.2 Solution conformation of peptides

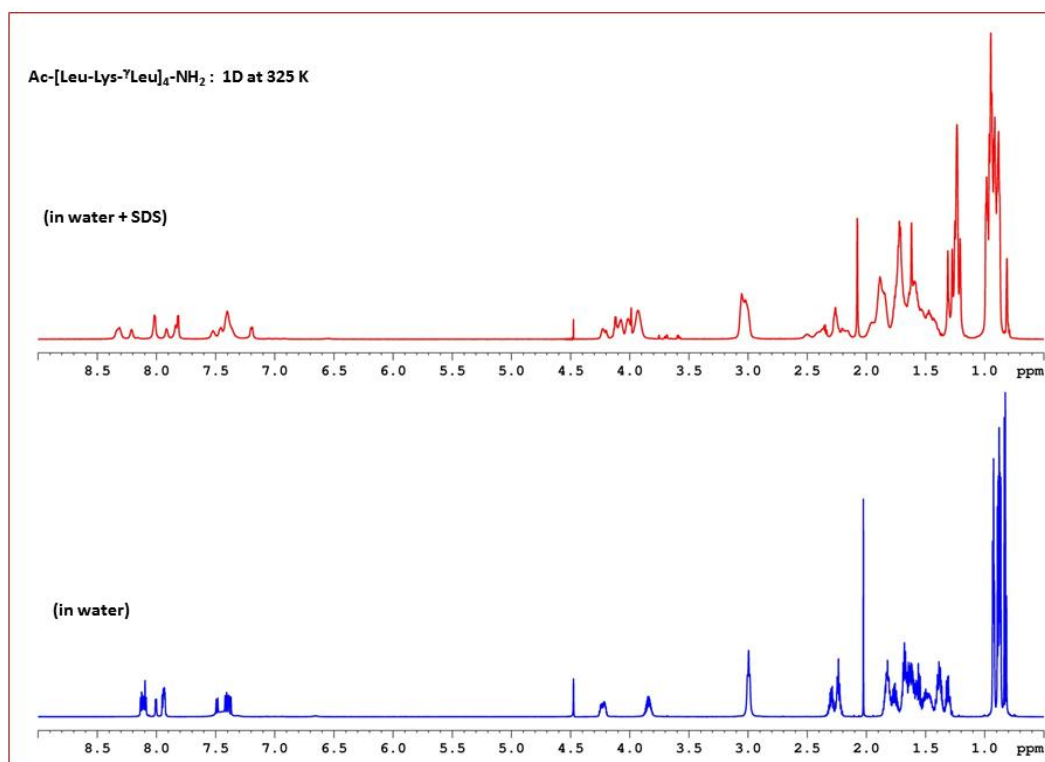


Figure 4.2: 800 MHz ¹H plot of peptide **H6**: Ac-[Leu-Lys-γLeu]₄-CONH₂ in water and with SDS.

Though resonance were broadened, spectral dispersion especially in amide region were observed.

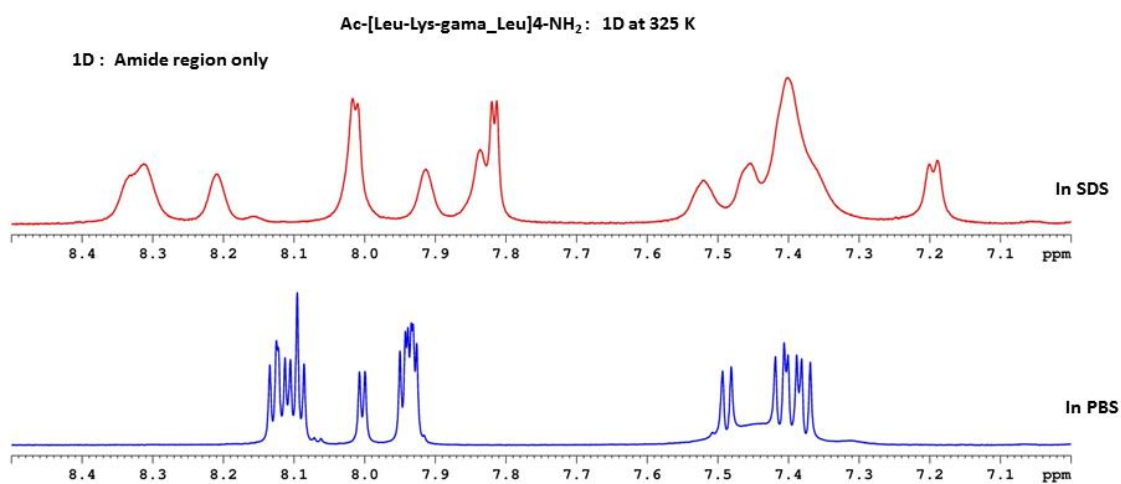


Figure 4.3: Partial ¹H NMR spectrum of **H6** depicting the amide NH chemical shifts

Table 4.1: Chemical shifts of Peptide **H6** in SDS

Residue	Chemical shifts							
	HN	H ^α	H ^β	H ^γ	H ^δ	H ^ε	Others	dδ/dt (ppb/°C)
L1	7.83	4.25	1.74	1.66	0.99	-	-	4.59
K2	8.03	4.22	1.90/1.78	1.47	1.57	3.08	7.42	-
γL3	7.21	1.99	2.39/2.23	3.94	1.63/1.51	1.25	CH ₃ - 0.92/0.88	3.51
L4	7.85	4.05	1.73	1.64	0.98	-	-	3.78
K5	8.31	4.10	1.88	1.50	1.74	3.02	7.42	-
γL6	7.47	1.97	2.52/2.19	3.96	1.60/1.43	1.27	CH ₃ -0.92	3.24
L7	8.02	4.04	1.90/1.73	1.63	0.98	-	-	-
K8	8.34	4.15	1.92/1.73	1.33	1.54	3.04	7.42	-
γL9	7.53	1.96/1.77	2.43/2.26	3.95	1.45/1.59	1.28	CH ₃ -0.92	4.05
L10	7.92	4.12	1.68	1.61	0.97	-	-	5.13
K11	8.21	4.26	1.90/1.74	1.54	1.62	3.07	7.42	4.59
γL12	7.42	1.85/1.75	2.29	3.97	1.60/1.49	1.33	CH ₃ -0.93	1.89

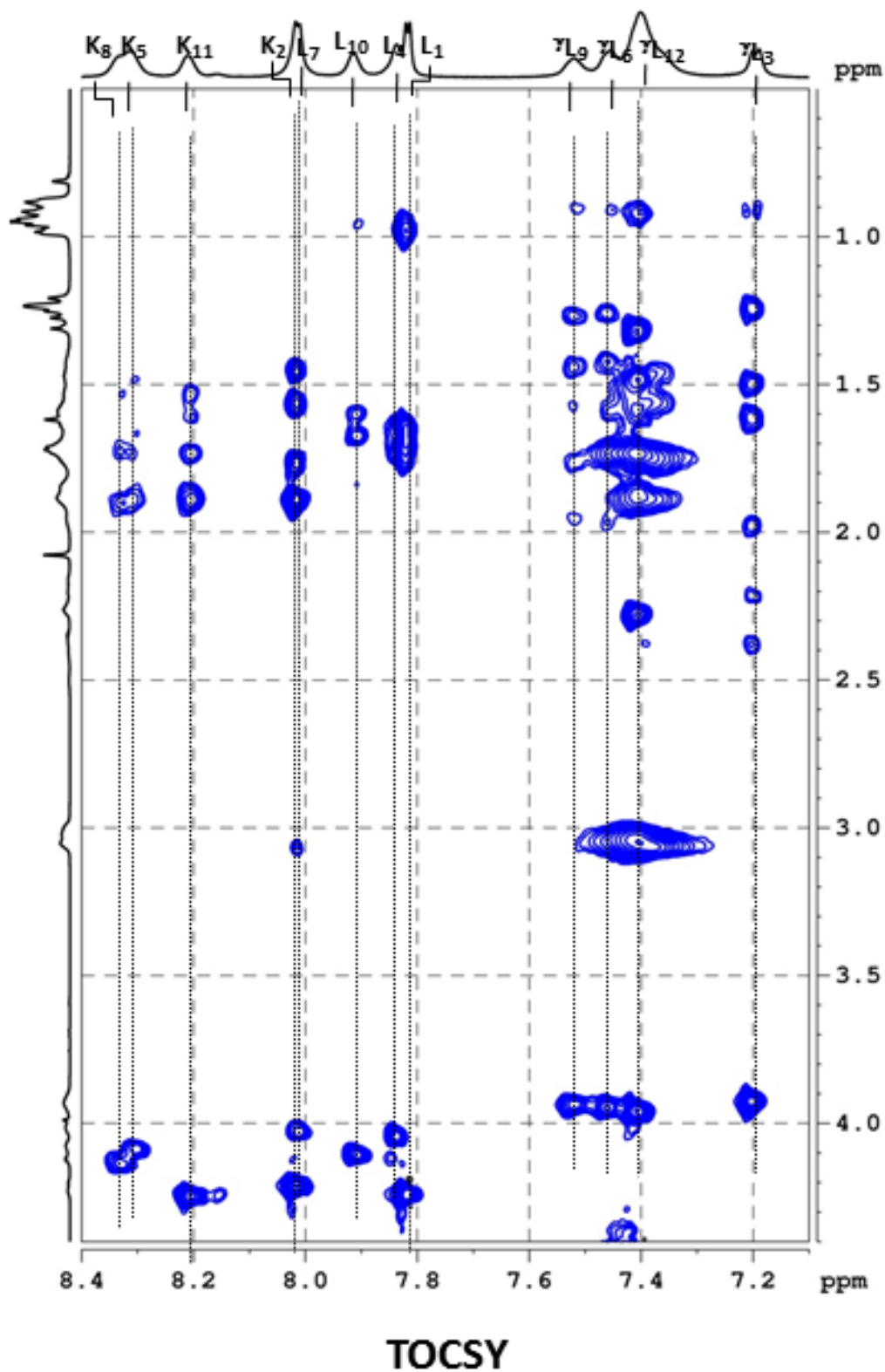


Figure 4.4: Partial 800 MHz TOCSY plot of **H6**. Residue specific TOCSY pattern for each residue is shown.

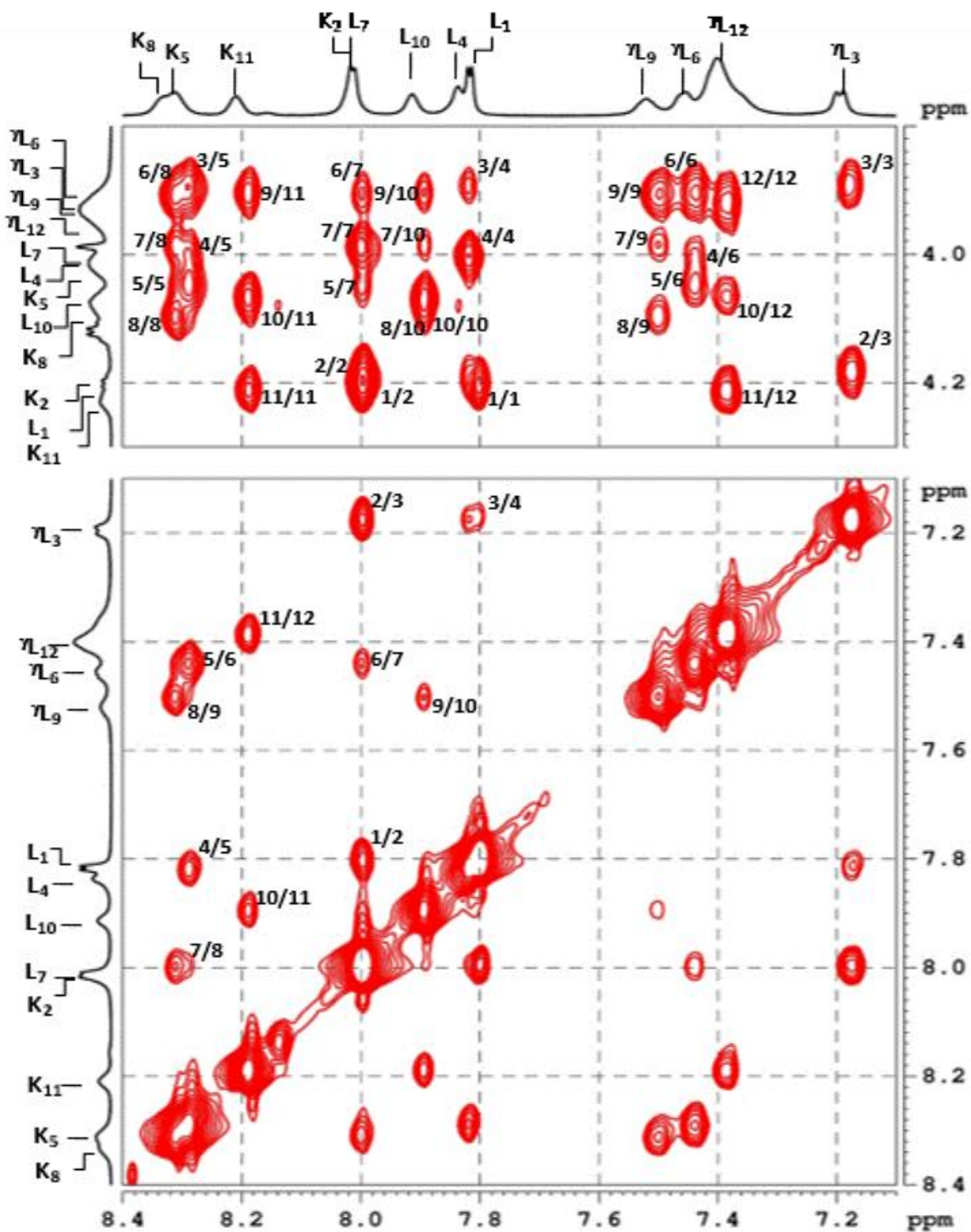


Figure 4.5: Partial NOESY spectrum of H6 depicting the d_{NN} and $d_{CH\alpha N}$ NOEs of hybrid peptide H6.

Table 4.2. NOE's observed for **H6**.

NOE	Upper limit (Å°)	Distance in NMR structure (Å°)
L1H α -K2NH	3.5	3.46
L1NH-K2NH	3.5	2.70
K2NH- γ L3NH	3.5	2.79
K2H α - γ L3NH	3.5	3.48
γ L3NH-L4NH	3.5	3.58
γ L3H γ - L4NH	5.0	3.88
γ L3H γ -K5NH	3.5	2.97
γ L3NH-K5NH	5.0	4.53
L4NH-K5NH	3.5	3.19
L4H α -K5NH	3.5	3.58
L4NH- γ L6NH	3.5	4.42
L4H α - γ L6NH	3.5	3.78
K5H α - γ L6NH	3.5	3.45
K5NH- γ L6NH	3.5	2.61
γ L6NH-L7NH	3.5	3.60
γ L6H γ -L7NH	3.5	3.55
γ L6H γ -K8NH	3.5	2.46
L7NH-K8NH	3.5	3.01
L7H α -K8NH	3.5	3.54
L7H α - γ L9NH	5.0	3.80
K8NH- γ L9NH	3.5	2.74
γ L9NH-L10NH	3.5	3.46
γ L9H γ -L10NH	5.0	3.97
γ L9H γ -K11NH	3.5	3.03
L10NH-K11NH	3.5	2.93
L10H α -K11NH	3.5	3.47
L10H α - γ L12NH	3.5	3.56
K11NH- γ L12NH	3.5	2.95
K11H α - γ L12NH	2.5	3.05

In order to understand the solution conformation of $\alpha\alpha\gamma$ -hybrid peptides, we subjected all peptides to 2D NMR (TOCSY and NOESY) analysis. Peptides gave poor quality ^1H NMR in aqueous solution except **H6**, however better spectrum was obtained in membrane mimicking sodium salt of dodecyl-*d*25 sulfate (SDS). Though the resulting 1D spectrum had relatively larger line widths, resonances show better dispersion in SDS. The ^1H NMR spectrum of **H6** in aqueous solution and in SDS is shown in Figure 4.2. Chemical shifts of proton are given in Table 4.1. Instructively, a clear distinction in the chemical shifts between α - and γ - residue amide NHs has been observed in ^1H NMR of **H6**. Similar trend has also been observed in the solution conformations of α,γ -hybrid peptide 12-helices.¹⁸ The amide NHs of γ -residues are relatively up-field shifted compared to the NHs of α -residues. Fully assigned partial TOCSY spectrum of peptide **H6** is shown in Figure 4.4. The 2D NOESY spectrum in SDS was rich in cross peaks. The partial NOESY spectrum depicting $\text{NH}\leftrightarrow\text{NH}$ and $\text{C}_\alpha\text{H}\leftrightarrow\text{NH}$ NOEs is shown in Figure 4.5. The strong d_{NN} NOEs followed by $d_{\alpha\text{N}}(i, i+1)$ NOEs clearly indicating helical fold in **H6**. The sequential $\text{NH}(i)\leftrightarrow\text{NH}(i+1)$ and $\text{C}^\alpha\text{H}(i)\leftrightarrow\text{NH}(i+1)$ NOEs observed in the NOESY spectrum are tabulated in the Table 4.2. The NOEs observed between $\text{NH}\gamma\text{Leu}(i)\leftrightarrow\text{NH}\text{Leu}(i+1)$ were found to be weaker than the other sequential $\text{NH}\leftrightarrow\text{NH}$ NOEs. Using these unambiguous NOE constraints, energy minimized NMR structures were generated. The superposition of ten energy minimized structures is shown in Figure 4.6. As anticipated, peptide **H6** adopted 10/12 helical conformation in solution. The top-view depicting the side-chain projection of the peptides is shown in Figure 4.6. The torsion angles derived from the solution structure are in excellent agreement with the previously reported X-ray structures.^{16,17} Nevertheless, the C-terminal amide NH is involved in the 9-membered H-bonding with the CO of Leu11 ($i\rightarrow i+2$). All γ -Leu residues adopted g^+ , g^+ backbone conformation along $\text{C}^\gamma\text{-C}^\beta$ and $\text{C}^\beta\text{-C}^\alpha$ bonds. As expected, the side-chains of Lys residues are

projected at one face of the helix. Thus the amphiphilic helices can be readily generated using $\alpha\alpha\gamma$ -hybrid peptides.

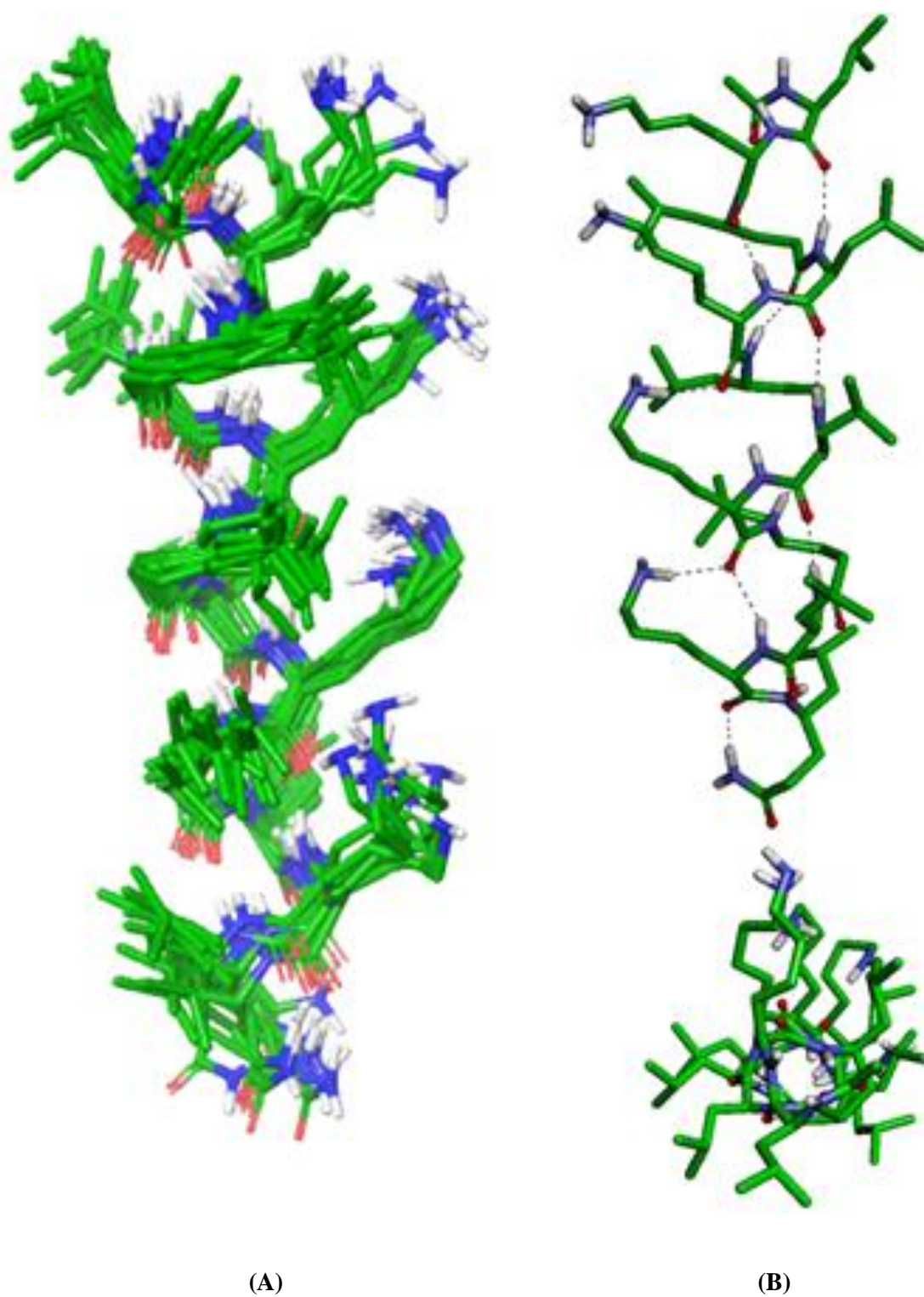


Figure 4.6: A) Superposition of 10 lowest energy structures of peptide **H6** in SDS. B) Single conformer and top view of the 10/12-helix of **H6**.

4.3.3 Antibacterial activities

Antibacterial activities of $\alpha\gamma$ -hybrid peptides, **H1-H7**, and the control α -peptide (**H8**) were examined against *Escherichia coli*, *Escherichia coli* K12, *Klebsiella pneumonia*, *Pseudomonas aeruginosa*, *Staphylococcus aureus*, *Salmonella typhimurium*, Methicillin-sensitive *Staphylococcus aureus* and Methicillin-resistant *Staphylococcus aureus* strains and the activities were determined by measuring their minimum inhibitory concentrations (MICs). The MIC values are given in the Table 4.3. The hexapeptide, **H1** showed the low inhibitory profiles against the all strains. In comparison with **H1**, the nonapeptide **H2** displayed 16 fold better antibacterial activities against *K. pneumonia* and *P. aeruginosa* and 8 fold better activities against *S. typhimurium*. Peptides **H3-H6** showed excellent activity across various bacterial strains including MSSA and MRSA. Both 15-mer **H4** and **H6** (*N*-acetylated analogue of **H3**) showed pronounced activities against MSSA and MRSA bacterial strains. Peptide **H3** was found to be best among all active peptides. In contrast to the peptide **H3**, replacement of γ -Leu with γ -Ala in **H7** leads to the poor antibacterial activities across the panel of bacterial strains. In addition, the α -peptide **H8** also showed the antibacterial activities on par with the designed hybrid peptides. As all individual active peptides displayed similar antibacterial activities across the panel of microorganisms suggesting that these peptides may be adopting similar mode of action.

Table 4.3. Antibacterial and Hemolytic Activity (HD₁₀) of $\alpha\alpha\gamma$ -hybrid peptides. The MIC values are given in $\mu\text{g/mL}$.

	H1	H2	H3	H4	H5	H6	H7	H8
<i>Escherichia coli</i>	>250	62.5	1.9	3.9	3.9	3.9	250	3.8
<i>Escherichia coli K12</i>	>250	62.5	3.9	3.9	3.9	3.9	250	3.8
<i>Klebsiella pneumoniae</i>	125	7.8	1.9	3.9	3.9	7.8	62.5	3.8
<i>Pseudomonas aeruginosa</i>	250	15.6	7.8	7.8	3.9	15.6	125	7.8
<i>Staphylococcus aureus</i>	250	62.5	3.9	7.8	3.9	7.8	>250	15.6
<i>Salmonella typhimurium</i>	250	31.2	3.9	3.9	3.9	7.8	125	3.8
MSSA	>250	62.5	3.9	1.9	3.9	1.9	62.5	a
MRSA	>250	62.5	3.9	1.9	3.9	1.9	250	a
HD ₁₀	>500	>500	445	53	134	170	>500	62

^a not determined.

4.3.4 Hemolytic activities

As peptides **H3-H6** and α -peptide **H8** displayed excellent antimicrobial activities, we subjected them to hemolytic activities to evaluate their specificity against the human red blood cells. The hemolytic activity of peptide H1-H8 is shown in Figure 4.7. The specificity of hybrid peptides against the bacteria versus mammalian cells is of particular interest. The

10% hemolytic dose (HD_{10}) values are given the Table 4.3. We defined the selectivity ratio (SR) as a quotient of HD_{10} and the MIC values. Hence, SR is an estimate of the peptides tendency to kill bacteria than the mammalian cells. Remarkable results were obtained from the hemolytic studies. The active peptide **H3** showed least hemolysis compared to the other active peptides in the series. The selectivity ratio of **H3** against *E. coli* and *Klebsiella pneumonia* was found to be 234, and the peptide also displayed good selectivity ratio against other bacteria.

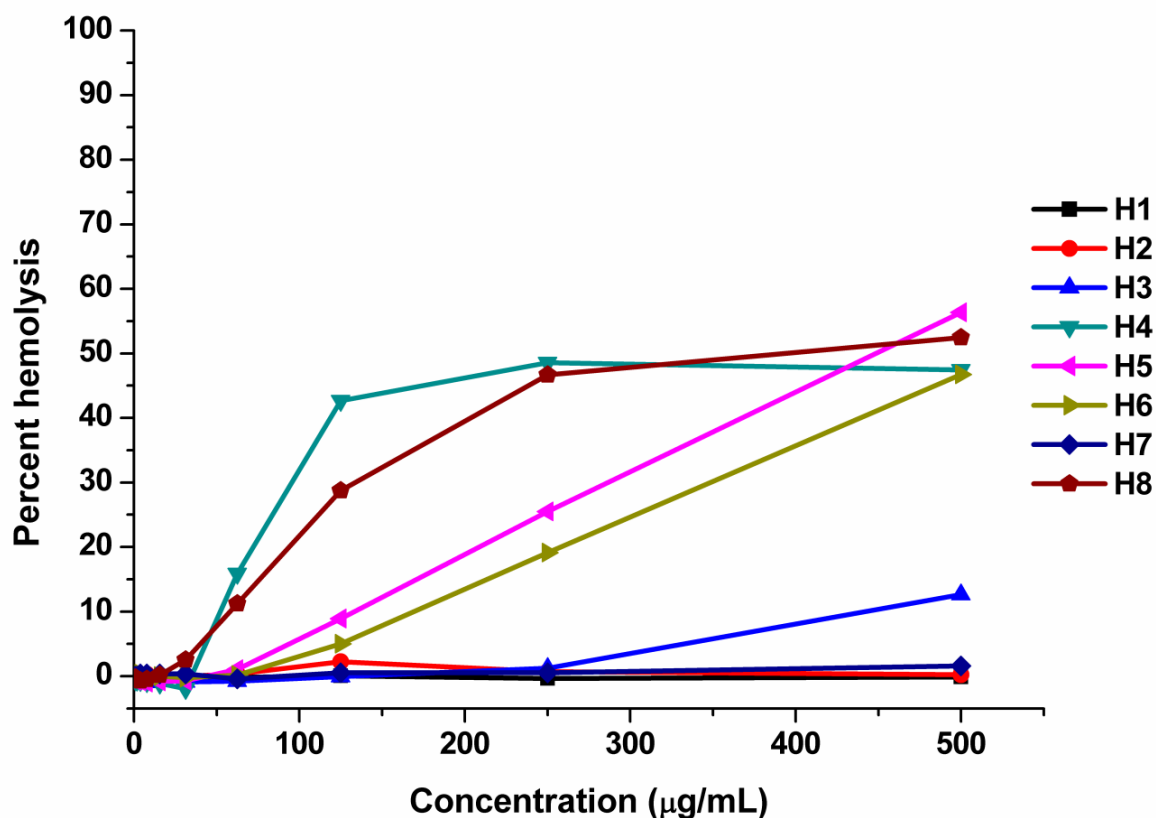


Figure 4.7. Hemolytic activities of the peptides **H1-H8**.

In contrast, the α -peptide analogue **H8** with the same length showed the higher hemolytic activity and subsequently lower selectivity ratio. The selectivity ratio of **H8** against *E. coli* and *Klebsiella pneumonia* was found to be 16, which is 14 fold lower than the peptide **H3**. Surprisingly, **H6** displayed higher hemolytic values (HD_{10} :170) compared to **H3** (HD_{10} : 445).

Though the peptide **H4** showed 2 fold better activity against MSSA and MRSA, however **H3** displayed better selectivity ratio (84 Vs. 114). Thus, the specificity displayed by these peptides against the bacteria compared to the mammalian cells provided wide opportunity to explore them as antibacterial agents.

4.3.5 Field emission scanning electron microscopy studies

As all active hybrid helical peptides displayed similar MIC values against the various bacteria, we examined the mechanism of action of these peptides. Many natural AMPs were

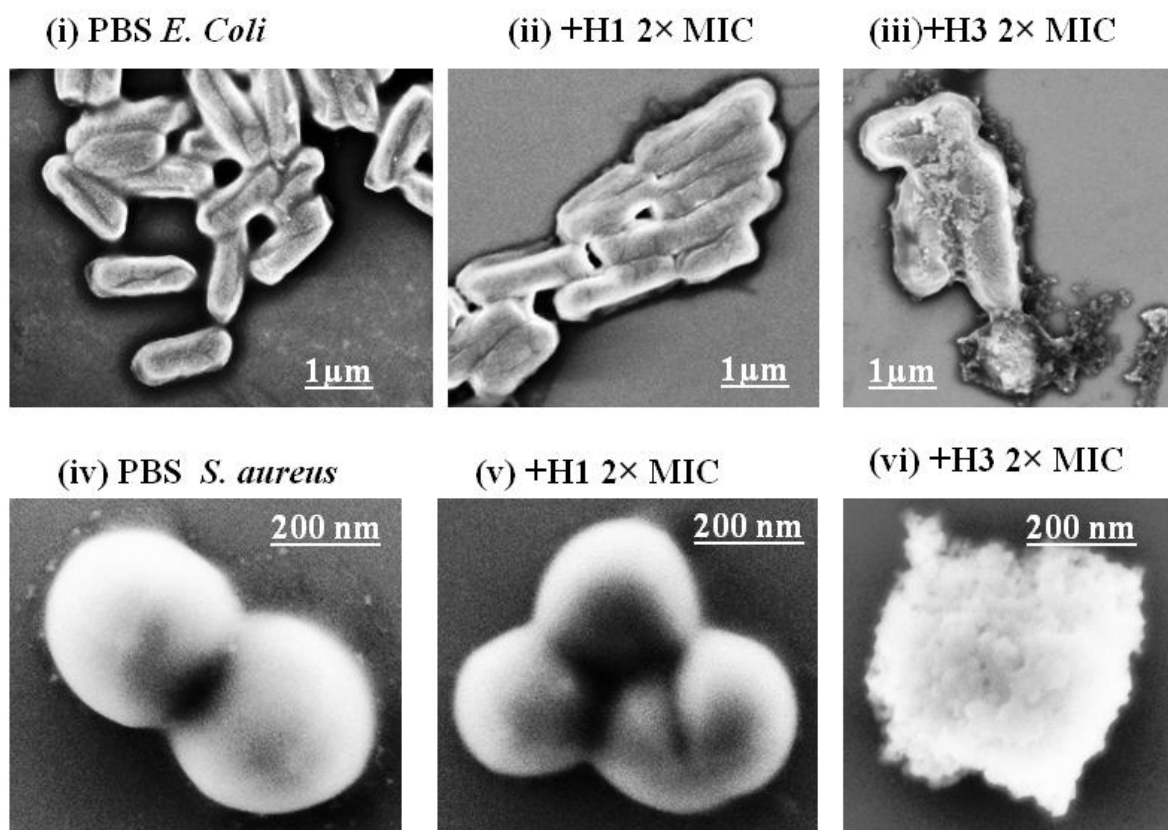


Figure 4.8. Field Emission Scanning Electron Microscopy images of *Escherichia coli* K12 (i) and *S. aureus* (iv) before the treatment of peptides, (ii) and (v) after the treatment with peptide **H1** and (iii) and (vi) after the treatment with peptide **H3** respectively.

found to be disrupting the membrane after binding through the difference in the electrochemical potential.³ To understand whether these helical peptides are disrupting the

bacteria cell, we treated the *E. coli* and *S. aureus* with peptides **H1** and **H3** at $2 \times \text{MIC}$ concentration and subjected to the FE-SEM analysis. The SEM images of the bacteria before and after treatment of peptides are shown in the Figure 4.8. When compared to **H1**, **H3** showed the complete disruption of the bacterial cell wall. The change in the morphology of both microorganisms suggests that the possible action of these helical peptides is through the disruption of cell membrane.

4.3.6 β -Galactosidase leakage assay

We further subjected peptides **H1** and **H3** to cytolitic enzyme β -galactosidase leakage assay to understand the action of these hybrid helices on the inner cell membrane using *E. coli* (pUC19 plasmid transformed Top10 competent cells).¹⁹ In this assay, we exploited β -galactosidase from *E. coli* as an indicator to understand the disruption of the cytoplasmic membrane. Release of β -galactosidase upon treatment of peptides was measured using the initial velocity of the reaction on standard fluorogenic substrate. The release kinetics is shown in Figure 4.9. This assay provides intriguing information on the mode of action of hybrid peptides. The weak fluorescence intensity enhancement is observed in the case of peptide **H1** compared to the control experiment without peptides. In contrast, **H3** displayed huge fluorescence intensity indicating the significant discharge of β -galactosidase. This experiment suggests that both peptides act on membrane and facilitate the release of β -galactosidase, however **H3** disrupt the cell membrane better than the peptide **H1**.

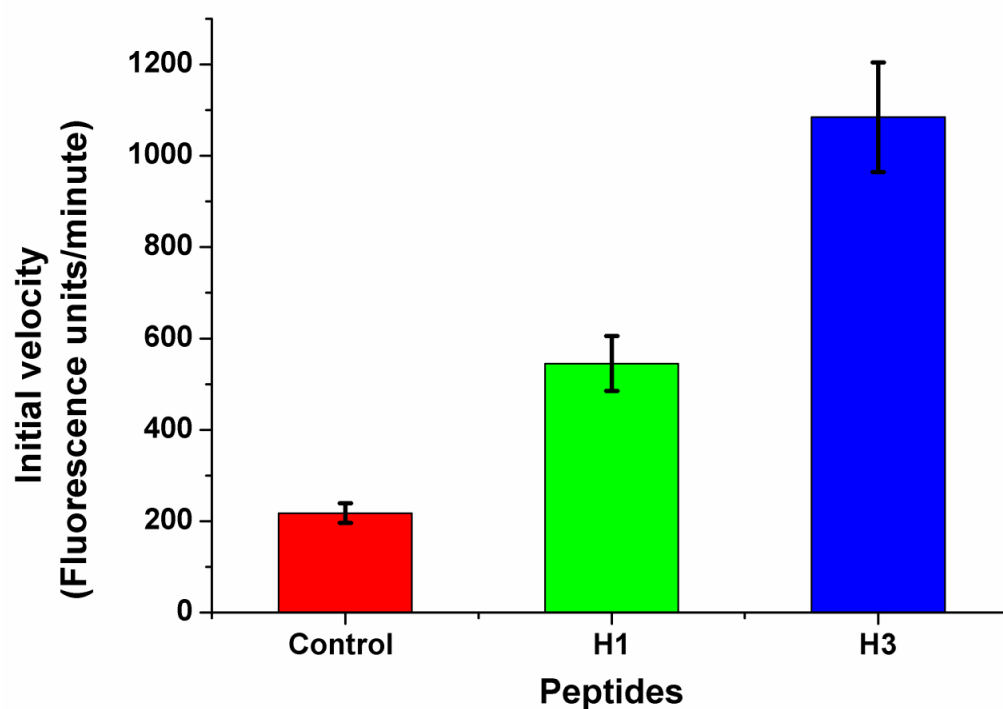


Figure 4.9. β -galactosidase leakage from *Escherichia coli* Top10 cells after treatment with α,α,γ -hybrid peptides. The bar graph represents relative amounts of β -galactosidase present in the medium after treating with the peptides **H1** and **H3**. The experiments were carried out in triplicate for each peptide and error bars are set.

4.3.7 DNA binding assay

The projection of cationic residues at one side along the helix motivated us to investigate their DNA binding ability.²⁰ We examined the DNA interacting ability of peptide **H3** by monitoring electrophoretic mobility of plasmid DNA on an agarose gel. Increasing concentrations of peptide **H3** were mixed with fixed concentration of plasmid DNA and subjected to electrophoresis on an agarose gel after incubating for 2 h (Figure 4.10). At the MIC concentration, complete retardation of the mobility of DNA was observed. These results suggest another mode of action of these $\alpha\alpha\gamma$ -hybrid peptide foldamers along with their membrane disruption.

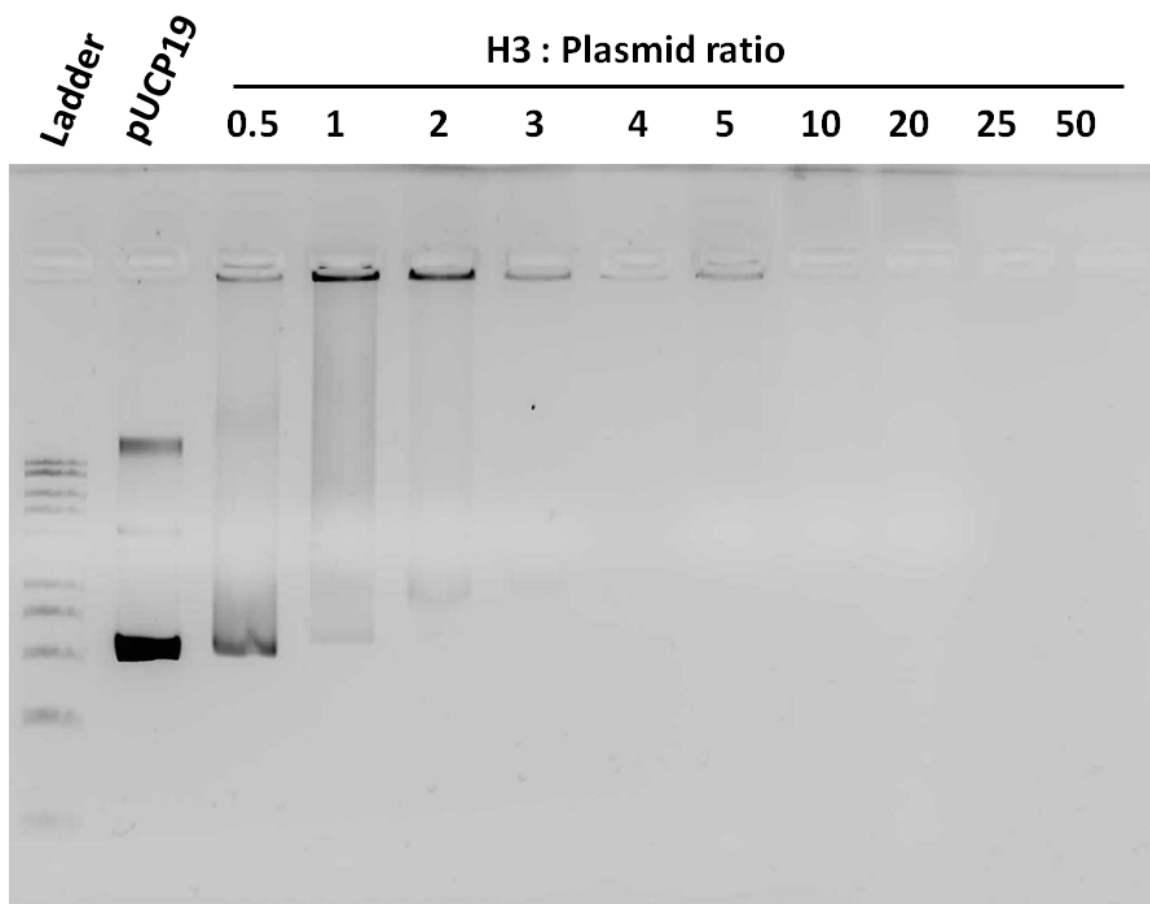


Figure 4.10. Retardation of plasmid pUCP19 DNA migration on a 1% agarose gel at different **H3**: Plasmid weight ratios.

4.3.8 Time kill kinetics assay

Further, we examined the rate at which the hybrid helical foldamers are acting on the bacteria.²¹ We chose *K. pneumoniae* and foldamer **H3** for time kill kinetics experiments. The foldamer was incubated with the bacterial solution at $2 \times \text{MIC}$ ($4 \mu\text{g/mL}$) and $20 \mu\text{L}$ of the peptide treated bacterial solution was drawn at different time intervals. The solution was plated again on Mueller Hinton agar plates and incubated at $37 \text{ }^\circ\text{C}$ for 24 h. The bacterial colonies were counted after the incubation. Results of time kill kinetics assay are shown in Figure 4.11. Results suggested that the complete clearance of bacteria within 20 min by peptide foldamer **H3**.

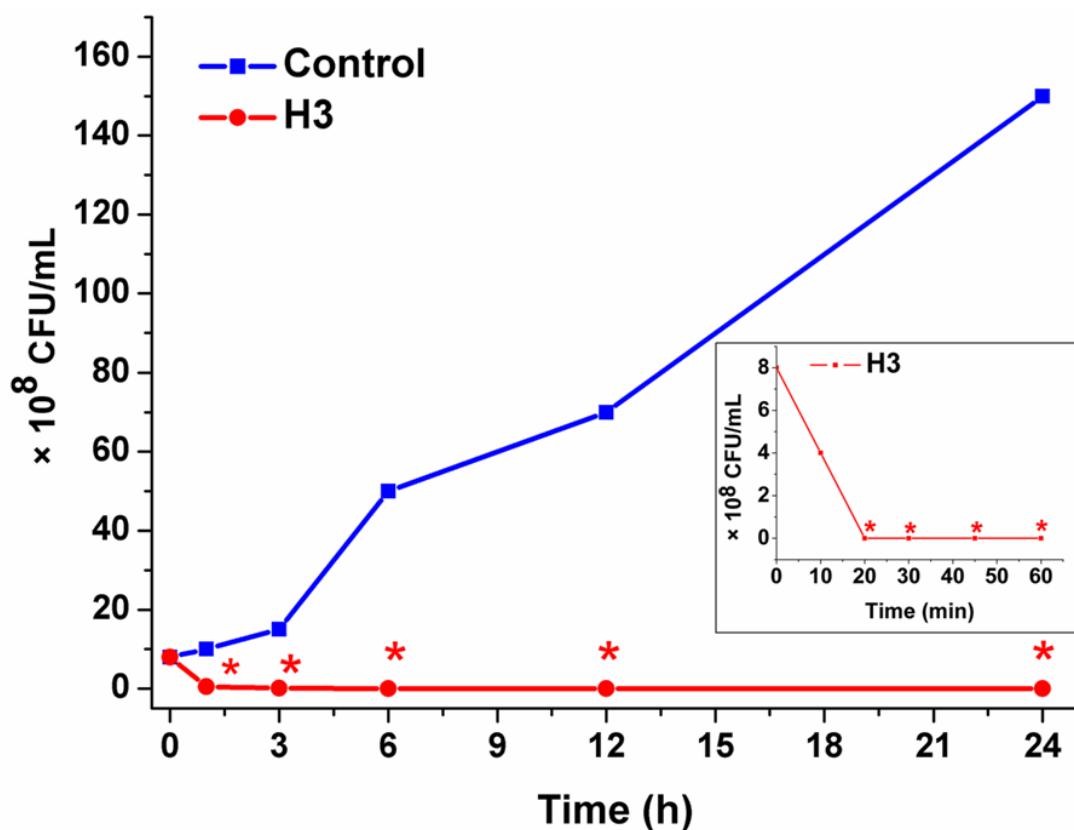


Figure 4.11. Time–kill kinetics profile of peptide **H3** ($2 \times \text{MIC}$) against *K. pneumoniae* (asterisks correspond to $<50 \text{ CFU/mL}$) for 24 h.

4.3.9 Serial passage assay

The potent and broad spectrum antibacterial activity of hybrid foldamers encouraged us to investigate the microbial resistance development against the hybrid peptides through serial passage assay. Based on the time-kill kinetics,²¹ the foldamer **H3** exposed *S. aureus* bacterial solution was drawn before 20 min and grown again in the absence of foldamers. The bacterial solution was further exposed to foldamer **H3** at ($3 \times \text{MIC}$) and 20 μL of the peptide treated bacterial solution was drawn before 20 min after exposing bacteria to antibiotic foldamer. The bacterial solution was further incubated in the absence of antibiotic. This protocol was repeated for about 18 days and monitored MIC values (Figure 4.12). Analysis

suggested that there is no change in the MIC values even after exposing bacteria to the foldamer antibiotics.

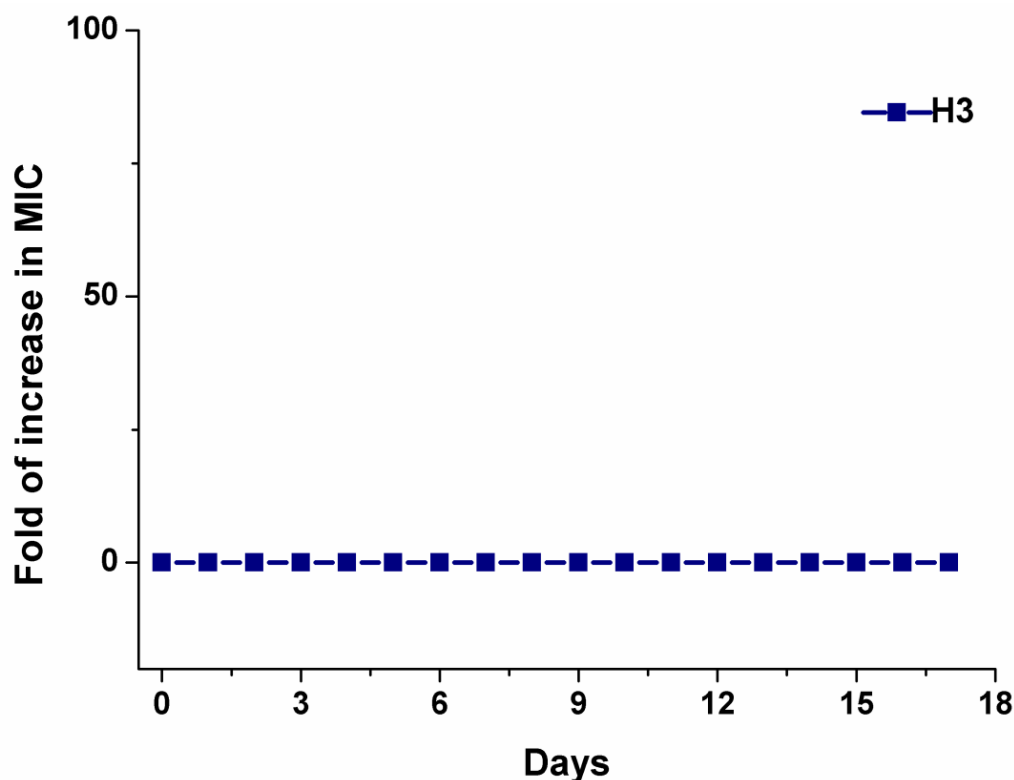


Figure 4.12. Assay to check development of resistance in *S. aureus* after 18 consecutive passages continuously treated with peptide **H3** at sub MIC levels.

4.4 Discussion

There are more than 2600 antimicrobial peptides have been reported do date.²² However, majority of these suffer from various inherent demerits such as length of peptides, poor activity, non-specificity and proteolytic instability. Focus of this work is to rationally design amphiphilic helices from $\alpha\alpha\gamma$ -hybrid peptides composed proteinogenic side-chains. Though the 10/12-helical conformations of $\alpha\alpha\gamma$ -hybrid peptides reported in single crystals, their solution conformations were proved here. Among all peptides, **H6** gave well dispersed ¹H NMR spectrum in SDS. The solution structure analysis of **H6** revealed that the peptide

adopted a 10/12-helical conformation in SDS. The structure of the peptide is stabilized by repetitive 10 and two 12-membered H-bonds along the helix. The hybrid helical foldamers described here represent an alternative approach to derive antimicrobial amphiphilic helices constituted with complete proteinogenic side-chains. These types of helices are of particular appeal due to their increased stability against proteases. The top view of the $\alpha\alpha\gamma$ -hybrid peptides 10/12-helices also resembles the α/β -hybrid peptides. This structural feature of 10/12-helix provided an excellent opportunity to design amphiphilic helices. As simple hexapeptide without N-terminal protection, showed similar type of NOEs as that of **H6**, we anticipate that other peptides in the series also adopt similar type of helical conformation. It is possible that these $\alpha\alpha\gamma$ -hybrid peptides may adopt helical conformation upon binding to the bacterial membrane. The sequences in the hybrid peptide foldamers **H1-H7** are designed to be globally amphiphilic to bind and block the growth of bacteria. The hexa and nonapeptides showed poor antimicrobial activity. Increasing the length from nonapeptide to 12-mer peptides (**H3** and **H6**) showed remarkable improvement in their antimicrobial activities. Further increasing in the length of the peptide from 12-mer to 15-mer (**H4**) and 18-mer (**H5**), no improvement in their antimicrobial activities was observed. Instructively, increasing in the length led to more hemolytic activity of the peptides. Thus 12-mer may be the optimum length for better antimicrobial activity and selectivity in $\alpha\alpha\gamma$ -hybrid peptide foldamer. In contrast, though the 12-mer α -peptide **H8** showed better antimicrobial activity across the panel of bacteria tested but displayed poor selectivity against mammalian cells. The reason for enhanced hemolytic activity observed in the longer **H4** and **H5** and α -peptide **H8** is not clear. Probably the hydrophobicity and side-chains projections play significant role in the activity and selectivity. Similar to many natural and synthetic AMPs, these foldamers also bind and disrupt the bacterial membrane as suggested by FE-SEM and β -galactosidase leakage analysis. Along with the membrane destruction, these cationic amphiphilic foldamers

also bind to the DNA and inhibits its mobility in electrophoresis, suggesting the dual mode of action of these peptides. Beguilingly, these foldamers eradicate the bacteria with 20 min after their exposure and no development of resistance were observed after constant exposing the bacteria to foldamer antibiotics even after 18 days in the serial passage assay. All these results suggested that amphiphilic $\alpha\alpha\gamma$ -hybrid foldamers may serve as potent antibacterial agents.

4.5 Conclusion

We have demonstrated the design, synthesis, conformational analysis and potent antibacterial activity and selectivity of $\alpha\alpha\gamma$ -hybrid peptide foldamers. As anticipated, the structural analysis of the one of the active peptide **H6** revealed that $\alpha\alpha\gamma$ -hybrid peptides adopted 10/12-helix conformation. Among the various lengths of $\alpha\alpha\gamma$ -hybrid peptides, 12-residue peptide was found to be optimum for better activity and selectivity. The 12-residue $\alpha\alpha\gamma$ -hybrid peptides showed excellent antibacterial activity across the panel of various bacterial strains including MRSA and MSSA with very low MIC values. The longer sequences of $\alpha\alpha\gamma$ -hybrid peptides suffer from poor selectivity between bacteria and mammalian cells. Moreover, these foldamer antibiotics completely inhibit the growth of bacteria within 20 min and no development of resistance was observed even after exposing bacteria to foldamer antibiotic for about 18 days. Mechanism of action showed that they not only act on bacterial membrane but also have the ability to bind DNA. The excellent antibacterial activity was also supported by the dual mode of action of foldamers. In contrast, the control 12-mer α -peptide showed poor selectivity over the mammalian and bacterial cells similar to many natural amphiphilic helices. Overall, the $\alpha\alpha\gamma$ -hybrid peptide foldamers provided a unique opportunity to design potent and selective antimicrobial candidates. The potency of these foldamers can be further improved by fine tuning the threshold of hydrophobicity and hydrophilicity.

4.6 Experimental section

4.6.1 Solid phase peptide synthesis and purification of $\alpha\alpha\gamma$ -hybrid peptides

Peptides (**H1-H8**) were synthesized on Knorr amide resin using standard Fmoc-chemistry (0.20 mmol scale). The coupling reactions were carried out by using HBTU/HOBt and monitored by Kaiser Test. After completion of the synthesis, cocktail mixture of TFA: water (95:5) was used to cleave the peptides from the resin. After cleavage, the resin was filtered and washed twice with TFA (2×5 mL). The combined TFA solution was then evaporated under reduced pressure. The peptides were precipitated out using diethyl ether. The precipitated peptide was dissolved in methanol and subjected to purification through reverse phase HPLC on C₁₈ column using methanol/water gradient.

4.6.2 NMR structure calculations

NMR experiments were carried out on 800 spectrometer attached with a cryo probe. Peptide with ~1mM concentration was dissolved in water (90% H₂O + 10% D₂O). A second sample with 1: 100 ratio of peptide: SDS (deuterated) was also made in water. All 2D experiments (TOCSY and NOESY) were carried out at different temperatures 308 K and 325 K to optimize on amide proton dispersion. Data were collected in phase sensitive mode using State- TPPI algorithm. Spectral width for 2D data was set at 8000 Hz and data were collected using 2 K points in the t₂ dimension and 450 points in the indirect (t₁) dimension. Zero filling was done in the t₁ dimension to yield a final data set of 2K X 1K before fourier transformation. A shifted square sine bell window was used while processing. Mixing times were set to 100 ms and 400 ms in case of TOCSY and NOESY respectively.

Amide proton temperature coefficients were obtained by collecting a series of 1D experiments at various temperatures between 278 K and 318 K in steps of 10 K. Slope of the

straight line plots obtained by plotting changes in chemical shifts vs temperature for each amide proton resonance yields its temperature coefficient.

Structure calculation was done using a simulated annealing protocol in vacuum using DESMOND and OPLS 2005 force field with NOE constraints. Upper limit for distance was kept at 3.5 Å for medium NOEs. All the lower distance limits were taken to be 1.8 Å. 1 Kcal/mol force constant was used for all the constraints.

Before production run simulation, a default NVT relaxation was done as implemented in DESMOND. NVT ensemble was used for the production run simulation. Berendsen thermostat with a relaxation time of 1 ps was used. A RESPA integrator was used in which for all the bonded interactions and near nonbonded interactions a time step of 1 fs was used and far nonbonded interaction time step of 3 fs was used. A cut-off of 9 Å was used for short range electrostatic interactions. A smooth particle mesh ewald method was used for treating long range electrostatic interactions. Simulated annealing was done in 6 stages. First stage consists of simulation for 30 ps at 10 K. In the second stage, temperature was linearly increased to 100 K till 100 ps. In the third stage, temperature was linearly increased to 300 K till 200 ps. In the fourth stage, temperature was linearly increased to 400 K till 300 ps. In the fifth stage, temperature was maintained at 400 K till 500 ps. In the sixth stage, temperature was linearly decreased to 300 K till 1000 ps and maintained at 300 K till 1200 ps. The lowest energy structure from the trajectory between 1000 ps and 1200 ps was taken and minimized using a steepest descent method using a convergence gradient threshold of 0.5 kcal/mol/Å.

4.6.3 Procedure for determining MIC

The bacteria *Escherichia coli* (NCIM 2065), *Escherichia coli* K12 (NCIM2563), *Klebsiella pneumoniae* (NCIM 2957), *Pseudomonas aeruginosa* (NCIM 5029), *Salmonella typhimurium* (NCIM 2501) were collected from National Collection of Industrial Microorganisms

(NCIM), and *Staphylococcus aureus* (NCIM 5021), Methicillin resistant *Staphylococcus aureus* (ATCC 33591) and Methicillin sensitive *Staphylococcus aureus* (ATCC 29213) from American type culture collection (ATCC). The Minimum Inhibitory concentration (MIC) of the peptides (**H1-H8**) was determined by microbroth dilution method using 96-well microtiter culture plate. The bacterial cultures were grown for 6 h at 37 °C and were serially diluted to a concentration of 10^6 colony forming units/mL with sterile MHB (Muller-Hinton broth) medium. For each peptide, Two-fold serial dilutions were performed with Mueller Hinton broth medium in a sterile 96-well plate making final volume of 50 μ L in each well. 50 μ L bacterial suspension was added to each well and the peptide treated bacteria were incubated at 37 °C for 14-16 h. The experiment was carried out in triplicate. No peptide was added in the control wells. The growth inhibition of bacteria was monitored by measuring the absorbance at 492 nm. MIC of the peptides were determined as the lowest concentration of peptide required for the complete killing of bacteria.

4.6.4 Procedure for hemolysis assay

Fresh hRBCs (Human Red Blood Cells) were collected and EDTA was added to avoid clotting. The hRBC's were washed with Tris buffer saline (10mM Tris, 150mM NaCl, and pH 7.2) four times and dilution with Tris buffer saline was done to make final concentration of 4% v/v. Sterile 96-well plates were used for the assay. The peptides (**H1-H8**) were two-fold serial diluted in Tris buffer (50 μ L) and aliquots of 50 μ L of hRBC suspension (4% v/v) were added to them. After completion of plating, the hRBCs were incubated at 37 °C for 1 h and then centrifuged for 15 mins at 3000 rpm. The cell debris settled down and supernatant (50 μ L) from each well was pipetted to another sterile 96-well plate containing 50 μ L of tris buffer in each well. The release of haemoglobin (absorbance-540 nm) was monitored as a measure of hemolysis. The hRBCs suspension with Tris buffer was taken as negative control

and with 1% Triton-X was taken as positive control. The experiments were performed in triplicate.

4.6.5 Procedure for β -galactosidase leakage assay

Escherichia coli (TOP10) cells were used to transform the pUC19 plasmid containing LacZ reporter gene. *E. coli* producing β -galactosidase were isolated and used for this assay. *E. coli* cells were grown in Luria Bertani broth with 100 $\mu\text{g/mL}$ of ampicillin at 37 °C to an absorbance 0.6 at 660 nm. The cells were centrifuged and extracellular β -galactosidase was removed by washing with fresh medium thrice. 10 μL of peptide of stock solution in deionised water (concentration 200 $\mu\text{g/mL}$) was added in a sterile 96-well plate. 90 μL bacterial suspension was added to each well and the bacteria were incubated at 37 °C for 1h. After incubation is over, cell debris was removed by centrifugation of the plate at 4000 rpm for 10 min. 80 μL of supernatant was transferred to sterile 96 well plate. An aliquot 20 μL (0.4 mg/mL) of fluorescent indicator 4-methylumbelliferyl- β -galactosidase (MUG) was added to each well and β -galactosidase release was monitored for 1 h at 5 min. intervals. Initial velocities of enzyme reaction were calculated from the linear plot of fluorescence versus time. The samples treated with water served as a blank.

4.6.6 Procedure for peptide:DNA binding assay

An agarose gel retardation assay was performed to evaluate binding of peptide **H3** to plasmid DNA as previously described with modifications.¹⁹ Culture of *E. coli* (Top 10/ pUCP19) cells was grown overnight and Unmodified pUCP19 plasmid was purified from them using a Plasmid Purification Kit (QIAGEN Inc.). Elution of the pUCP19 vector was carried out by using water, and a NanoDrop machine was used to find the concentration of the purified plasmid. Plasmid (200 ng) was incubated at 23 °C with **H3** in increasing ratios in 20 μL of binding buffer (5% glycerol, 10 mM Tris-HCl at pH 8.0, 1 mM EDTA, 1 mM dithreitol, 20

mM KCl, and 50 mg/ml BSA). After 1 hr of incubation, 2 mL of 103 loading buffer (Invitrogen) was added to the mixture. 100 ng of plasmid from each incubation mixture was loaded onto a 1% agarose gel in Tris-acetate-EDTA (TAE) buffer containing SYBR Safe DNA gel stain (Invitrogen). The gel was run at 100 V for approx. 50 min and the DNA bands were observed with UV light using a Chemigenius 2 Bio Imaging System.

4.6.7 Procedure for time kill kinetics assay

The rate at which the peptide **H3** kills the bacteria was determined by performing time kill kinetics assay. In brief, *K. pneumoniae* were grown in MHB broth at 37 °C for 6 h. Peptide **H3** solution in water (4 µg/mL, 2 × MIC) was added to the bacterial solution of *K. pneumoniae* (1.8×10^5 CFU/mL). The peptide treated bacteria samples were incubated at 37 °C. 20 µL aliquots were drawn at different time intervals (0, 1, 3, 6, 12, and 24 h) from that solution and were serially diluted 10-fold by using 0.9% saline. Then from the dilutions, 20 µL solutions were spread evenly on Mueller Hinton agar (MHA) plates and the plates were incubated at 37 °C for 20 h. After 20 h, the bacterial colonies were counted, and results are determined in CFU/mL scale. A similar experiment was performed using for shorter time intervals of 0, 10, 20, 30, 45, and 60 min to find out the exact time required to kill the bacteria.

4.6.8 Procedure for membrane deformation study

The bacteria (*E. coli* and *S. aureus*) were treated with peptide by using the broth micro dilution method for a shorter period of incubation. In brief, 100 µL peptide solution (2 × MIC) was pipetted into a sterile 96-well plate. Bacteria (*E. coli* and *S. aureus*) were first inoculated to enter its log growth-phase. An equal volume of bacterial solution (100 µL) was added into each well of the 96-well plate containing the peptide. The concentration of bacterial solution was maintained to give an initial optical density (O.D.) reading of 0.1-0.2 at 600 nm wavelength. The bacterial cells were incubated with peptide at 37 °C for 2 h with 8

replicates. After completion of incubation, all the replicates were mixed into a micro centrifuge tube and the solution was pelleted down at 5000 g for 5 min. Following the centrifugation, the supernatant was removed and bacterial cells were then washed with PBS for three times. The bacterial cells were then fixed with 2.5% glutaraldehyde for 15 min, followed by washing with PBS twice. Finally, the bacteria were washed by deionized water. The bacterial cells were pelleted down and dehydrated with a series of graded ethanol solution (30%, 50%, 70%, 95%, and 100%). Dehydrated bacterial samples were then drop casted on silicon wafer, sputtered with gold coating, and images were recorded under a field emission scanning electron microscope.

4.6.9 Procedure for serial passage assay

At first, the MIC value of peptide **H3** was determined against *S. aureus* as by micro broth dilution method. Bacteria treated with sub MIC concentration of the peptide **H3** (approx. 2 µg/mL) were cultured for the next day MIC experiment and subjected to MIC determination assay after incubation with the peptide **H3** for 6-8 h. On the next day, after the MIC determination, the bacterial solution treated with sub MIC concentration of peptide was inoculated freshly and incubated with the peptide **H3** for 6-8 h. The process was repeated for 17 days. The rate of increase in MIC for **H3** was plotted against the number of days for which the experiment was performed.

4.7 References

1. a) Levy, S. B.; Marshall, B. *Nat. Med.* **2004**, *10*, S122-S129. b) Tomasz, A. *N. Engl. J. Med.* **1994**, *330*, 1247-1251. c) Murray, B. E. *N. Engl. J. Med.* **2000**, *342*, 710-721. d) Aires de Sousa, M.; De Lencastre, H. *J. Clin. Microbiol.* **2003**, *41*, 3806-3815.
2. a) Zasloff, M. *Nature* **2002**, *415*, 389-395. b) Zasloff, M. *Proc. Natl. Acad. Sci. U.S.A.* **1987**, *84*, 5449-5453. c) Steiner, H.; Hultmark, D.; Engstrom, A.; Bennich, H.; Boman, H. G. *Nature* **1981**, *292*, 246-248.
3. a) Hancock, R. E. W. *Lancet* **1997**, *349*, 418-422. b) Brogden, K. A. *Nature* **2005**, *3*, 238-250. c) Straus, S. K.; Hancock R. E. W. *Biochim. Biophys. Acta* **2006**, *1758*, 1215-1223. d) Bishop, J. L.; Finlay, B. B. *Trends Mol. Med.* **2006**, *12*, 3-6. e) Perron G. G.; Zasloff, M.; Bell, G. *Proc. Biol. Sci.* **2006**, *273*, 251-256.
4. a) Fjell, C. D.; Hiss, J. A.; Hancock, R. E. W.; Schneider, G. *Nat. Rev. Drug Discov.* **2012**, *11*, 37-51. b) Hancock, R. E. W.; Sahl, H. G. *Nat. Biotechnol.* **2006**, *24*, 155-1557.
5. a) Tossi, A.; Sandri, L.; Giangaspero, A. *Biopolymers* **2000**, *55*, 4-30. b) Pag, U.; Oedenkoven, M.; Sass, V.; Shai, Y.; Shamova, O.; Antcheva, N.; Tossi, A.; Sahl, H. -G. *J. Antimicrob. Chemother.* **2008**, *61*, 341-352. c) Falla, T.; Karunaratne, D.; Hancock R. E. W. *J. Biol. Chem.* **1996**, *271*, 19298-19303. d) Oren, Z.; Lerman, J.; Gudmundsson, G.; Agerberth, B.; Shai Y. *Biochem. J.* **1999**, *341*, 501-513.
6. a) Shai, Y.; Oren, Z. *J. Biol. Chem.* **1996**, *271*, 7305-7308. b) Oren, Z.; Hong, J.; Shai, Y. *J. Biol. Chem.* **1997**, *272*, 14643-14649. c) Oren, Z.; Shai, Y. *Biochemistry* **1997**, *36*, 1826-1835. d) Bessalle, R.; Kapitkovsky, A.; Gorea, A.; Shalit, I.; Fridkin, M. *FEBS Lett.* **1990**, *274*, 151-155.
7. a) Raguse, T. L.; Porter, E. A.; Weisblum, B.; Gellman S. H. *J. Am. Chem. Soc.* **2002**, *124*, 12774-12785. b) Arvidsson, P. I.; Frackenpohl, J.; Ryder, N. S.; Liechty, B.; Petersen, F.; Zimmermann, H.; Camenisch, G. P.; Woessner, R.; Seebach D.

- ChemBioChem* **2001**, *2*, 771-773. c) Schmitt, M. A.; Weisblum, B.; Gellman, S. H. *J. Am. Chem. Soc.* **2007**, *129*, 417-428. d) Porter, E. A.; Weisblum, B.; Gellman, S. H. *J. Am. Chem. Soc.* **2002**, *124*, 7324-7330. e) Porter, E. A.; Wang, X.; Lee, H. S.; Weisblum, B.; Gellman, S. H. *Nature* **2000**, *404*, 565. f) Liu D.; DeGrado, W. F. *J. Am. Chem. Soc.* **2001**, *123*, 7553-7559. g) Hansen, T.; Alst, T.; Havelkova, M.; Strøm, M. B. *J. Med. Chem.* **2010**, *53*, 595–606.
8. a) Chongsiriwatana, N. P.; Patch, J. A.; Czyzewski, A. M.; Dohm, M. T.; Ivankin, A.; Gidalevitz, D.; Zuckermann, R. N.; Barron, A. E. *Proc. Natl. Acad. Sci. U.S.A.* **2008**, *105*, 2794-2799. b) Patch, J. A.; Barron, A. E. *J. Am. Chem. Soc.* **2003**, *125*, 12092-12093.
9. a) Schmitt, M. A.; Weisblum, B.; Gellman, S. H. *J. Am. Chem. Soc.* **2004**, *126*, 6848-6849. b) Schmitt, M. A.; Weisblum, B.; Gellman, S. H. *J. Am. Chem. Soc.* **2007**, *129*, 417-428.
10. a) Choi, H.; Chakraborty, S.; Liu, R.; Gellman, S. H.; Weisshaar, J. *ACS Chem. Biol.* **2016**, *11*, 113-120. (b) Liu, R.; Chen, X.; Falk, S.; Masters, K.; Weisblum, B.; Gellman, S. H. *J. Am. Chem. Soc.* **2015**, *137*, 2183-2186. c) Chakraborty, S.; Liu, R.; Hayouka, Z.; Chen, X.; Ehrhardt, J.; Lu, Q.; Burke, E.; Yang, Y.; Weisblum, B.; Wong, G.; Masters, K.; Gellman, S. H. *J. Am. Chem. Soc.* **2014**, *136*, 14530-14535.
11. a) Thangamani, S.; Nepal, M.; Chmielewski, J.; Seleem, M. *Drug Design, Development and Therapy* **2015**, *9*, 5749–5754. b) Nepal, M.; Thangamani, S.; Seleem, M.; Chmielewski, J. *Org. Biomol. Chem.* **2015**, *13*, 5930-5936. c) Hernandez, V.; Geisler, I.; Chmielewski, J. *Bioorg. Med. Chem. Lett.* **2014**, *24*, 556-559. d) Kuriakose, J.; Hernandez, V.; Nepal, M.; Brezden, A.; Pozzi, V.; Seleem, M.; Chmielewski, J. *Angew. Chem. Int. Ed.* **2013**, *52*, 9664 –9667.

12. a) Liu, D.; Choi, S.; Chen, B.; Doerksen, R. J.; Clements, D. J.; Winkler, J. D.; Klein, M. L.; William F. DeGrado, W. F. *Angew. Chem. Int. Ed. Engl.* **2004**, *43*, 1158–1162. b) Tew, G. N.; Liu, D.; Chen, B.; Doerksen, R. J.; Kaplan, J.; Carroll, P. J.; Klein, M. L.; DeGrado, W. F. *Proc. Natl. Acad. Sci. USA* **2002**, *99*, 5110–5114.
13. a) Fisher, B. F.; Gellman, S. H. *J. Am. Chem. Soc.* **2016**, *138*, 10766-10769. (b) Giuliano, M.; Maynard, S.; Almeida, A.; Guo, L.; Guzei, I.; Spencer, L.; Gellman, S. H. *J. Am. Chem. Soc.* **2014**, *136*, 15046-15053. c) Basuroy, K.; Dinesh, B.; Shamala, N.; Balaram, P. *Angew. Chem. Int. Ed.* **2012**, *51*, 8736-8739. (d) Basuroy, K.; Dinesh, B.; Reddy, M. B. M.; Chandrappa, S.; Raghothama, S.; Shamala, N.; Balaram, P. *Org. Lett.*, **2013**, *15*, 4866-4869.
14. a) Bouillère, F.; Thétiot-Laurent, S.; Kouklovsky, C.; Alezra, V. *Amino Acids* **2011**, *41*, 687-707. b) Guo, L.; Chi, Y.; Almeida, A. M.; Guzei, I. A.; Parker, B. K.; Gellman, S. H. *J. Am. Chem. Soc.* **2009**, *131*, 16018-16020.
15. a) Jadhav, S. V.; Bandyopadhyay, A.; Gopi, H. N. *Org. Biomol. Chem.* **2013**, *11*, 509-514. (b) Bandyopadhyay, A.; Jadhav, S. V.; Gopi H. N. *Chem. Commun.* **2012**, *48*, 7170-7172.
16. Basuroy, K.; Dinesh, B.; Shamala, N.; Balaram, P. *Angew. Chem. Int. Ed.* **2013**, *52*, 3136-3139.
17. Ganesh Kumar, M.; Benke, S. N.; Raja, K. M. P.; Gopi, H. N. *Chem. Commun.*, **2015**, *51*, 13397-13399.
18. Misra, R.; Saseendran, A.; George, G.; Veeresh, K.; Raja, K. M. P.; Raghothama, S.; Hofmann, H. -J.; Gopi, H. N. *Chem. Eur. J.* **2017**, *23*, 3764 – 3772.
19. Uljasz, A. T.; Grenader, A.; Weisblum, B. *J. Bacteriol.* **1996**, *178*, 6305-6309.
20. a) Yan, J.; Wang, K.; Dang, W.; Chen, R.; Xie, J.; Zhang, B.; Song, J.; Wang, R. *Antimicrob. Agents Chemother.* **2013**, *57*, 220–228. b) Haney, E. F.; Petersen, A. P.; Lau,

C. K.; Jing, W.; Storey, D. G.; Vogel, H. J. *Biochim. Biophys. Acta* **2013**, *1828*, 1802–1813.

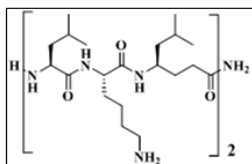
21. Mohamed, M. F.; Abdelkhalek, A.; Seleem, M. N. *Sci. Rep.* **2016**, *6*, 29707

22. Wang, G.; Li, X; Wang, Z. *Nucleic Acids Res.* **2016**, *44*, D1087–D1093.

4.8 Appendix IV: Characterisation data of synthesized peptides

Designation	Description	Page No.
H1	HPLC trace and Mass spectrum	162
H2	HPLC trace and Mass spectrum	162
H3	HPLC trace and Mass spectrum	163
H4	HPLC trace and Mass spectrum	163
H5	HPLC trace and Mass spectrum	164
H6	HPLC trace and Mass spectrum	164
H7	HPLC trace and Mass spectrum	165
H8	HPLC trace and Mass spectrum	165

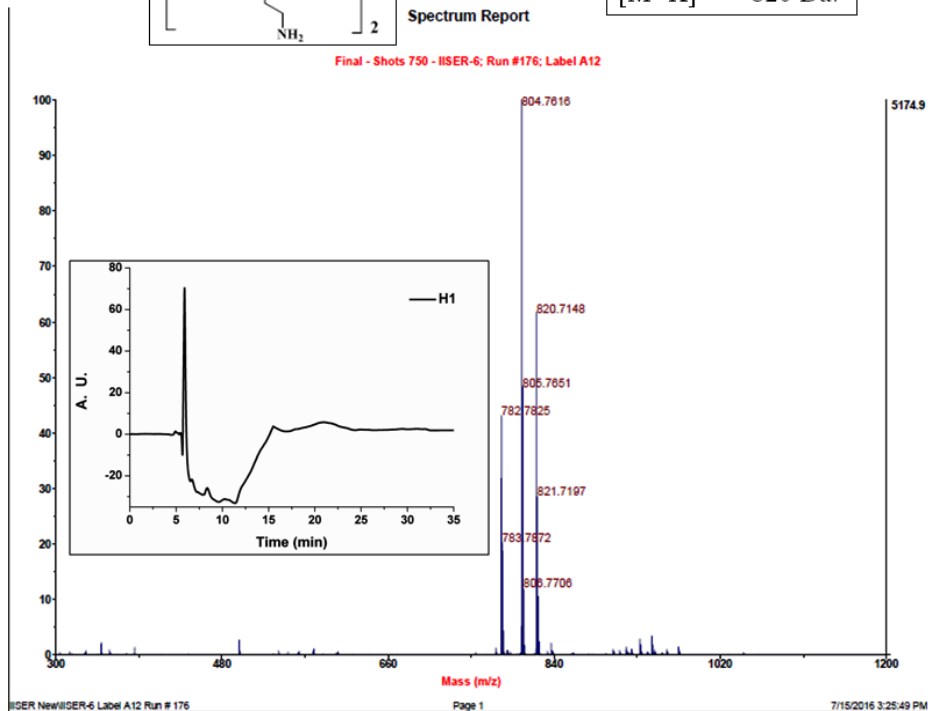
H1



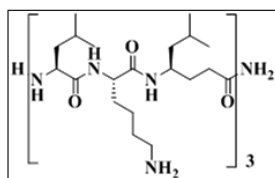
Spectrum Report

Mol wt. = 781 Da.
[M+Na]⁺ = 804 Da.
[M+K]⁺ = 820 Da.

Final - Shots 750 - IISER-6; Run #176; Label A12



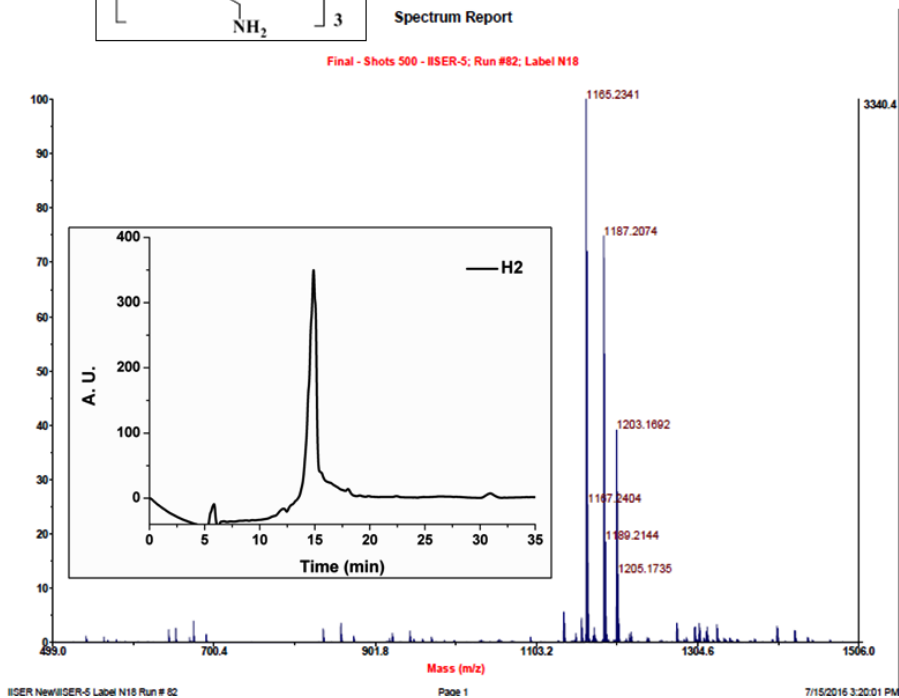
H2



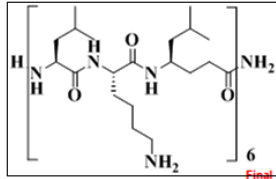
Spectrum Report

Mol wt. = 1164 Da.
[M+Na]⁺ = 1187 Da.
[M+K]⁺ = 1203 Da.

Final - Shots 500 - IISER-5; Run #82; Label N18



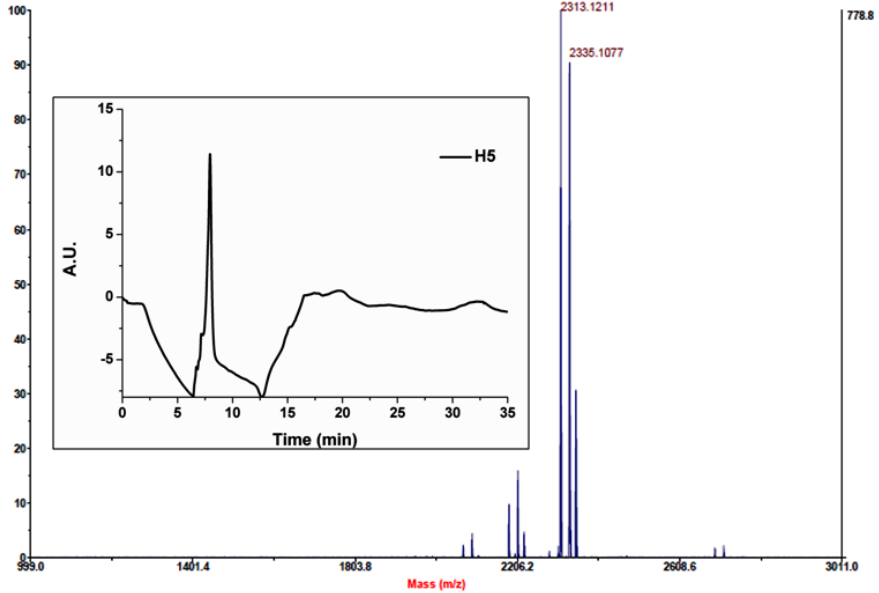
H5



Spectrum Report

Mol wt. =2312 Da.
[M+H]⁺ = 2313 Da.
[M+Na]⁺ =2335 Da.

Final - Shots 500 - IISER-6; Run #283; Label P19

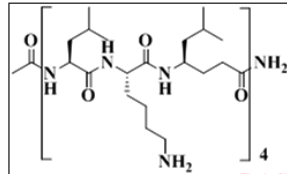


IISER New/IISER-6 Label P19 Run # 283

Page 1

7/15/2016 3:27:39 PM

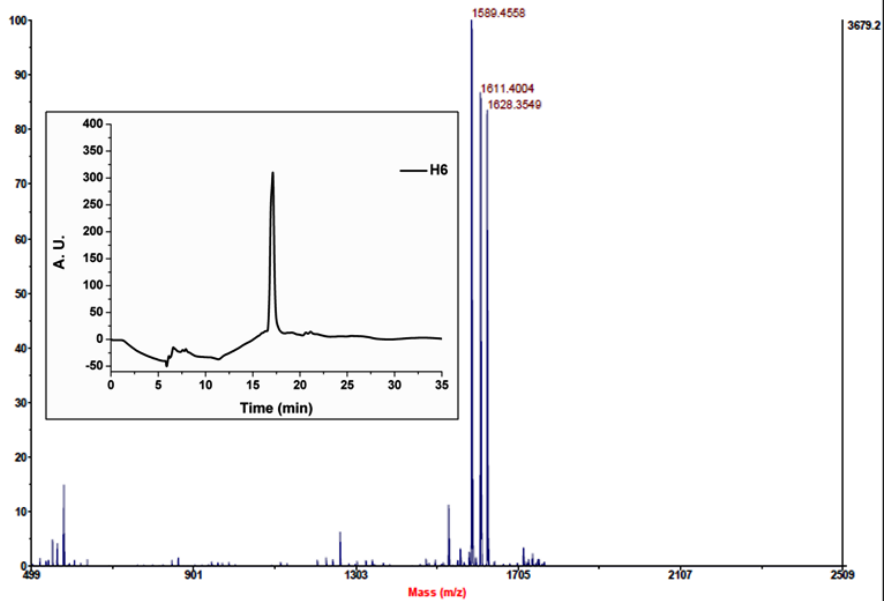
H6



Spectrum Report

Mol wt. =1588 Da.
[M+Na]⁺ =1611 Da.
[M+K]⁺ =1627 Da.

Final - Shots 500 - IISER-6; Run #167; Label I4

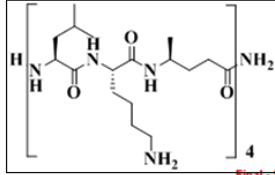


IISER New/IISER-6 Label I4 Run # 167

Page 1

7/15/2016 3:23:20 PM

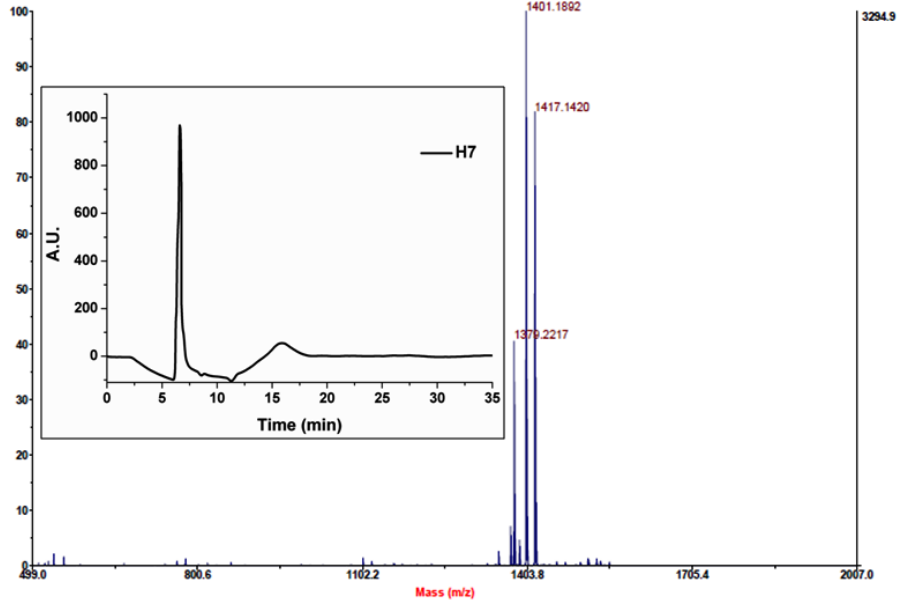
H7



Spectrum Report

Mol wt. = 1378 Da.
[M+Na]⁺ = 1401 Da.
[M+K]⁺ = 1417 Da.

Final - Shots 500 - IISER-5; Run #173; Label E1

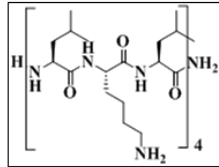


SER New/IISER-5 Label E1 Run # 173

Page 1

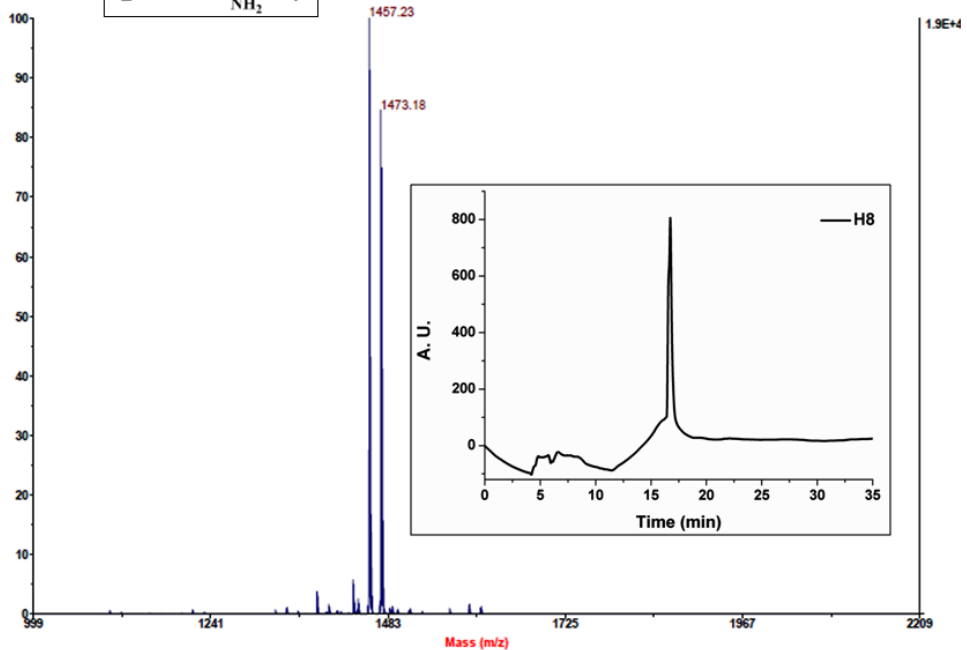
7/15/2016 3:18:10 PM

H8



Final - Shots 600 - IISER-96-1; Run #61; Label A11

Mol wt. = 1434 Da.
[M+Na]⁺ = 1457 Da.
[M+K]⁺ = 1473 Da.



Synopsis

Abstract:

The emergence and spread of antibiotic resistant pathogens is one of the major health concerns of the 21st century, giving rise to an urgent need to develop new antibiotics with different mode of action. Peptides derived from non canonical amino acids such as β - and γ -amino acids have attracted greater interest due to their proteolytic resistance and predictable folding properties. These fascinating features encouraged us to explore the anti-microbial properties of hybrid peptides composed of α - and γ -amino acids. In this regard, we have designed two types of hybrid peptides-short lipopeptides and amphiphilic hybrid helices and investigated their antimicrobial properties. The short lipopeptides are composed of 1:1 α -, and γ -amino acids with varied length of lipid tail and the helical peptides are composed of repeating units of $\alpha\alpha\gamma$ tripeptide segment. These peptides were tested against various Gram positive, Gram negative bacteria as well as Fungi. In the first series, the designed lipopeptides displayed broad spectrum antimicrobial activity. The FITC uptake assay, β -galactosidase assay and AFM analysis reveal that peptides adopted different modes of action through membrane perturbation. In contrast to the lipopeptides composed of alpha and *E*-vinyllogous γ -amino acids, the second series of lipopeptides composed of 1:1 α - and saturated γ -amino acids showed better antimicrobial properties with less haemolytic activity. In the third series, the amphiphilic helical peptides were designed based on the single crystal conformation of α , α , γ -hybrid peptide 10/12-helices to mimic the structural and functional properties of natural helical antibiotic magainin and LL37. As predicted, the 2D NMR (TOCSY and NOESY) experiments reveal that the α,α,γ -hybrid peptides adopted 10/12-helical conformations of in SDS. Similar to the lipopeptides, these α,α,γ -helical peptides displayed potent broad spectrum antimicrobial activity across the panel of Gram positive and Gram negative bacteria including MRSA. The mode of action suggests that they not only inhibit the bacterial growth through membrane depolarisation but also showed their ability to bind DNA. These results suggest the dual mode of action of hybrid helical peptides. Overall, this study underlines the potential of α,γ -hybrid peptides in the development of next generation antimicrobial therapeutics.

Based on the types of investigation, this thesis is divided into following four chapters.

1. Introduction to Antimicrobial Peptides
2. Design, Synthesis, and Broad Spectrum Antimicrobial Properties of Short Hybrid *E*-Vinylogous Lipopeptides
3. a) Potent Antimicrobial Activity of Lipidated Short α , γ -Hybrid Peptides
b) Synthesis and Utilization of New $\gamma\gamma$ -diamino acids from *E*-Vinylogous Amino Acids and Their Utility in Design of α,γ -Hybrid Peptide Foldamers
4. Design, Structure and Potent Antimicrobial Activity of $\alpha\alpha\gamma$ -Hybrid Peptide Helical Foldamers

Chapter 1

Antimicrobial peptides

Antibiotics have been serving as powerful medicines to combat pathogenic infections and are playing crucial role in improving the human health. Constant exposure to antibiotics has initiated various mutations in the microbes which have made many of the microbes resistant towards the antibiotics in use.¹ Rapid emergence of antibiotic resistance and its escalating spread across the globe has created urgent need to look out for other sustainable alternatives such as antimicrobial peptides (AMP). AMP's are evolutionarily conserved component of innate immune system and are ubiquitously found in plant and animal kingdoms.² AMP's are generally 10-50 amino acid long amphipathic peptides, carry a net positive charge more than 2 and have ~50% hydrophobic amino acids. More than 2600 AMP's have been reported so far and they can be classified on the basis of their secondary structure in various classes such as linear, helical, β -sheet, cyclic or mixed peptides.³ Mode of action of AMP's is different than that of other antibiotics. They not only disrupt the bacterial membrane but also bind to various intracellular targets leading to the death of microorganisms.⁴ The amphipathic design of AMP's helps them to specifically act on the bacterial cells versus erythrocytes (Figure 1). Although natural AMP's show potent antimicrobial activity, very few of them have entered clinical trials and fewer have been approved as drugs.⁵ This is due to the inherent limitations of AMP's such as lack of selectivity, proteolytic instability and poor bioavailability. Backbone modification of the peptide has been proved to be excellent strategy to increase the stability of peptides against proteases and several antimicrobial peptidomimetics such as synthetic peptides,⁶ β -peptides,⁷ α/β -peptides,⁸ peptoids,⁹ lipo- β -peptides,¹⁰ Nylon-3 polymers,¹¹ α -AA peptides¹² have been investigated in this regard but there are no report

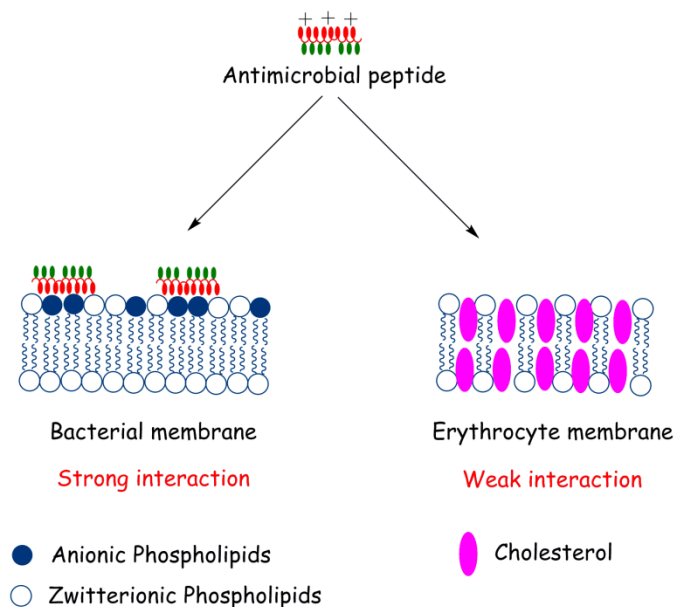
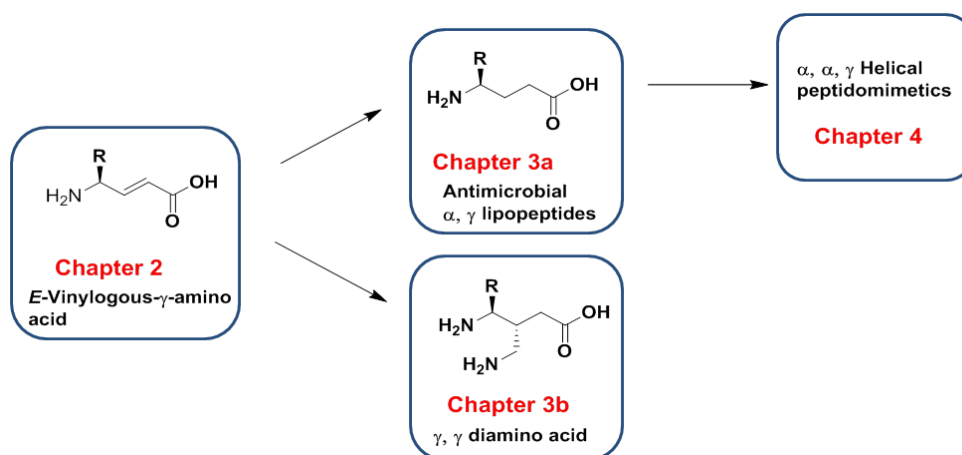


Figure 1. The specificity in action of AMP's on bacterial cell membrane versus erythrocyte cell membrane.

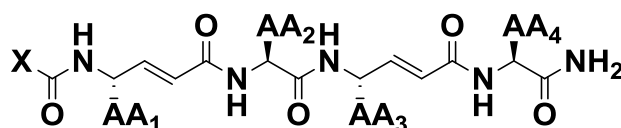
on the utility of γ -amino acids in the design of antimicrobial peptidomimetics so far. We have been working the area of foldamers composed of various non-natural amino acids and demonstrated the successful incorporation of various γ -amino acids in secondary structural peptidomimetics such as α -helix, β -sheet and β -hairpin.¹³ Also, the preliminary protease studies suggested that the γ -amino acids containing peptides are more stable against proteases as compared to natural peptides.¹⁴ In this regard, we designed two classes of antimicrobial peptidomimetics composed of γ -amino acids - lipopeptides and helical peptides and investigated their antimicrobial activity including drug resistant bacteria, hemolytic activity and mechanism of action.



Chapter 2

Design, Synthesis, and Broad Spectrum Antimicrobial Properties of Short Hybrid *E*-Vinylogous Lipopeptides

α , β -Unsaturated γ -amino acids (*E*-vinylogous amino acids) are important components of many biologically active peptides and also have been used as potential candidates for design of inhibitors of serine and cysteine protease. We have explored the *E*-vinylogous amino acids in the design of secondary structural mimics of proteins.¹³ As *E*-vinylogous amino acids promote β -sheet type structures, we sought to explore the antimicrobial properties of short hybrid lipopeptides containing geometrically constrained *E*-vinylogous amino acids. We designed amphipathic lipopeptides containing two hydrophilic residues (Lys or Arg) and two *E*-vinylogous amino acids. The lipid tail is attached to the N-terminus of the peptides. The peptide sequences are listed in Scheme 1.



- S1** C₁₁H₂₃-dgAla-Lys-dgAla-Lys-CONH₂
S2 C₇H₁₅-dgAla-Lys-dgAla-Lys-CONH₂
S3 C₁₁H₂₃-dgTyr-Lys-dgTyr-Lys-CONH₂
S4 C₇H₁₅-dgTyr-Lys-dgTyr-Lys-CONH₂
S5 C₁₁H₂₃-dgAla-Arg-dgAla-Arg-CONH₂
S6 C₇H₁₅-dgAla-Arg-dgAla-Arg-CONH₂
S7 C₁₁H₂₃-dgPhe-Lys-dgPhe-Lys-CONH₂
S8 C₇H₁₅-dgPhe-Lys-dgPhe-Lys-CONH₂
S9 C₇H₁₅-dgLeu-Lys-dgVal-Lys-CONH₂
S10 CH₃-dgPhe-Lys-dgPhe-Lys-CONH₂
S11 C₇H₁₅-Leu-Lys-Val-Lys-CONH₂
dg- dehydro gamma amino acid

Scheme 1. List of α,γ -hybrid vinylogous lipopeptides

All the peptides were subjected to antimicrobial activity against bacterial strains, *Escherichia coli*, *Escherichia coli* K12, *Klebsiella pneumoniae*, *Pseudomonas aeruginosa*, *Salmonella typhimurium*, and *Staphylococcus aureus* and fungi, *Candida albicans*, *Candida glabrata*, *Cryptococcus neoformans*, and *Saccharomyces cerevisiae*. Interestingly, peptides **S1**, **S3** and **S8** were found to be active in micro molar range (1.56-

3.12 $\mu\text{g/mL}$). We then subjected all the peptides to hemolysis assay. Peptide **S1** showed specificity in action (Figure 2B). The mechanism of action of the lipopeptides was investigated by atomic force microscopy studies (Figure 2A) and β -galactosidase leakage assay (Figure 2C).

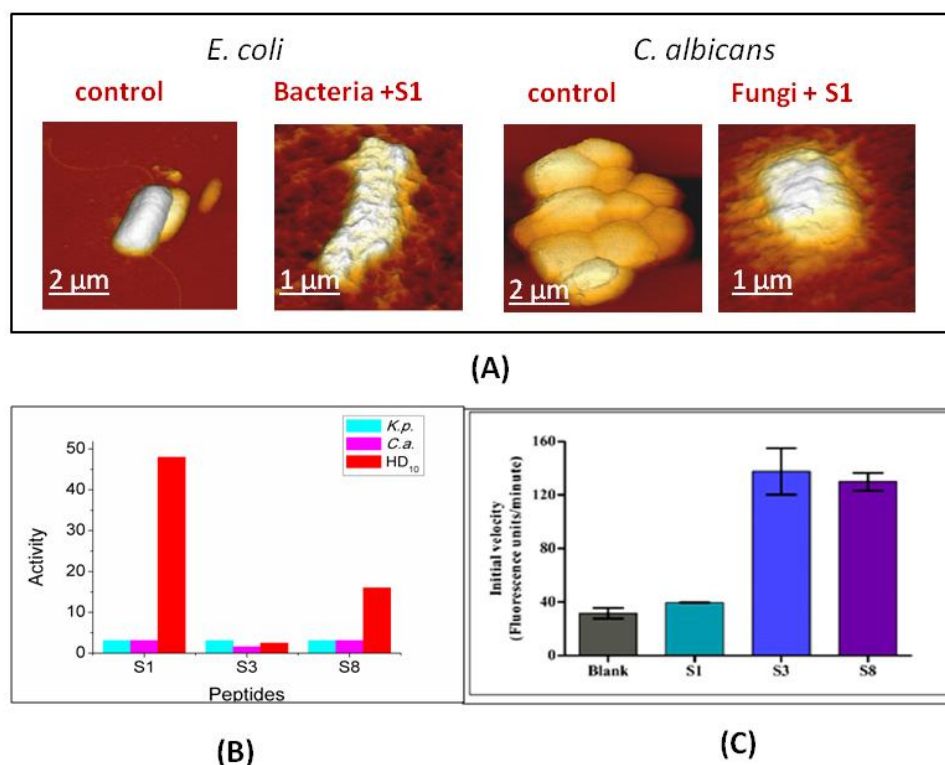


Figure 2 (A) Atomic Force Microscopy (AFM) images of *Escherichia coli* K12 and *Candida albicans* before the treatment of lipopeptide, and after the treatment lipopeptide **S1**. (B) Specificity of the peptides **S1**, **S3** and **S8**. (C) Peptide induced leakage of β -galactosidase from *Escherichia coli* Top10 (Invitrogen) cells. The graph represents relative amount of β -galactosidase present in the medium after treating with the peptides. Error bars are based on triplicate experiments for each peptide.

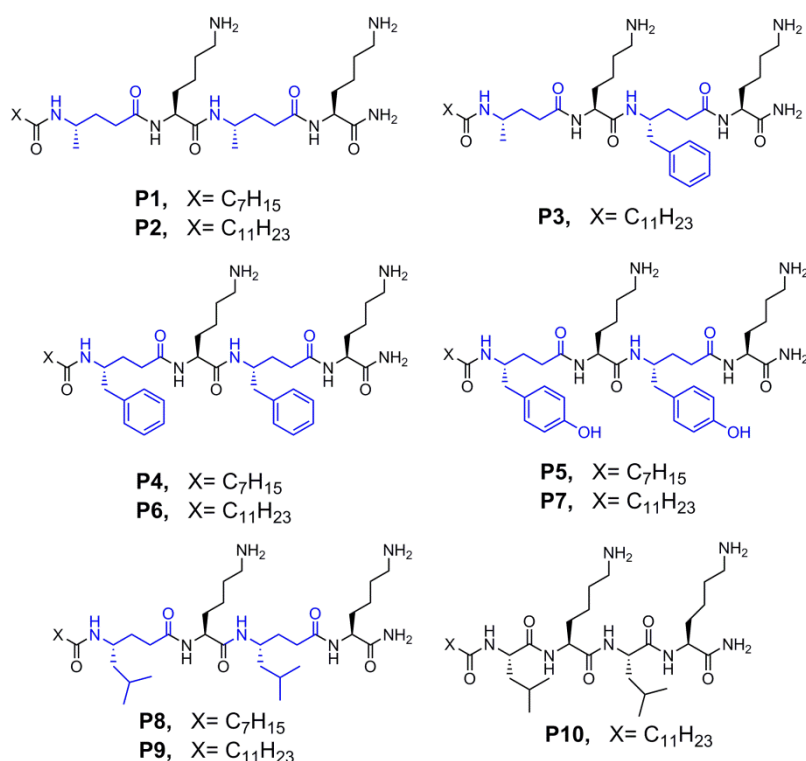
The AFM images confirmed that the peptides act through membrane perturbation. β -galactosidase leakage was found to be more for **S3** and **S8** compared to **S1** suggesting different mode of action. Due to their geometrical restriction of the backbone double bonds, these short hybrid peptides showed highly potent antimicrobial activity compared to that of their α -peptide counterparts. In addition, hybrid peptides with C_{12} and C_8 N-terminal fatty acids displayed better activity than the α - as well as β -lipopeptides containing C_{16} fatty acid at the N-terminal. The hybrid peptides with moderate

hydrophobicity and high electrical potential of self-assemblies showed high antimicrobial and low hemolytic activities. These peptides may possibly bind to the negatively charged outer membrane of the microorganisms and affecting the transmembrane electric potential. The antimicrobial activity, the mode of action and the self-assembly patterns of these short *E*-vinylogous hybrid lipopeptides, particularly **S1** and **S8** provide a unique opportunity to further design potent antimicrobial candidates as well as to explore their utility as smart biomaterials.

Chapter 3a

Potent Antimicrobial activity of Lipidated Short α , γ -hybrid peptides

In the previous chapter, we have studied the antimicrobial activities of the short lipopeptides composed of α - and *E*-vinylogous residues. In this chapter, we sought to investigate the antimicrobial activities of short α,γ -hybrid peptides composed saturated γ -amino acids. We designed short α,γ -hybrid peptides **P1-P9** and control α -peptide **P10** varying the hydrophobicity. The sequences of the peptides are shown in Scheme 2.



Scheme 2. Sequences of α,γ -hybrid lipopeptides (**P1-P9**) and control α -lipopeptide (**P10**).

The peptides were subjected to antimicrobial assay against various Gram positive and Gram negative bacteria. Instructively, peptides **P6**, **P7**, and **P9** displayed potent antimicrobial activity against all the bacterial strains with minimum inhibitory concentration (MIC) in micro molar range (3-6 $\mu\text{g}/\text{mL}$). In addition to their antibacterial activity, we also investigated their mechanism of action and hemolytic activity. The peptide **P9** with aliphatic amino acids displayed less hemolytic activity as compared to aromatic amino acid containing peptides **P6** and **P7** (Figure 3A).

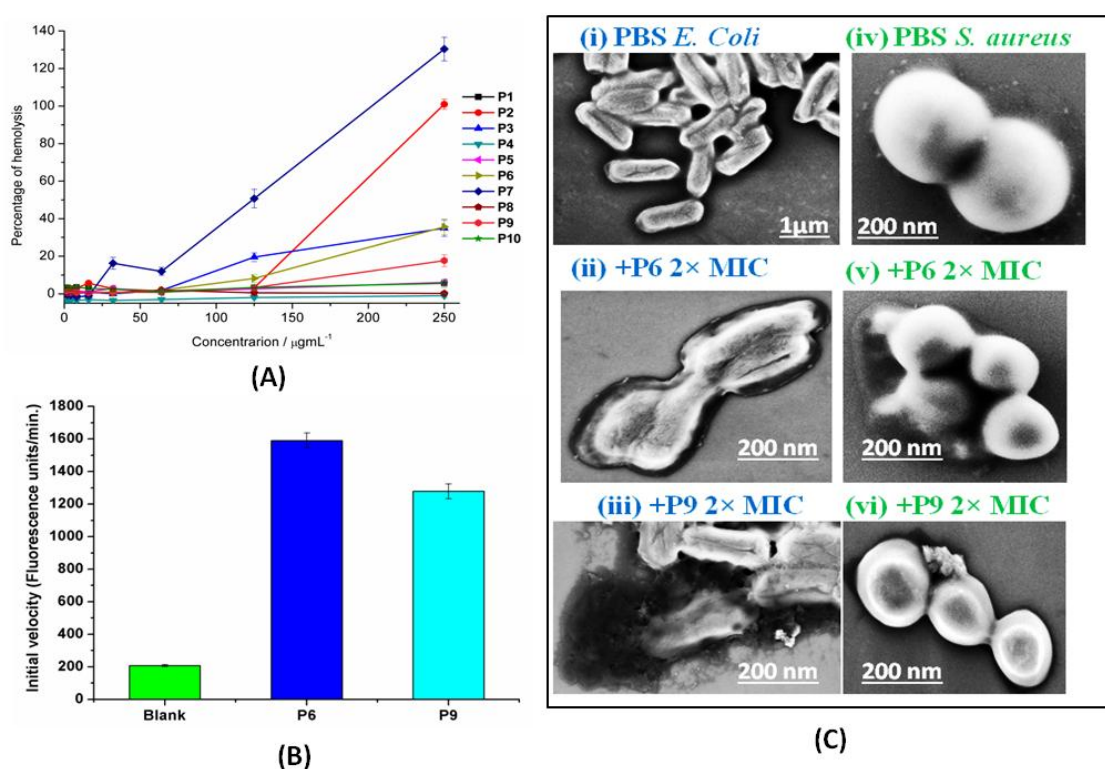


Figure 3. (A) Hemolytic activity of short lipopeptides. (B) Peptide mediated β -galactosidase leakage. The height of the graphs indicates the relative amount of β -galactosidase present in the medium after the treatment of peptides. (C) FE-SEM images of bacteria *E. coli* K12 (i) and *S. aureus* (iv) without lipopeptides. Images of *E. coli* after the treatment with lipopeptides **P6** (ii) and **P9** (iii). Images of *S. aureus* after the treatment with lipopeptides **P6** (v) and **P9** (vi).

In order to understand whether these peptides act through membrane disruption similar to other native antimicrobial peptides, we undertook Field-emission scanning electron microscopy analysis (FE-SEM) which suggested the change in morphology of the microorganisms after the treatment of α,γ -hybrid lipopeptides (Figure 3C). In addition, outer membrane disruption of bacterial membrane by **P6** and **P9** was confirmed by β -

galactosidase leakage assay (Figure 3B). Moreover, the time kill kinetics assay suggested that the lipopeptide **P9** completely inhibit the growth of bacteria within 20 min.

Overall, the potent antibacterial activity, mechanism of action, and fast killing of bacteria, less haemolytic activity displayed by the short α,γ -hybrid peptides, particularly peptide **P9**, provided an unique opportunity to further design peptide antibiotics.

Chapter 3b

Synthesis and Utilization of New γ -diamino acids from *E*-Vinyllogous Amino Acids and Their Utility in Design of α,γ -Hybrid Peptide Foldamers

In chapter 3b, we have demonstrated the synthesis of new γ -amino acids starting from *E*-vinyllogous amino acids through the Michael addition. we have recently demonstrated utility of the esters of *E*-vinyllogous γ -amino acids as Michael acceptors to derive β -substituted γ -amino acids. Using nitromethane Michael donor, we have synthesized a variety of β -nitromethyl substituted γ -amino acids and demonstrated their utility in design of hybrid peptide foldamers.

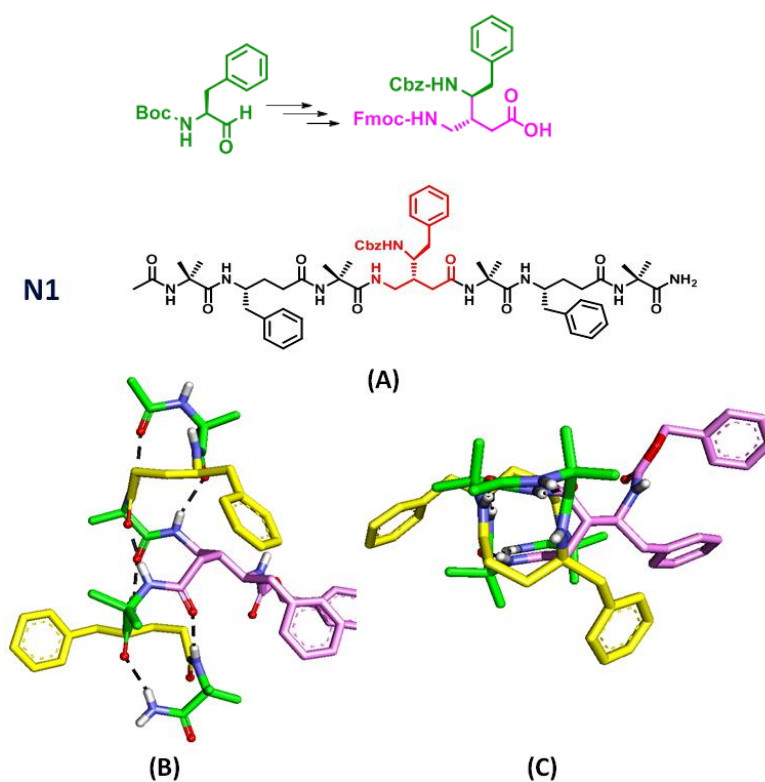


Figure 4. (A) Peptide sequence of hybrid Foldamer **N1** containing new 3-substituted γ -amino acid. (B) Crystal structure of **N1**-side view and (C) top view.

Using the mild reduction of β -nitromethyl group, orthogonally protected new 3-substituted γ -amino acids were isolated in excellent yields and utilized in the construction of hybrid peptide foldamer (Figure 4). The single crystal conformational analysis of hybrid heptapeptide suggested that these amino acids can be accommodated into the helix similar to the other γ -amino acids. More importantly, the amine and side-chain functionality of the α -amino acids can be now placed as a single side-chain on the helical peptide backbone. Overall, the synthesis and isolation of different side-chain substituted γ -amino acids and their conformations in single crystals reported here can be explored to design functional peptide foldamers.

Chapter 4

Design, Structure and Potent Antimicrobial Activity of α,α,γ -Hybrid Peptide Helical Foldamers

In this chapter, we are reporting the design, synthesis, conformational analysis in solution and antimicrobial properties of various amphiphilic $\alpha\alpha\gamma$ -hybrid peptides. Our recent

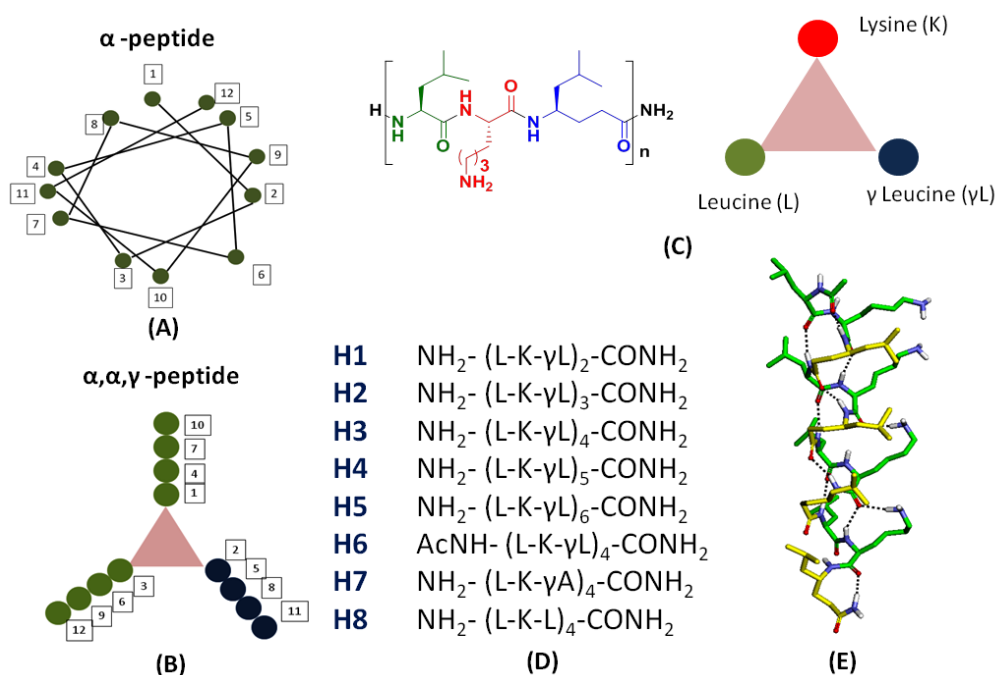


Figure 5. Helical orientation of amino acid side chains in (A) α -helix. (B) α,α,γ -helix. (C) sequence design template of antimicrobial α,α,γ -helical peptides. (D) Peptide sequences **H1-H8**. (E) Solution state conformation of **H6**.

structural analysis of $\alpha\alpha\gamma$ -hybrid peptide foldamers reveals the unique projection of amino acid side-chains along the helical cylinder.¹⁵ The helical distribution of amino acid residues is global in α -helical peptides (Figure 5A) whereas three side aggregation of side chains of amino acid residues is observed in $\alpha\alpha\gamma$ -hybrid peptides (Figure 5B). The distinctive distribution of amino acid side-chains in the $\alpha\alpha\gamma$ -hybrid peptide foldamers provided excellent opportunity to design amphiphilic antimicrobial foldamers.

Based on the crystal structure evidence, we designed amphipathic peptide helices with 2:1 ratio of hydrophobic (Leu, γ Leu) and cationic (Lys) amino acids (Figure 5C). The sequences of the hybrid peptides are shown in Figure 5D. The 2D NMR analysis of the peptide **H6** suggested that the peptide adopts 10/12 helix in solution having amphipathic orientation of side chain (Figure 5E). Based on the knowledge of side chain pre-organization in amphipathic α,α,γ -helices, we designed peptides **H1-H8** with variations in length and hydrophobicity. To understand the antibacterial activity of these designed amphiphilic foldamers, various Gram positive and Gram negative bacteria and Methicillin-resistant *Staphylococcus aureus* (MRSA) and Methicillin-sensitive *Staphylococcus aureus* (MSSA) were tested.

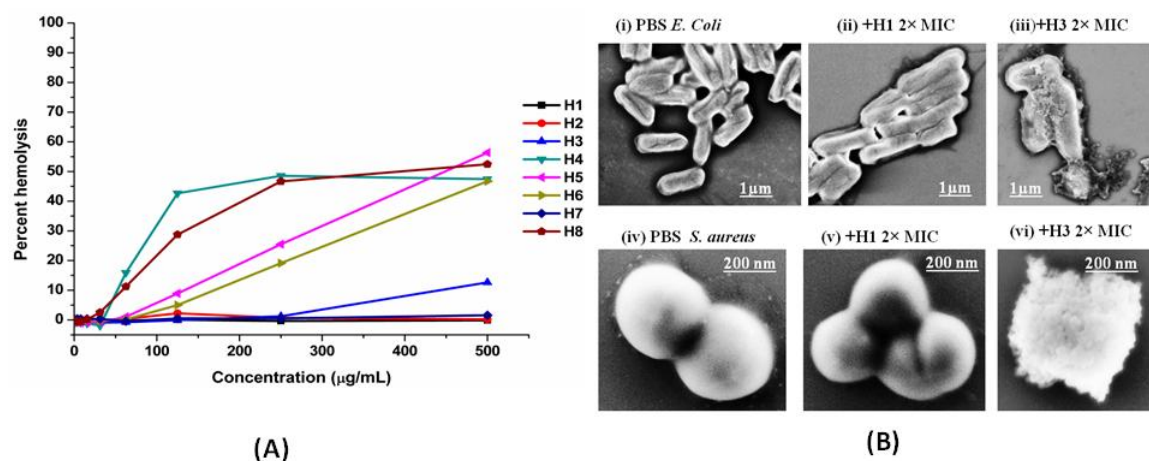


Figure 6. (A) Hemolytic activities of **H1-H8**. (B) Field Emission Scanning Electron Microscopy images of *Escherichia coli* K12 (i) and *S. aureus* (iv) before the treatment of peptides, (ii) and (v) after the treatment with peptide **H1** and (iii) and (vi) after the treatment with peptide **H3** respectively.

The peptides **H3**, **H4** and **H5** showed potent antimicrobial activity with MIC in micro molar range. Also, **H3** displayed less hemolytic activity as compared to the control α -peptide **H8**. Similar to many natural and synthetic AMPs, these foldamers also bind and

disrupt the bacterial membrane as suggested by β -galactosidase leakage assay and FE-SEM analysis (Figure 6B). Along with the membrane destruction, these cationic amphiphilic foldamers also bind to the DNA and inhibits its mobility in electrophoresis, suggesting the dual mode of action of these peptides. Beguilingly, these foldamers eradicate the bacteria within 20 min after their exposure and no development of resistance was observed after constant exposing the bacteria to foldamer antibiotics even after 18 days in the serial passage assay. All these results suggested that amphiphilic $\alpha\alpha\gamma$ -hybrid foldamers may serve as potent antibacterial agents.

References

1. Read, A. F.; Woods, R. J. *Evol. Med. Public Health* **2014**, *1*, 1-147.
2. a) Zasloff, M. *Nature*, **2002**, *415*, 389-395. b) Nakatsuji, T.; Gallo, R.L. *J. Investig. Dermat.* **2012**, *132*, 887-895. c) Hancock, R. E. W.; Brown, K. L.; Mookherjee, N. *Immunobiol.* **2006**, *211*, 315-322. d) Bulet, P.; Stocklin, R.; Menin, L. *Immunol. Rev.*, **2004**, *198*, 169-184.
3. a) Zelezetsky, I.; Tossi, A. *Biochim. Biophys. Acta.* **2006**, *1758*, 1436-1449. b) Nguyen, L. T.; Haney, E. F.; Vogel, H. J. *Trends in Biotechnol.* **2011**, *29*, 464-472. c) Epanand, R. M.; Vogel, H. J. *Biochim. Biophys. Acta.* **1999**, *1462*, 11-28. d) Hancock, R. E. W.; Chapple, D. S. *Antimicrob. Agents. Chemother.* **1999**, *43*, 1317-1323.
4. a) Shai, Y. *Biochim. Biophys. Acta.* **1999**, *1462*, 55-70. b) Saberwal, G.; Nagaraj, R. *Biochim. Biophys. Acta.* **1994**, *1197*, 109-131.
5. Hancock, R. E. W. *Lancet*, **1997**, *349*, 418-422.
6. Wade, D.; Englund, J. *Prot. Pep. Lett.*, **2002**, *9*, 53-57.
7. a) Hamuro, Y.; Schneider, J. P.; DeGrado, W. F. *J. Am. Chem. Soc.* **1999**, *121*, 12200 - 12201. b) Liu, D.; DeGrado, W. F. *J. Am. Chem. Soc.* **2001**, *123*, 7553 - 7559. c) Porter, E. A.; Wang, X.; Lee, H. S.; Weisblum, B.; Gellman, S. H. *Nature* **2000**, *404*, 565 - 565.
8. a) Schmitt, M. A.; Weisblum, B.; Gellman, S. H. *J. Am. Chem. Soc.* **2007**, *129*, 417 - 428. b) Raguse, T. L.; Porter, E. A.; Weisblum, B.; Gellman, S. H. *J. Am. Chem. Soc.* **2002**, *124*, 12774 - 12785. c) Porter E. A.; Weisblum, B.; Gellman S. H. *J. Am. Chem. Soc.* **2002**, *124*, 7324-7330.
9. a) Chongsiriwatana, N. P.; Miller, T. M.; Wetzler, M.; Vakulenko, S.; Karlsson, A. J.; Palecek, S. P.; Mobashery, S.; Barron A. E. *Antimicrob. Agents.*

- Chemother.* **2011**, *55*, 417-420. b) Chongsiriwatana, N. P.; Patch, J. A.; Czyzewski, A. M.; Dohm, M. T.; Ivankin, A.; Gidalevitz, D.; Zuckermann, R. N.; Barron A. E. *Proc. Natl. Acad. Sci. USA* **2008**, *105*, 2794-2799. c) Skovbakke, S. L.; Larsen, C. J.; Heegaard, P. M. H.; Moesby, L.; Franzyk, H. *J. Med. Chem.* **2015**, *58*, 801–813.
10. Serrano, G.; Zhanel, G.; Schweizer, F. *Antimicrob. Agents. Chemother.* **2009**, *53*, 2215–2217.
11. a) Liu, R.; Chen, X.; Falk, S. P.; Masters, K. S.; Weisblum, B.; Gellman, S. H. *J. Am. Chem. Soc.* **2015**, *137*, 2183. b) Chakraborty, S.; Liu, R.; Hayouka, Z.; Chen, X.; Ehrhardt, J.; Lu, Q.; Burke, E.; Yang, Y.; Weisblum, B.; Wong, G. C.; Masters, K. S.; Gellman, S. H. *J. Am. Chem. Soc.* **2014**, *136*, 14530.
12. a) Hu, Y.; Amin, M. N.; Padhee, S.; Wang, R. E.; Qiao, Q.; Bai, G.; Li, Y.; Mathew, A.; Cao, C.; Cai J. *ACS Med. Chem. Lett.* **2012**, *3*, 683-686. b) Niu, Y.; Padhee, S.; Wu, H.; Bai, G.; Qiao, Q.; Hu, Y.; Harrington, L.; Burda, W. N.; Shaw, L. N.; Cao, C.; Cai J. *J. Med. Chem.* **2012**, *55*, 4003-4009.
13. a) Jadhav, S. V.; Bandyopadhyay, A.; Gopi, H. N. *Org. Biomol. Chem.* **2013**, *11*, 509-514. b) Bandyopadhyay, A.; Jadhav, S. V.; Gopi H. N. *Chem. Commun.* **2012**, *48*, 7170-7172. c) Misra, R.; Saseendran, A.; George, G.; Veeresh, K.; Raja, K. M. P.; Raghothama, S.; Hofmann, H. -J.; Gopi, H. N. *Chem. Eur. J.* **2017**, *23*, 3764 – 3772. d) Ganesh Kumar, M.; Thombare, V. J.; Katariya, M. M.; Veeresh, K.; Raja, K. M. P.; Gopi, H. N. *Angew. Chem. Int. Ed.* **2016**, *55*, 7847-7851.
14. Frackenpohl, J.; Arvidsson, P. I.; Schreiber, J. V.; Seebach, D. *ChemBioChem* **2001**, *2*, 445- 455.
15. Ganesh Kumar, M.; Benke, S. N.; Raja, K. M. P.; Gopi, H. N. *Chem. Commun.* **2015**, *51*, 13397-13399.

List of Publications

1. A facile synthesis and crystallographic analysis of *N*-protected β -amino alcohols and short peptaibols. Sandip V. Jadhav, Anupam Bandyopadhyay, **Sushil N. Benke**, Sachitanand M. Mali and Hosahudya N. Gopi, *Org. Biomol. Chem.*, 2011,9 4182-4187.
2. Self-Assembly to Function: Design, Synthesis, and Broad Spectrum Antimicrobial Properties of Short Hybrid *E*-Vinyllogous Lipopeptides S. Shiva Shankar, **Sushil N. Benke**, Narem Nagendra, Prabhakar Lal Srivastava, Hirekodathakallu V. Thulasiram, and Hosahudya N. Gopi. *J. Med. Chem.*, 2013, 56, 8468-8474.
3. Engineering polypeptide folding through trans double bonds: transformation of miniature β -meanders to hybrid helices. Mothukuri Ganesh Kumar, **Sushil N. Benke**, K. Muruga Poopathi Raja and Hosahudya N. Gopi. *Chem commun.*, 2015, 51, 13397-13399
4. Potent Antimicrobial activity of Lipidated Short α , γ -hybrid peptides. **Sushil N. Benke**, H. V. Thulasiram and H. N. Gopi. *ChemMedChem*, 2017,12, 1610-1615.
5. Novel γ -amino acids for the design of Hybrid peptide foldamers. **Sushil N. Benke** and H. N. Gopi. (Manuscript Submitted)
6. Foldamer antibiotics: Design, Structure and Potent Antimicrobial Activity of α,α,γ -hybrid helices. **Sushil N. Benke**, Mothukuri G. K., Shiva Shankar, G. George, S. S. Ragothama, H. V. Thulsiram, and H. N. Gopi. (Manuscript Submitted)